



**HAL**  
open science

# Supervision, analysis and optimization of electrical distribution networks with integration of renewable energies and energy storage means

Daniel Martinez Montana

► **To cite this version:**

Daniel Martinez Montana. Supervision, analysis and optimization of electrical distribution networks with integration of renewable energies and energy storage means. Electric power. Université de Picardie Jules Verne, 2021. English. NNT : 2021AMIE0038 . tel-03852774

**HAL Id: tel-03852774**

**<https://theses.hal.science/tel-03852774v1>**

Submitted on 15 Nov 2022

**HAL** is a multi-disciplinary open access archive for the deposit and dissemination of scientific research documents, whether they are published or not. The documents may come from teaching and research institutions in France or abroad, or from public or private research centers.

L'archive ouverte pluridisciplinaire **HAL**, est destinée au dépôt et à la diffusion de documents scientifiques de niveau recherche, publiés ou non, émanant des établissements d'enseignement et de recherche français ou étrangers, des laboratoires publics ou privés.



# Thèse de Doctorat

*Mention Sciences pour l'ingénieur  
Spécialité Génie Electrique*

présentée à l'Ecole Doctorale en Sciences Technologie et Santé

**de l'Université de Picardie Jules Verne**

par

**Daniel MARTINEZ MONTANA**

pour obtenir le grade de Docteur de l'Université de Picardie Jules Verne

*Supervision, analyse et optimisation des réseaux de distribution électrique avec intégration d'énergies renouvelables et des moyens de stockage d'énergie*

Soutenue le 28/06/2021, après avis des rapporteurs, devant le jury d'examen :

M. Gabriel VELU, Professeur, Université d'Artois	Président
M. Gianfranco CHICCO, Professeur, Politecnico di Torino	Rapporteur
M. DEBUSSCHERE Vincent, Maître de Conférences HDR, Grenoble INP	Rapporteur
M. Seddik BACHA, Professeur, Université Joseph Fourier	Examineur
M. Bruno MEYER, Docteur, Réseau de Transport d'Electricité	Examineur
M. Humberto HENAO, Professeur, Université de Picardie Jules Verne	Directeur de thèse
M. Gérard-André CAPOLINO, Professeur, Université de Picardie Jules Verne	Co-encadrant





# Doctoral Thesis

*Engineering Sciences  
Electrical Engineering*

presented to *Ecole Doctorale en Sciences Technologie et Santé*

**of Université de Picardie Jules Verne**

by

**Daniel MARTINEZ MONTANA**

to obtain the degree of Doctor in Université de Picardie Jules Verne

*Supervision, analysis and optimization of electrical  
distribution networks with integration of renewable energies  
and energy storage means.*

Defended on 28/06/2021, after the opinion of the rapporteurs, in front of the jury:

M. Gabriel VELU, Professor, Université d'Artois	President
M. Gianfranco CHICCO, Professor, Politecnico di Torino	Rapporteur
M. DEBUSSCHERE Vincent, Associate Professor, Grenoble INP	Rapporteur
M. Seddik BACHA, Professor, Université Joseph Fourier	Reviewer
M. Bruno MEYER, Doctor, Réseau de Transport d'Electricité	Reviewer
M. Humberto HENAO, Professor, Université de Picardie Jules Verne	Thesis advisor
M. Gérard-André CAPOLINO, Professor, Université de Picardie Jules Verne	Co-advisor



Dedicated to the loving memory of Humberto MONTANA.

1933 – 2020



*"All people everywhere should have free energy sources." [...]  
"Electric power is everywhere present in unlimited quantities  
and can drive the world's machinery without the need for coal, oil or gas.*

— Nikola Tesla

## ACKNOWLEDGEMENTS

---

This research was achieved within the project VERTPOM<sup>1</sup> supported by the French Environment and Energy Management Agency (ADEME), as part of the "Future Investment Program of the French government".

First of all I would like to thank my parents, Giovanna and Alberto, who always supported me from the beginning of this journey. Also, I sincerely thank the rest of my family for their patience and the encouraging messages received during this time.

I wish to thank my advisors, Dr. Humberto Henao and Dr. Gérard-André Capolino, for giving me a chance in the project and for their continued guidance and support throughout the last three years. I am extremely grateful for their mentoring, time and attention. Likewise, a special thanks to my fellow Juan Perez, together we were able to commit all the challenges.

I would like to thank the team of CIAC IT for their unwavering support of my academic ambitions. These thanks are extensive to Gabriel Garcia who always knew how to guide the goals of the project.

I want also say thanks to Dr. Gustavo Ramos and Dr. Davis Montenegro who with their ability to teach and advice, I found a passion in this field of the engineering. I would have ever imagined possible to go further without their inspiration and motivation.

I want to say thanks to all the amazing people I have met during the development of this project. To my friends in the different parts of the world: Alonso Mena, Wiem Benatia, Willy Valverde, Florian Porquet, Carolina Ruiz, Julian Valle, Felipe Rodriguez, Freddy Ruiz, thanks for being there in the difficult moments. Thanks to the UniAndes team Camilo Dominguez, Ernesto Rincon, Edison Maldonado and Ivan Bonilla for your true friendship.

---

<sup>1</sup> Agence de la transition écologique. "VERTPOM: Véritable énERgie du Territoire POSitif et Modulaire". Online: <https://www.ademe.fr/vertpom>



# CONTENTS

---

Acknowledgements . . . . .	v
Abbreviations . . . . .	xvii
Résumé substantiel . . . . .	xix
Extended Summary . . . . .	xli
General Introduction . . . . .	lxi
<b>I A NOVEL PLATFORM FOR SUPERVISION, ANALYSIS AND OPTIMIZATION OF POWER DISTRIBUTION SYSTEMS</b>	<b>1</b>
<b>1 INTRODUCTION TO CONDITION MONITORING SYSTEMS FOR POWER DISTRIBUTION GRIDS</b>	<b>3</b>
1.1 Introduction . . . . .	4
1.2 Condition monitoring for smart grids . . . . .	6
1.2.1 Fault diagnosis for power distribution grids . . . . .	7
1.2.1.1 Fault diagnosis methodology . . . . .	7
1.2.1.2 Feature extraction . . . . .	8
1.2.1.3 Diagnosis method . . . . .	9
1.3 Smart grid monitoring . . . . .	10
1.3.1 Electromagnetic transients simulation (EMT) . . . . .	13
1.3.2 Transient simulation analysis (TSA) . . . . .	13
1.3.3 Hybrid simulation (EMT and TSA) . . . . .	14
1.4 Real-time (RT) simulation . . . . .	14
1.4.1 Fully real-time digital simulator (DRTS) . . . . .	15
1.4.2 Hardware in the loop (HIL) simulator . . . . .	16
1.4.2.1 Control HIL (CHIL) simulator . . . . .	17
1.4.2.2 Power HIL (PHIL) simulator . . . . .	17
1.5 Experimental platforms for power distribution system analysis . . . . .	18
1.5.1 Consumption and generation forecast . . . . .	19
1.5.2 Cyber resilience . . . . .	19
1.5.3 Supervisory control and data acquisition . . . . .	19
1.5.4 RT capabilities . . . . .	20
1.6 Challenges of RT simulators for smart grids innovation . . . . .	20
1.6.1 RT simulation of large-scale power systems . . . . .	21
1.6.2 Accuracy of power electronics (PE) simulation . . . . .	22
1.6.3 Power distribution fault detection . . . . .	22
1.6.4 Demand side management (DSM) . . . . .	23
1.6.5 RT and intelligence requirements for business . . . . .	24
1.6.6 Artificial intelligence (AI) for smart distribution grids . . . . .	24
1.6.7 Security and privacy . . . . .	25
1.7 Chapter summary . . . . .	26
<b>2 DISTRIBUTION SYSTEM ANALYSIS USING THE BANK OF ENERGY</b>	<b>27</b>
2.1 Introduction . . . . .	28
2.2 The new Bank of Energy concept . . . . .	29



2.3	Hardware architecture of the experimental platform for real-time simulation . . .	31
2.3.1	Workstation peripherals . . . . .	31
2.3.2	Display for supervision, monitoring and visualization . . . . .	31
2.3.3	Hardware in the loop system emulators . . . . .	32
2.3.3.1	Grid emulators . . . . .	32
2.3.3.2	Electronic load emulators . . . . .	33
2.3.3.3	Electrical enclosure . . . . .	33
2.3.4	Equipment rack . . . . .	33
2.3.4.1	Workstation . . . . .	34
2.3.4.2	Data acquisition and data control device . . . . .	34
2.3.4.3	Data server . . . . .	35
2.3.4.4	Network switch . . . . .	35
2.3.4.5	Uninterruptible power supply (UPS) . . . . .	35
2.3.5	Intelligent electronic devices . . . . .	35
2.3.6	Remote control devices . . . . .	35
2.3.7	Workspace . . . . .	36
2.4	Software architecture of the experimental platform . . . . .	36
2.4.1	Event-driven architecture . . . . .	37
2.4.1.1	Graphic user interface . . . . .	38
2.4.1.1.1	User interaction . . . . .	40
2.4.1.1.2	Metering and reporting . . . . .	40
2.4.1.1.3	Heat mapping . . . . .	41
2.4.1.1.4	Simulation and equipment configuration . . . . .	42
2.4.1.2	Containerized applications . . . . .	42
2.4.1.3	Database . . . . .	43
2.4.2	API layer . . . . .	43
2.4.2.1	OpenDSS simulator . . . . .	44
2.4.2.2	Web service applications . . . . .	45
2.4.3	External devices connection . . . . .	46
2.5	Validation of the experimental platform concept . . . . .	46
2.5.1	Real case: Fault study analysis . . . . .	47
2.5.1.1	Case 1: Single phase short-circuit and overcurrent fault . . . . .	47
2.5.1.1.1	Causes of faults detected . . . . .	50
2.5.1.1.2	Possible corrective solution . . . . .	52
2.5.1.2	Case 2: Three-phase short-circuit . . . . .	52
2.5.2	Test case studies . . . . .	54
2.5.2.1	Speed test . . . . .	54
2.5.2.2	Performance of multiple simulations concurrently using the parallel processing features . . . . .	56
2.6	Advantages of using the Bank of Energy . . . . .	59
2.6.1	Fault analysis . . . . .	60
2.6.2	System reconfiguration . . . . .	60
2.6.3	Energy forecasting and operational planning . . . . .	60
2.6.4	Hosting capacity . . . . .	61
2.6.5	Battery energy installation and management . . . . .	61
2.6.6	Penetration of electric vehicles . . . . .	61
2.7	Chapter summary . . . . .	62

<b>II</b>	<b>A NOVEL METHODOLOGY TO INTEGRATE BATTERY ENERGY STORAGE SYSTEMS IN POWER DISTRIBUTION NETWORKS</b>	<b>63</b>
<b>3</b>	<b>BATTERY ENERGY STORAGE SYSTEM INTEGRATION IN POWER DISTRIBUTION SYSTEMS</b>	<b>65</b>
3.1	Introduction . . . . .	66
3.2	The power distribution system . . . . .	67
3.2.1	DERs in a power distribution system . . . . .	68
3.2.2	BESSs for an efficient power distribution system . . . . .	69
3.2.2.1	Power quality . . . . .	71
3.2.2.2	Voltage support and regulation . . . . .	72
3.2.2.3	Frequency control . . . . .	73
3.2.2.4	Peak shaving and load levelling . . . . .	73
3.2.2.5	Energy arbitrage . . . . .	74
3.2.2.6	Distribution upgrade deferral . . . . .	74
3.2.3	Impact of BESS on the power distribution system . . . . .	75
3.2.3.1	BESS placement and sizing in MV and LV systems . . . . .	77
3.3	BESS testing model . . . . .	77
3.3.1	OpenDSS storage element . . . . .	78
3.3.2	Storage element operation . . . . .	79
3.3.2.1	Charging state . . . . .	80
3.3.2.2	Discharging state . . . . .	81
3.3.2.3	Idling state . . . . .	82
3.3.3	Dispatch modes . . . . .	83
3.4	BESS placement and sizing background . . . . .	84
3.4.1	Optimal placement of BESSs in distribution systems . . . . .	85
3.4.1.1	Centralized BESS installation . . . . .	86
3.4.1.2	Decentralized BESS installation . . . . .	86
3.4.2	Optimal sizing of BESSs in distribution systems . . . . .	86
3.4.2.1	Financial criteria . . . . .	87
3.4.2.2	Technical criteria . . . . .	87
3.4.2.3	Hybrid criteria . . . . .	87
3.4.3	Methodologies for placement and sizing of BESSs . . . . .	88
3.4.3.1	Probabilistic methods . . . . .	88
3.4.3.2	Analytical methods . . . . .	91
3.4.3.3	Directed search-based methods . . . . .	93
3.4.3.3.1	Mathematical optimisation based methods . . . . .	93
3.4.3.3.2	Heuristic methods . . . . .	93
3.4.3.4	Hybrid techniques . . . . .	101
3.5	Chapter summary . . . . .	103
<b>4</b>	<b>METHODOLOGY FOR BESS PLACEMENT AND SIZING USING PARALLEL COMPUTING</b>	<b>105</b>
4.1	Introduction . . . . .	106
4.2	Diakoptics and the actor-oriented model concept . . . . .	107
4.2.1	Diakoptics for tearing networks . . . . .	107
4.2.2	Actor-oriented model . . . . .	108
4.2.3	Actor based diakoptics in OpenDSS . . . . .	109
4.2.3.1	Using the OpenDSS parallel processing suite . . . . .	110
4.2.3.2	Parallel computing communication between NI LabVIEW® and OpenDSS . . . . .	113

4.3	BESS installation based on A-Diakoptics framework . . . . .	117
4.3.1	Sensitivity analysis algorithm for BESS placement applying parallel computing . . . . .	119
4.3.1.1	Formulation of the parallel sensitivity analysis . . . . .	120
4.3.1.2	Test case study . . . . .	121
4.3.1.2.1	Sensitivity results . . . . .	122
4.3.1.2.2	Error validation . . . . .	122
4.3.1.3	Real test case: French distribution network . . . . .	123
4.3.1.3.1	Sensitivity results . . . . .	123
4.3.1.3.2	Interactive data visualization . . . . .	124
4.3.2	BESS sizing methodology for power distribution systems applying parallel computing . . . . .	125
4.3.2.1	Parallel genetic algorithm (PGA) . . . . .	125
4.3.2.1.1	PGA classes . . . . .	127
4.3.2.1.2	PGA implementation . . . . .	129
4.3.2.1.3	Single-core genetic algorithm . . . . .	132
4.3.2.2	Test case study . . . . .	133
4.3.2.2.1	Optimization results . . . . .	134
4.3.2.3	Real test case: A French distribution network . . . . .	134
4.3.2.3.1	Algorithm performance evaluation . . . . .	135
4.3.2.3.2	Case study I: Real test case system without a BESS installation . . . . .	135
4.3.2.3.3	Case study II: Centralized placement of BESS at the most sensitive bus for voltage profile improvement . . . . .	136
4.3.2.3.4	Case study III: Distributed placement of BESS at the most three sensitive buses for voltage profile improvement . . . . .	138
4.3.2.3.5	Case study IV: Centralized placement of BESS at the most sensitive bus for loss minimization . . . . .	139
4.3.2.3.6	Case study V: Distributed placement of BESS at the most three sensitive buses for loss minimization . . . . .	140
4.3.2.3.7	Results analysis . . . . .	142
4.4	Other future applications . . . . .	145
4.5	Chapter summary . . . . .	147
	General Conclusions and Prospects . . . . .	149

**III APPENDIX AND COMPLEMENTARY MATERIAL** 151

A	POWER DISTRIBUTION SYSTEM OF GAZELEC OF PERONNE	153
A.1	Distribution system description . . . . .	153
A.2	Renewable energy production . . . . .	154
A.3	Electrical model in OpenDSS . . . . .	156
A.4	Radial distribution description . . . . .	160
B	POWER DISTRIBUTION TEST FEEDERS	165
B.1	The IEEE 8500 node test feeder . . . . .	165
B.2	The IEEE European test feeder . . . . .	166
B.3	Non- IEEE test cases . . . . .	167
B.3.1	EPRI test circuits . . . . .	167
B.3.2	Iowa distribution test systems . . . . .	169

BIBLIOGRAPHY . . . . . 173  
Publications . . . . . 187

## LIST OF FIGURES

---

Figure 1.1	AMI, ADA, and EMS architecture through a smart distribution system . . . . .	4
Figure 1.2	Monitoring enhancement for the distribution system landscape . . . . .	5
Figure 1.3	RT decision-making tool key elements . . . . .	6
Figure 1.4	Smart grid monitoring at various stages of development . . . . .	6
Figure 1.5	General fault diagnosis . . . . .	8
Figure 1.6	Fault diagnosis methods classification . . . . .	10
Figure 1.7	Condition monitoring applied to power distribution systems . . . . .	11
Figure 1.8	Overview of time ranges of power system dynamics . . . . .	13
Figure 1.9	Evolution of high-accurate simulators . . . . .	15
Figure 1.10	RT power system simulation categories . . . . .	16
Figure 1.11	HIL simulator architecture . . . . .	17
Figure 1.12	RT smart grid innovation necessity . . . . .	21
Figure 1.13	Actual situational challenges . . . . .	21
Figure 2.1	Grid computational paradigm . . . . .	28
Figure 2.2	Block diagram of the software/hardware implementation of the experimental platform . . . . .	30
Figure 2.3	General hardware structure of the experimental platform . . . . .	31
Figure 2.4	GE & EL internal power architecture . . . . .	32
Figure 2.5	GE & EL emulator power supply protection and wiring diagram . . . . .	33
Figure 2.6	Internal arrangement of the equipment rack . . . . .	34
Figure 2.7	General view of the experimental platform workspace . . . . .	36
Figure 2.8	General software structure of the experimental platform . . . . .	37
Figure 2.9	Event-driven model . . . . .	38
Figure 2.10	Event-driven model . . . . .	39
Figure 2.11	Human machine interface of the experimental platform . . . . .	40
Figure 2.12	Pop-up windows . . . . .	41
Figure 2.13	Producer/consumer architecture . . . . .	41
Figure 2.14	Heat mapping painting . . . . .	42
Figure 2.15	Containerized applications in the experimental platform . . . . .	43
Figure 2.16	Topology of the microservices architecture . . . . .	44
Figure 2.17	Client-server architecture for restful applications . . . . .	45
Figure 2.18	Master-slave architecture for external devices . . . . .	46
Figure 2.19	Normal state of GoP distribution system . . . . .	47
Figure 2.20	One-day voltage data set from CT-IBox meters . . . . .	48
Figure 2.21	Fault clearing procedure detected by the CT-IBox meters . . . . .	49
Figure 2.22	Single-phase short-circuit in the line 78 . . . . .	49
Figure 2.23	Timeline of the single-phase short-circuit case study . . . . .	50
Figure 2.24	Blackout due to a three-phase short-circuit . . . . .	51
Figure 2.25	GoP system before the overcurrent . . . . .	51
Figure 2.26	New reconfiguration suggested . . . . .	52
Figure 2.27	Three-phase short-circuit in the Gens du voyage transformer . . . . .	53
Figure 2.28	Timeline of the second fault case study . . . . .	53

Figure 2.29	Average calculation time based on the number of electrical nodes of the simulated system . . . . .	56
Figure 2.30	CPU utilization under speed test . . . . .	56
Figure 2.31	Calculation time based on the number of nodes of the simulated systems and cores of the processor . . . . .	58
Figure 2.32	Parallel simulation execution of the Ckt24 test feeder . . . . .	59
Figure 2.33	Overhead produced in the CPU during the Ckt24 test feeder execution . . . . .	59
Figure 3.1	Power systems have more technologies and locations to the DERs . . . . .	66
Figure 3.2	Constraints through the whole life-cycle of the distribution grid system . . . . .	68
Figure 3.3	Impacts of DER penetration on grid operation . . . . .	69
Figure 3.4	Services provided by BESS according to the time scale . . . . .	71
Figure 3.5	Peak load shaving using BESS . . . . .	74
Figure 3.6	LV problems caused by a BESS installation . . . . .	76
Figure 3.7	BESS generic architecture and controls . . . . .	78
Figure 3.8	General model of the storage element in OpenDSS . . . . .	79
Figure 3.9	Internal power flow of the storage element during the charging state in OpenDSS . . . . .	80
Figure 3.10	Internal power flow of the storage element during the discharging state in OpenDSS . . . . .	82
Figure 3.11	Internal power flow of the storage element during the idling state in OpenDSS . . . . .	83
Figure 3.12	Objectives of BESS sizing . . . . .	87
Figure 3.13	Methodologies for BESS placement & sizing . . . . .	88
Figure 3.14	General placement and sizing algorithm . . . . .	89
Figure 3.15	Flowchart of probabilistic methods . . . . .	90
Figure 3.16	Flowchart of analytical methods . . . . .	92
Figure 3.17	Flowchart of direct search-based methods . . . . .	93
Figure 3.18	Crossover GA operator: Single-point . . . . .	98
Figure 3.19	Mutation GA operators . . . . .	98
Figure 3.20	Schematic representation of the motion of a particle in PSO . . . . .	101
Figure 4.1	Power system decomposition in primitive subsystems . . . . .	108
Figure 4.2	Actor-oriented specification of an application . . . . .	109
Figure 4.3	A-Diakoptics algorithm in OpenDSS . . . . .	110
Figure 4.4	Operational architecture for A-Diakoptics algorithm in OpenDSS . . . . .	111
Figure 4.5	Event-base state machine design pattern . . . . .	113
Figure 4.6	Event-Base State Machine structure . . . . .	114
Figure 4.7	Functional Event-Base State Machine using NI LabVIEW . . . . .	114
Figure 4.8	OpenDSS-PM parallel computing example. Actor's initialization . . . . .	115
Figure 4.9	OpenDSS-PM parallel computing example. Actor's definition . . . . .	115
Figure 4.10	OpenDSS-PM parallel computing example. Actor's configuration . . . . .	116
Figure 4.11	OpenDSS-PM parallel computing example. Simulation execution . . . . .	116
Figure 4.12	OpenDSS-PM parallel computing example. Actor's progress status . . . . .	116
Figure 4.13	OpenDSS-PM parallel computing example. Actor's statistics . . . . .	117
Figure 4.14	A flow chart of the novel placement and sizing BESS methodology . . . . .	118
Figure 4.15	Parallel computing methodology for the integration of the sensitivity analysis and the genetic algorithm . . . . .	119
Figure 4.16	A flow chart of a novel sensitivity analysis with using computing . . . . .	121
Figure 4.17	Test network topology . . . . .	121

Figure 4.18	Sensitivity calculation in Gazelec distribution system . . . . .	123
Figure 4.19	Sensitivity calculation results . . . . .	124
Figure 4.20	Sensitivity heat map visualization result in the Bank of Energy experi- mental platform marking the three most sensible buses. . . . .	125
Figure 4.21	Parallel genetic algorithm . . . . .	126
Figure 4.22	Master-Slave model . . . . .	127
Figure 4.23	Coarse-grained parallel model . . . . .	128
Figure 4.24	Fine-grained parallel model . . . . .	128
Figure 4.25	Sequence diagram of master-slave PGA . . . . .	129
Figure 4.26	Flowchart of the single-core GA model . . . . .	133
Figure 4.27	Voltage profile of GoP distribution system . . . . .	136
Figure 4.28	Voltage profile with a centralized BESS for voltage improvement . . . . .	137
Figure 4.29	Voltage profile with decentralized BESSs for voltage improvement . . . . .	139
Figure 4.30	Voltage profile with a centralized BESS for loss minimization . . . . .	140
Figure 4.31	Voltage profile with decentralized BESSs for loss minimization . . . . .	142
Figure 4.32	Speedup factor calculated to evaluate the PGA performance . . . . .	143
Figure 4.33	User data visualization panel of the toolkit developed . . . . .	146
Figure A.1	Gazelec of Peronne distribution feeder map . . . . .	153
Figure A.2	Load profile curve extrapolated of the city for 2019 . . . . .	154
Figure A.3	Wind farm 1 power production for 2017 . . . . .	155
Figure A.4	Wind farm 2 power production for 2017 . . . . .	155
Figure A.5	GoP distribution network modeled in the experimental platform . . . . .	156
Figure A.6	Tape shielded cable geometric properties . . . . .	157
Figure A.7	Load profile extrapolation for each zone . . . . .	157
Figure A.8	Load profile consumption from transformers in the pilot site database . . . . .	158
Figure A.8	(Continued) Load profile consumption from transformers in the pilot site database . . . . .	159
Figure A.9	Load profile for transformers with CT-Ibox installed . . . . .	160
Figure A.10	Radial GoP distribution system diagram . . . . .	161
Figure B.1	One-line diagram of the 8500 node test system . . . . .	165
Figure B.2	Load profile curve of the 8500 node test system . . . . .	166
Figure B.3	One-line diagram of the IEEE European test system . . . . .	166
Figure B.4	Load profile curve of the IEEE European test system . . . . .	167
Figure B.5	One-line diagram of the EPRI test circuits . . . . .	168
Figure B.6	Load profile curve of the EPRI test circuits . . . . .	169
Figure B.7	One-line diagram of the Iowa State University test system . . . . .	170
Figure B.8	Load profile curve of the Iowa State University test system . . . . .	170
Figure B.8	Load profile curve of the Iowa State University test system . . . . .	171
Figure B.9	Total load profile curve of the Iowa State University test system . . . . .	171

## LIST OF TABLES

---

Table 1.1	Terminology used in fault diagnosis. . . . .	7
Table 1.2	Comparison between feature extraction methods. . . . .	9
Table 1.3	Fields to apply smart grid monitoring. . . . .	12
Table 1.4	Summary of salient features of real-time simulators reported in the literature . . . . .	18
Table 2.1	Summary of the test circuits integrated in the experimental platform (1). . . . .	54
Table 2.2	Summary of the test circuits integrated in the experimental platform (2). . . . .	55
Table 2.3	Speed test results using one core. . . . .	55
Table 2.4	Yearly simulation of the test feeders using single and multi-core processing. . . . .	57
Table 3.1	Distribution grid-related BESS Applications . . . . .	70
Table 3.2	Technical considerations for some grid applications of battery energy storage systems. . . . .	71
Table 3.3	Summary of relevant differences between MV and LV systems . . . . .	77
Table 3.4	Dispatch modes of the storage element available in OpenDSS . . . . .	84
Table 3.5	Summary of BESS sizing techniques . . . . .	102
Table 4.1	Sensitive results for the test case system. . . . .	122
Table 4.2	Error statistics for the sensibility test case between the algorithm developed and the reference set. . . . .	122
Table 4.3	Solution time for selected test case. . . . .	122
Table 4.4	Voltage sensitive indices of the most sensitive buses. . . . .	124
Table 4.5	Validation results of the optimization problem using the test case study. . . . .	134
Table 4.6	Architecture description of the GA tested. . . . .	135
Table 4.7	Power flow results for the real test case study without a BESS. . . . .	136
Table 4.8	Power flow results for a centralized BESS in the case study II. . . . .	137
Table 4.9	GA performance in the case study II. . . . .	138
Table 4.10	Power flow results for distributed BESS in the case study III. . . . .	138
Table 4.11	GA performance in the case study III. . . . .	139
Table 4.12	Power flow results for a centralized BESS in the case study IV. . . . .	140
Table 4.13	GA performance in the case study IV. . . . .	141
Table 4.14	Power flow results for distributed BESS in the case study V. . . . .	141
Table 4.15	GA performance in the case study V. . . . .	142
Table 4.16	Optimal BESS sizing results with a charging installation. . . . .	144
Table 4.17	Optimal BESS sizing results with a discharging installation. . . . .	144
Table A.1	Synthesis description of the distribution network of the city. . . . .	155
Table A.2	Generators. . . . .	161
Table A.3	Lines characteristics. . . . .	162
Table A.4	Transformer characteristics. . . . .	163
Table A.5	(Continued) Transformer characteristics. . . . .	164
Table A.6	Type line properties description. . . . .	164
Table A.7	Type line geometric properties description. . . . .	164
Table B.1	Summary of EPRI Test Circuits. . . . .	168



## LISTINGS

---

Listing 1	Perturb-and-Observe algorithm for sensitivity generation . . . . .	97
Listing 2	Pseudo code of GA algorithm . . . . .	99
Listing 3	Pseudo code of PSO algorithm . . . . .	100

## ABBREVIATIONS

---

ADA	Advanced Distribution Automation
AMI	Advanced Metering Infrastructure
BESS	Battery Energy Storage Systems
DER	Distributed Energy Resources
DG	Distributed Generation
DRTS	Digital Real-Time Simulation
DS	Distributed Storage
DSO	Distribution System Operator
EL	Electronic Load
EMS	Energy Management System
EMT	Electromagnetic Transients Simulation
ESS	Energy Management System
GA	Genetic Algorithm
GE	Grid Emulator
GoP	Gazelec of Peronne
HIL	Hardware In The Loop
IED	Intelligent Electronic Device
PGA	Parallel Genetic Algorithm
PM	Parallel Machine
QSTS	Quasi Static Time Series
RT	Real-Time
VI	Virtual Instrument



## RÉSUMÉ SUBSTANTIEL

---

### LE PROJET VERTPOM

#### *Contexte*

Dans un territoire en pleine mutation, les réseaux d'énergie doivent être de plus en plus réactifs et flexibles. Passer de la maîtrise de l'Énergie à l'efficacité énergétique, créer de nouveaux modèles de gestion multi fluide et de production d'énergie est une nécessité régionale, nationale et internationale.

Le projet VERTPOM® (ADEME, 2018b) est porté par un consortium qui développera et déploiera un outil d'aide à la décision VERTPOM-BANK® appelé Banque de l'Énergie qui aura comme objectif de maintenir un bilan optimisé entre l'énergie disponible issue de la production (conventionnelle et ENR) au regard des utilisations (consommations et pertes techniques), en liaison avec des moyens de stockage d'énergie. Avec cet outil, le but est d'aider un territoire au travers des GRD/ELD, à devenir moins dépendant des énergies traditionnelles (fossiles et fissiles) et prétendre à terme à devenir à énergie positive.

La Banque de l'Énergie sera articulée autour d'algorithmes de prédiction des niveaux de production d'énergie renouvelable, des consommations et des pertes techniques sur les différents systèmes de distribution. Ces algorithmes exploiteront une base commune de données où l'utilisation de l'intelligence artificielle sera privilégiée. En amont, le bilan d'énergie (positif ou négatif) du territoire sera évalué. Puis les outils de la Banque de l'Énergie seront utilisés pour étudier tous les scénarii possibles permettant d'améliorer le bilan production/consommation d'énergie, tout en identifiant les énergies renouvelables propres au territoire en y associant des moyens de stockage pour une utilisation optimale de ces dernières.

#### *Objectifs généraux du projet VERTPOM*

Le projet VERTPOM a pour finalité la création scientifique et technologique tant sur le plan environnemental que sociétal grâce à la création de la Banque de l'Énergie : VERTPOM BANK®. Le Territoire des Hauts de France, avec son parc éolien en Picardie et ses laboratoires spécialisés de l'Université de Picardie Jules Verne, se trouve au carrefour de ces enjeux, et, représente le cadre propice pour devenir un territoire à énergie positive produisant plus d'Énergie qu'il n'en consomme.

La Banque de l'Énergie est un outil basé sur une approche technico-financière pour la gestion énergétique efficace d'un territoire. De ce fait, la constitution de cet outil doit s'appuyer sur une connaissance représentative de la consommation énergétique, des moyens de distribution et des ressources énergétiques disponibles du territoire. Cette base d'informations est néces-

saire pour définir avec certitude le processus conduisant à terme à la gestion d'un territoire à énergie positive.

Développer la Banque de l'Énergie, un outil informatique d'arbitrage énergétique entre les énergies renouvelables ENR et énergies conventionnelles à partir d'une base de données intelligente, qui fonctionne dans un système informatique associé, sécurisé, capable d'optimiser les consommations et productions d'énergie locales en quasi temps réel, est l'objectif de ce projet ambitieux.

La Banque de l'Énergie est le « Chef d'Orchestre » qui corrèle l'ensemble des données permettant une gestion intelligente prédictive des énergies et fluides (multi-énergies et multi-fluide). À partir de la puissance installée conventionnelle et renouvelable disponible et de la consommation énergétique du territoire dans l'année, il s'agit de déterminer les différents scénarios qui transformeraient le territoire en territoire à énergie positive ou neutre dans le pire des cas, tout en identifiant le déficit ou l'excédent des énergies renouvelables par rapport à la consommation énergétique du territoire.

Les réseaux énergétiques doivent être plus réactifs, flexibles, et ainsi favoriser les interactions entre les acteurs du marché. La banque de l'énergie contribuera à ces objectifs en proposant différentes fonctionnalités :

- Recueillir les données sur les réseaux grâce à des capteurs et dispositifs contrôlables à distance (compteurs communicants multi fluides, capteurs).
- Analyser dans un délai rapide l'état du réseau d'électricité.
- Anticiper la production locale à partir des ENR et du stockage de l'énergie.
- Permettre le développement de services de maîtrise de l'énergie (MDE): en fournissant de l'information sur les consommations d'énergie et en permettant la gestion des usages.
- Optimiser la pointe de consommation et interagir intelligemment avec le consommateur final (consomm'acteur).
- Permettre le déploiement de nouveaux services.
- Contribuer à la mise en œuvre et au contrôle de nouvelles flexibilités : stockage, programmes de gestion de la pointe, gestion des puissances (production et demande), tarifs dynamiques, etc.
- Donner de l'information aux clients, fournisseurs et autres acteurs du marché et assurer la sûreté et la stabilité du réseau.

### *Objectifs de cette thèse*

Sur la base des informations transmises par des compteurs communicants et des capteurs supplémentaires qui seront installés sur différents points d'alimentation et de consommation d'électricité, il s'agit de développer pour ce sujet de thèse intitulé : "Supervision, analyse et optimisation des réseaux de distribution électrique avec intégration d'énergies renouvelables et des moyens de stockage d'énergie", un système de supervision et de diagnostic des réseaux de distribution d'électricité, afin d'améliorer la qualité de fourniture. Des algorithmes d'analyse sont à développer pour avoir une image globale des conditions de fonctionnement.

Le système proposé dans ce sujet de thèse sera validé sur un banc de test à échelle réduite avant sa validation à échelle réelle sur le réseau de distribution de la ville. Ce banc de test est à réaliser dans le cadre de cette thèse, dans le laboratoire LTI et plus particulièrement dans les locaux de l'équipe EESA.

Par ailleurs, aider à l'introduction des unités de stockage d'énergie participant de manière active à la gestion énergétique et à la supervision de la qualité du réseau électrique du territoire est l'un des objectifs majeurs de ce travail.

### SOMMAIRE DE LA THÈSE

#### *Chapitre I*

Dans ce chapitre sont examinés l'ensemble de technologies de pointe qui permettent la surveillance d'état des réseaux de distribution électrique. Actuellement, des efforts considérables sont développés pour contribuer à la modernisation de ces derniers, mais dans la plupart des cas, leur complexité croissante est devenue le thème principal des systèmes de surveillance où même les méthodes de diagnostic ne sont pas les plus appropriées pour évaluer le comportement de ce système en pleine évolution.

Dans ce contexte, la disponibilité permanente des données nécessite une analyse précise, afin de s'orienter dans la recherche du système de surveillance le plus adéquat pour les réseaux électriques de distribution. Donc, la solution réalisable est celle qui consiste à utiliser la surveillance en temps réel, avec un haut débit et des moyens de stockage des données, pour suivre de près les variations des paramètres de fonctionnement et l'état de santé de ce système, de manière à déterminer à tout instant les actions les plus appropriées pour sa gestion (Qiao and Lu, 2015).

La conception d'un réseau électrique intelligent nécessite l'utilisation d'équipements largement répandus, tous associés à un système de surveillance capable de les observer en permanence. A ce propos, il est important d'introduire dans ce réseau électrique, un système des

compteurs intelligents avec communication bidirectionnelle, de même qu'un système intelligent de contrôle, afin de mieux manager la production et la consommation d'énergie. De cette manière, une solution est de réaliser premièrement un projet du processus d'analyse chargé d'évaluer l'état du système électrique dans des conditions réelles, en y incluant les méthodologies de conception et d'optimisation pour déterminer l'état de fonctionnement de chaque élément du réseau électrique et du système en général (Figure 1). Néanmoins, l'expérimentation sur un réseau électrique réel est extrêmement limitée et dans certains cas, irréalisables à cause des conditions nécessaires pour sa mise en place (taille et complexité du réseau de distribution).

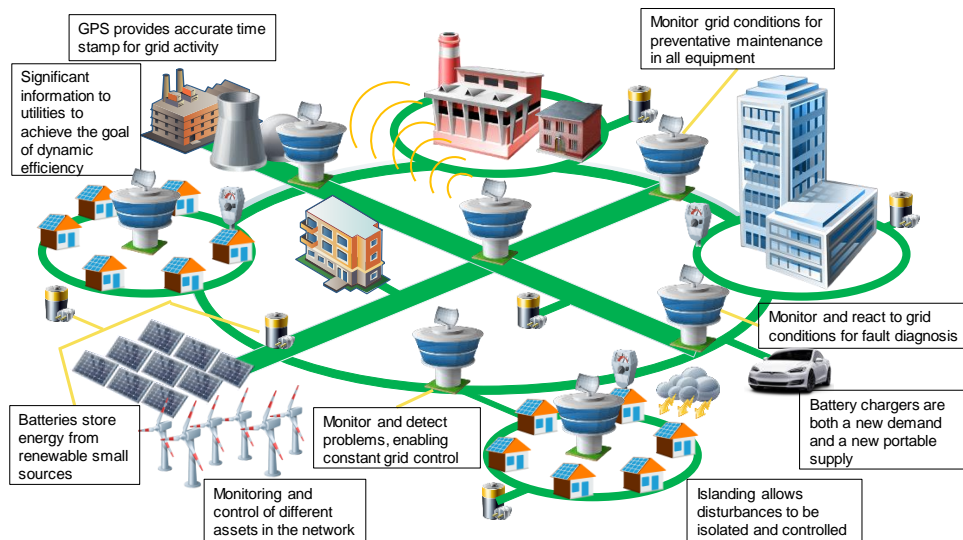


Figure 1: Augmentation de la surveillance dans le panorama actuel des réseaux de distribution d'électricité.

C'est pour cela que l'utilisation des outils de modélisation et de simulation numérique du comportement électromagnétique des composants d'un réseau électrique à grande échelle, représentent une alternative intéressante pour évaluer leur comportement, tout en estimant l'impact relatif aux différentes conditions d'intervention ou de contrôle sur le système lui-même (Borlase, 2018). De plus, l'utilisation d'une architecture de surveillance temps réel, pourrait constituer à terme une norme de gestion du réseau de distribution pour le faire évoluer vers un réseau électrique intelligent, en tenant compte de considération comme le diagnostic de défauts, l'analyse de contingences, la supervision et l'optimisation de l'utilisation des différents éléments qui le constituent, la sûreté de fonctionnement des composants critiques, les informations d'importance pour les fournisseurs d'électricité afin de garantir la meilleure efficacité dynamique, les questions de la qualité de l'énergie, etc. (Martinez, Henao, and Capolino, 2019). En conséquence, le développement d'une plateforme décisionnelle pour l'opérateur du système électrique de distribution est essentiel, pour assurer de manière appropriée la surveillance des conditions de fonctionnement et intégrer les décisions d'un système automatique de gestion d'énergie (Jalili-Marandi and Dinavahi, 2009).

A présent, il y a un large marché en croissance pour introduire les outils de modélisation, simulation et contrôle des systèmes en temps réel dans l'industrie. Pour cette raison, leur utilisation nécessite des modèles précis de représentation des phénomènes physiques mis en jeu, des données en temps réel des conditions de fonctionnement sur le terrain, des algorithmes de calcul et du matériel informatique de pointe, pour une exécution dans des délais

raisonnables (Ilamparithi, Abourdia, and Kirk, 2016). Mais, il s'avère que la littérature récente dans le domaine des réseaux électriques de distribution, montre que les outils temps réel de modélisation et simulation n'atteignent pas l'efficacité informatique nécessaires pour la gestion des conditions de fonctionnement de ce type de système, ce qui peut conduire à des retards inadmissibles dans la réponse pour des situations critiques.

Dans la plupart des cas observés, les plateformes décisionnelles expérimentales relatives aux réseaux électriques de distribution sont limitées à cause de différentes restrictions, comme le prix excessif d'achat ou l'obligation d'achat de licences supplémentaires pour activer toutes les options, mis à part le fait que les options proposées, ne répondent pas toujours aux besoins des opérateurs et que leur efficacité informatique pour le traitement des données en temps réel ne réunit pas les conditions pour une utilisation efficace. Dans ces conditions, il est fondamental le développement d'un nouveau type de plateforme décisionnelle expérimentale, en considérant les caractéristiques temporelles de la dynamique des phénomènes électromagnétiques traités. A cette fin, les outils d'analyse temps réel les plus adaptés sont ceux du type hybride, où les conditions d'haute-fidélité des signaux analogiques électriques donnant une image des différents éléments associés au réseau électrique en question, seront associées à celles provenant du modèle du réseau lui-même reproduit de manière discrète dans le temps utilisant un système numérique (Guillaud et al., 2015).

L'évaluation dynamique du comportement électromagnétique d'un réseau électrique de taille réelle dans ces conditions, requiers précision et vitesse d'exécution. Ces exigences sont essentielles pour la formulation du système de surveillance temps réel, de la future architecture d'automatisation d'un réseau électrique de distribution (Noureen, Roy, and Bayne, 2017). Ce système de surveillance doit permettre une évaluation précise du réseau de distribution électrique lui-même en temps réel, pour alimenter en informations le pilotage automatique et la supervision de l'ensemble de composants associés. La qualité d'exécution de ce système peut varier en fonction de la technologie utilisée et des de la configuration du réseau étudié et des application envisagées.

Les outils d'analyse temps réel sont classifiés en 4 principales catégories (Figure 2) : 1. Entièrement numérique ; 2. Les signaux d'entrée et de sortie réels d'un dispositif électrique sont associées à un système numérique ; 3. Le système de contrôle réel d'un dispositif électrique est associé à un système numérique ; 4. Le dispositif électrique associé à un système numérique, produit un transfert de puissance électrique sur un autre dispositif électrique. Ces technologies représentent une solution rentable pour évaluation de méthodes de gestion de réseaux électriques intelligents, couvrant même les aspects relatifs au contrôle de l'ensemble et aux dispositifs de protection, de manière fonctionnelle et robuste (Ibarra et al., 2017).

Les défis des outils d'analyse temps réel pour les réseaux électriques intelligents sont de plus en plus sélectifs. Dans ce sens, l'industrie exige des outils d'analyse temps réel à chaque fois plus puissants pour faire face à leur complexité croissante et à l'intégration des nouvelles technologies d'utilisation de l'électricité qui changent les modèles et les profils de consommation. Ces dernières conditions introduisent en particulier des nouvelles dynamiques dans le réseau électrique de distribution, qui représentent également des nouveaux challenges pour les gestionnaires des réseaux de distribution. La gestion et utilisation optimale de ce système électrique pour continuer à réunir toutes les conditions d'une fourniture de qualité, en présence de nouvelles contraintes et à venir, constituent des défis inattendus, spécialement pour le développement des nouvelles techniques d'évaluation, lesquelles devront incorporer





électrique et les algorithmes de prédictions du comportement production - consommation d'énergie. Dans ces conditions, plusieurs scénarios sont déployés pour déterminer les décisions d'opération les plus appropriées pour l'obtention d'un bilan énergétique production-consommation positif ou au mois nul, tout en considérant la production d'énergie d'origine renouvelable locale, la minimisation des pertes techniques, ainsi que la maîtrise de l'énergie au niveau des consommateurs. Cette vision énergétique d'un territoire, ouvre les possibilités de gestion d'un réseau électrique de distribution, du point de vue de son efficacité avec une perspective technico-financière. Cette efficacité dans la gestion doit intégrer de manière optimale, le prix d'achat de l'énergie, son stockage qui est essentiel dans cette démarche, ainsi que la production locale d'énergie d'origine renouvelable. Cette optimisation est formulée sous forme de modèle mathématique, pour atteindre les différents critères opérationnels et de gestion définis par l'opérateur du réseau en question.

Pour développer le concept de Banque de l'Energie, une plateforme décisionnelle expérimentale est planifiée comme point de départ de cette démarche. Cette plateforme décisionnelle a pour objectif d'intégrer les éléments caractéristiques et principaux de ce type d'outils d'analyse, pour résoudre les besoins immédiats ainsi que les planifiés d'un réseau de distribution électrique (Figure 3). Cette plateforme est conçue sur la base d'une architecture modulaire afin d'optimiser ses caractéristiques d'exécution tant du point de vue matériel que logiciel. La communication entre les différents éléments matériels peut être programmée par différents canaux de communication, de manière à assurer la scalabilité et la flexibilité de la solution proposée. En plus, cette plateforme possède une base de données sécurisée qui permet le stockage de toutes les statistiques sur la consommation et sur la disponibilité d'énergie électrique dans le territoire. Ces conditions permettent le développement de nouvelles méthodologies de gestion des réseaux électriques intelligents avec un large éventail de choix, en partant d'analyses statiques ou dynamiques exécutées hors ligne ou en ligne pour le temps réel et en considérant une flexibilité dans le choix de fenêtres temporelles d'analyse pour l'évaluation dans toute la gamme des phénomènes transitoires d'un tel système.

L'architecture matérielle de cette plateforme est montrée sur la Figure 4. Elle est basée sur une structure évolutive multi-terminal et multi-plateforme, permettant la communication à distance et distribuée avec différents modules. Cette architecture est constituée des éléments suivants :

- **Les périphériques du poste de travail** : Eléments qui assurent un espace de travail pour l'opérateur pour interagir avec la plateforme.
- **Ecran de visualisation pour la supervision et la surveillance** : Cet écran principal représente l'interface homme-machine de la plateforme.
- **Emulateurs temps réel** : Ces émulateurs permettent une évaluation réaliste en laboratoire de la plupart d'applications de tests dans le domaine des réseaux électriques intelligents, comme l'injection des énergies renouvelables, les bornes de recharge des véhicules électriques, les systèmes de stockage d'énergie, les défauts électriques sur les lignes de distribution, etc..
- **Poste de travail** : Cet élément représente le cerveau de la plateforme. Il contient l'application principale, les modules et les algorithmes avec lesquels les analyses numériques sont réalisées et interfacées avec les composants matériels et logiciels externes.

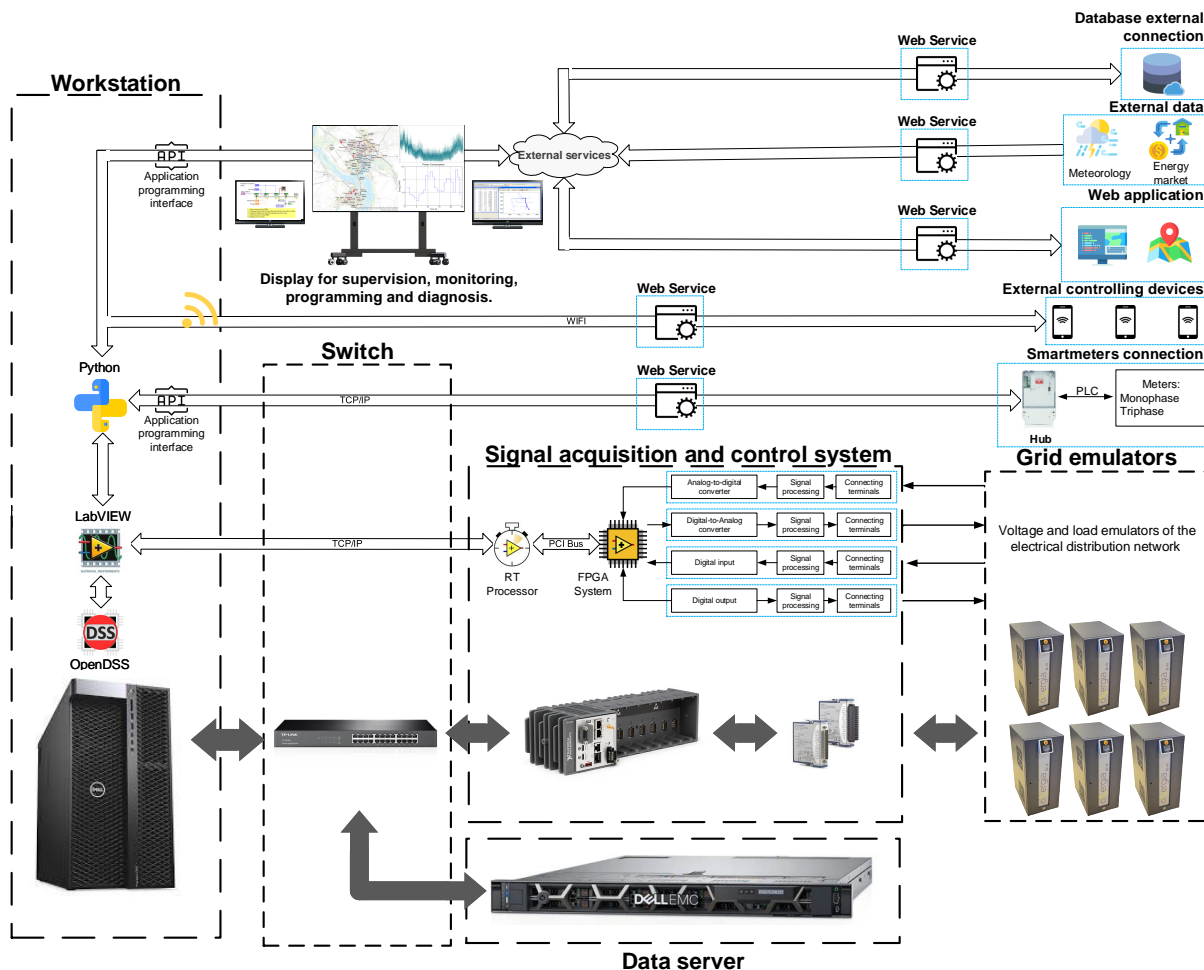


Figure 3: Schéma-bloc d'implémentation du concept Banque de l'Énergie.

- **Acquisition de données et dispositif de contrôle des données :** Cette unité est en charge du contrôle et de la gestion des signaux analogiques et numériques utilisés pour développer une analyse en temps réel.
- **Serveur des données :** Toutes les données collectées dans la plateforme sont stockées dans ce serveur.
- **Dispositifs électroniques intelligents :** Ces dispositifs sont principalement représentés par les compteurs intelligents et les concentrateurs des données associés, installés sur le terrain ou en laboratoire.
- **Dispositifs de contrôle à distance :** Ce type de dispositif est intégrée à la plateforme pour exécuter à distance certaines tâches de simulation numérique.

L'architecture logicielle de cette plateforme est le composant le plus important pour le développement réussi de l'application logicielle dans son ensemble du projet VERTPOM®, appelée VERTPOM BANK®. Ce style d'architecture est mis en place à plusieurs niveaux modulaires de manière à exécuter efficacement toutes les fonctionnalités disponibles dans la plateforme. Ce type de construction permet l'intégration de nouvelles fonctionnalités à n'importe quel

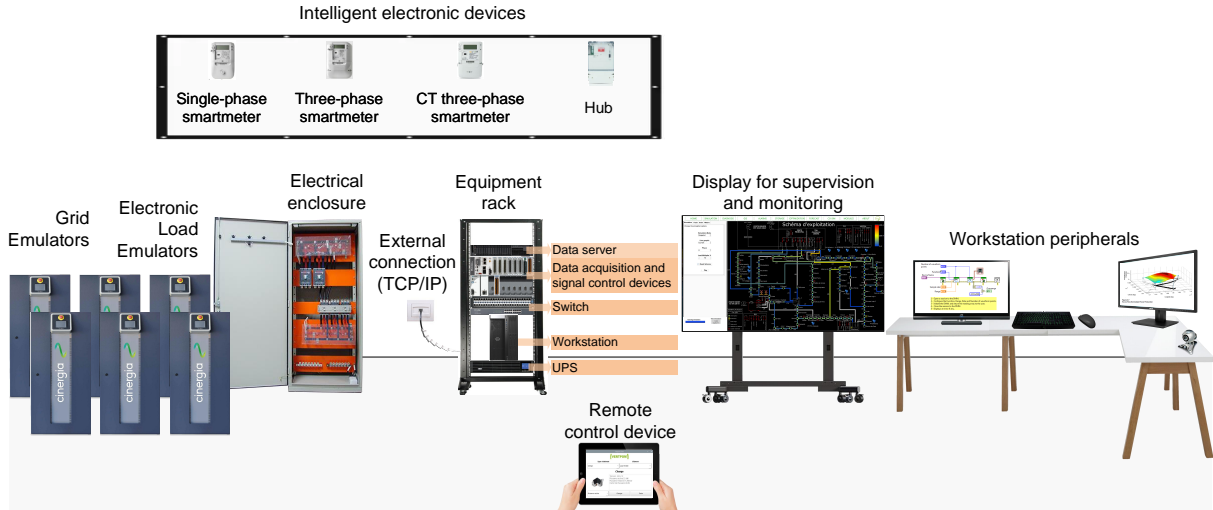


Figure 4: Structure matérielle générale du Banc d'Expérimentation VERTPOM®.

niveau en accord avec leur propre structure. Cette architecture logicielle est présentée sur la Figure 5.

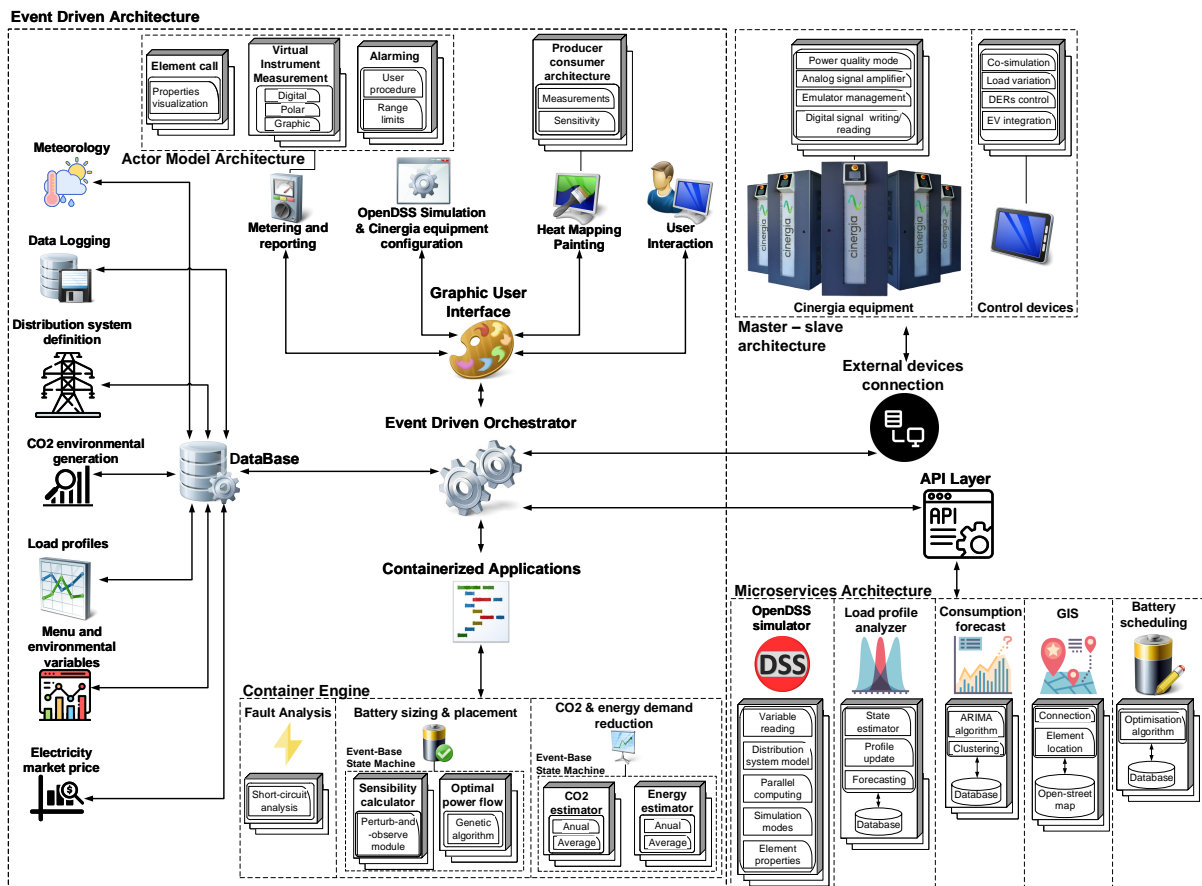


Figure 5: Structure logicielle générale du Banc d'Expérimentation VERTPOM®.

Les styles utilisés respectent les caractéristiques architecturales, les décisions architecturales et les principes de construction nécessaires pour définir la structure appropriée du système logiciel proposé. Les caractéristiques architecturales sont basées dans la définition de critères

de succès de manière à ce que le système fonctionne correctement. Ces critères de succès sont soutenus par des considérations opérationnelles et structurelles telles que la qualité d'exécution, la fiabilité, la scalabilité, la portabilité, l'évolutivité, la sécurité informatique, etc.. Les décisions architecturales fixent les règles de comment les styles architecturaux utilisés vont interagir entre eux. Finalement, les principes de construction sont les consignes suivies dans les techniques de programmation dans la mise en œuvre logicielle.

Pour l'évaluation de la précision et de la qualité d'exécution du Banc d'Expérimentation VERTPOM®, un cas réel et plusieurs cas de test ont été étudiés. Pour le cas d'étude réel, il s'agit d'émuler les incidents déclarés dans le réseau de distribution d'électricité réel de la ville, à l'occasion de plusieurs défaillances constatées par les opérateurs du système. Ce cas permet en particulier d'évaluer la précision de cette plateforme décisionnelle par rapport aux incidents déclarés. Les cas de test effectués correspondent à plusieurs scénarios de validation de manière à tester et évaluer les performances temporelles d'exécution de la plateforme, dans des conditions de calcul obtenues avec un traitement de données en parallèle.

Ces plusieurs cas d'évaluation du Banc d'Expérimentation VERTPOM® ont permis de démontrer, que l'architecture matérielle et logicielle choisie pour cette plateforme, suffit largement pour la supervision et l'analyse en temps réel des systèmes électriques de distribution de taille réelle. Cette plateforme est conçue pour être installée dans un centre de recherche ou dans un laboratoire ou centre de contrôle de la distribution d'un réseau électrique intelligent. Dans le contexte informatique actuel, l'utilisation d'une architecture de distribution libre du grand public avec une infrastructure modulaire, facilitent pour VERTPOM BANK®, la diffusion des contrats de licence, son installation et sa mise en service.

### *Chapitre III*

La haute pénétration dans la production d'énergie électrique d'origine renouvelable dans les réseaux de distribution électrique et spécialement du secteur éolien, a évolué de manière très substantielle ces dernières années. Pour garantir une intégration convenable et une utilisation optimale localement dans le territoire où elles sont captées, l'installation de systèmes de stockage d'énergie devient une exigence pour contribuer à la transition énergétique. De ce fait, ces dispositifs attirent énormément l'attention ces dernières années également. Le principe de fonctionnement de ce système est basé sur la conversion à haut rendement de l'énergie électrique provenant du réseau électrique, en une forme d'énergie stockable, laquelle est utilisée ensuite en cas de besoin (Prieur and Fau, 2015). Ce processus de conversion permet d'utiliser l'électricité pour la stocker aux moments où la consommation est faible, le prix de génération est bas ou quand l'énergie disponible provient des ressources renouvelables intermittentes, pour être ensuite utilisée aux moments de haute consommation quand les prix de génération sont élevés où quand aucun autre moyen de génération est disponible (Raihan, 2016).

Les applications de ces moyens de stockage d'énergie électrique sont variées et dépendent de l'utilisation envisagée, soit sous forme de source de puissance soit sous forme de source d'énergie (Entsoe, 2018). Sous forme de source de puissance cette application requiert un niveau important de puissance, générée usuellement pendant des courtes périodes de temps. Tandis que sous forme de source d'énergie, l'application requiert une grande quantité d'énergie

stockée, souvent pour durations de décharge allant de quelques minutes à quelques heures (Eyer and Corey, 2011). Quelques applications de ce dispositif sont illustrées sur la Figure 6.

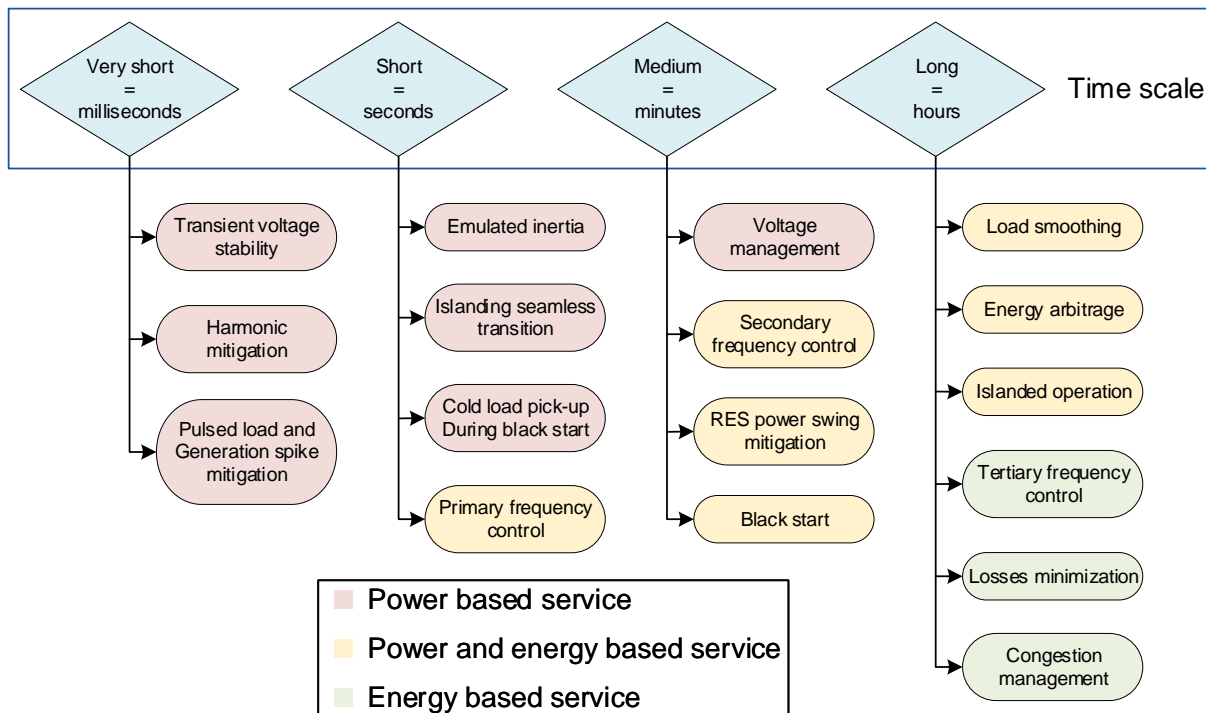


Figure 6: Principales applications d'un système de stockage d'énergie dans un réseau électrique en fonction de l'échelle de temps d'utilisation (Stecca et al., 2020).

Pour les réseaux électriques de distribution, un système de stockage d'énergie lui permet d'appliquer ce processus de conversion d'énergie, en fonction des potentiels bénéfiques pour qu'on peut obtenir pour répondre à la courbe de consommation ou au prix horaire d'achat de l'énergie, ou à tous les deux. Les principaux indicateurs pour une utilisation efficace d'un système de stockage d'énergie sont les suivants :

- **Dispatchabilité :** C'est la réactivité aux fluctuations de la consommation d'énergie qui peuvent se produire à différents cycles (journaliers, hebdomadaires et saisonniers) en raison des variations dans la consommation résidentielle et industrielle et à des changements de quelques facteurs environnementaux.
- **Interruptibilité :** C'est la réactivité à l'intermittence provenant des sources de puissance d'origine renouvelable comme l'éolienne ou la solaire, les comportements alternatifs saisonniers de la puissance hydraulique ou de la biomasse, mais également aux instabilités périodiques relatives à l'approvisionnement de combustible fossile.
- **Efficacité :** C'est la capacité à récupérer et à réutiliser l'énergie qui autrement serait perdue.

Les systèmes de stockage d'énergie sont de plus en plus utilisés dans les réseaux électriques, mais dans certains cas, sans une véritable stratégie d'impact d'intégration pour les gestionnaires des réseaux de distribution électrique (Key, 2000). Aujourd'hui, un système de stockage d'énergie représente un vrai facteur déterminant dans la distribution économique et la

planification technique d'un réseau de distribution électrique. Ainsi, une stricte analyse sur la manière de gérer sa pénétration croissante est nécessaire.

Dans ce chapitre on donne une description des méthodes analytiques et des considérations les plus couramment utilisées pour l'intégration d'un système de stockage d'énergie d'un un réseau distribution électrique, en tenant compte principalement des aspects concernant la localisation et le dimensionnement de sa puissance, sans tenir compte du type de technologie utilisée. Pour développer n'importe quelle méthodologie de localisation et de dimensionnement en puissance d'un tel système, avant tout est nécessaire de disposer d'un modèle d'analyse pour cet élément dans réseau de distribution d'électricité. Le modèle de système de stockage d'énergie utilisé dans le Banc d'Expérimentation VERTPOM®, est celui provenant du logiciel OpenDSS (Rocha et al., 2020). Ce modèle est montré sur la Figure 7, lequel est assez solide pour effectuer n'importe quel type d'étude de stockage d'énergie ou de gestion énergétique en fonction de l'application envisagée. Il permet l'analyse d'impact dû à installation d'un système de stockage d'énergie dans un réseau de distribution électrique.

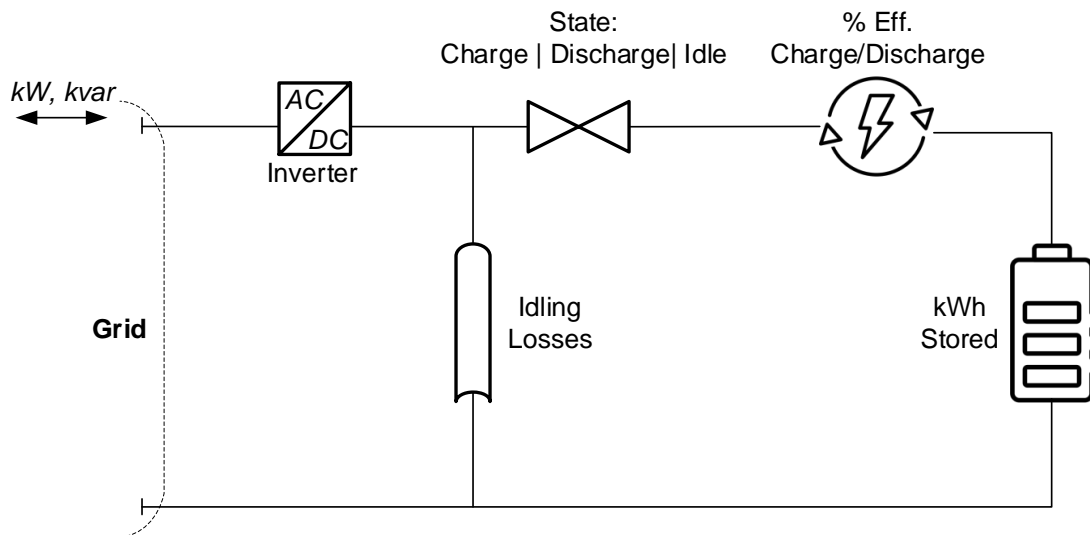


Figure 7: Modèle général de l'élément de stockage d'énergie utilisé dans OpenDSS (Rocha et al., 2020).

En fonction de l'application spécifique d'un système de stockage d'énergie et de la définition la stratégie opérationnelle correspondante à son utilité dans un réseau de distribution d'électricité particulier, il est nécessaire de définir la procédure la plus adaptée pour déterminer sa localisation et son dimensionnement en puissance, afin que ces deux facteurs minimisent le prix d'achat de l'énergie et les pertes techniques de puissance du système électrique de distribution en question (Zhong Qing et al., 2013). Ainsi, il convient de développer les algorithmes capables de cette analyse et de conclure avec la localisation et le dimensionnement de puissance optimaux du système de stockage en étude.

Trouver le site adéquat, fixe le premier pas du processus vers l'installation d'un système de stockage d'énergie. Son installation dans un réseau électrique peut être imaginée de deux manières, centralisée ou décentralisée (Kumar et al., 2019). Ensuite, le dimensionnement de ce système implique trouver son dimensionnement en puissance et sa capacité en énergie, avec l'intérêt de minimiser la fonction objectif du problème considéré. Les études sur ce sujet, peuvent être classées d'après le critère d'optimisation utilisé, financier, technique ou l'hybride des deux (Yang et al., 2018).

La localisation et le dimensionnement en puissance de ce système de stockage peut être déterminé par un large éventail de méthodes. Le problème le plus complexe est de déterminer sa localisation car il est non linéaire, non convexe et requiert une formulation dimensionnelle élevée. Cette formulation est en effet un problème d'optimisation en nombres entiers mixtes et non linéaire, qui traite la difficulté combinatoire d'optimisation sur des ensembles à variable discrète avec des fonctions non linéaires. En tenant compte de la complexité de ce problème, différents types de méthodes avec différentes fonctions objectif sont proposées dans la littérature (Jayashree and Malarvizhi, 2020). Ces méthodes sont classées de la manière suivante (Yang et al., 2018) :

- **Méthodes probabilistes** : Des méthodes probabilistes sont utilisées pour la génération des données. Ces méthodes sont les plus simples pour déterminer la localisation et le dimensionnement du système de stockage d'énergie. Le principe de ces méthodes est d'utiliser la nature stochastique des éléments actifs du réseau comme les sources de puissance distribuées et les consommateurs pour ce problème d'optimisation.
- **Méthodes analytiques** : Les méthodes analytiques sont amplement adaptées pour l'analyse du comportement dynamique du système et par ce moyen permettent de trouver la localisation et le dimensionnement adaptés.
- **Optimisation mathématique** : La localisation et le dimensionnement du systèmes de stockage sont exprimés comme des problèmes de programmation linéaire, de programmation en nombre entiers mixtes ou même de programmation non linéaire. La solution à ces problèmes sont formulés par la recherche de la solution optimale à travers d'un processus itératif sur la fonction objectif.
- **Optimisation mathématique** : La localisation et le dimensionnement du systèmes de stockage sont exprimés comme des problèmes de programmation linéaire, de programmation en nombre entiers mixtes ou même de programmation non linéaire. La solution à ces problèmes sont formulés par la recherche de la solution optimale à travers d'un processus itératif sur la fonction objectif.
- **Méthodes heuristiques** : Ce type de méthode est utilisé pour des problèmes réels où la solution optimale exacte n'est pas obligatoire et une solution approximative est suffisante. Ces méthodes évitent les calcul complexes tels que les dérivées pour un problème d'optimisation non linéaire, améliorant ainsi l'utilisation de la mémoire CPU et le temps de calcul nécessaire pour trouver la solution.
- **Méthodes hybrides** : Cette méthode combine la robustesse de chacune des méthodes précédentes dans la recherche de la solution requise.

#### *Chapter IV*

On peut trouver dans la littérature différentes études réalisées afin de trouver la localisation et le dimensionnement en puissance d'un système de stockage d'énergie dans des réseau de distribution électrique mais de topologie radiale. Néanmoins, dans le cas qui occupe ce travail de recherche dans le cadre du projet VERTPOM®, le cas français, ces études ne sont



pas applicables directement car la topologie principalement utilisée en France est donnée par une alliance entre deux topologies, la radiale et la maillée, pour assurer plus fiabilité et une meilleure qualité de service (ADEME, 2018a). Dans ces conditions et avec l'utilisation des capacités de calcul avancées développées dans les Banc d'Expérimentation VERTPOM®, une nouvelle méthodologie adaptée au cas français des réseaux de distribution électrique est proposée.

Dans ce chapitre est présenté la nouvelle méthodologie développée laquelle est intégrée à l'architecture logicielle présentée dans le chapitre 3, comme une boîte à outils de la plateforme expérimentale. Cette méthodologie simplifie de manière considérable l'étude d'insertion d'un système de stockage d'énergie, dans un réseau de distribution électrique, avec l'utilisation du logiciel de simulation numérique OpenDSS évoqué précédemment. Une programmation de calcul parallèle avec une architecture de processeur multicœurs est considérée, pour améliorer la qualité d'exécution computationnelle de la plateforme expérimentale. D'après la littérature, cette dernière fonctionnalité n'a jamais été implémentée auparavant et les résultats obtenus montrent, qu'elle offre des nombreux avantages permettant d'accélérer les calculs numériques, en partageant les analyses des scénarios et du réseau en étude, entre les différents acteurs disponibles qui sont relatifs à chaque cœur du processeur.

Avec cette nouvelle méthodologie, la localisation et le dimensionnement en puissance d'un système de stockage d'énergie sont combinés, avec l'utilisation de la stratégie propre au cadre de développement de OpenDSS par EPRI (Montenegro and Dugan, 2019). Cette stratégie appelée A-Diakoptics, décompose un problème physique en plusieurs sous-problèmes, qui peuvent être résolus de manière séparée les uns des autres, avant d'être tous réunis pour l'obtention de la solution exacte du problème entier initial. De cette manière, l'évaluation numérique de tous les scénarios possibles concernant la localisation et le dimensionnement en puissance du système de stockage en question, sont gérés en parallèle et de manière concurrente avec cette option. Dans ce cas, l'utilisation d'une interface de programmation applicative directe (Direct DLL API) de OpenDSS permet une intégration facile de ce type de méthode heuristique, qui est particulièrement adaptée au traitement multi-tâches du logiciel LabVIEW® de National Instruments® (Montenegro, 2017), utilisé initialement pour le dispositif d'acquisition et contrôle des données ainsi que pour l'utilisation des toutes les catégories des méthodes temps réel de la plateforme expérimentale.

La nouvelle méthodologie proposée crée la fusion de deux techniques efficaces, la première pour définir la localisation du système de stockage à partir d'une analyse de sensibilité du réseau électrique en question et la seconde celle de son dimensionnement en puissance par une approche génétique, lesquelles sont renforcées par un calcul par un calcul parallèle, pour l'obtention d'outil performant en termes d'efficacité et de rapidité de calcul. Le diagramme de flux de cette solution est présenté sur la [Figure 8](#).

Premièrement, l'analyse de sensibilité est réalisée pour permettre l'introduction du niveau système de stockage, sans affecter ou perturber le fonctionnement normal du système électrique de distribution en question (Christakou et al., 2013). Cependant, ce type d'analyse de sensibilité est l'une des plus consommatrices de temps dans ce processus computationnel, dont son efficacité consiste à déterminer les nœuds les plus sensibles, permettant ainsi de définir la localisation qui potentiellement est la plus adaptée à cet intérêt. Dans ces conditions, le calcul parallèle est appliqué pour la première fois à l'analyse de sensibilité, avec l'application d'une méthodologie dédiée au logiciel LabVIEW® mais potentiellement applicable dans d'autres en-

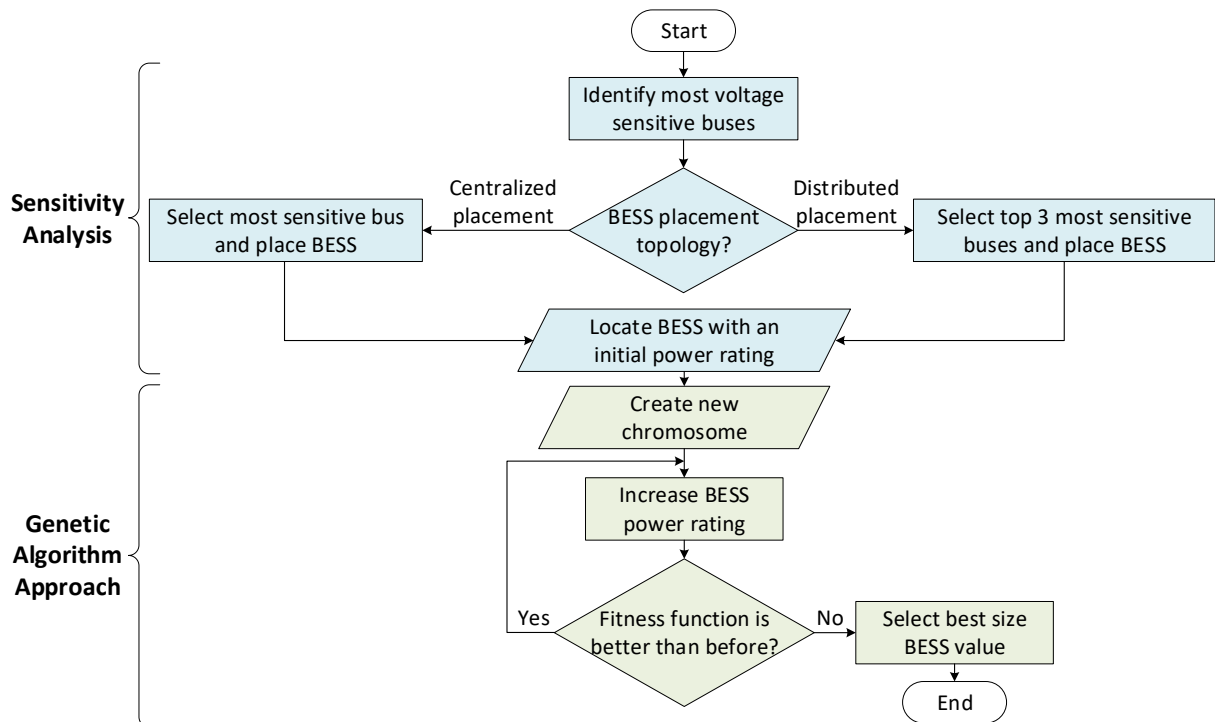


Figure 8: Diagramme de flux de la nouvelle méthodologie de localisation et de dimensionnement en puissance d'un système de stockage d'énergie pour un réseau de distribution électrique.

vvironnements logiciels. . Une fois que cette analyse est réalisée pour tous les nœuds du réseau électrique, le post-traitement des résultats obtenus consiste à classer l'ensemble de nœuds selon son niveau de sensibilité, en partant du plus haut niveau jusqu'au niveau le plus bas observés (entre 0 et 1). Ce classement permet ensuite d'observer de manière visuelle sur l'écran principal de la plateforme, la sensibilité de chaque nœud avec un code de couleurs du type carte thermique, comme illustré dans la Figure 9, pour le schéma d'exploitation du réseau de distribution d'électricité de la ville.

De manière à comparer à comparer la précision et la rapidité de calcul de cette analyse de sensibilité dans le Banc d'Expérimentation VERTPOM®, un réseau électrique de test a été programmé dans OpenDSS avec une programmation de l'algorithme perturber et observer dans l'environnement logiciel de LabVIEW®. Cette comparaison est réalisée par rapport aux tests de référence présentés dans (Tamp and Ciufu, 2014). Les résultats obtenus sur le Tableau 1 montrent les performances remarquables de cet algorithme quand il déployé dans une architecture de calcul multicœurs, avec une réduction du temps de calcul d'environ la moitié par rapport au cas classique.

Après avoir déterminé la sensibilité des nœuds du réseau de distribution, l'opérateur peut sélectionner le ou les lieux où les unités de stockage pourront être installées, soit une seule sur le nœud le plus sensible ou plusieurs sur les nœuds qui partagent un niveau de sensibilité importante également. C'est en fonction de ce choix, que la nouvelle approche par calcul parallèle de l'algorithme d'optimisation génétique proposée, est utilisée pour déterminer le dimensionnement en puissance du système de stockage envisagé. Le diagramme de séquence de la programmation en calcul parallèle de cet algorithme est présenté sur la Figure 10.

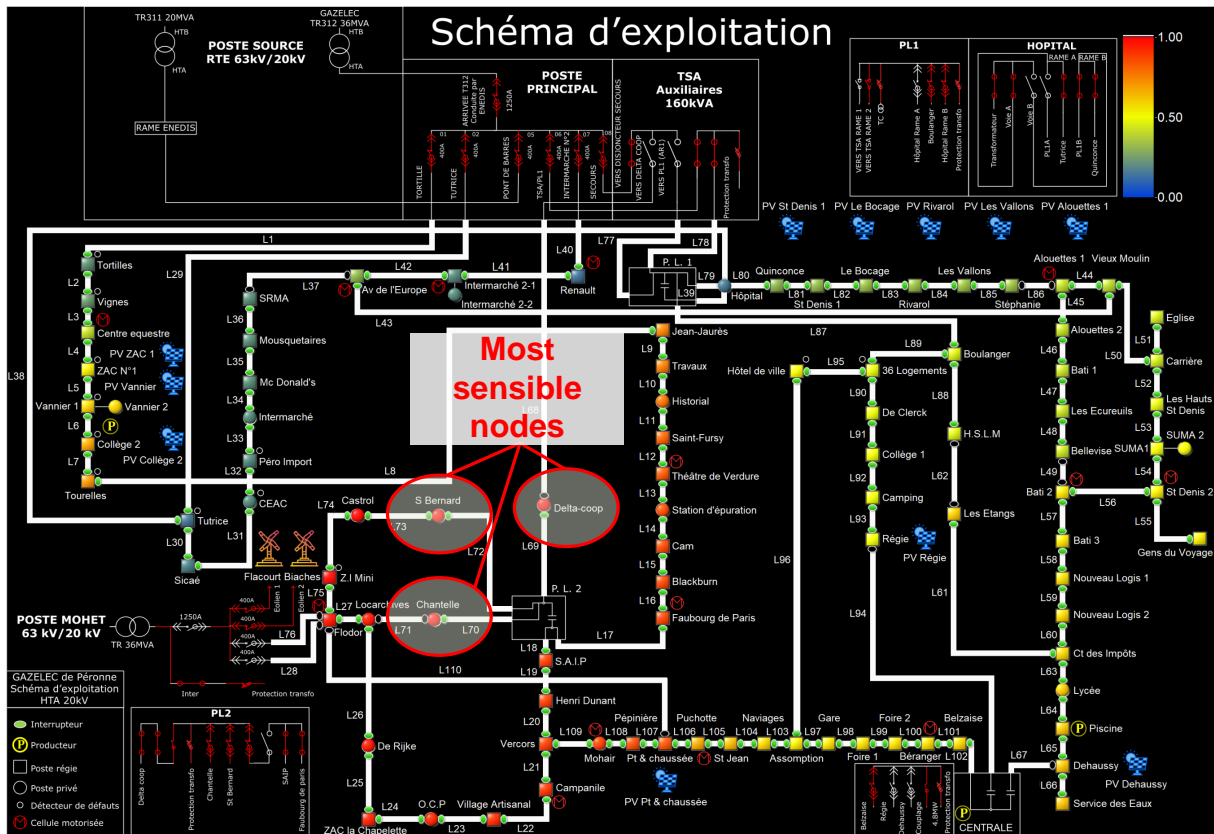


Figure 9: Visualisation de la carte de sensibilité du réseau de distribution d'électricité de la ville dans le Banc d'Expérimentation VERTPOM®.

Table 1: Comparaison des résultats de temps de calcul de l'algorithme perturber et observer par rapport à la solution de référence (Tamp and Ciufu, 2014).

Temps de calcul	Temps de référence	Processeur à un cœur	Processeur multicœurs
Temps moyen, ms	170.4	147.4	82.6
Temps minimum, ms	157	144	68
Temps maximum, ms	183	156	98

Cette procédure d'optimisation est réalisée en plusieurs étapes. Premièrement, les conditions initiales sont définies en faisant un choix sur le nombre d'unités de stockage à installer, en fixant les valeurs de puissance et le pas de recherche en fonction de l'expérience de l'opérateur, ainsi que les restrictions techniques d'évolution de la fonction objectif. Le processus génétique d'optimisation qui s'en suit dans la création de nouveaux chromosomes, est vérifié par co-simulation de manière permanente entre OpenDSS et LabVIEW®, afin de respecter les restrictions techniques fixées. Cet algorithme est exécuté jusqu'à ce que les critères de convergence de la solution soient obtenus, donnant à la fin le meilleur dimensionnement en puissance du système recherché. Cet algorithme a été appliquée initialement pour le réseau électrique de référence (Tamp and Ciufu, 2014), en considérant deux approches séparément, l'amélioration du profil de tension et la minimisation des pertes de puissance techniques. Les

résultats obtenus sont présentés dans le Tableau 2 et montrent son effectivité pour ces deux conditions.

Après cette validation, l'algorithme génétique avec calcul parallèle est appliqué au réseau de distribution d'électricité de la ville, à partir de l'analyse sensibilité présenté dans la Figure 9, en considérant les cas d'étude suivants :

- **Cas d'étude I** : Réseau électrique sans système de stockage.
- **Cas d'étude II** : Réseau électrique avec système de stockage centralisé sur le nœud le plus sensible pour améliorer le profil de tension (poste de livraison Delta-coop).

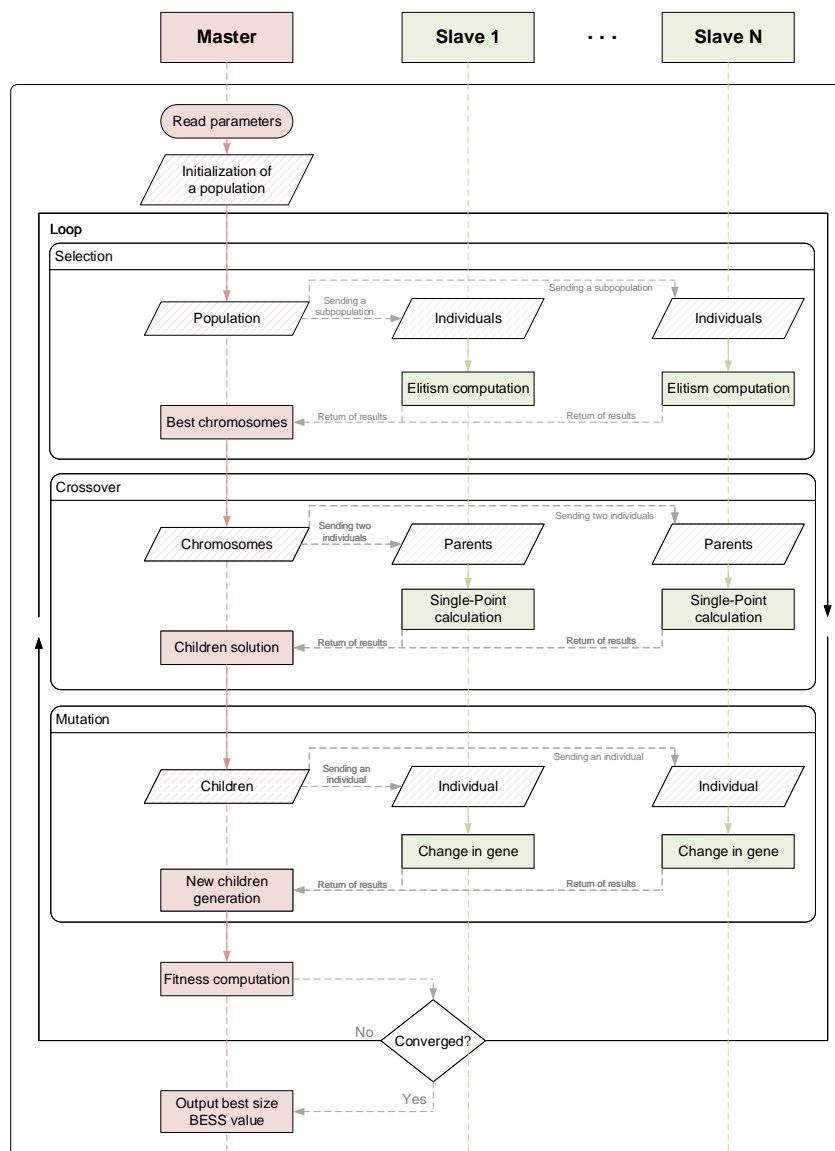


Figure 10: Diagramme de séquence de la programmation en calcul parallèle de l'algorithme génétique pour le dimensionnement en puissance du système de stockage.

Table 2: Validation de l'utilisation de l'algorithme génétique sur le cas de référence.

	Puissance active total consommée, MW	Plage des tensions, p.u.	Puissance totale de pertes techniques, MW	Dimensionnement du système de stockage centralisé sur le nœud le plus sensible, MW
Sans système de stockage	598.511	1-0.88	19.51	-
Avec système de stockage et amélioration du profil de tension	103.257	1-0.929	10.25	477
Avec système de stockage et minimisation de la puissance des pertes techniques	263.165	1-0.925	7.16	314

- **Cas d'étude III** : Réseau électrique avec système de stockage distribué sur les 3 nœuds les plus sensibles pour améliorer le profil de tension (postes de livraison Delta-coop, Chantelle et Saint Bernard).
- **Cas d'étude IV** : Réseau électrique avec système de stockage centralisé sur le nœud le plus sensible pour minimiser les pertes de puissance techniques (poste de livraison Delta-coop).
- **Cas d'étude V** : Réseau électrique avec système de stockage distribué sur les 3 nœuds les plus sensibles pour minimiser les pertes de puissance techniques (postes de livraison Delta-coop, Chantelle et Saint Bernard).

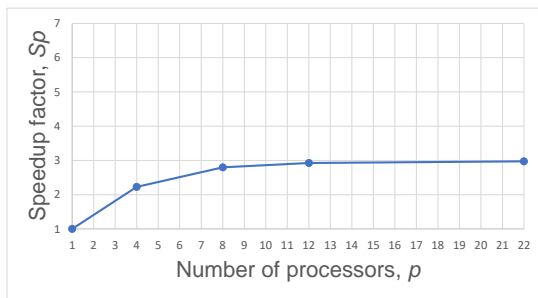
Dans ces conditions les algorithmes de calcul *génétique* simple cœur et multicœurs sont déployés afin d'établir les performances relatives pour ce dernier. Deux scénarios sont examinés pour cette comparaison, l'un avec un système localisé et l'autre avec un système distribué, sur les nœuds les plus sensibles du réseau de distribution d'électricité. Les conditions de fonctionnement de ce réseau électrique sont celle du pire scénario avec 100% de charge sur tous les postes de livraison. Le Tableau 3, montre les conditions d'utilisation de chaque version de cet algorithme.

Les performances de calcul de ces deux algorithmes se font sur la base de l'estimation du facteur d'accélération dont les résultats obtenus sont présentés sur la Figure 23, pour les scénarios précédemment considérés. Ces résultats démontrent l'amélioration générale de la nouvelle formulation proposée de l'algorithme génétique avec calcul parallèle.

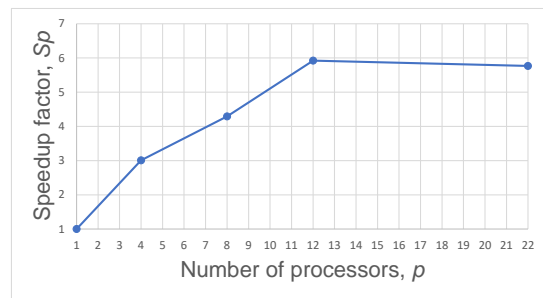
Du point de vue des résultats obtenus pour le dimensionnement de la puissance du système de stockage, les résultats obtenus sont présentés dans le Tableau 4 pour évaluer son effet dans des conditions de charge du système de stockage (comportement charge) et dans le Tableau 5 pour évaluer son effet dans des conditions de décharge (comportement générateur), pour tous les scénarios évalués.

Table 3: Description des paramètres utilisés pour chaque algorithme *génétique*.

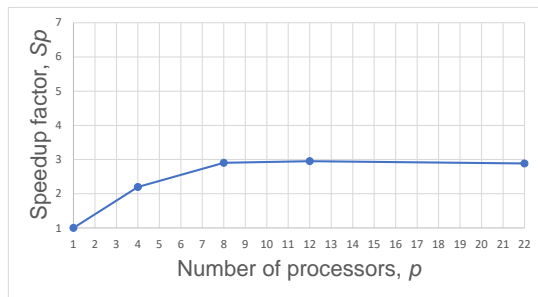
Fonctions d'évaluation	Algorithme génétique classique	Algorithme génétique pour calcul parallèle
Nombre de populations	1	1
Nombre de sous populations ( $\lambda$ )	1	4, 8, 12, 22
Nombre d'individus ( $\mu$ )	50, 20	20
Méthode d'opération	-	Synchrone
Nombre de points de synchronisation	-	Plusieurs points



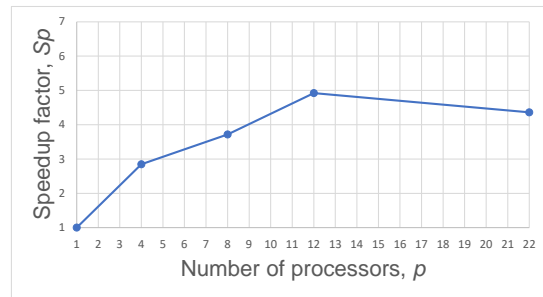
(a) Installation centralisée du système de stockage pour améliorer le profil de tension.



(b) Installation décentralisée du système de stockage pour améliorer le profil de tension.



(c) Installation centralisée du système de stockage pour minimiser les pertes de puissance techniques.



(d) Installation décentralisée du système de stockage pour minimiser les pertes de puissance techniques.

Figure 11: Résultats d'estimation du facteur d'accélération en fonction du nombre de processeurs pour les scénarios considérés.

Sur ces deux tableaux on peut observer qu'en général, l'approche de minimisation des pertes de puissance techniques introduit une amélioration plutôt légère sur l'ensemble du réseau électrique, par rapport à celle qui introduit l'approche d'amélioration du profil de tension. Ces performances sont obtenues avec un dimensionnement en puissance plus faible pour la première approche par rapport à la seconde. Ces résultats montrent les bénéfices qui peuvent être obtenus avec ce système de stockage d'énergie avec des flexibilités qui peuvent s'adapter aux besoins du système, tout en contribuant au lissage de la courbe de consommation par une gestion énergétique locale du territoire qui reste à définir.

Table 4: Effet du système de stockage optimal sur le réseau électrique dans des conditions de charge.

Cas d'étude	Localisation et dimensionnement en puissance	Puissance active totale, MW	Plage des tensions, p.u.	Puissance totale des pertes techniques, MW
I	No BESS	24.99	1-0.94	0.438
II	Delta-coop (6.9 MW)	32.09	1-0.9	1.049
III	Delta-coop (2.5 MW) Chantelle (2.4 MW) Saint Bernard (2.4 MW)	32.5	1-0.9	1.08
IV	Delta-coop (5.6 MW)	30.8	1-0.907	0.903
V	Delta-coop (2 MW) Chantelle (2 MW) Saint Bernard (2 MW)	31.22	1-0.906	0.93

Table 5: Effet du système de stockage optimal sur le réseau électrique dans des conditions de décharge.

Cas d'étude	Localisation et dimensionnement en puissance	Puissance active totale, MW	Plage des tensions, p.u.	Puissance totale des pertes techniques, MW
I	No BESS	24.99	1-0.94	0.438
II	Delta-coop (6.9 MW)	17.97	1-0.949	0.313
III	Delta-coop (2.5 MW) Chantelle (2.4 MW) Saint Bernard (2.4 MW)	17.55	1-0.9494	0.301
IV	Delta-coop (5.6 MW)	19.25	1-0.947	0.304
V	Delta-coop (2 MW) Chantelle (2 MW) Saint Bernard (2 MW)	18.84	1-0.948	0.294

Cette nouvelle méthodologie est intégrée au Banc d'Expérimentation VERTPOM® comme une boîte à outils avec laquelle, on peut lancer initialement l'analyse de sensibilité et continuer ensuite avec le dimensionnement du système de stockage pour le réseau électrique en étude, pour n'importe quelle configuration du système électrique de base, en donnant comme résultat l'évaluations des performances potentielles pour la configuration choisie.

A titre d'exemple, sur la [Figure 12](#) est présenté le panneau sur l'écran principal montrant les résultats obtenus pour le cas d'étude II traité précédemment. Avec les possibilités de calcul parallèle programmés pour cette méthodologie, elle est énormément extensible sur la plateforme expérimentale, selon les résultats d'évaluation obtenus. La combinaison proposée entre une analyse de sensibilité et un algorithme d'optimisation évolutif, se prêtent pour d'autres type d'études dans les réseaux électriques de distribution. La technique proposée convient

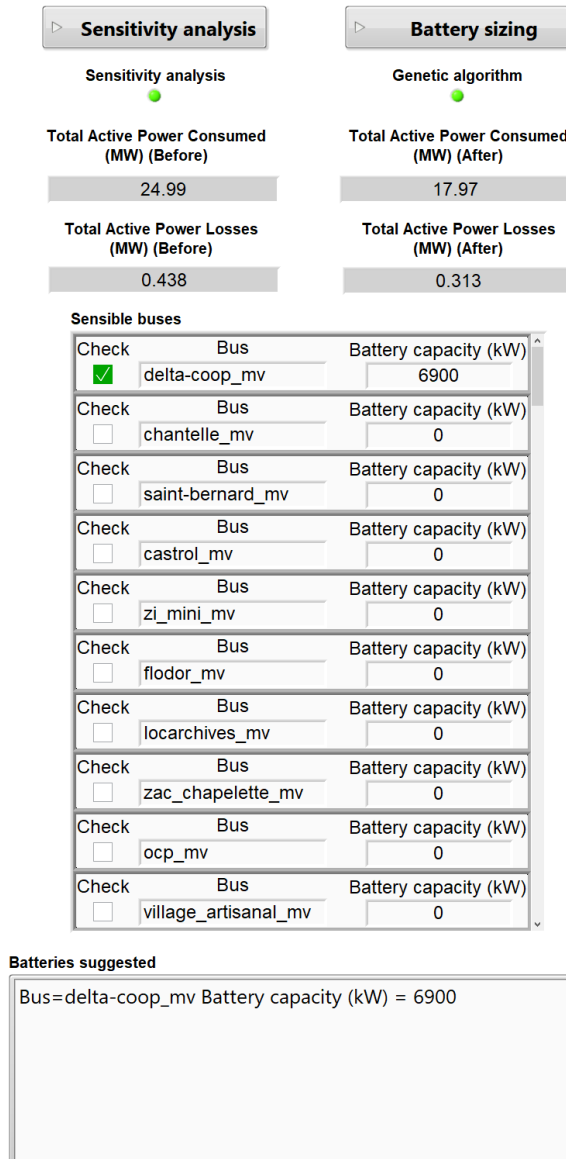


Figure 12: Visualisation du panneau d'affichage dédié à l'étude et à la présentation des résultats obtenus pour un système de stockage d'énergie dans l'écran principal du Banc d'Expérimentation VERTPOM®. Les informations et les résultats affichés correspondent au cas d'étude II.

amplement pour des études temps réel dans le contrôle de différentes configurations d'un réseau électrique, en incluant des dispositifs matériels dans l'analyse. Cette évolution dans les configurations successives d'un réseau électrique, nécessite un recalcul périodique des conditions de fonctionnement du système. Le temps de traitement dans ces conditions peut être réduit de manière significative avec l'utilisation d'une approche multi-tâches pour la gestion de ces procédures d'analyse.



## CONCLUSIONS

Le travail de recherche présenté dans ce mémoire de thèse, couvre le sujet associé à la supervision, l'analyse et l'optimisation des systèmes électrique de distribution, tenant en considération la pénétration des ressources électriques distribuées ainsi que les systèmes de stockage d'énergie électrique. Premièrement, une étude est présentée sur l'état de l'art des différentes méthodologies et outils à ce sujet, pour avoir une compréhension complète des challenges qui doivent être satisfaits pour assurer la surveillance et l'analyse d'un réseau de distribution d'électricité.

Sur la base des concepts collectés, une plateforme matérielle/logicielle expérimentale est initialement conçue et réalisée de manière à développer un nouveau paradigme dans le déploiement dans l'analyse des réseaux électriques de distribution, paradigme basé sur les outils de test et d'analyse temps réel. Après la réalisation de plusieurs tests de performance sur cette plateforme expérimentale, il s'est avéré que le bien fondé de l'architecture choisie est largement suffisant pour les études en temps réel de la supervision et de l'analyse d'un réseau de distribution d'électricité.

En raison du type de réseau de distribution électrique étudié, dans le cas français avec de la production d'électricité distribuée d'origine renouvelable provenant de deux parcs éoliens et des multiples panneaux photovoltaïques installés tous tout au long du réseau, une étude est réalisée pour évaluer la manière la plus adaptée d'intégrer un système de stockage d'énergie à un réseau électrique réel. Une analyse du contexte permettant d'évaluer les méthodologies actuelles pour définir sa localisation et son dimensionnement en puissance, est également réalisée. Le résultat de cette analyse a permis de formuler une nouvelle méthodologie de conception d'un système de stockage avec du calcul parallèle. La méthodologie hybride a été programmée et évaluée dans la plateforme expérimentale, avec un cas de test et un cas réel, avec des résultats montrant que la programmation multi-tâches de ce type de calcul, réduit de manière intéressante le temps d'exécution avec l'obtention de résultats précis pour déterminer la localisation et le dimensionnement en puissance d'un tel système. Ceci contribue à une meilleure intégration de ces dispositifs dans les réseaux électriques intelligents, avec beaucoup d'efficacité et réduction des coûts de conception.

Finalement, la conception un système de gestion d'énergie du système de stockage localisé et dimensionné en puissance, est le pas suivant dans l'étude de son intégration définitive au réseau de distribution d'électricité. Dans ce sens, une nouvelle méthodologie est en perspective d'être développée, pour évaluer sa capacité en énergie, de la même manière que l'optimisation du nombre des cycles de charge et décharge en accord avec la production d'électricité d'origine renouvelable locale et les besoins de consommation du territoire correspondant.

**Note:** *Le projet VERTPOM a été conçu initialement pour évaluer les systèmes multi-fluides présents sur un territoire, mais en raison d'une forte demande pour améliorer le système de distribution électrique, cette thèse entend traiter en premier lieu ce dernier objectif. De nouvelles perspectives seront intégrées en tenant compte des autres fluides dans les projets à venir.*

## EXTENDED SUMMARY

---

### VERTPOM PROJECT

#### *Context*

The territory is at the crossroads of energy, climate, economic, environmental, social issues. The increase in the volume of information will multiply the opportunities for their use, with the need to develop new technical solutions to manage them, while guaranteeing their safety (cybersecurity) and consumer privacy.

VERTPOM® (ADEME, 2018b) is a project led by a consortium to develop and deploy the VERTPOM-BANK® decision support tool called the Bank of Energy, which will maintain an optimized balance between the available produced energy (conventional and renewable) uses (consumption and losses), in connection with the energy storage means. This tool will help territories to become positive energy territory "TEPOS" (Territoire à Energie POSitive).

The Bank of Energy will be based on algorithms for prediction and simulation of energy production levels, consumption and losses on the various distribution systems. They will exploit a common data base. The use of artificial intelligence will be preferred.

#### *General objectives of VERTPOM project*

VERTPOM® is a GLOBAL offer made up of techno-economic components: energy control, social monitoring tool, scalable storage system, public infrastructure energy performance... adapted to the market of French and international distribution network managers.

One of the first tasks is to note the level of energy (positive or negative) of the territory. Then the energy bank will look for and simulate all possible scenarios to improve the production/-consumption balance, while identifying the specific renewable energies of the territory.

The fundamental role and responsibilities for data management will essentially be: to be a market facilitator, to allow network access and connection in a transparent and nondiscriminatory way, to ensure the security of the provision and quality of service.

Energy networks need to be more responsive, flexible, and thus promote interactions between market players. The Bank of Energy will contribute to these objectives listed below:

- Collect data on networks using sensors and remotely controllable devices (smart multi-fluids IBox, sensors).
- Analyze in a quick time the network status (electricity, water, gas).

- Anticipating local production from REN and energy storage.
- Enabling the development of energy management services by providing information on energy consumption and allowing the management of uses.
- Optimize consumption and intelligently interact with the end-user (consumer/actor).
- Enable the deployment of new services.
- Contribute to the implementation and control of new flexibilities: storage, state-of-the-art management programs, power management (production and demand), dynamic tariffs.
- Provide information to customers, suppliers and other market participants and ensure the safety and stability of the network.

#### SUPERVISION, ANALYSIS AND OPTIMIZATION OF ELECTRICAL DISTRIBUTION NETWORKS WITH INTEGRATION OF RENEWABLE ENERGIES AND ENERGY STORAGE MEANS

##### *Objectives of this thesis*

Based in the data collected over the smart meters and sensors installed in multiple electrical feeding and consumption points, this thesis has the objective to develop a supervision and diagnosis system for power distribution networks to improve the service quality. Data analysis and optimisation algorithms have to be developed to understand the global system operation.

The methodologies proposed in this thesis are validated using an experimental platform before to be implemented in the real network. The experimental platform is conceived as well in this thesis, this tool has been installed and put in service in the facilities of the LTI laboratory more precisely in the EESA building.

Moreover, one of the most important objectives of this thesis is the introduction of energy storage systems to participate in the electricity management and the supervision of the energy quality.

#### THESIS SUMMARY

##### *Chapter I*

In [Chapter 1](#), it is provided a comprehensive survey on the state-of-the-art of condition monitoring technologies as enabling the fault detection for the power distribution grids. Several engineering efforts have already been initiated to modernize the power grid, but in most cases, the increasing complexity of distribution systems has become a major topic for monitoring techniques, and even the diagnostic methods are not suitable to assess the system behavior progress.

The constant availability of the power distribution system data requires a detailed analysis for a fault diagnosis solution. Hence, a real-time monitoring with high data rates and the possibility to data storage is a feasible solution to monitor the changes on the operating parameters and system health in order to determine the most appropriate action.

The vision of a smart distribution system requires a widespread equipment and system monitoring capability. For this purpose, it is fundamental to introduce an advanced metering infrastructure and an advanced distribution automation to manage the energy consumption. In this way, one alternative is to realize a scheme analysis process in charge to estimate the state of the system under real conditions, including the design and optimization process, to determine the power system elements ratings and to analyze the power systems grid state in general. As shown in Figure 13, these alternatives can provide the necessary monitoring and alarm detection in several changes which can occurs in the parameters of the physical system (Qiao and Lu, 2015). However, the experimentation with the real distribution network is very limited and in some cases infeasible, mostly due to its large size and high complexity.

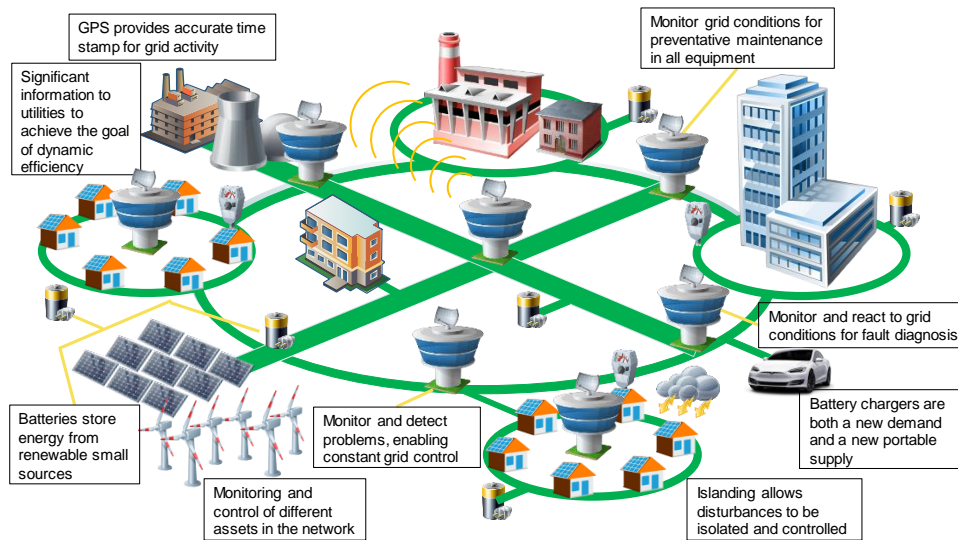


Figure 13: Augmentation de la surveillance dans le panorama actuel des réseaux de distribution d'électricité.

According to the literature (Borlase, 2018), the simulation process is an alternative solution to study the electromagnetic phenomena behaviour in the power grids and to realise the impact related to an operation or control procedure. Moreover, the use of a real-time monitoring architecture could represent an enhanced evolution of the grid towards a smart grid according with different considerations such as fault diagnosis and contingency analysis, supervision and optimization of different assets in the network, security of critical components, significant information to utilities to achieve the goal of dynamic efficiency, power quality issues, among others (Martinez, Henao, and Capolino, 2019).

In consequence, the development of a real-time decision-making platform for the system operator is essential to provide a properly way to monitor the current distribution system conditions and supporting decisions made in an automated energy management system (Jalili-Marandi and Dinavahi, 2009).

Currently, there is a large and growing market for real-time simulation and control technology in industry. Because of this, simulation requires accurate representative models, real-time

data for situational awareness, computational algorithms and hardware capabilities for timely execution (Ilamparithi, Abourdia, and Kirk, 2016). But, the literature reveals that the existing real-time simulators does not accomplish the computational efficiency in grid operations, which can lead in delays to respond to critical events.

In most of the cases the experimental platforms for power distribution system analysis are limited to several restrictions, in some others, these platforms are over-priced or it is mandatory the purchase of extra licenses to enable all features. Thus, the development of a new experimental platform solution is fundamental considering certain functionalities. These functionalities required are belonged to the simulation-based application which is evaluated including temporal characteristic of the dynamic phenomena. For this purpose, hybrid simulators can deal with both conditions combining the fidelity of the analog simulators with the models recreated in the discrete time domain using a digital system (Guillaud et al., 2015).

For a dynamic evaluation of realistic-size power networks, it is necessary accuracy and speed. In both aspects, the real-time condition monitoring is a key component of the future automation architecture in the power distribution grid. It provides an accurate evaluation of the network in real-time to feed the automatic and supervisory control of the network components (Noureen, Roy, and Bayne, 2017). Its performance can vary depending on the hardware technology and based on the setup of the simulation and its application. As shown in Figure 14 based on the setup of the simulation and its application, RT simulators can be classified into four main categories: fully RT digital simulator, hardware in the loop (HIL) simulator, control HIL (CHIL) simulator, and power HIL (PHIL) simulator.

A HIL simulator is which a part of the system is modeled and simulated in real-time, while the remainder is the actual hardware, connected in closed loop through various input/output interfaces (Faruque and Dinavahi, 2010). In a control HIL simulator, a hardware controller is tested and linked to a power network simulated entirely (Panwar et al., 2013). Finally, the interaction assessment and response between a couple of power equipment can be tested using a power HIL methodology (Ibarra et al., 2017). All these methodologies offers a cost-effective and comprehensive means of testing smart grid control and protection schemes by covering functional and robustness testing.

The challenges of real-time simulation tools for smart grids are increasingly more selective. The industry is demanding more powerful simulation tools since the complexity is getting bigger, and the integration of new technologies is changing loading patterns and profiles introducing dynamics at the distribution grid that present new grid management challenges for utilities.

Managing and optimizing the grid to meet all the traditional requirements in the presence of new and upcoming constraints pose unanticipated challenges, especially to provide novel testing techniques, which incorporate more detail and reduce the simulation time (Ilamparithi, Abourdia, and Kirk, 2016).

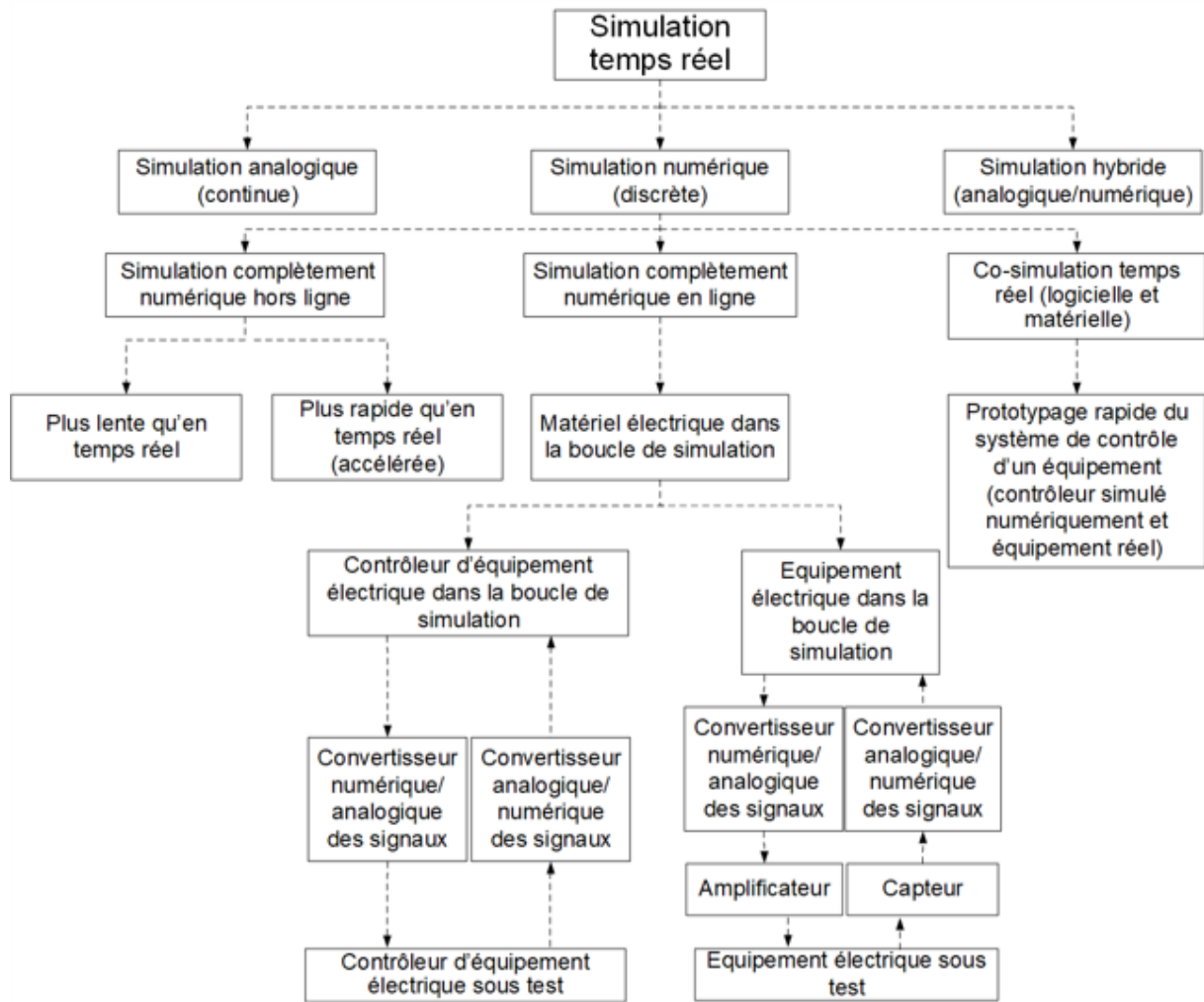


Figure 14: RT power system simulation categories.

## Chapter II

Chapter 2 introduces the development of a novel comprehensive experimental platform intended to monitor, supervise and simulate the state of a power distribution system based in the prediction and the integration of real-time capabilities and HIL integration. The description is done from the main hardware/software components, as well as the test validation of different test scenarios performed.

The Bank of Energy® is developed as a hardware/software interface for energy arbitrage between the energy produced in a territory (conventional and distributed), the energy consumed (clients), and the assets belonged to the distribution network (ADEME, 2018b). In other words, the purpose of the Bank of Energy is to optimize in real-time the local energy production and consumption through a robust and a resilient architecture, resulting in the principles and conceptions towards a smart power distribution grid definition.

The operation of the Bank of Energy is based in the correlation of the data obtained from the intelligent electronic devices (IED) installed in site and the algorithms developed to guarantee the prediction of the energy production/consumption behaviour. Then, several scenarios

are deployed to determine the suitable operation decisions considering the system balance production/consumption to be considered as positive, by identifying the energy surplus in the relationship between the local renewable energy production and the consumer energy management.

This kind of approach opens the possibility to manage the energy efficiency of a distribution system by a technical-financial perspective. So, an efficient energy management of the distribution system is deployed by the optimization of the energy production by the different DERs, the energy purchase, the load consumption and the storage systems that can be installed into the grid. The optimization is formulated as a mathematical model to accomplish the different operational and management criteria of the system operator.

To develop this concept, the Bank of Energy is based in an experimental platform as a starting point of development. This platform aims to integrate the principal characteristics identified in power systems simulators to solve current and planned needs. The architecture designed is shown in Figure 15.

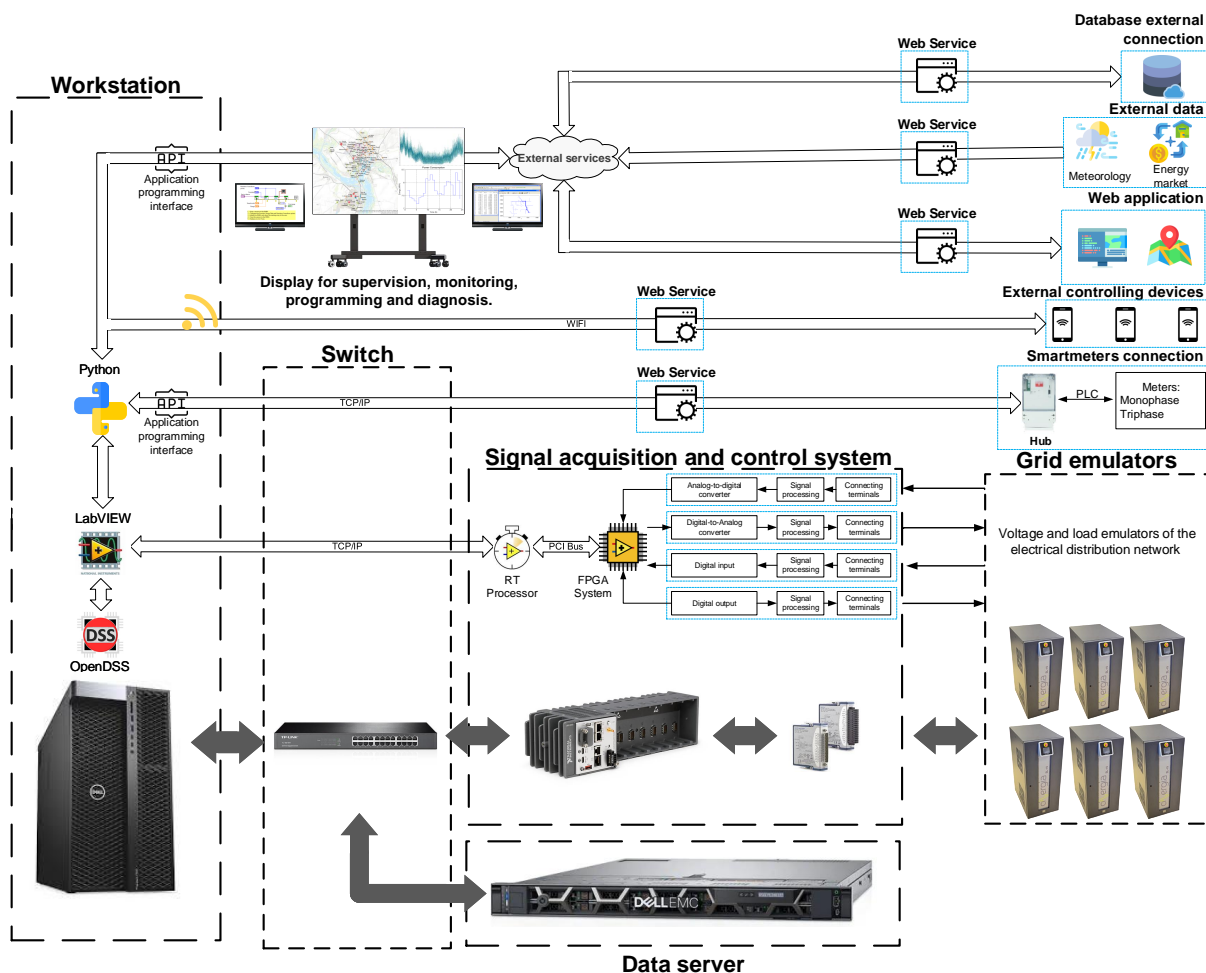


Figure 15: Block diagram of the software/hardware implementation of the Bank of the Energy.

The experimental platform has been designed based in a modular architecture to maximize the optimal performance of the hardware and software capabilities. The communication between the hardware elements through different communication channels programmed assure the scalability and flexibility of the platform. Moreover, the experimental platform merges all the

information collected in a secured database, saving the data in statistics corresponding to the energy availability in a time range from minutes to hours for different periods of time.

The interface between the elements that join the experimental platform has settled a novel methodology to manage the smart grids. It enables the possibility of a wide-range of studies starting from static and dynamic analyses, running in off-line or RT step simulation, and considering a flexible temporal window to analyze the use of advanced algorithms capable to evaluate the complete range of transient phenomena in electrical power distribution systems.

The hardware architecture of the experimental platform shown in [Figure 16](#), is based on a multi-terminal and multi-platform scalable structure that allows the remote and distributed communication with different modules. Multiple elements conform the experimental platform, a brief description of their utilities are explained below:

- Workstation peripherals: These elements provide a workspace for operators to interact with the experimental platform.
- Display for supervision, monitoring and visualization: This central screen displays the Human-Machine-Interface (HMI) of the experimental platform.
- Hardware in the loop system emulators: These emulators allow the simulation of the majority of test applications in the field of renewable energies, smartgrids, batteries and electric vehicles.
- Workstation: This element is the brain of the experimental platform. It stores the main application, modules and algorithms whereby the simulations are performed and interfaced with external hardware and software components.
- Data acquisition and data control device: This is a unit in charge to control and manage the analog and digital signals utilized to deploy a real-time simulation.
- Data server: All data collected in the experimental platform is stored in this data server.
- Intelligent electronic devices: These devices correspond to the smart meters and data concentrators installed in field interfaced in the experimental platform.
- Remote control devices: These units are integrated in the experimental platform to perform a remote control of certain simulation tasks.

The software architecture of the experimental platform is the most important component to the successful development of the software system. The type of architecture style is implemented in function to modular layers to perform efficiently all the functionalities available. This design assures that new functionalities can be added in any layer according to its own structure. The software structure of the experimental platform is illustrated in [Figure 17](#).

The styles used obey a certain architecture characteristics, architecture decisions, and design principles to define the suitable structure of the software developed. The architecture characteristics are based in the definition of a successful criteria in order to function the system properly. This criteria is supported in operational and structural considerations such as performance, reliability, scalability, portability, upgrade-ability, security, among others. The architecture decisions has set the rules of how the styles are going to interact between them. Finally,



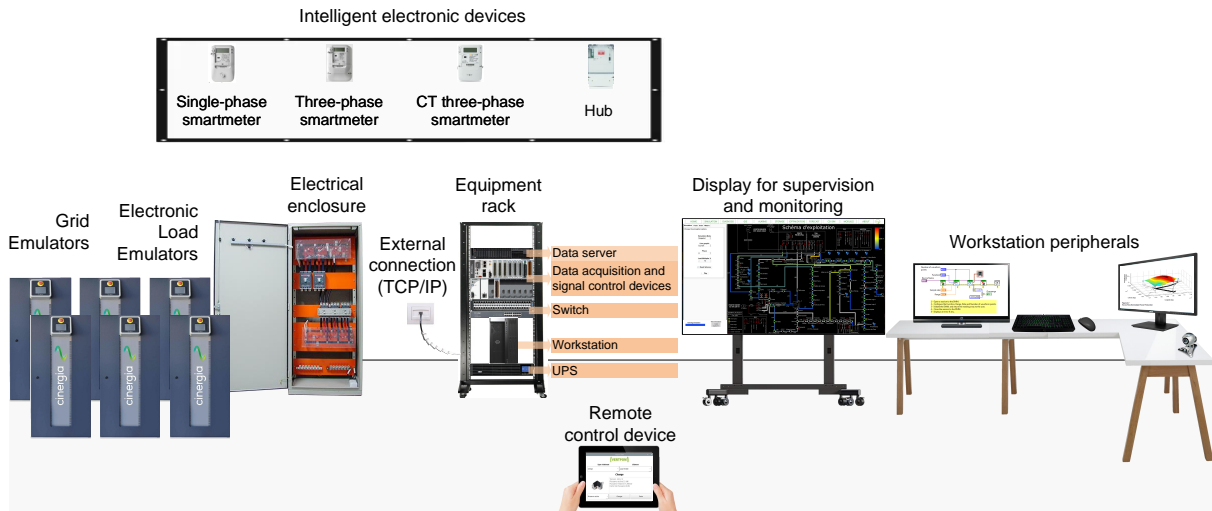


Figure 16: General hardware structure of the experimental platform.

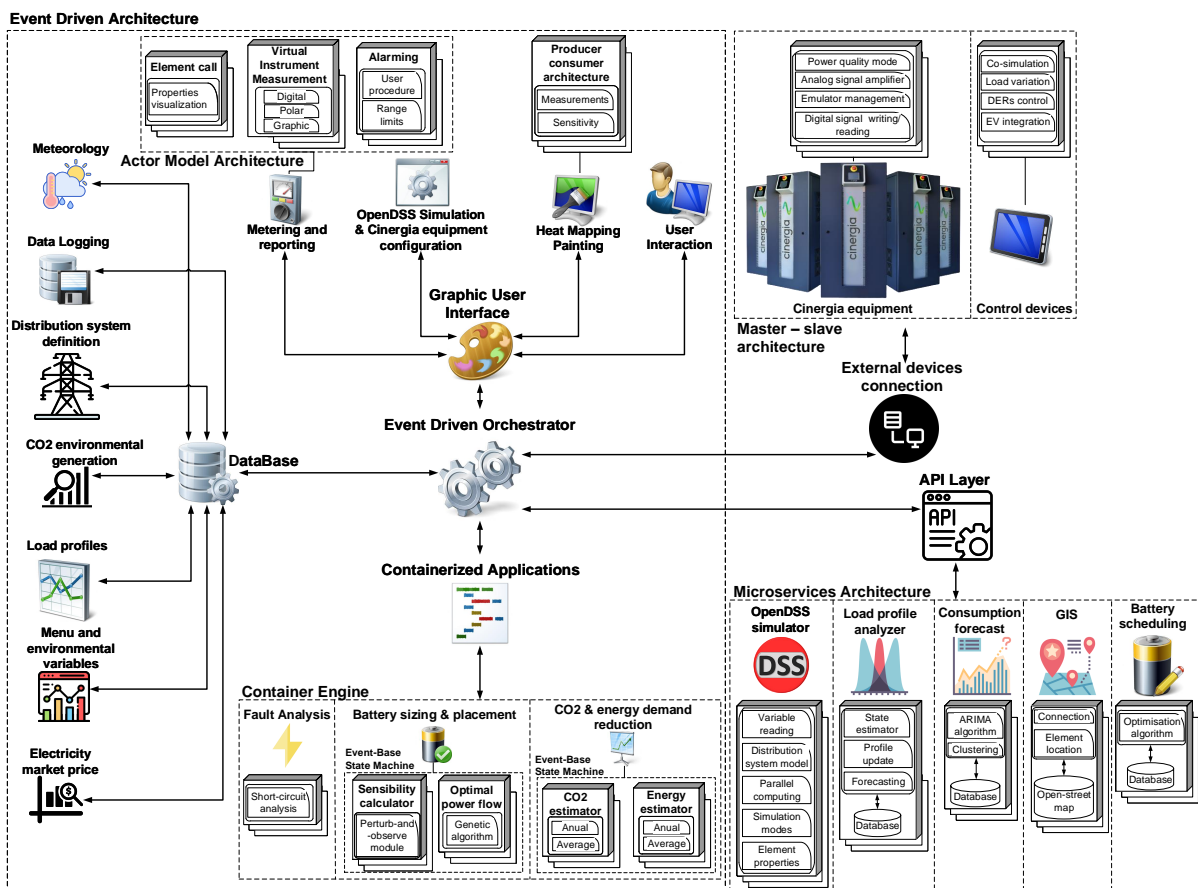


Figure 17: General software structure of the experimental platform.

the design principle is the guideline of the programming techniques followed in the software implementation. The architecture styles are established in a hierarchy order to solve both the requirements and all the other architectural characteristics.

For evaluating the accuracy and performance of the experimental platform, a real case and some test cases are used. First, the real case intends to emulate the incidents reported in

a real distribution system, allowing to evaluate the accuracy of the experimental platform comparing the results obtained with the system operator's report. The system model and the fault analysis simulation functionalities are also tested. Second, a series of testing scenarios are integrated in order to stress the experimental platform and evaluate their performance in the temporal parallelization process.

After the execution of these test cases, it is proven that the experimental platform performance based in the architecture selected is largely enough for the real-time supervision and analysis of the power distribution systems. Moreover, the scalability of the experimental platform is not unique for the Gazelec distribution system but for any other power distribution system.

The experimental platform belonged to the Bank of Energy is a platform that can be installed at research centers, laboratories or smart grid distribution control centers. The use of an open-source architecture and a modular infrastructure facilitates the license agreements and installation commissioning. As a result, multiple grid operators, researchers and students would be able to receive a beneficial implementation of the proposed approach.

### *Chapter III*

The high penetration of renewable energy production in the Gazelec of Peronne distribution system, specially wind energy has increased to a substantial level in recent years (Prieur and Fau, 2015). To ensure the proper integration and controllability of the renewable energy resources, the installation of a battery energy storage system (BESS) is getting wide attention in recent years.

BESS is based in the process of converting electrical energy from the power system into a storable form of energy to be used back when needed (Entsoe, 2018). This process allows to produce the electricity at times of either low demand, low generation cost or from intermittent energy sources and to be used at times of high demand, high generation cost or when no other generation means is available (Raihan, 2016).

The applications can be power applications or energy applications (Entsoe, 2018). Power applications require high power output, usually for short periods of time, whereas, energy applications uses large amount of stored energy, often for discharge durations of many minutes to hours (Eyer and Corey, 2011). Some of these application are illustrated in [Figure 18](#).

For distribution networks, a BESS allows to store the energy from a power network and use it back when needed depending on the demand or cost benefits. Benchmarks for an effective BESS include:

- **Dispatchability:** Responsiveness to electricity demand fluctuations that may occur on various cycles (daily, weekly, and seasonal) due to variations in domestic and industrial loads and changes in some environmental factors.
- **Interruptibility:** Reactivity to the intermittency of renewable energy supplies such as wind and solar, the seasonally alternating behaviors of hydropower and biomass, and the recurring instabilities associated with fossil fuel supplies.

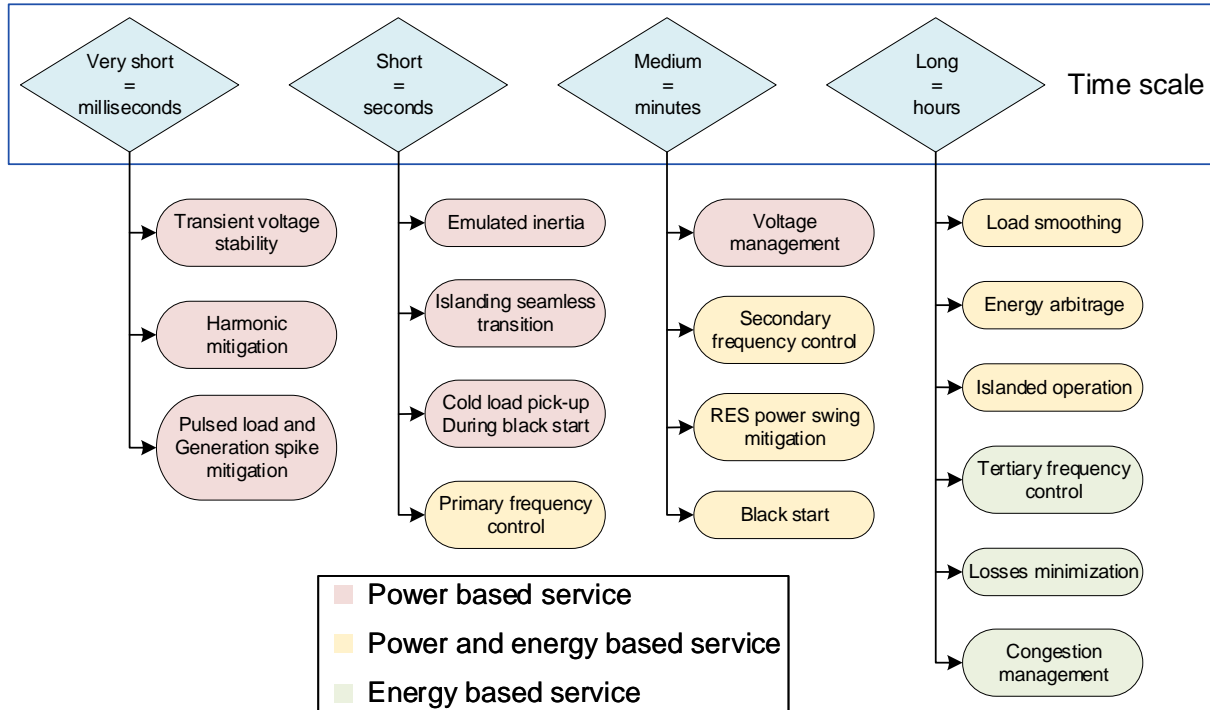


Figure 18: Services provided by BESS according to the time scale (Stecca et al., 2020).

- Efficiency: The capacity to recover and reuse energy that is otherwise wasted.

The BESS are increasingly being installed around the grid, but in some cases without a clear strategy that impacts the integration of BESS concerning the electric power distribution industry (Key, 2000). The BESS are being a determining factor into distribution economic and technical planning, so an strict assessment of how to manage the growing penetration is necessary.

Chapter 3 provides a description of the most common analytical methods and considerations from the integration of BESS into the power distribution systems, taking into account mainly the aspects of placement and sizing, without taking into account the type of technology of the BESS.

To develop any algorithm to perform the placement and sizing of a BESS installation, first, it is necessary to find a suitable model of analysis in a distribution system. The BESS used in the experimental platform comes from the OpenDSS simulator (Rocha et al., 2020). This model is shown in Figure 19. This storage element is robust enough to perform any kind of storage study or battery management system according to the application. It will allow to analyze the impact due to a BESS installation in the distribution grid.

According to an specific BESS application and an operational strategy, there is a need to execute a suitable procedure to determine the power rating size and the location of a BESS, due to the fact that an adequate BESS size and location minimize the costs and losses in the system (Zhong Qing et al., 2013). So, it is pertinent to develop algorithms capable to analyze and conclude the optimal size and location of a BESS.

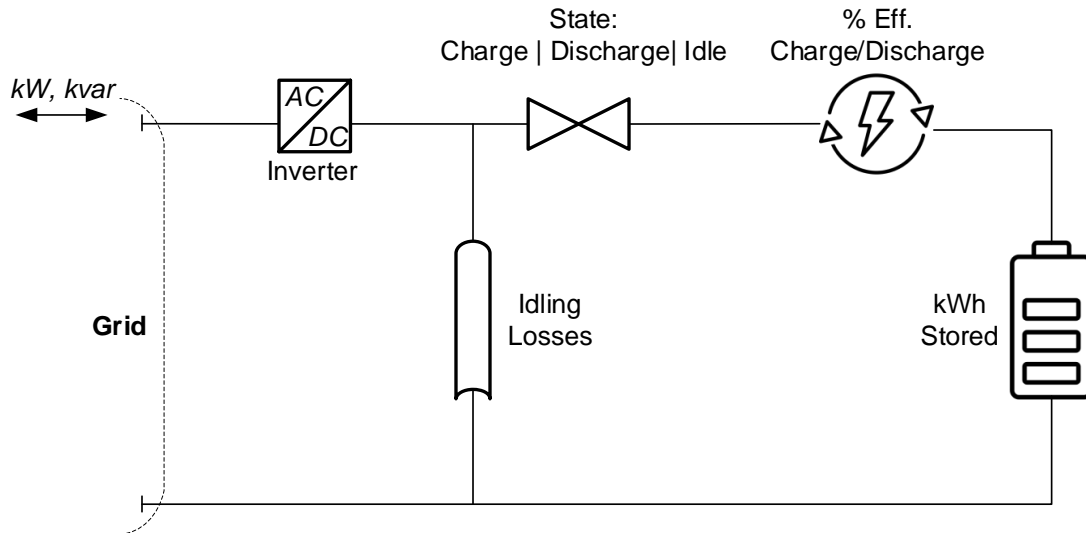


Figure 19: General model of the storage element in OpenDSS (Rocha et al., 2020).

Find a suitable site is among the first steps in the process of a BESS installation. The deployment of BESS technologies on the power distribution systems can be centralized or decentralized (Kumar et al., 2019). Then, sizing the output power rating of the BESS involves finding the optimal battery power and energy capacity with the aim of minimize the fitness function of the problem desired. Studies on sizing BESS can be classified according to an optimization criteria in financial, technical an hybrid (Yang et al., 2018).

The placement and sizing of BESS can be determined by a wide variety of approaches. The major issue of determine the placement and size of BESS is that in general this problem is a complex, non-linear, non-convex and requires a high dimensional formulation. The formulation is indeed a mixed-integer non-linear optimization problem, it handles the combinatorial difficulty of optimizing over discrete variable sets combined with the complexity of handle with non-linear functions. On account of this problem complexity, various types of methods with different objective functions are suggested in the literature (Jayashree and Malarvizhi, 2020). The methodologies can be categorized in five ways (Yang et al., 2018):

- Probabilistic methods: The probabilistic methods are used for data generation. These methods are the simplest way to determine the placement and sizing of a BESS. The basis is to use the stochastic nature of the active elements of the grid such as DERs and customers, to optimise the BESS siting and size.
- Analytical methods: The analytical methods are broadly suitable for analyzing the dynamic behavior of the system, and thus allowing to find the suitable location and size of a BESS. The analytical methods are based in the variation of the system elements in the power system configuration to find the optimal performance criteria.
- Mathematical optimization: The BESS placement and sizing problem can be expressed as linear programming, mixed-integer programming or even non-linear programming problems. Expressed the problem as a fitness function, the objective is to find the optimal solution by an iterative process.

- **Heuristic Algorithms:** The heuristic methods are widely used in real problems where the exact optimal solution is not mandatory and it is possible to have an approximate solution. The major advantage of heuristic methods is that they can avoid complex calculations such as derivatives for non-linear optimisation problems, improving the CPU memory usage and the computation time required to find a solution.
- **Hybrid techniques:** It combines the robustness of each method while it searches for the global optimal with the required resolution.

## Chapter IV

Different studies have been carried out to find out the proper placement and optimal size of BESS. However, pressed by the proper French distribution system complexity to integrate a new facility without changing its reliability and power quality (ADEME, 2018a), and motivated by the latest computational advancements, a novel methodology is proposed.

Chapter 4 presents the methodology developed which works as a toolkit of the experimental platform. It simplifies the introduction of BESS in the distribution systems using OpenDSS as a back-end simulator. A parallel programming within a multi-core architecture is considered to improve the computing performance of the experimental platform. According to literature, this feature was never implemented before and it has a lot of advantages allowing to accelerate the simulations performed, spreading the scenarios and network analysis in every actor available related for each core processor.

In this new methodology, BESS placement and sizing analysis is combined using an strategy of the A-Diakoptics framework of EPRI's OpenDSS (Montenegro and Dugan, 2019). It means that everything is treated as an actor, giving the capacity to handling placement and sizing scenarios in a parallel and concurrent way. The use of the Direct DLL API of OpenDSS allows an easy integration of this kind of heuristic methods suitable for multi-thread processing in NI LabVIEW (Montenegro, 2017).

This methodology is the merge of two efficient techniques which are boosted by a parallel computing capability, achieving a faster and effective user decision tool to place and size either centralized or decentralized BESS. A flow chart of this solution is presented in the Figure 20.

First, a sensitivity analysis is performed enabling the introduction of new system elements to support the load demand without affecting or disturbing the correct operation of the system (Christakou et al., 2013). However, the sensitivity analysis is one of the most time-consuming computational process applied to BESS placement regardless its effectiveness to determine the sensible nodes in a power system network. As a result, a parallelization of the sensitivity analysis is applied for BESS placement to speedup the most time-consuming computational part of the traditional algorithm used over the years, which itself can be decomposed into parallel subsystem tasks.

When the algorithm simulation is finished, a post-processing of the sensible data is done to arrange the values from the highest to the lowest sensible bus. This list is then prepared as an

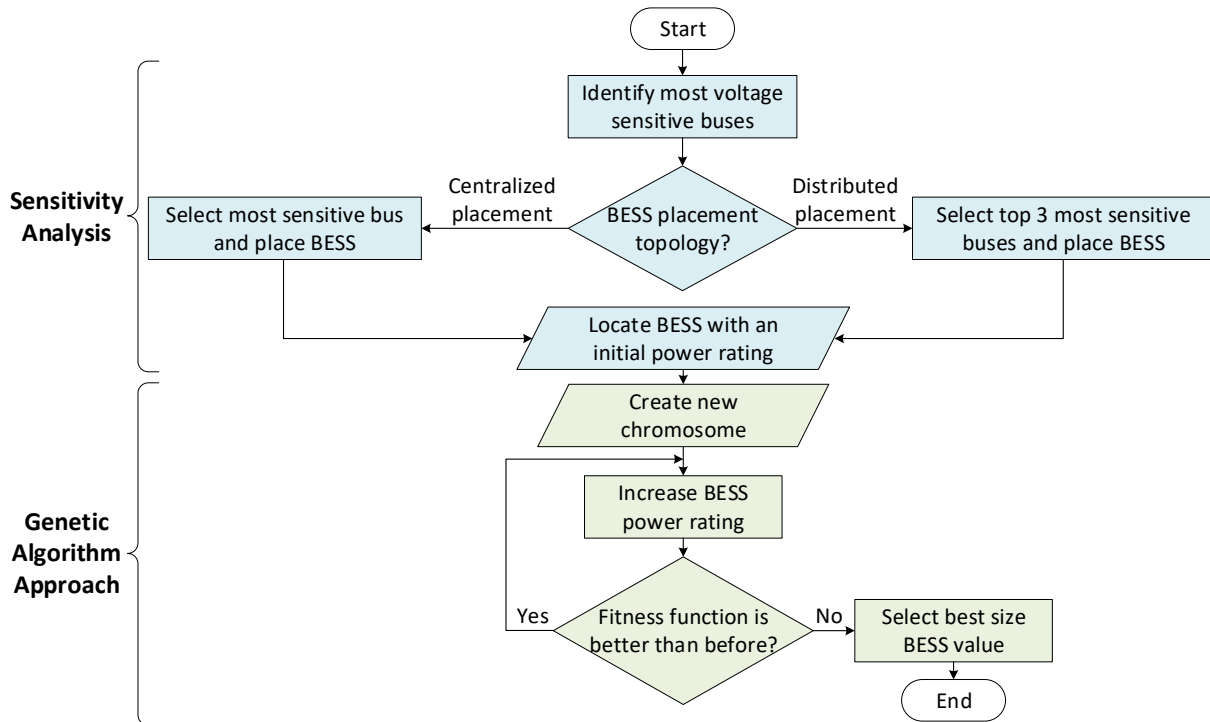


Figure 20: A flow chart of the novel placement and sizing BESS methodology.

input of a visualization toolkit developed for the experimental platform (Figure 21), generating a sensible heat map of the distribution system.

It is used a test network implemented in OpenDSS and the development of the perturb and observe algorithm for sensibility analysis in NI LabVIEW in order to validate the developed method. These sensitivities are compared according to a reference set (Tamp and Ciufu, 2014).

The results listed in the Table 6 reveal an outstanding performance when the algorithm is deployed in a multi-core architecture, reducing the solution time almost in a half of a normal solution. This characteristic provides an excellent opportunity for sensitivity calculation of large-scale distribution systems.

Table 6: Solution time for the test network implemented.

Speed test	Reference set	One-core	Multi-core
Average time, ms	170.4	147.4	82.6
Minimum time, ms	157	144	68
Maximum time, ms	183	156	98

After knowing the sensible buses, the system operator can select the number of BESS to install. Then, a parallel genetic algorithm (PGA) approach is implemented in order to determine the size of the BESS in a low calculation time. The sequence diagram of the PGA implemented is illustrated in the Figure 22.

Due to the easy architecture implementation, the size of the power distribution system, and the actor-oriented model used between OpenDSS and NI LabVIEW, this approach is programmed

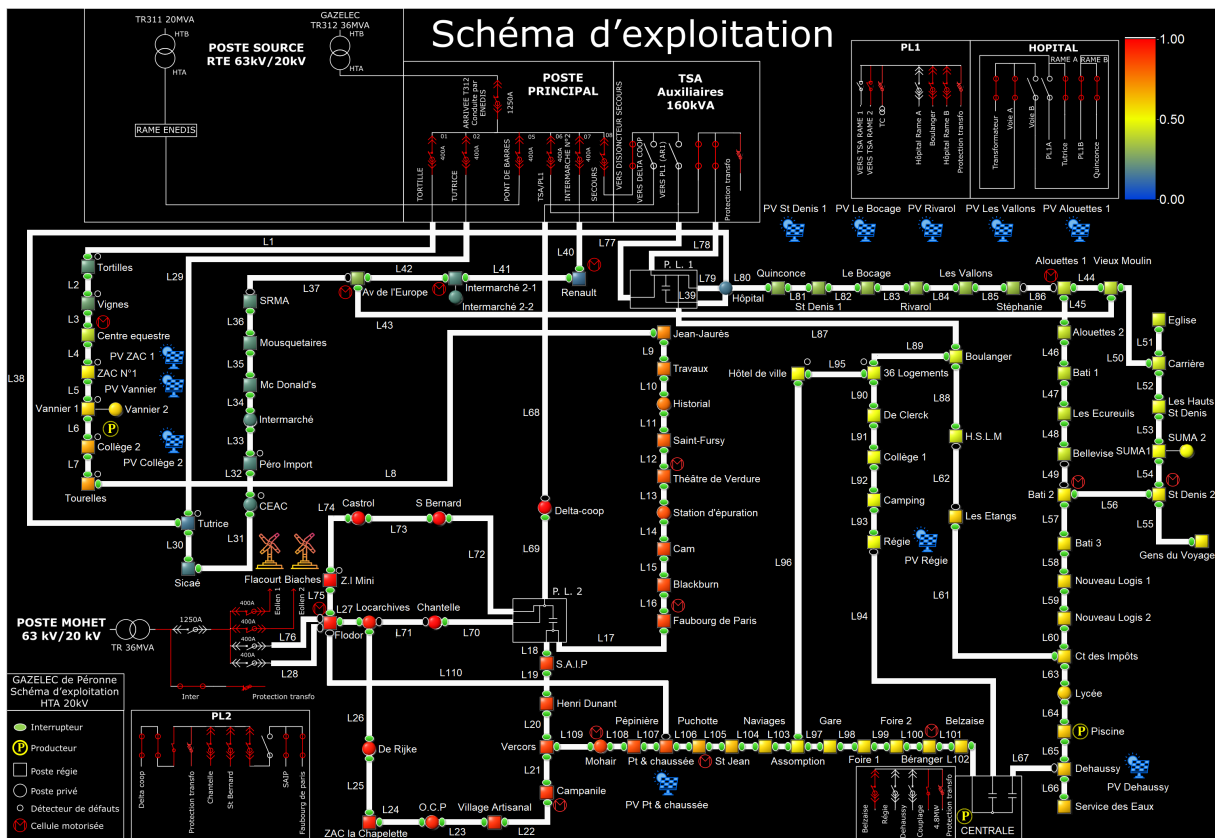


Figure 21: Sensitivity heat map visualization result on the Bank of Energy experimental platform.

using a master-slave genetic algorithm parallelization. The function of the master is allocating tasks to the slaves, collecting the results, and synchronizing the processes. In the other hand, the function of the slaves is to execute the genetic operations at each generation.

The PGA procedure is executed in multiple steps. First the initial system conditions are defined, choosing the number of batteries and setting their initial values and constraints. Then, the fitness function is calculated for the parents generation. A new BESS chromosome is created and evaluated in the power distribution system, the co-simulation between OpenDSS and NI LabVIEW is done to review the optimization constraints. After the constraints are validated, the PGA operations are executed to determine a new generation. The algorithm is executed according to the termination criteria, finding at the end the best BESS output power rating installation for the distribution system.

The PGA is applied to find the optimal power rating size of a BESS in the Gazelec power distribution system considering two system approaches: the voltage profile improvement and the loss minimization. As a result, the fitness function of the PGA is equal to each approach of the BESS application to be analyzed. The optimization problem is validated using the same test case study integrated in the sensitivity analysis. The results listed in the [Table 7](#) show an improvement in the distribution system when a BESS is installed using both approaches.

After the optimization problem is validated, the PGA is deployed to evaluate the solution performance in the Gazelec of Peronne distribution system considering the following case study conditions:

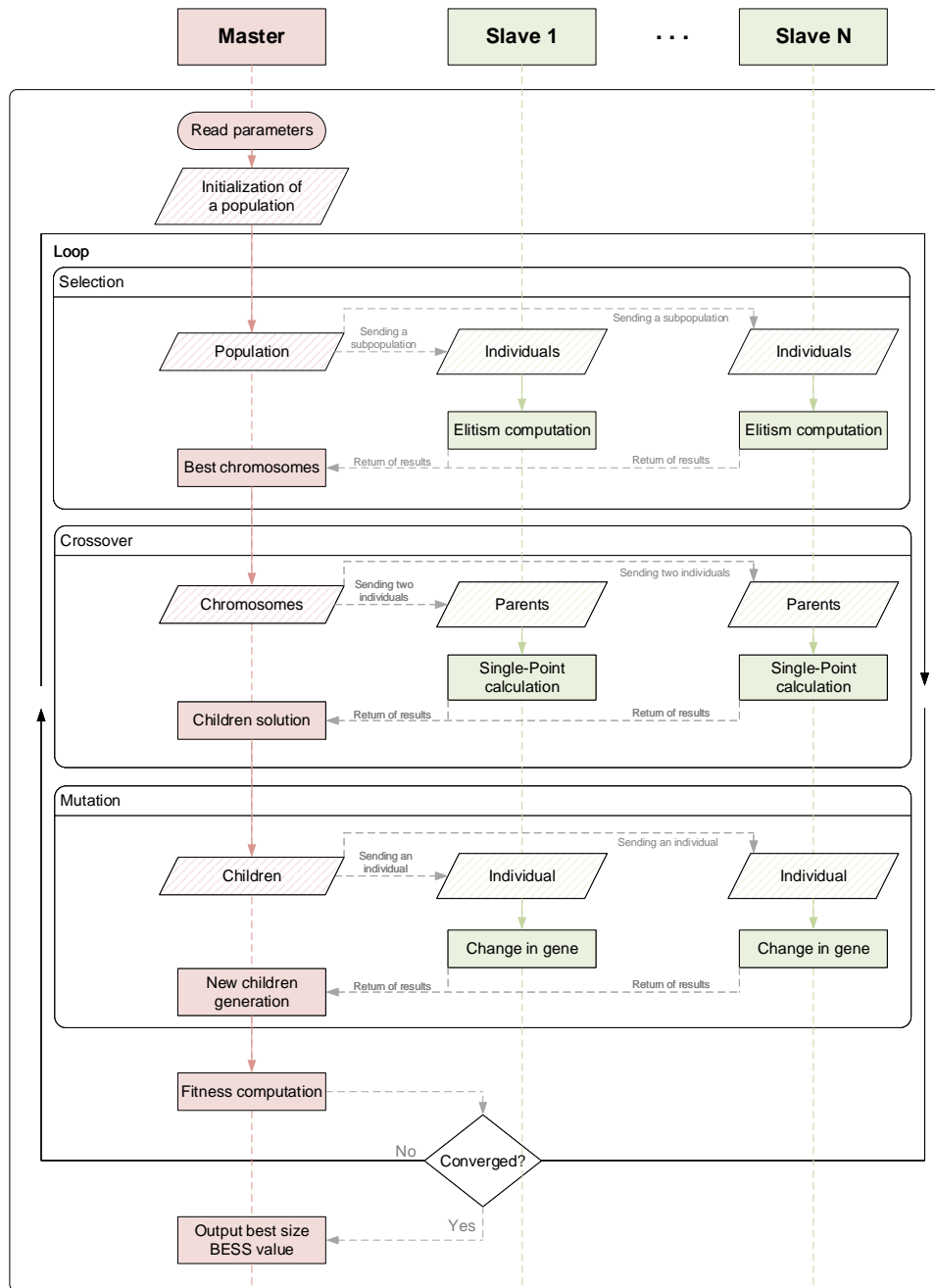


Figure 22: Sequence diagram of the PGA implemented.

- Case study I: The system without a BESS installation.
- Case study II: The system with a centralized BESS installation in the most sensitive bus improving the voltage profile.
- Case study III: The system with a distributed BESS installation in the three most sensitive buses improving the voltage profile.
- Case study IV: The system with a centralized BESS installation in the most sensitive bus minimizing the system losses.



Table 7: Validation results of the optimization problem using the test case study.

	Total active power, MW	Voltage range, p.u.	Total active power losses, MW	BESS output power rating, MW
Without BESS	598.511	1-0.88	19.51	-
BESS for voltage profile	103.257	1-0.929	10.25	477
BESS for system losses	263.165	1-0.925	7.16	314

- Case study V: The system with a distributed BESS installation in the three most sensitive buses minimizing the system losses.

The single-core GA and the PGA are deployed to compare the solution performance of both algorithms. Moreover, a BESS power installation is suggested according to the simulation results. For this purpose, a BESS is installed under two perspectives: centralized and decentralized localization considering the most sensitive buses found in the sensitivity analysis. The distribution system is analyzed considering the worst scenario of load chargeability (100%).

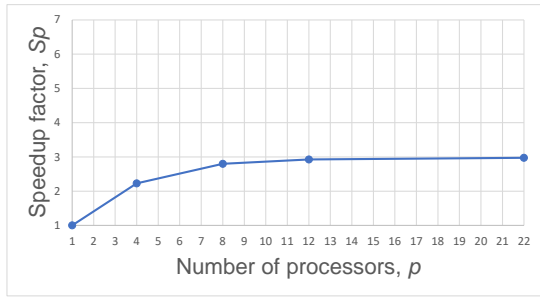
The performance evaluation of the PGA is a difficult task by itself. To do the evaluation, it is used as performance measure the average number of function evaluations to compute the optimum as well as the time needed to complete the computation. These performance measurements are compared with the single-core GA to demonstrate the advantages to use this algorithm in a parallel architecture. The [Table 8](#) shows the parameter set of each GA architecture.

Table 8: Architecture description of the GA tested.

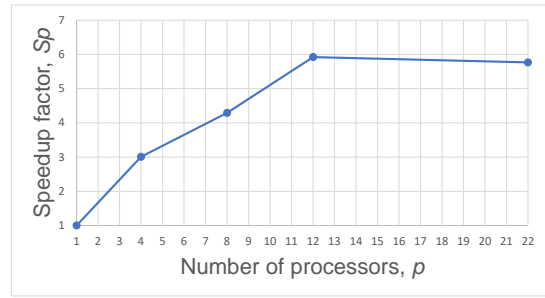
	Classical GA	PGA
# of populations	1	1
# of subpopulations ( $\lambda$ )	1	4, 8, 12, 22
# of individuals ( $\mu$ )	50, 20	20
Method of operation	-	Synchronous
# of sync points	-	many

In order to evaluate the PGA performance capability, the speedup factor is calculated considering the algorithm performance results obtained for each test case study. The speedup factor results are shown in [Figure 23](#) demonstrating a general improvement in the use of a parallel architecture.

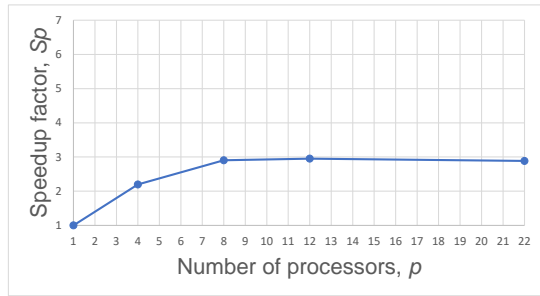
In the other hand, the optimal BESS power rating results based on the different study cases using the two optimization approaches and the solution aforementioned are shown in [Table 9](#) and [Table 10](#). The states of charging and discharging of the BESS are analyzed to evaluate the impact of both conditions over the Gazelec of Peronne distribution system.



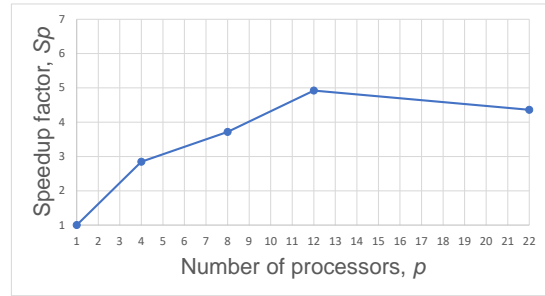
(a) Centralized BESS installation for voltage profile improvement.



(b) Distributed BESS installation for voltage profile improvement.



(c) Centralized BESS installation for system losses reduction.



(d) Distributed BESS installation for system losses reduction.

Figure 23: Speedup factor calculated to evaluate the PGA performance for a:

Table 9: Optimal BESS sizing results with a charging installation.

Case study	Optimal sizing of BESS	System results when BESS is charging		
		Total active power, MW	Voltage range, $p.u.$	Total active power losses, MW
I	No BESS	24.99	1-0.94	0.438
II	Delta-coop (6.9MW)	32.09	1-0.9	1.049
III	Delta-coop (2.5MW) Chantelle (2.4MW) Saint Bernard (2.4MW)	32.5	1-0.9	1.08
IV	Delta-coop (5.6MW)	30.8	1-0.907	0.903
V	Delta-coop (2MW) Chantelle (2MW) Saint Bernard (2MW)	31.22	1-0.906	0.93

The loss minimization approach shows a slight improvement in the system results with regard to the voltage profile improvement approach. A smaller BESS sizing is also needed with a loss minimization approach for a centralized and a decentralized BESS installation. The system results shows that BESS can significantly introduce great benefits to the Gazelec of Peronne distribution system operation providing peak shaving, improving the voltage profile and an active power losses reduction. Moreover, the different optimal BESS test scenarios schemes

Table 10: Optimal BESS sizing results with a discharging installation.

Case study	Optimal sizing of BESS	System results when BESS is discharging		
		Total active power, MW	Voltage range, p.u.	Total active power losses, MW
I	No BESS	24.99	1-0.94	0.438
II	Delta-coop (6.9MW)	17.97	1-0.949	0.313
III	Delta-coop (2.5MW) Chantelle (2.4MW) Saint Bernard (2.4MW)	17.55	1-0.9494	0.301
IV	Delta-coop (5.6MW)	19.25	1-0.947	0.304
V	Delta-coop (2MW) Chantelle (2MW) Saint Bernard (2MW)	18.84	1-0.948	0.294

with different BESS installation illustrate that the solution for optimal BESS sizing proposed can provide planners flexibility according to the system needs.

A new toolkit panel is integrated in the software layer of the experimental platform to deploy the BESS integration procedure. This panel places a heavy emphasis on a simple and an analytical examination state of the distribution system, providing an infrastructure for integrate a BESS solution in the distribution system. The [Figure 24](#) shows the data visualization panel designed after simulated the case study II.

This new methodology based in parallel computing are highly extensible. The combination between the sensitivity analysis and an evolutionary algorithm lends itself to application to other studies. The techniques presented become suitable for real-time network control scenarios including hardware devices into the analysis. The changes in the network loading requires that the system be re-calculated periodically. The processing time could be significantly reduced using a multi-threading approach.

### *Conclusions and perspectives*

The work reported in the present thesis covers the subject concerning the supervision, analysis and optimization of power distribution systems considering the penetration of distributed energy resources and energy storage systems.

First, a comprehensive survey is developed about the state of the art of the different methodologies, tools and challenges necessary to allow a complete understanding of the challenges that must be fulfilled for ensuring the supervision and analysis of the distribution networks.

Based in the concepts collected, a hardware/software experimental platform is designed in order to develop a new paradigm to deploy power distribution system analysis, based in RT simulations and hardware in the loop testing. After the execution of different test cases, it

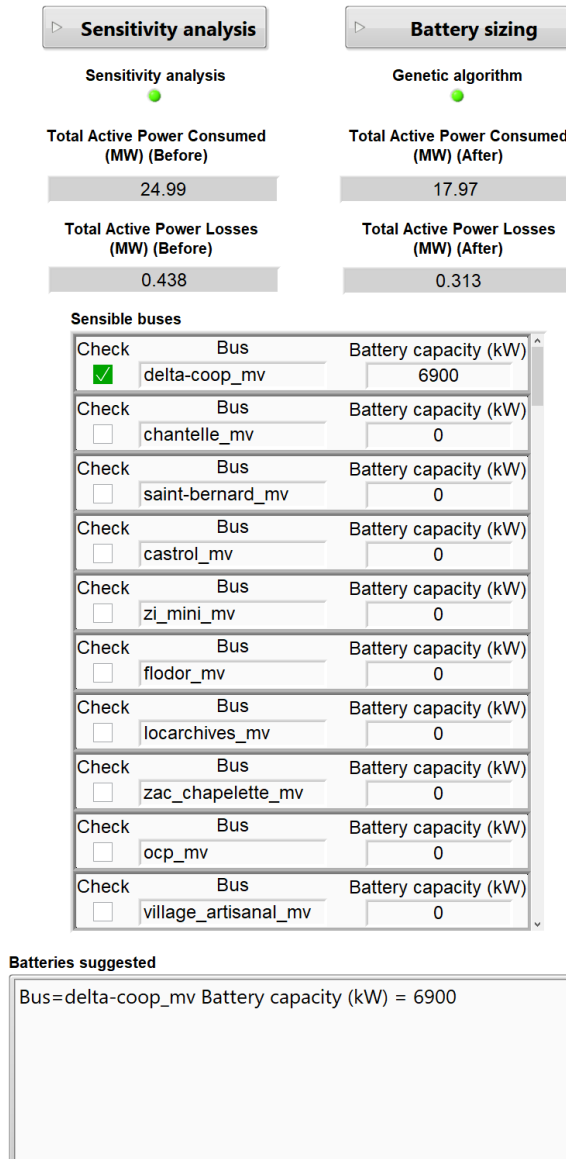


Figure 24: User data visualization panel of the toolkit developed.

is proven that the experimental platform performance based in the architecture selected is largely enough for the RT supervision and analysis of the power distribution systems.

Because the power system modeled is a real French distribution network with distributed generation composed of two wind farms and multiple photovoltaic panels installed along the grid, a study is performed to evaluate and determine the suitable integration of battery energy storage systems into the grid. A background analysis is also done to know the existing methodologies to locate and size the battery energy storage systems.

As a result of this study, a novel methodology is presented for BESS placement and power sizing using parallel computing. The hybrid methodology implemented is evaluated under a test case and a real case scenario. The results reveal that the use of a multi-threaded approach reduce the execution time to find an accurate answer for BESS location and output power rating. Moreover, a correct power rating sizing and placement evaluation of the BESS is crucial

in the integration into a smart grid. The development of algorithms for placement and sizing for BESS provides a higher efficiency and reduces the installation cost.

An energy management system of the BESS is the next step to be integrated into the system. For this purpose, a new methodology have to be developed to determine the energy capacity of the BESS, as well as, the optimization of the number of charge/discharge cycles according to the system needs.

**Note:** *VERTPOM project is conceived to evaluate the multi-fluid systems found in a territory, but due to a high demand to improve the electrical distribution system, this thesis intends to deal firstly with this objective. New insights will be incorporated considering the other fluids in the upcoming projects.*

## GENERAL INTRODUCTION

---

The rapid evolution of the power systems has resulted in an impact over the system network. Based on the classical model of the energy consumption chain (generation, transmission, and distribution), the power distribution system is the most concerned due to the technological developments, regulatory policies and environmental requirements.

Consequently, the system operator deals with several challenges to maintain a well-functioning network, as well as the system stability and load balancing. To attend to these challenges, the use of an energy management system is necessary based on an advanced metering infrastructure and an advanced distribution automation.

This has resulted in the development of the Bank of Energy experimental platform, a real-time platform designed for the supervision and analysis of power distribution systems, allowing to perform several studies such as power flow, sensibility evaluation, state estimation, condition monitoring, fault diagnosis, dynamics simulation, among others. This platform is composed of an architecture hardware/software capable to deploy hardware in the loop testing, providing a comprehensive decision-making tool properly to monitoring the current distribution system conditions and supporting the decisions made by the system operator.

A real distribution system network is used to validate the Bank of Energy experimental platform concept. A French 20 kV distribution system is modeled in OpenDSS and a human machine interface is also developed in NI LabVIEW® to improve the user experience. The consumption data is retrieved from the CT-IBox smart meters installed in the city related. The distributed energy resources were modeled as well. The electromagnetic system behavior is validated under different operating conditions by the technical operators of the real system.

Due to the increased presence of distributed energy resources in this system (wind farms, photovoltaic energy and thermal energy) and considering the total power losses from the system assets, a penetration study of battery energy storage systems (BESS) is performed as the first stage for the best integration of them in this context. As a result, a new methodology for BESS placement and sizing is proposed.

This methodology is divided in two approaches. First, a sensitivity analysis algorithm to evaluate the introduction of BESS elements which supports the system without affecting or disturbing its correct operation. Knowing the most sensible buses, a second algorithm based on an evolutionary approach determines the optimal output power rating size of the number of BESS chosen. These algorithms are upgraded to exploit the parallel processing capabilities of the Bank of Energy experimental platform and to cover the basic needs for the simulation of smart grids.

Part I

A NOVEL PLATFORM FOR SUPERVISION, ANALYSIS AND  
OPTIMIZATION OF POWER DISTRIBUTION SYSTEMS





# INTRODUCTION TO CONDITION MONITORING SYSTEMS FOR POWER DISTRIBUTION GRIDS

---

## Contents

---

1.1	Introduction . . . . .	4
1.2	Condition monitoring for smart grids . . . . .	6
1.2.1	Fault diagnosis for power distribution grids . . . . .	7
1.3	Smart grid monitoring . . . . .	10
1.3.1	Electromagnetic transients simulation (EMT) . . . . .	13
1.3.2	Transient simulation analysis (TSA) . . . . .	13
1.3.3	Hybrid simulation (EMT and TSA) . . . . .	14
1.4	Real-time (RT) simulation . . . . .	14
1.4.1	Fully real-time digital simulator (DRTS) . . . . .	15
1.4.2	Hardware in the loop (HIL) simulator . . . . .	16
1.5	Experimental platforms for power distribution system analysis . . . . .	18
1.5.1	Consumption and generation forecast . . . . .	19
1.5.2	Cyber resilience . . . . .	19
1.5.3	Supervisory control and data acquisition . . . . .	19
1.5.4	RT capabilities . . . . .	20
1.6	Challenges of RT simulators for smart grids innovation . . . . .	20
1.6.1	RT simulation of large-scale power systems . . . . .	21
1.6.2	Accuracy of power electronics (PE) simulation . . . . .	22
1.6.3	Power distribution fault detection . . . . .	22
1.6.4	Demand side management (DSM) . . . . .	23
1.6.5	RT and intelligence requirements for business . . . . .	24
1.6.6	Artificial intelligence (AI) for smart distribution grids . . . . .	24
1.6.7	Security and privacy . . . . .	25
1.7	Chapter summary . . . . .	26

---

## 1.1 INTRODUCTION

The power systems evolution is fundamental to the modern society and its economy. Driven by technological development, regulatory policies, and environmental requirements, energy challenges are continually expanding electricity distribution (Tan and Novosel, 2017). The power systems growth is more obvious in the distribution system landscape because of the proliferation of new technology trends and multiple challenges which are emerging such as (Cai et al., 2019; Gharavi and Ghafurian, 2011; Qi et al., 2011; Arnold, 2011; Annaswamy and Amin, 2013):

- Integration and management of distributed energy resources (DER) and energy storage systems to address global climate change and enable an overall energy cost reduction.
- Active customer participation to ensure better energy conservation.
- Efficient utilization of existing assets to achieve a suitable performance and a long term sustainability.
- Reliable and secure two-way optimized power quality flow to reduce losses and the cost of energy.
- Incorporation of real-time (RT) monitoring and control across distribution systems to guarantee safety and operational flexibility.

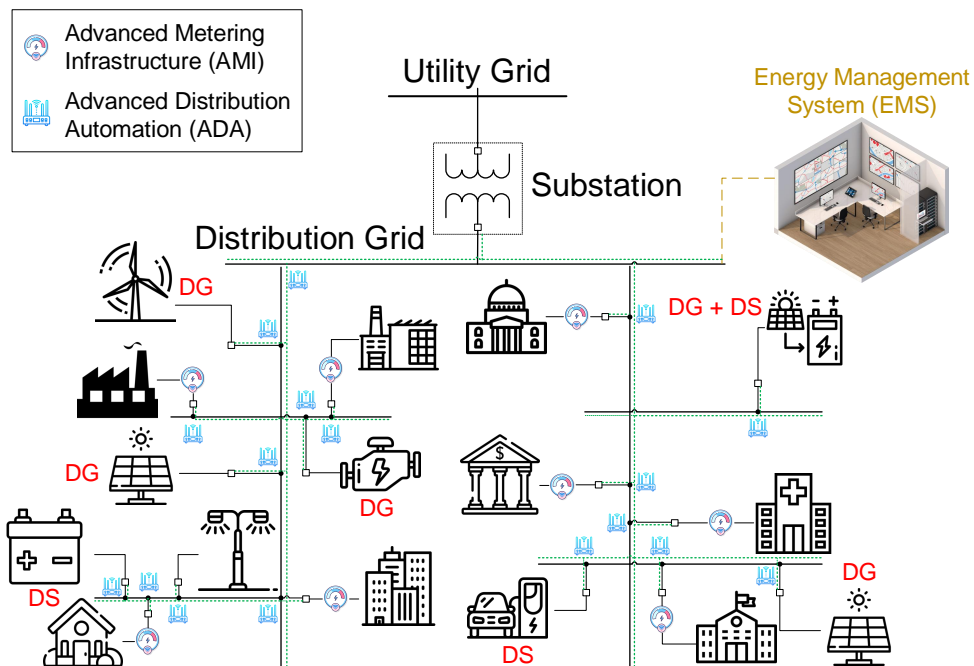


Figure 1.1: AMI, ADA, and EMS architecture through a smart distribution system.

This vision of a smart distribution system shown in Figure 1.1, it has belonged to a widespread equipment and system monitoring capability, where an advanced metering infrastructure (AMI), and advanced distribution automation (ADA) plays a fundamental role to achieve an energy management system (EMS) architecture (Arritt and Dugan, 2011; Valencia et al., 2016). In consequence, it ensures a flexible, controllable and automated distribution system,

including the integration of DER to enhance system reliability, energy management among the distributed generation (DG) and distributed storage (DS), and a safe and reliable operation (Sugumar et al., 2019; McGranaghan and Goodman, 2005; Goodman and McGranaghan, 2005; Madani et al., 2015).

This has resulted in an increased demand for knowledge to apply AMI and ADA well-working. In this way, one possible alternative is to realize a scheme analysis process in charge to estimate the state of the system under real conditions, including the design and optimization process, for the determination of power electronics components ratings and for analyzing power systems grid in general. As shown in Figure 1.2, its capabilities can provide the necessary monitoring and alarm detection in several changes which can occur in the parameters of the physical system (Qiao and Lu, 2015), allowing an earlier detection and localization of fault events to mitigate their impacts on the overall stability of the distribution grid (He and Zhang, 2011).

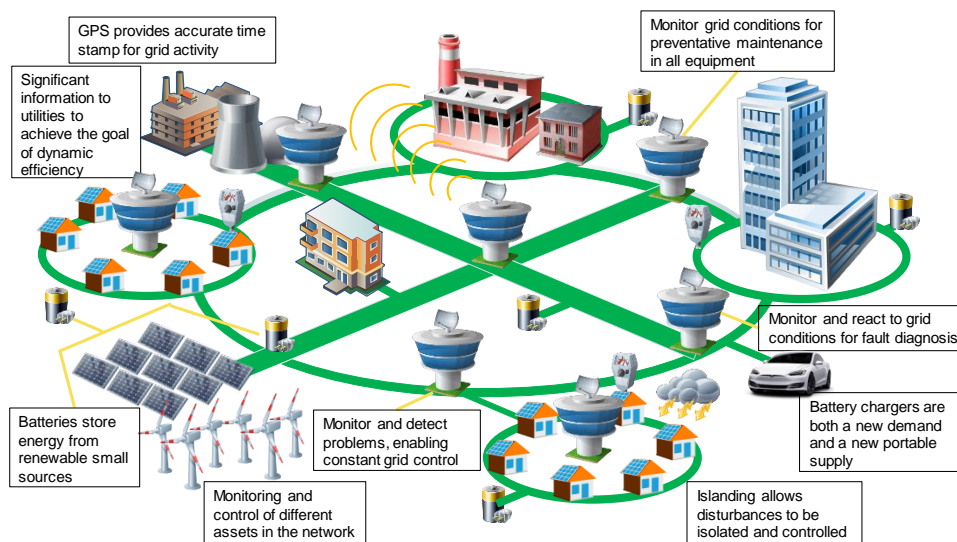


Figure 1.2: Monitoring enhancement for the distribution system landscape.

As it is described in Figure 1.3, the use of a RT monitoring architecture represents an enhanced evolution of the grid towards a smart grid according to different considerations including: fault diagnosis, contingency analysis, supervision and optimization of different assets in the network, security of critical components, significant information to utilities to achieve the goal of dynamic efficiency, power quality issues, among others (Isaac et al., 2011).

Altogether will allow a platform able to provide the operator with a RT decision-making tool, properly to monitor the current distribution system conditions and supporting decisions made in an automated EMS (Martinez, Henao, and Capolino, 2019). Additionally, digital RT simulations (DRTS) provides functions such as supervisory control and data acquisition (SCADA), alarming, system state estimation, optimization and contingency analysis (Byrne et al., 2018; Giri, 2015; Forth and Tobin, 2002). These situations will vary based upon some factors, including day time, forecast system load, and weather conditions for local and interconnected areas (Luna et al., 2018; Taha, Abdeltawab, and Mohamed, 2018; Podmore and Robinson, 2010).

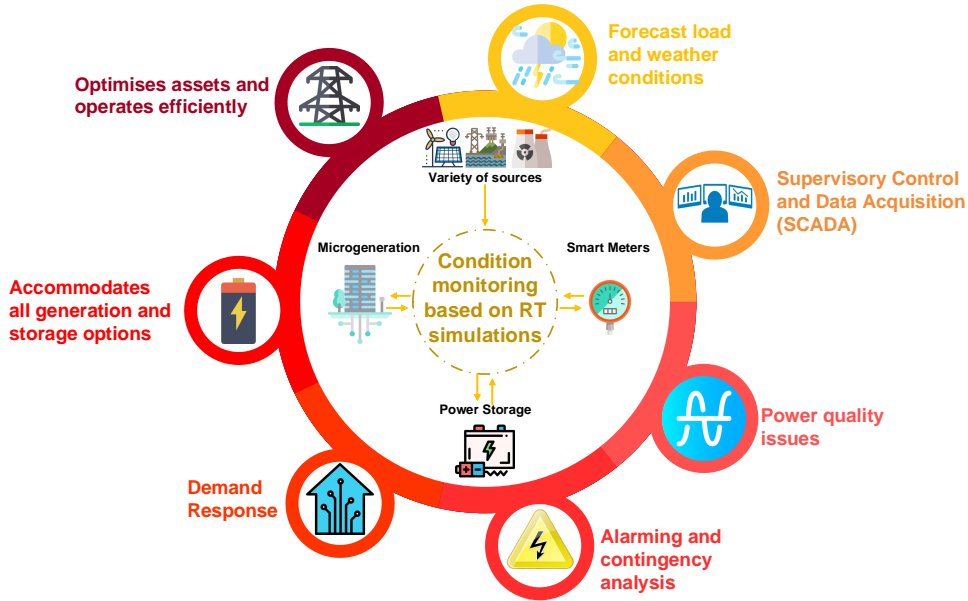


Figure 1.3: RT decision-making tool key elements.

1.2 CONDITION MONITORING FOR SMART GRIDS

Condition monitoring is an important method of monitoring the condition state of systems, devices, components and so on. It basically could be defined as a systematic collection of data over a period of time, which monitors the changes on the operating parameters and system health in the system in order to determine the most appropriate action (Groom, 2014).

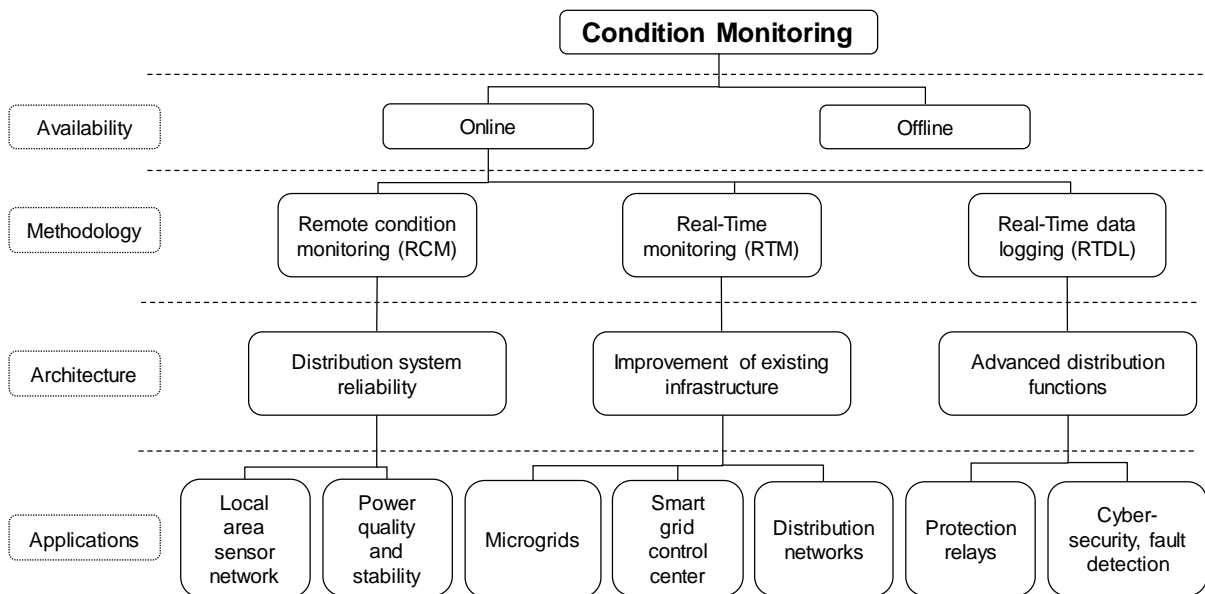


Figure 1.4: Smart grid monitoring at various stages of development.

In Figure 1.4 a modular description of condition monitoring is presented based on the requirements and considerations of each application. The constant availability of a collection of data allows to do a permanent analysis of the online information. Furthermore, this process of collecting data in condition monitoring is categorized in three methodologies:

- **Remote condition monitoring:** Transmits periodic updates and alerts to a remote host in long periods of time, often limited by power and data communication restrictions.
- **Real-time monitoring (RTM):** Allows maintenance scheduled to view data in field, with high data rates.
- **Real-time data-logging:** Uses higher sampling rates than RTM, but often requires data storage, that later transmitted or retrieved.

### 1.2.1 Fault diagnosis for power distribution grids

Fault diagnosis is a multidisciplinary technology that involves mathematics, control, information and reliability theories. Fault diagnosis could be applied to any system including power distribution systems. Fault diagnosis is critical to ensure the safety of the power distribution system and its assets. [Table 1.1](#) shows the common definitions of the terminology used in fault diagnosis.

Table 1.1: Terminology used in fault diagnosis.

Term	Definition
Fault	An anomaly due to which a system is unable to perform a specified function.
Fault mode	The macroscopic behavior of a fault, also known as the type of fault.
Fault cause	The key factors causing a fault.
Fault mechanism	The nature of changes in physical processes that eventually develop into a fault.
Fault feature	The feature or parameter that reflects the abnormality caused by a fault.
Fault detection	The process of determining whether a fault has occurred.
Fault isolation	The process of determining the type and/or location of a fault.
Fault identification or estimation	The process of determining the magnitude/intensity of a fault.
Fault diagnosis	The process of detecting, isolating, and estimating a fault.

#### 1.2.1.1 Fault diagnosis methodology

Fault diagnosis could be represented by the flowchart seen in [Figure 1.5](#). The process is divided into multiple sections. First, data acquisition is used to process and store information from experimental measurements and high-fidelity simulation models, mainly including the

main variables like voltage, current, power, and losses for the distribution system. The processed data will be used for demand response, improvement in the power quality, fault characterization, reduction in active and reactive power losses, enhancement in voltage profile, among others. The electrical characteristics are extracted by the smart grid monitoring, including information from intelligent electronic devices (IEDs), modeling, analysis and simulation. Then, the fault diagnosis and the fault prognosis can be performed based on the characteristics extracted (Hu et al., 2020).

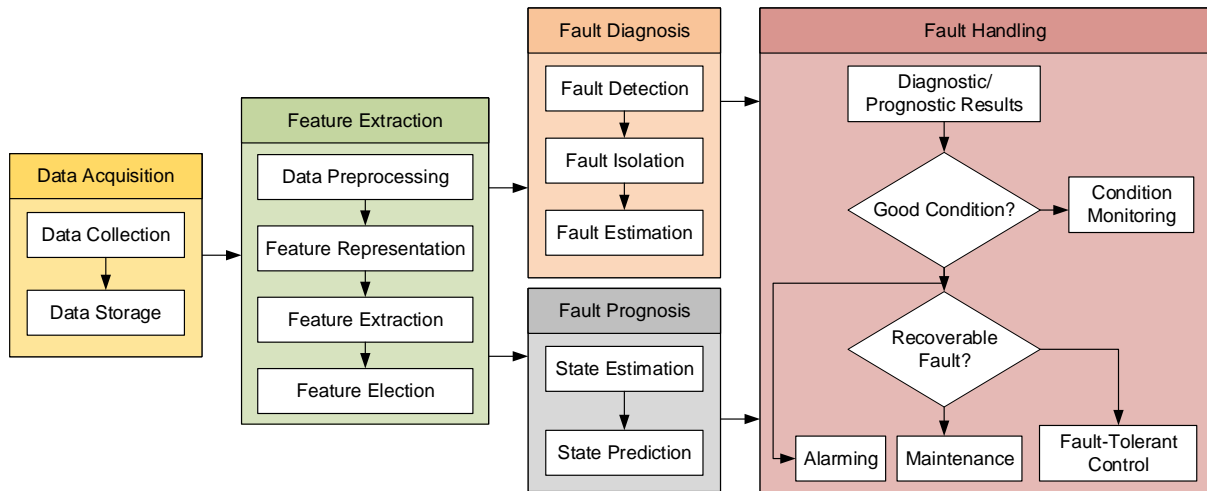


Figure 1.5: General fault diagnosis (Hu et al., 2020).

After to collect the data information, the methodology to react enabling the indication of future failure occurrences and preventive maintenance is based on two operating procedures (Groom, 2014):

- **Diagnosis:** Addressed by three main components when a fault occurs.
  - **Fault detection:** Indicates a deteriorated condition in the monitored system.
  - **Fault isolation:** Allows to locates the component that is faulty.
  - **Fault estimation:** Enables the recognition of the fault pattern when is detected.
- **Prognostics:** Allows to predict if a fault is impeding, estimating the time and type of the fault that will happen. It permits as well to predict remaining useful life of the device.

Finally, the fault-handling module analyzes and assesses the results from the fault diagnosis and the fault prognosis and makes decisions, such as alarming, initiating fault-tolerant control to maintain safe operation and meet certain performance, isolating system equipment or feeders, activating system protections, and even cutting off the power supply.

#### 1.2.1.2 Feature extraction

Feature extraction is a pre-processing step for fault diagnostics. The accuracy of feature extraction highly depends on the method used. Here, we focus on two main feature extraction

methods: signal processing-based and model-based. Based on the measurements, model-based state estimation and parameter estimation methods can be used to extract fault features.

Theoretically, artificial intelligence algorithms can also be applied to extract fault features as an alternative to the physics-based model. This method is expected to extract more accurate features with online training and continuous improvement but with the computational cost of continuous training.

The signal processing method does not require modeling work, but it may not achieve fault isolation. In contrast, it is easier for the model-based method to quantify and locate specific faults by exploiting the relationship between faults and model states or parameters.

Table 1.2: Comparison between feature extraction methods.

Feature extraction methodology	Description	Advantages	Disadvantages
Signal processing	Measures the variables directly to the distribution system to determine the fault.	More practicable to analyze qualitatively. No need for system modeling.	Difficult to detect failures and to achieve fault isolation.
Model-based	Apply estimation techniques to identify changes in the system state and model parameters.	Suitable for quantitative application analysis and fault isolation	Depends on the model accuracy.
Artificial intelligence	Recognize fault features based in a machine learning process.	Recommended for forecasting and prognostics.	Computational cost of continuous training.

### 1.2.1.3 Diagnosis method

According to (Hu et al., 2020) and how is shown in [Figure 1.6](#), diagnosis methods can be classified in three domains:

- **Knowledge-based methods:** These diagnostic methods utilize the knowledge and observation of distribution systems and are specially suitable for nonlinear and complex systems, without need for developing mathematical models.
- **Model-based method:** It is based on a residual signal obtained by comparing the measurable signal with the signal generated by the model. After, the residual signal will be evaluated to determine the diagnostic results. These methods can not only detect faults but also locate faults and estimate their magnitude.

- **Data-driven method:** These methods directly analyze and process the running data to detect faults without relying on the accurate analytical model and the experience of experts.

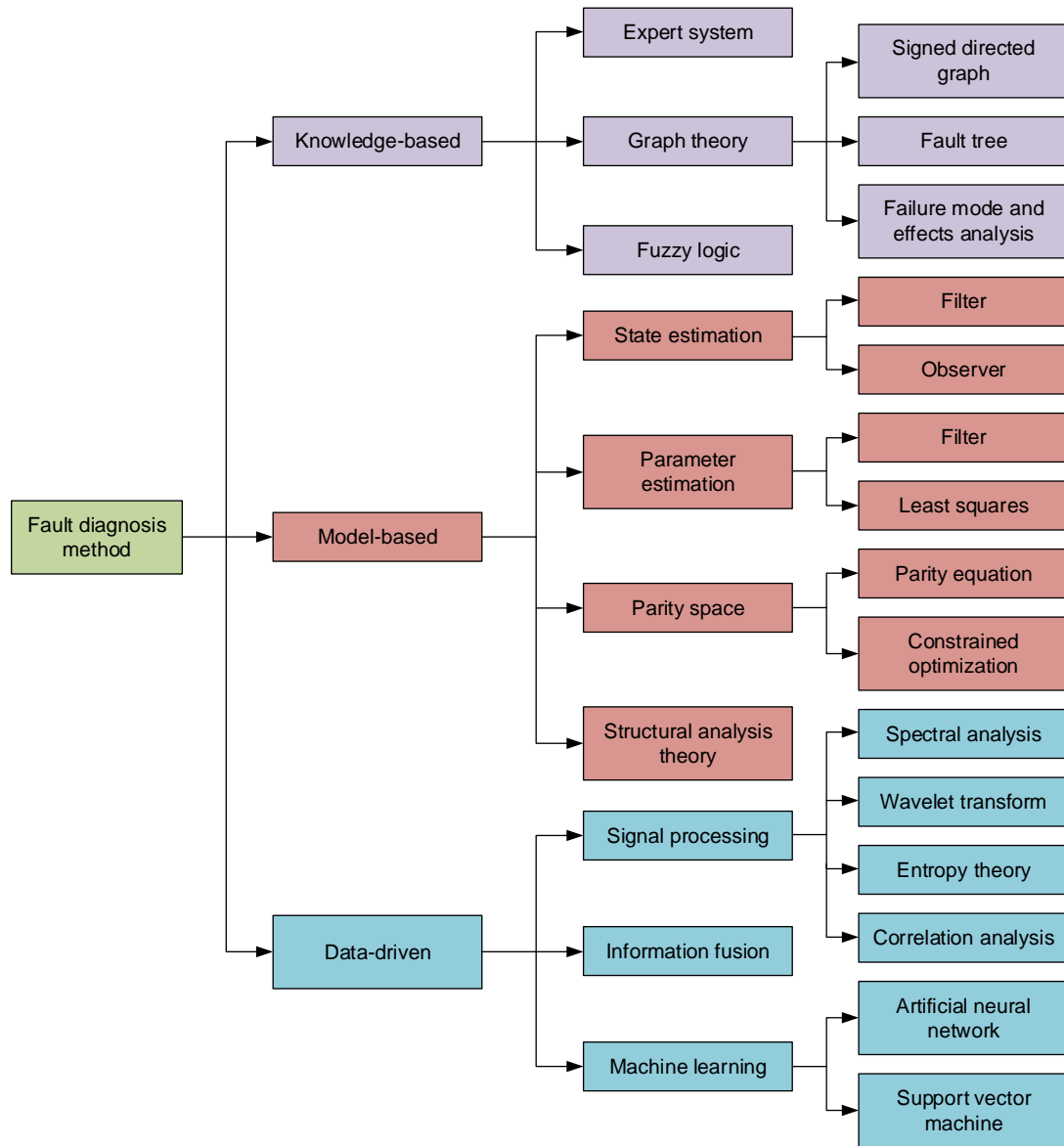


Figure 1.6: Fault diagnosis classification (Hu et al., 2020).

### 1.3 SMART GRID MONITORING

The power grid system has atypical behaviors and outages that despite the measurement devices and SCADA systems installed around the system are not enough to supply a complete information of situational awareness of the network system. Due to these shortcomings, a simple and cost effective solution for smart detection is based on the smart grid monitoring.

Smart grid monitoring is a technique or process that implies to observe all important components in all critical locations, requires the collection of large amount of data to predict a



system failure precisely and timely, and thus to obtain a highly reliable and non-disruptive smart grid system (Soliman, Wang, and Blaabjerg, 2016). A block diagram representation of smart grid monitoring for diagnosis and fault detection in a power distribution system is shown in Figure 1.7.

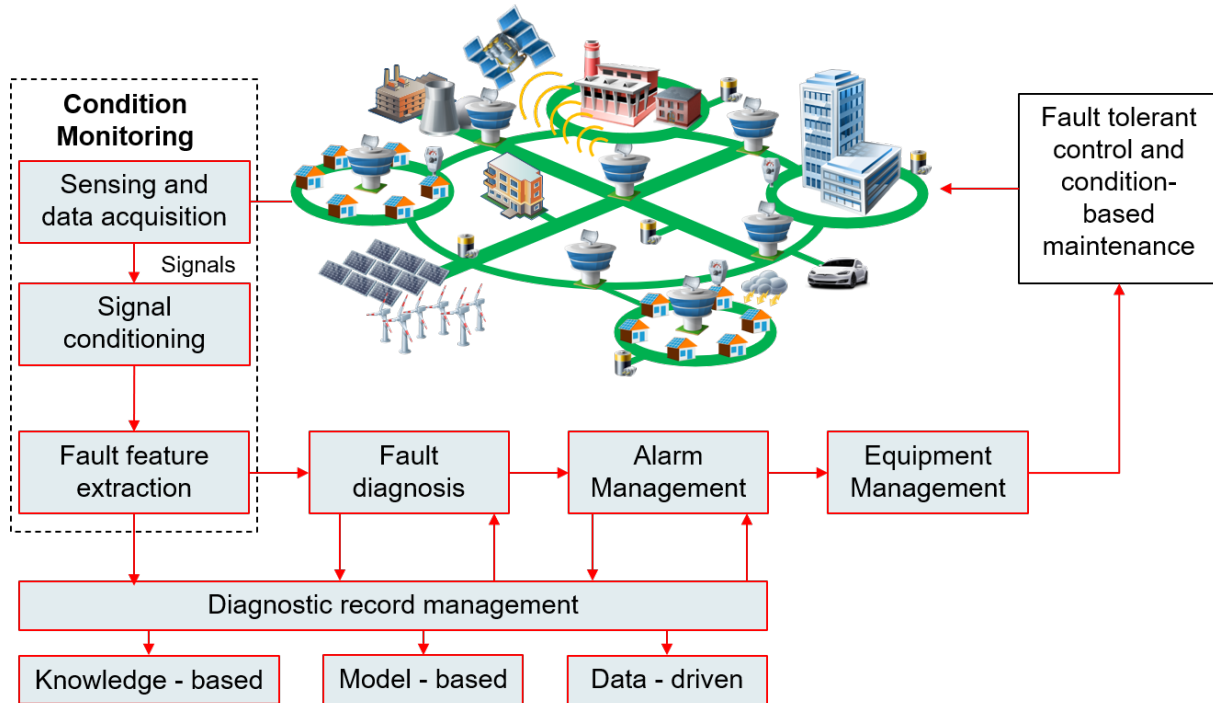


Figure 1.7: Condition monitoring applied to power distribution systems.

Since the smart grid monitoring was implemented in the current power system, robust intelligent monitoring systems have evolved continuously to reinforce the smart grid and power systems monitoring (Table 1.3) (Baki, 2014; Zhang and Lai, 2012; Ilonen et al., 2005; Salvadori et al., 2013). The result is a monitoring architecture that provides a wide variety of advanced functions (McGranaghan and Deaver, 2012):

- **Distribution system reliability:** The monitoring system provides continuous monitoring of vital operating parameters to allow strategic operation of the distribution grid for reconfiguration, fault diagnosis, and other functions to improve reliability.
- **Improved utilization of existing infrastructure:** The monitoring system enables efficient operation of the distribution grid, allowing closer control of voltage profiles and minimizing electrical losses.
- **Advanced distribution functions:** The monitoring system enables fault detection in the distribution grid, that contribute to the outage prevention and recovery, optimal system performance under changing conditions, and reduced operating costs, by the strategic use of IEDs and other new distribution system technologies.

To understand the information for supporting activities such as ADA, AMI, or EMS, simulations are the primary tool that one must rely on (Chakraborty and Bose, 2017; Chiniforoosh et al., 2010). Accurate simulations are oriented to different functional applications such as design, operation, planning, modeling, control, testing, post event analysis, fault diagnosis,

Table 1.3: Fields to apply smart grid monitoring.

Application	Purposes
Local area sensor network	Provide benefits to power quality, grid efficiency and health monitoring.
Power quality and stability	Track the modes of voltage collapse and identify vulnerable areas.
Microgrids	Integrate DERs modeling, monitoring and control.
Smart grid control center	Implement parallel computing infrastructure.
Distribution networks	Increase customer satisfaction, improve the delay of the network, enhance the control and management system of the active distribution network.
Protection relays	Allow new power system problem-solving, cost saving.
Cyber security, fault detection and communication	Facilitate the control of power system, collect data information, and protects from small leaks and theft.

among others (Panwar et al., 2013; Montenegro, Ramos, and Bacha, 2017). According to the architecture, simulators can be differentiated as follows:

- **Analog simulators:** These are composed of two different approaches. The build of scaled models using electrical elements for reproducing the behavior of a real system, and the inclusion of active electronic circuits to overcome speed limits in digital simulators (Nagel et al., 2010).
- **Digital simulators:** These are computer based and consists of algorithms for solving linear and nonlinear equations in order to reproduce the behavior of the physical system. These simulators can work offline, on-line and in RT for recreating different scenarios (Ren et al., 2011). In (Montenegro, Ramos, and Bacha, 2016), the author reveals the most recognized digital simulation tools available nowadays.
- **Hybrid simulators:** For addressing the limits identified in analog and digital simulators, the hybrid simulator combines their strengths for evolving into an advanced simulation platform. This simulator combines the fidelity of the analog simulators with the models recreated in the discrete time domain using digital systems (Gick, Gallenkamp, and Wess, 1996).

Based on the simulation high fidelity-based applications, simulations can be classified in terms of temporal characteristics as a snapshot or time-sequential. However, time-sequential simulations are essential for interoperability validation and other time dynamic phenomena as shown in Figure 1.8 (Hernandez et al., 2017; Gurralla et al., 2016).

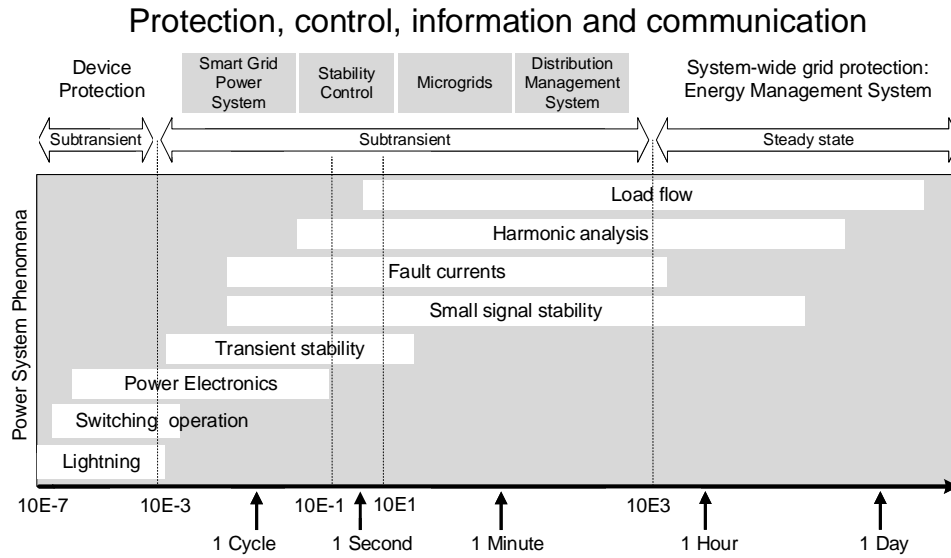


Figure 1.8: Overview of time ranges of power system dynamics.

### 1.3.1 Electromagnetic transients simulation (EMT)

EMT simulation is a valuable preliminary step for detailed representation of power electronic devices design and performance testing, and for analyzing power systems in general (Su, Duan, and Zeng, 2008; Su et al., 2004). According to (Jalili-Marandi et al., 2009) definition, EMT is the response of the power system elements to a perturbation caused by external electromagnetic fields or to a change in the physical configuration of the network. EMT simulation tools may be classified into two categories (Mahseredjian, Dinavahi, and Martinez, 2009):

- **Off-line:** Conducts simulations on a generic computer using a programmed mathematical solution. The off-line tools are usually more precise for the network solution part.
- **On-line:** Capable of generating results in synchronicity with a RT clock. RT methods are most useful for studying actual manufacturer equipment and embedded algorithms.

### 1.3.2 Transient simulation analysis (TSA)

TSA mainly deals with the power transfer stability of large power systems. Basically, AC network power system stability depends on the synchronicity of its machines when the system is perturbed by a large disturbance (Jalili-Marandi et al., 2009; Dufour, Jalili-Marandi, and Bélanger, 2012; Jalili-Marandi and Dinavahi, 2009).

Instead of EMT simulation, this type of simulation has a larger time scale, going from milliseconds to weeks, months or years. However, large integration time-step of the TSA programs is the main restriction for the detailed representation of nonlinear elements (power electronic devices) and dynamically fast events (line energization, switching, resonance analysis) (Nagel et al., 2013).

### 1.3.3 Hybrid simulation (EMT and TSA)

For transient evaluation of realistic-size power networks, it is necessary both accuracy and speed. In the last years, several advances for integrating TSA and EMT simulations have been developed (Huang and Vittal, 2018; Shu et al., 2018; Huang and Vittal, 2016); the aim is to satisfy both the accuracy requirements of detailed power electronic devices and the efficiency of large-scale power systems. Such requirements reduce the computational burden by focusing the EMT approach on a certain part of the system and leave the rest of the power system to the TSA approach (Guillaud et al., 2015). The main issues interfacing TSA and EMT simulators, and creating a hybrid simulator are as follows:

- Equivalent models of external and detailed systems.
- Identifying the domains of study and locations of interface buses.
- Exchanging data between TSA and EMT simulators.
- Organizing interaction protocol between TSA and EMT simulators.

## 1.4 REAL-TIME (RT) SIMULATION

A key component of the future automation architectures in the power distribution grid is the RT condition monitoring system. Since it provides an accurate evaluation of the network in RT, to feed the automatic and supervisory control of the network components (Westermann and Kratz, 2010; Angioni et al., 2016). Due to advancements on the computer hardware, several RT simulators have been developed for multiple applications (Montaña et al., 2018; Hernandez et al., 2018; Ibarra et al., 2017; Faruque et al., 2015), which have been exploited for EMT simulation of power networks (Rehtanz and Guillaud, 2016). Therefore, RT simulation has become an integral part of the planning, design and operation of power systems (Jalili-Marandi and Dinavahi, 2009), ensuring a solid framework and a realistic view of the system behavior to test the new control/protection concepts, as well as detect, analyze, and correct any potential problems before commissioning (Dinavahi, Iravani, and Bonert, 2004).

RT simulator is a system which is designed to provide the exact behavioral characteristics when is compared with a real system (Noureen, Roy, and Bayne, 2017). In a traditional discrete simulation (off-line simulation), the wall clock time required to solve all equations of a system can be lower or higher than the fixed time step. However, in RT simulation (on-line simulation), computation of the system equations as well as communication with other simulation nodes can only be run if RT is ensured, as the surrounding events react under wall-clock timing (Ilamparithi, Abourdia, and Kirk, 2016; Guo et al., 2015). To accomplish this accuracy, these simulators need to process the models for one time-step at a time, synchronized with real-world clock.

RT simulators can be classified as commercial and lab-made RT simulators (Chen and Dinavahi, 2014). The simulators evolution is shown in Figure 1.9, where the performance can vary depending on the hardware technology as micro-controllers, digital signal processors (DSPs), field-programmable gate array (FPGAs) and even personal computers (PCs) with a

compliant operating system (Faruque et al., 2015). Most RT simulators have the following common characteristics (Westermann and Kratz, 2010):

- Multiple processors which operate in parallel to form the target platform on which the simulation runs in RT.
- A host computer used to prepare the model off-line, then compile and load it on the target platform. Host computers are also used for monitoring the results of RT simulation.
- Input-output (I/O) terminals to interface with external hardware.
- A communication network to exchange data between multiple targets when the model is split into many subsystems. A separate communication link is required for data exchange between the host and the target.

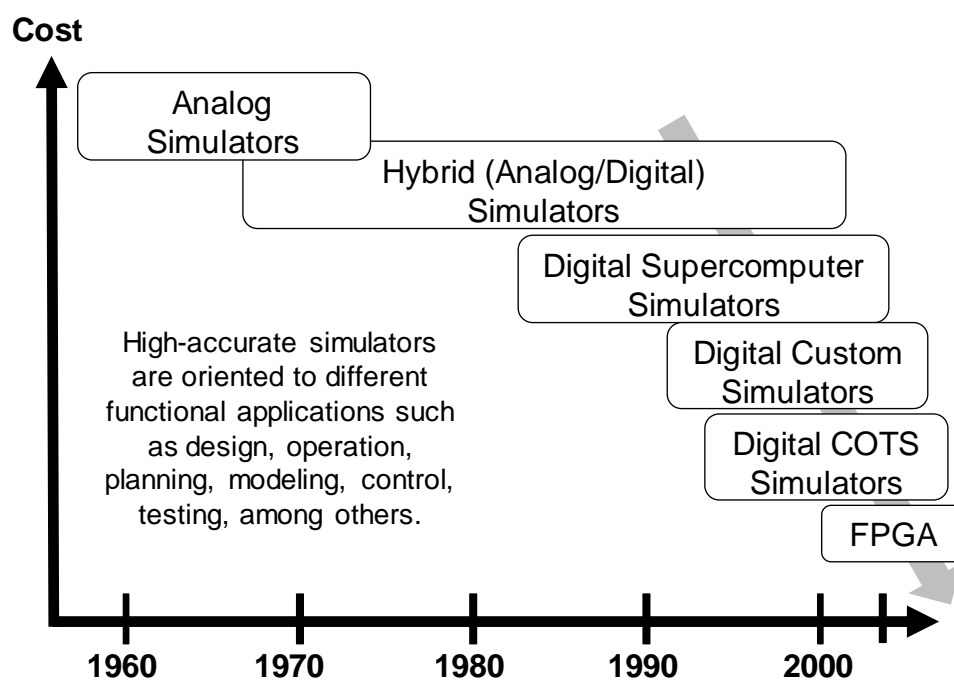


Figure 1.9: Evolution of high-accurate simulators.

As shown in [Figure 1.10](#) based on the setup of the simulation and its application, RT simulators can be classified into four main categories: fully RT digital simulator, hardware in the loop (HIL) simulator, control HIL (CHIL) simulator, and power HIL (PHIL) simulator.

#### 1.4.1 Fully real-time digital simulator (DRTS)

DRTS is a simulator in which, the entire system, including the control, event sequence, protection, and so on, is entirely modeled on the simulator platform and does not involve any interfacing with the external world using I/O terminals (Vijay, Doolla, and Chandorkar, 2017). It provides an identical behavioral characteristics when compared to a real event into the system.

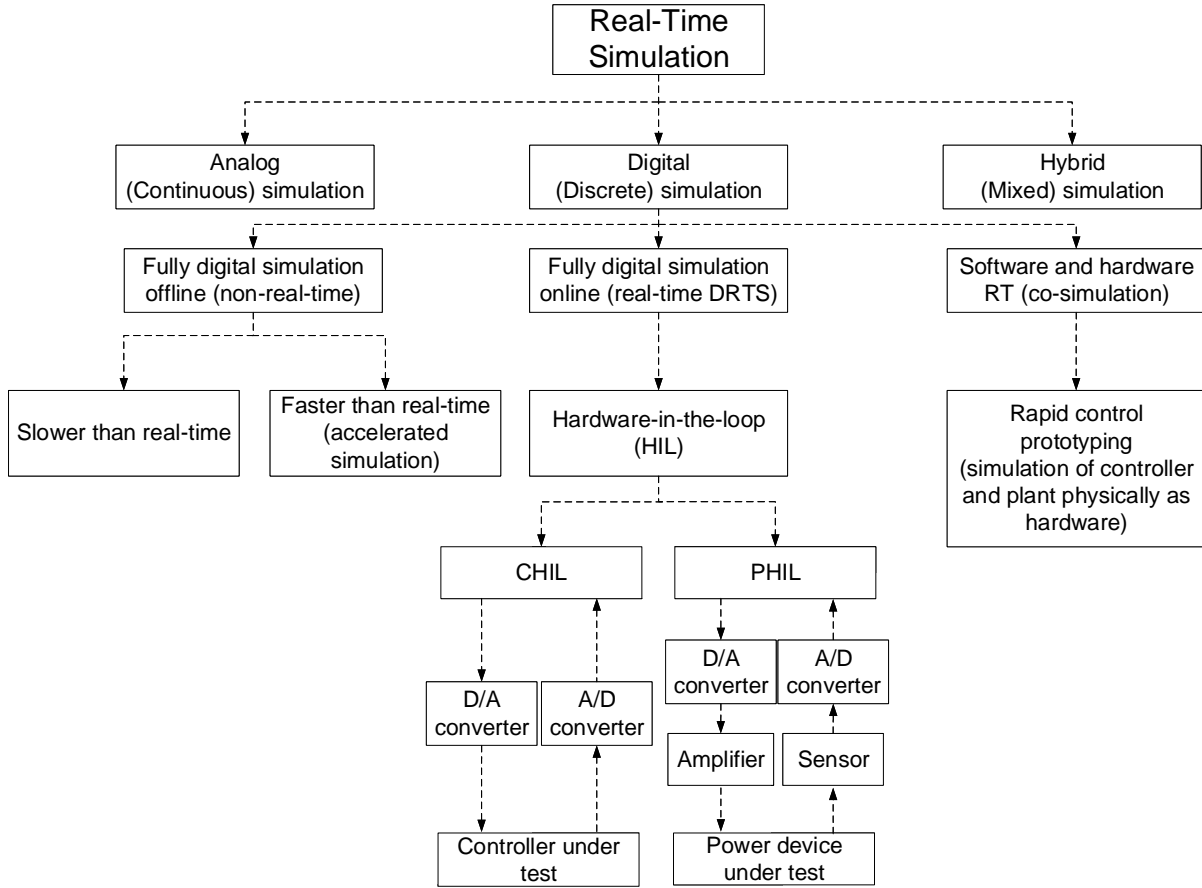


Figure 1.10: RT power system simulation categories.

The execution of a DRTS needs to process the models for one time-step at a time, assuring the fidelity with a real network and synchronizing the clock accuracy. As a result, the signal output is based on a discrete time period (Noureen, Roy, and Bayne, 2017).

#### 1.4.2 Hardware in the loop (HIL) simulator

As the name implies, a HIL simulator has a part of the system modeled and simulated in RT, while the remainder is the actual hardware, connected in closed loop through various I/O interfaces such as analog-to-digital (A/D) and digital-to-analog (D/A) converters, and signal conditioning equipment (Faruque and Dinavahi, 2010; Thornton et al., 2018).

The important requirements of a RT HIL simulator setup are to ensure high fidelity of the system modeled and a minimum loop latency between the physical device and the virtual system in the simulator. HIL simulator offers a cost-effective and comprehensive means of testing micro-grid/smart grid control and protection schemes by covering functional and robustness testing at both the algorithmic and communication/interface levels (Jeon et al., 2010). As shown in Figure 1.11, the HIL system is generally composed of three indispensable parts (Ren et al., 2011):

- A piece of hardware simulated named hardware under test (HuT), which is a real device to be developed or tested.
- A DRTS, which supplies the test environment based on software modes to test the HuT.
- An interface that links the hardware and the simulated system.

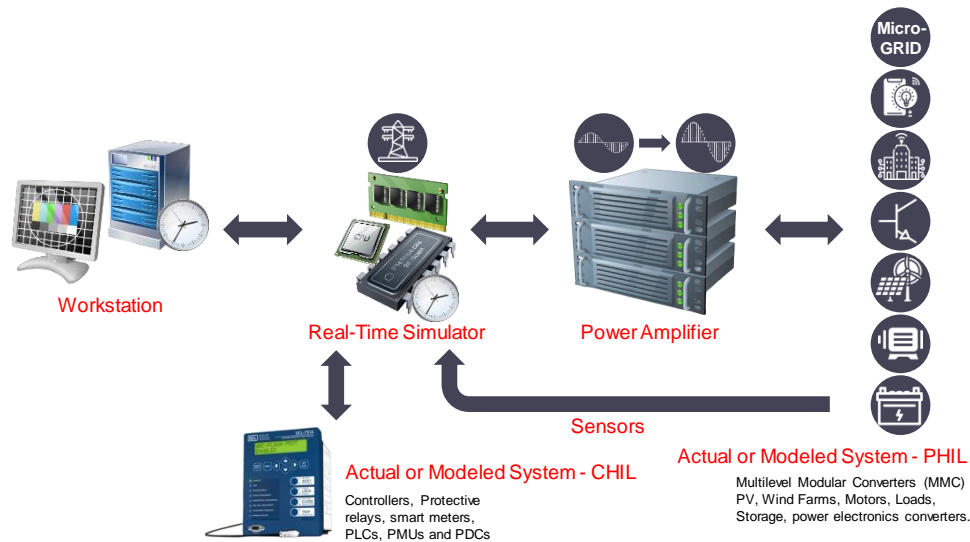


Figure 1.11: HIL simulator architecture.

#### 1.4.2.1 Control HIL (CHIL) simulator

In CHIL simulator, a hardware controller is tested and linked to a power network simulated entirely in the DRTS, in which case the interfaces to the simulated system are through control level signals, with no significant power being transferred to or from the HuT (Panwar et al., 2013).

It involves closed-loop simulation of two or more subsystems, where at least one is a physical device and another a software simulation subsystem executed in a DRTS. Because the use of CHIL simulators, hardware testing elements can be emulated in a RT environment evaluating the flexibility and complexity of multiple system components (Lauss et al., 2017).

#### 1.4.2.2 Power HIL (PHIL) simulator

The interaction assessment and response between power equipment can be tested using a PHIL methodology. A PHIL simulator is an HIL simulator involving real power/energy transfer to/from the HuT, so a power source generating, or absorbing power is required (Ibarra et al., 2017). Normally, the HuT is a power device so an appropriate power amplification is necessary to establish the interface (Kotsampopoulos et al., 2018). PHIL simulation is an outstanding solution to a controlled test environment, easier permitting, full instrumentation and the potential to evaluate alternate point of common coupling, feeders and operating conditions with the same hardware setup (Palmintier et al., 2015).

## 1.5 EXPERIMENTAL PLATFORMS FOR POWER DISTRIBUTION SYSTEM ANALYSIS

Experimental platforms are a key point to evaluate the technological changes and the arise of new opportunities in the electrical power grid. As shown in Table 1.4, the current market offers several experimental platform solutions for power distribution systems known as advanced distribution management systems (ADMS). The ADMS allows the system operator to have an overall idea of the current state of the grid, this kind of tools facilitate the decision-making task to maintain a proper functioning of the distribution system.

Table 1.4: Summary of salient features of real-time simulators reported in the literature. (Omar Faruque et al., 2015).

Real-Time Simulator	Hardware	OS and Application Software	Communication, Protocols, Interfacing and I/O	Modeling and Solution	Application	Other
RTDS from RTDS Technologies, Inc.	PowerPC RISC processors are implemented in cards (PB5), GTFPGA.	Host OS: Windows Target OS: VxWorks Application software: RSCAD	Optical fiber, fast back plane, global bus hub, Gigabit Ethernet, DNP3, IEC61850, TCP/IP, analog and digital I/O, third party I/O through GTNET.	EMTP type library of component models, small time step models for some components, Dommel's algorithm based Nodal solver.	Real-time simulation of power systems, power electronics, control systems, testing of equipment through HIL simulation.	Allows multi-rate simulation.
eMEGAsim from OPAL-RT Technologies Inc.	Multi-core CPU, FPGA, commercial of the shelf motherboard.	Host OS: Windows Target OS: Linux based Application software: Matlab / Simulink, RT-Lab.	Shared memory, Gigabit Ethernet, Dolphin networking, IEC61850, TCP/IP, DNP3, FPGA-based analog & digital I/O terminals, supports third party I/O.	Simulink and in house toolboxes, code (C/C++, MATLAB, Fortran) wrapped with S-function, discrete Simulink solvers, vendor specific solvers such as ARTEMIS-SSN.	Real-time simulation of power electronics, power systems, control and automotive systems, multi-domain simulation, HIL testing and simulation.	Multi-rate simulation, e-PHASORSim transient stability extension available, EMT models can be implemented on FPGA cards, multi-domain as it supports all Simulink block sets.
HYPERSIM from OPAL-RT Technologies Inc.	CPUs are used with SGI's NUMalink processors interconnect architecture.	Host OS: Windows Target OS: Linux based Application software: Hypersim software suite	Gigabit Ethernet, IEC 61850, standard PCIe interface with DSP based A/D and D/As.	GUI based component library is available through which system model is built, state space solution method is used with multiple integration rules.	Real-time simulation of power systems with power electronics, control systems, HIL testing.	Implementable in eMEGAsim platform for smaller scale transmission systems, automatic task mapping to available processors.
dSPACE from dSPACE GmbH.	CPU.	Host OS: Windows Target OS: QNX ROS	Gigabit Ethernet, PCIe based communication with other hardware and I/O uses proprietary dSPACE protocol, IOCNET.	Simulink, state-flow, AUTOSAR, C coded models	Mainly used for real-time control and rapid prototyping for automotive engineering, aerospace and industrial control.	
VTB-RT from University of South Carolina.	DSP cluster or multi-core CPU/FPGA.	Host OS: Windows Target OS: Linux		Modified resistive companion.	Power systems.	Multi-physics possible.

However, in most of the cases the current ADMS have several restrictions to develop new algorithms to interact with the distribution system. ADMS can also be limited by a number



of nodes allowed to analyze the system as same as the number of phases. Moreover, many of these tools are over-priced, needing extra licenses to enable the full potential of the software.

As a result, the development of new ADMS solutions is required considering certain functionalities, so, a review of the main functionalities to be integrated in an ADMS is listed below considering the existing features in the available platforms.

#### 1.5.1 *Consumption and generation forecast*

An important action of an ADMS is to consider the forecast of the renewable energy expected to be generated and the load profile of the distinct clients connected in the distribution network. This information allows to the operator to plan the optimal settings of the system, modify the topology, and manage the different events of the grid.

Several methods have been implemented to forecast the load profile of the clients. Some methods use statistical theory (ARIMA, Decision Trees) (Goswami, Ganguly, and Sil, 2018; Dehalwar et al., 2017). Other methods are implemented with Artificial Intelligence (neuronal networks, support vector machines, etc.) (Niu, Wang, and Li, 2005; Singh, Hussain, and Bazaz, 2018). Nevertheless there is a need to integrate this useful tool to other possibilities of the grid to improve a general knowledge.

#### 1.5.2 *Cyber resilience*

A digital era is always exposed to cyber attacks. The flow of huge quantities of information in distribution systems must be protected from malicious conducts. Similarly, the communication channels in the ADMS has to be protected from cyber attacks. For instance in (Hammad, Ezeme, and Farraj, 2019), a platform system is developed to test a communication network from possible cyber attacks in a distribution system. The system was modeled in the PSCAD/EMTDC simulator, then, a third party software is used to emulate the communication layer of the system and plan possible attacks to the grid.

Other solution is found in (Garau et al., 2018), focusing in specific attacks to ADMS such as the fault location isolation and service restoration (FLISR).

#### 1.5.3 *Supervisory control and data acquisition*

The monitoring process has to be based on a supervisory control and data acquisition (SCADA) tool. The primary purpose of an utility SCADA is to acquire and monitor RT data from the grid, then send the data to a central computer in a control center, which is used to manage and control the grid remotely.

The most common applications monitored and controlled in distribution SCADA systems allow the system operator to supervise the meters present in the network and control some system elements such as recloser controllers, tap changer, switches, among others intelligent

electronic devices (IED). Distribution systems have established some SCADA requirements, it includes a RT monitoring and control of the main distribution assets typically in the range of 1-5 s (Lin, 2020).

New meters are being installed to improve the data acquisition process and measurements in the system. This is the case of the phasor measurement unit (PMU), which has been largely introduced in some researches like (Rocha-Doria et al., 2018). A shorter timestamp is a priority in the measurement process increasing the accuracy to a smaller fractions (Prabakar et al., 2020). Another feature is related to the geographical information system (GIS), as (Devanand et al., 2020) a GIS is used to give more information at the outage management system to get less time interruption for the clients of the network.

#### 1.5.4 RT capabilities

RT grid management is mandatory to assure a reliable, optimized and safe operation of the grid. It opens a new vision of smartgrid monitoring as a predictive and corrective actions, from avoiding the system congestion while maximizing efficiency and minimizing supply cost, to an improved fast reaction to system faults ensuring the power availability as many customers as possible.

New experimental platforms have integrated RT analysis in their ADMS. In the literature, a vast number of scientific papers are available offering platforms with RT approaches. This RT capability is enabling the development of smart grids, handling the different DERs of the network, assuring the system stability in a two-way flow and assuring a permanent monitoring and control of the system. More of these details will be discussed in the following [Section 1.6](#).

Finally to confront the next challenges in the development of ADMS for power distribution grids, it is important to integrate all of these features in a single solution. Moreover, the use of open-source algorithms can be a further support to minimize the extra cost produced.

## 1.6 CHALLENGES OF RT SIMULATORS FOR SMART GRIDS INNOVATION

In recent years, the demand for RT control, condition monitoring, interaction operation and lean management of distribution networks are increasing. The industry is demanding more powerful simulation tools as shown in [Figure 1.12](#), since the complexity is getting bigger, and the integration of new technologies is changing loading patterns and profiles, introducing dynamics at the distribution grid that present new grid management challenges for utilities (Moghe, Tholomier, and Divan, 2016). Managing and optimizing the grid to meet all the traditional requirements in the presence of new and upcoming constraints pose unanticipated challenges, especially to provide novel testing techniques, which incorporate more detail and reduce the time (Ilamparithi, Abourdia, and Kirk, 2016).

Engineering research and development activities are vital to identify leading industry practices and assess emerging industry trends, solutions, challenges, and needs pertaining to electric utility technology, business, regulatory, policy, and customer experience aspects. Research

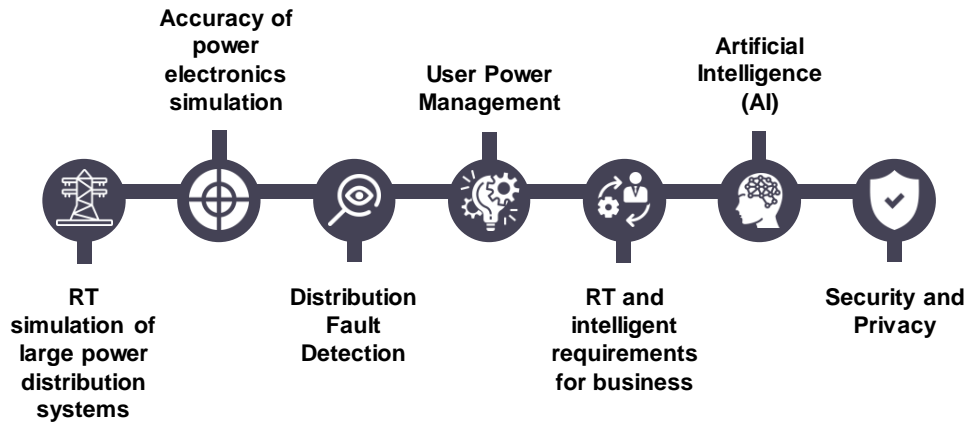


Figure 1.12: RT smart grid innovation necessity.

and development activities are important to identify market changes and auto reference inputs to update the selected utility of the future strategy as it is shown in Figure 1.13 (Romero Agüero, Khodaei, and Masiello, 2016).

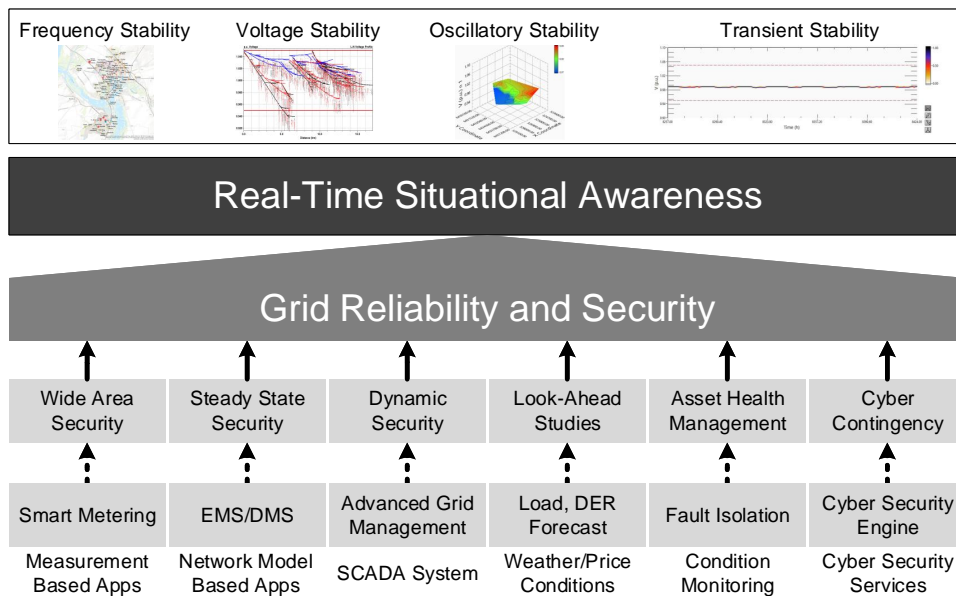


Figure 1.13: Actual situational challenges.

### 1.6.1 RT simulation of large-scale power systems

The volume of distribution grid is high, which requires large-scale deployment. EMT of power grids requires a high processing power to perform significant numerical computations (Ilamparithi, Abourdia, and Kirk, 2016). Then, the challenge is to solve all the grid equations in a simulation cycle. Dividing the grid model into groups and assigning each group to one of the multi-processors included in the simulator stands as the only possible solution (Andreev et al., 2018).

Nowadays there are some advances focused on the creation and enhancement of RT tools for large-scale power system simulation, but simplified physical and mathematical models

of the system characteristics are still used. Also the limitation in software tools which are inappropriate for simulation of large-scale power systems, the lack of adequate equipment for the emulation of the power grid phenomena, the absence of computers with the capacity to perform fast numerical calculations. All of these disadvantages restrict the precision of large-scale modeling results (Andreev et al., 2018).

### 1.6.2 Accuracy of power electronics (PE) simulation

Modern grids have a higher degree of DERs interfaced using PE converters. The transient behavior of such networks becomes difficult to analyze and predict. The accuracy of the simulator depends on the simulation step size, which should be small, since RT processors must solve all the equations in limited time cycles (Vijay, Doolla, and Chandorkar, 2017).

PE system devices switch their semiconductors at a few rate of kHz, so it is required time steps too small, in the order of microseconds, to be integrated in the RT simulators for an accurate testing. Conventional PE simulators works with single large time steps, it means implementing an interpolation scheme to improve switching accuracy. But in the RT simulators, these methods are not effective due to some issues when multiple semiconductors switching occurs at different instants in one time step. New RT simulators are being developed with an FPGA as a computation core to achieve to run simulations in a small time step (Le-Huy et al., 2006).

### 1.6.3 Power distribution fault detection

Fault incidents in low voltage are a major problem in the power grid operations and maintenance. Similarly, correct protection and control performance is most critical to power system stability and operation, resulting in a new equipment protection like digital/numerical relays (Phadke et al., 2016), which are being installed in power distribution systems to provide most critical functions in grid protection, system communication, monitoring, and recording of disturbances and faults.

So, an accurate simulation of the system and the protection devices is mandatory before the commissioning phase, avoiding a possible wrong operation of the distribution grid. But major simulations tools are based on an incomplete modeling of the system, allowing an incorrect performance of relays and related automation and control equipment; that may cause potential damage or problems for the system.

To evaluate the protection devices in an accurate way, it is necessary a fault modeling and system protection functions included into the RT simulator. HIL protection testing is suitable to evaluate and assure a proper functioning, allowing to handle failures situations when faults occur in a real system. Fault detection testing has to consider the following characteristics for protection devices (Tang, 2014):

- **Reliability:** Evaluate the operational needs, assuring an early fault detection and a proper protection operation.

- **Selectivity:** Dispose of different simulation sequences of operation as desired according to the system conditions, considering the available resources and maximizing the usage of the distribution system.
- **Economy:** Ensure a simulated environment for a smart design for protection and control systems, allow to reduce unnecessary equipment or complex design which might cause trouble to expand the network or generate too much investment to modify it.
- **Speed:** The simulation system is fast enough to test a protection scheme under a failure, creating emulated conditions to isolate a fault and react to avoid system damages.
- **Simplicity:** The simulation environment allows to evaluate a system reconfiguration under a failure detection, finding the simple way to re-organize the network and isolate the fault.

Power system fault simulation and modeling needs to advance in a more standardized way to test protection and control systems and commissioning practices, the fidelity is critical to ensure an improved system reaction under failure conditions, affecting the reliability and quality of the distribution grid.

#### 1.6.4 Demand side management (DSM)

Despite the development of AMI systems, the management of a high volume of users, the increasing sampling frequency in the evaluated conditions and the precision of terminals, and the gradual diversification of business requirements, make that RT simulation is still faced with problems of communication delays, channel blocking and personal privacy leaks (Noureen, Roy, and Bayne, 2017).

A modern power automation platform is strongly desired to support and coordinate variety of subsystems, such as demand side management, operation control, monitoring and management, etc., to maintain the high operation quality of power systems. This approach solves and reduces the energy consumption in most of the cities. A DSM methodology helps customers and system operators to take decision regarding the use of electricity in aspects such quantity and the optimal moment.

It is necessary to have RT tools for load shifting and load analysis. The first one, helping to the analysis of demand response shifting the load from peak hours to off peak hours, increasing the reliability and efficiency in operation, minimizing the cost and peak demand. The second method is related to move some loads from one feeder to other, balancing the system.

The addition of smart meters enables a two-way communication between the end-user and the system operator, performing a real analysis improving the energy consumption. Different DSM methodologies could be tested as well such as load shifting, valley filling, peak clipping, strategic load growth and flexible load shape (Anjana and Angel, 2017).

### 1.6.5 *RT and intelligence requirements for business*

The energy market becomes more complex where power producers/consumers submit the production/demand bids, the DER installation has changed the paradigm of the market competing either in spot markets, and the operator has to deal with all these information.

Building a RT simulator which contemplates the electricity market is not an easy task. There are a huge diversity between the markets, involving different bidding rules, and different clearing algorithms (Bernal-Agustín et al., 2007).

As a result, there are a lot of business scenarios which require a high RT response, such as RT response of demand side, dynamic optimization of energy usage, forecasting of the energy price, among others. (Jinming et al., 2018).

### 1.6.6 *Artificial intelligence (AI) for smart distribution grids*

The evolution of smart distribution grids is an important area of research, due to critical issues related to optimization, provision of smart customizable networks and efficient computational algorithms and methods based on AI and machine learning techniques requiring a lot of investigation. Considering the increased use of smart meters installed in residential and industrial customers, and the evolution in the hardware capabilities, AI implementation requires a RT computing infrastructure able to handle a high volume of newly available data sets, optimal to train AI models and deploy them inside the smart distribution grid.

DERs installation requires as well the use of AI methodologies in order to respond to the energy demand of the system. It is necessary to develop AI algorithms to enhance the design of the energy infrastructure, the deployment and production of renewable energy to becomes more resilient and cost-effective. The advantages of its large deployment include the possibility of performing prediction and generalization at high speed, flexibility, explanation capabilities and symbolic reasoning (Şerban and Lytras, 2020). The areas of smart distribution grid where AI could be applied are:

- Prediction of renewable energy production based on local weather information in close to RT techniques.
- BESS management according to energy prices available from the grid.
- Optimal utilization of energy based on the demand consumption.
- Load management considering AI predictive algorithms to reduce the consumption of energy in RT and to smooth out the demand side curves

To test the efficiency of AI methods applied to smart distribution grids, the literature suggest the following tasks to consider (Khan et al., 2018):

- **Energy usage:** Prediction of energy usage (demand side) based on a holistic set of metrics associated with the time of day, vehicle traffic patterns, human presence density, weather, commercial and industrial activity and historical energy usage information.
- **Energy production:** Prediction of energy generation based on a holistic set of metrics associated with installed generation capacity, salient weather signals, and historical generation information.
- **Savings:** Estimation of net savings or loss is associated with the energy available in batteries based on the price of energy stored originally, and compared with future energy generation and usage predictions, in the light of the prices of the energy mix available.

AI is the solution that should be integrated at economic level, for reducing the risk of variability of DERs, by performing predictive analysis, identifying patterns, reducing the storage cost, better connectivity between grids and users, thus conducting to grid stability, reliability and sustainability.

#### 1.6.7 Security and privacy

Contingency analysis in distribution systems is widely accepted for the operational security assessment, which uses case by case to verify if the current load of the grid meets the safety operation conditions. Currently, RT distribution simulation have to integrate efficient algorithms because in some cases, the contingency simulation time is highly prohibitive; so it is important to integrate new ways to evaluate all the operating points satisfying N-1 operational constrains.

The information technology of the distribution system is also a priority in terms of cybersecurity, the deployment of new IEDs on the feeders, the data exchanged among different entities interconnected in the system, and the evolution in the communication protocols are a constant risk against cybersecurity attacks and unintentional misuses (Jang-Jaccard and Nepal, 2014). A robust design of cybersecurity has to be carried out under a RT simulation platform, assuring a safety data exchange and mitigating the possibilities of an intentional blackout of the system.

The privacy is another important element in the side of the customer, a big number of user power consumption behavior data are collected and converged. It is necessary to ensure security and user privacy through management and technical means such as lightweight and efficient identity authentication, access control, encryption and decryption, and data desensitization. Also, several types of cyber-attacks threatening power distribution grid can be recreated using RT simulators (Ilamparithi, Abourdia, and Kirk, 2016).

Nevertheless, these challenges can be turned into an opportunity by introducing smart grid technologies with intelligence. Application solutions as edge computing for distribution grids provide full digitization of distribution grids, makes the grid observable and stable, and enables the delivery of flexible services from DERs (Moghe, Tholomier, and Divan, 2016). Due to the availability of measurement data, the edge computing solution is thoroughly positioned to provide further applications such as power quality analysis, fault detection, and failure predic-

tion as well as to support data-driven and automated applications such as asset management and network planning (Jinming et al., 2018).

In this context, a vision and strategy of the smart grid of the future is critical to ensure that utilities empower, provide opportunities, and fulfill customer needs, while remaining profitable, sustainable, and vital organizations.

## 1.7 CHAPTER SUMMARY

This chapter has presented a detailed review of condition monitoring and fault detection tools for power distribution grid analysis.

The RT simulators provides an accurate and flexible way for testing different control and protection systems by interfacing them with physical components, exchanging the information through the appropriate communication protocols. To ensure proper testing and validation, the RT simulation solution must be able to replicate the smart grid system with high fidelity. RT simulation is classified depending on its technical capabilities, so a complementary analysis has been done.

RT simulator limitations are related to performance and capability limits of the processors, non-availability of assessment methodologies, cost, and optimization, which still needs to be overcome by researchers on the path to implement these methods successfully and widely for testing purposes.

On the other hand, an efficient and reliable condition monitoring system is important for smart grid technology deployment. The monitoring system to support the future smart distribution system will need to be distributed and flexible, in order to design and implement a novel platform for supervision, analysis and optimization of power distribution systems.



---

**Contents**


---

2.1	Introduction . . . . .	28
2.2	The new Bank of Energy concept . . . . .	29
2.3	Hardware architecture of the experimental platform for real-time simulation . . . . .	31
2.3.1	Workstation peripherals . . . . .	31
2.3.2	Display for supervision, monitoring and visualization . . . . .	31
2.3.3	Hardware in the loop system emulators . . . . .	32
2.3.4	Equipment rack . . . . .	33
2.3.5	Intelligent electronic devices . . . . .	35
2.3.6	Remote control devices . . . . .	35
2.3.7	Workspace . . . . .	36
2.4	Software architecture of the experimental platform . . . . .	36
2.4.1	Event-driven architecture . . . . .	37
2.4.2	API layer . . . . .	43
2.4.3	External devices connection . . . . .	46
2.5	Validation of the experimental platform concept . . . . .	46
2.5.1	Real case: Fault study analysis . . . . .	47
2.5.2	Test case studies . . . . .	54
2.6	Advantages of using the Bank of Energy . . . . .	59
2.6.1	Fault analysis . . . . .	60
2.6.2	System reconfiguration . . . . .	60
2.6.3	Energy forecasting and operational planning . . . . .	60
2.6.4	Hosting capacity . . . . .	61
2.6.5	Battery energy installation and management . . . . .	61
2.6.6	Penetration of electric vehicles . . . . .	61
2.7	Chapter summary . . . . .	62

---

## 2.1 INTRODUCTION

Power grid planning and operation rely heavily on modeling and numerical evaluation tools (simulators). The experimentation with the real distribution network in RT is very limited and in some cases infeasible, mostly due to its large size and high complexity (Borlase, 2018). In consequence, numerical simulation is almost the unique solution to understand the electromagnetic phenomena behaviour in the power grids and to realise the impact related to an operation or control procedure.

With the current trend towards more complex large-scale systems, an increased energy transition must be performed based in energy efficiency and novel models to manage the production and consumption of the system. As seen in Chapter 1, there is a large and growing market for RT simulation and control technology in industry. Because of this, simulation requires accurate representative models, real-time data for situational awareness, computational algorithms and hardware capabilities for timely execution.

The current computational efficiency in power distribution grid operations is low, which can lead in delays to respond to critical events. As a result, advanced smart grid applications requires an efficient computing calculation to respond as quickly as possible to these events.

The analysis layers in an advanced smart grid application are shown in Figure 2.1. The analytical analysis corresponds to complex system modelling combined with optimization techniques. Off-line analysis is focused in deploy the classical methods which allow to evaluate the system stability. Finally, RT analysis can predict the system behaviour to respond in few minutes to possible failures in the grid. In particular, RT systems supported by the ability to include the evaluation of feedback control strategies, are finding increasing use and acceptance for tasks such as operator training, fault detection and investigation, and safe testing of prototype systems.

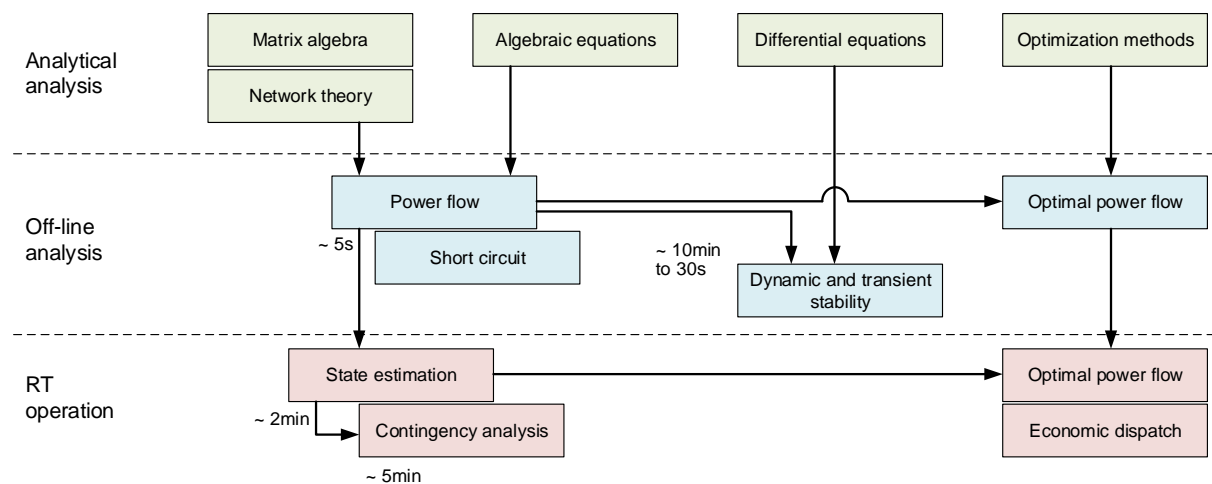


Figure 2.1: Grid computational paradigm (Borlase, 2018).

From this point of view, this chapter introduces the development of a novel and comprehensive tool intended to monitor, supervise and simulate the state of a power distribution system based in the prediction and the integration of RT capabilities and HIL integration. The description is done from the main hardware/software components, as well as a test validation

of different test scenarios is performed. Finally, some applications in development are also listed.

## 2.2 THE NEW BANK OF ENERGY CONCEPT

A novel tool denominated the Bank of Energy is developed as a hardware/software interface for energy arbitrage between the energy produced in a territory (conventional and distributed), the energy consumed (clients), and the assets belonged to the distribution network (ADEME, 2018b). In other words, the purpose of the Bank of Energy is to optimize in RT the local energy production and consumption through a robust and a resilient architecture, resulting in the principles and conceptions towards a smart power distribution grid definition.

The operation of the Bank of Energy is based in the correlation of the data obtained from the intelligent electronic devices (IED) installed in site, and the algorithms developed to guarantee the prediction of the energy production/consumption behaviour. Then, several scenarios are deployed to determine the suitable operation decisions considering the system balance production/consumption to be considered as positive, by identifying the energy surplus in the relationship between the local renewable energy production and the consumer energy management.

The Bank of Energy concept aims to make a real contribution to the current energy transition, to participate in sustainable global development and to reduce the greenhouse gas emissions. This approach opens the possibility to manage the energy efficiency of a distribution system by a technical-financial perspective. So, an efficient energy management of the distribution system is deployed by the optimization of the energy produced by the different DERs, the energy purchase, the load consumption and the storage systems installed into the grid. The optimization is formulated as a mathematical model to accomplish the different operational and management criteria of the system operator (SO).

The Bank of Energy is developed considering all the concepts presented in the previous chapter. A hardware/software architecture is designed to an effective evaluation of any scenario of a power distribution grid. The parameters considered to achieve an optimal Bank of Energy architecture are based in the following criteria:

- A generic simulation tool to analyze the behaviour of any distribution system.
- The use of multi-core information systems capable to perform RT simulations and execute optimization algorithms in a deterministic way to guarantee a faster response.
- The introduction of external equipment enable to interact in the supervision, control and diagnosis of the distribution system elements associated.
- The user-friendliness for the SO in maneuvers such as the modification of the system topology due to perturbation in the network.
- The possibility to perform several electrical studies based in different time ranges of power system dynamics.

In this way, to develop this concept, the Bank of Energy is based in an experimental platform as a starting point of development. This experimental platform has been designed following the architecture shown in Figure 2.2. Both hardware and software architecture of this experimental platform will be described in the next sections.

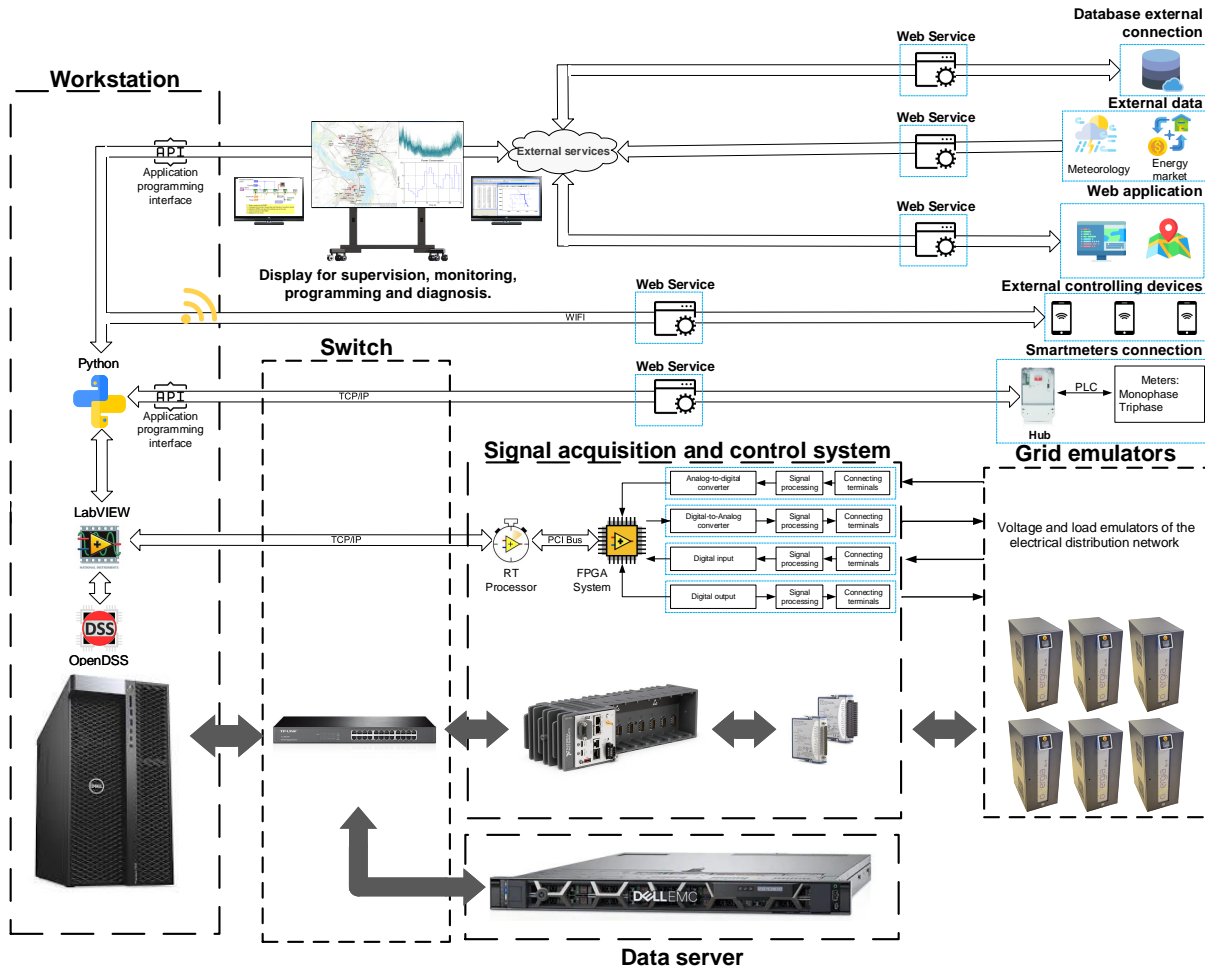


Figure 2.2: Block diagram of the software/hardware implementation of the experimental platform.

The experimental platform belonged to the Bank of Energy aims to integrate the principal characteristics identified in power systems simulators to solve current and planned needs. These characteristics are related to model's flexibility, data management and accuracy, interoperability with other validation platforms, and an advance integration of automation algorithms (Hernandez et al., 2018).

The interface between the elements that join the experimental platform has settled a novel methodology to manage the smart grids. It enables the possibility of a wide-range of studies starting from static and dynamic analyses, running in off-line or RT step simulation, and considering a flexible temporal window to analyze the use of advanced algorithms capable to evaluate the complete range of transient phenomena in electrical power distribution systems.

Similarly for daily, weekly, monthly, seasonal or annual simulations, the experimental platform optimizes the use of the local renewable resources in the short, medium and long term.

### 2.3 HARDWARE ARCHITECTURE OF THE EXPERIMENTAL PLATFORM FOR REAL-TIME SIMULATION

The hardware architecture of the experimental platform is based on a multi-terminal and multi-platform scalable structure that allows the remote and distributed communication with different modules. Figure 2.3 illustrates the general design of the hardware framework of the experimental platform. This hardware arrangement considers the different components detailed in Section 1.4 for a RT simulation platform. Multiple elements conform the experimental platform, a brief description of their utilities are explained below.

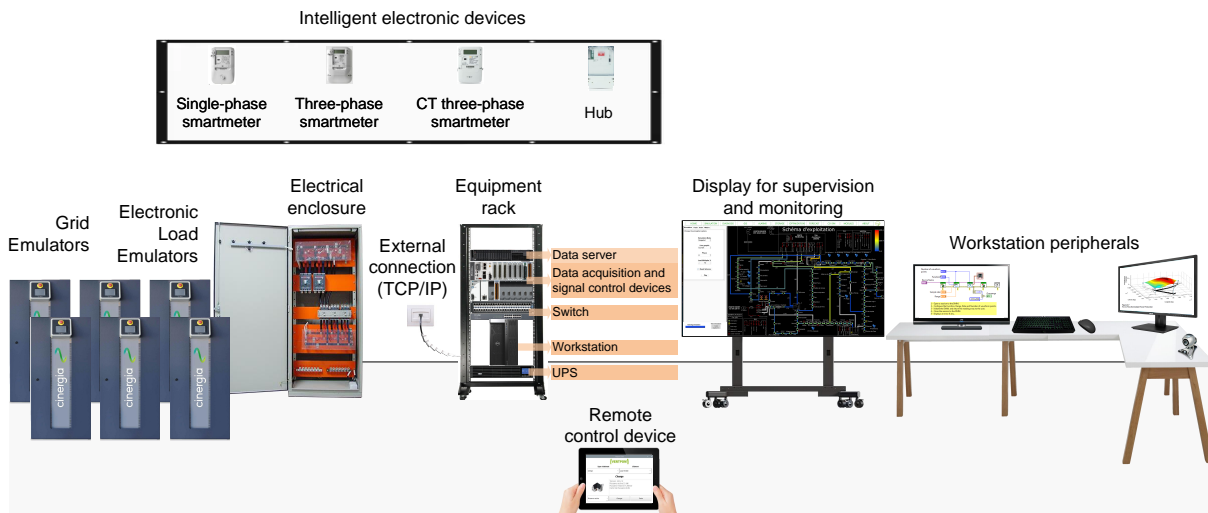


Figure 2.3: General hardware structure of the experimental platform.

#### 2.3.1 Workstation peripherals

This is formed by two monitors, a keyboard and a mouse. These elements provides a workspace for operators who can use the experimental platform. A methodology known as human-in-the-loop (HITL) is designed to assure an ergonomic engagement to respond to all user requests through a events generation (Zambrano et al., 2016).

The monitors show the different tasks and results from the available modules. A programming environment is also arranged in this configuration. As a result, new modules can be tested before to be integrated in the experimental platform.

#### 2.3.2 Display for supervision, monitoring and visualization

This central screen displays the human-machine-interface (HMI) of the experimental platform, allowing to visualize in an objective way the main software interface with the multiple modules and options developed.

This environment recreates a typical modern-day of an energy control center environment, keeping the maximum of similarities between the user experience and software disposition. The use of different display screens allow the operator to monitor and control the grid conditions. All modules and software functionalities are explained in [Section 2.4](#).

### 2.3.3 Hardware in the loop system emulators

Based in the different simulation architectures explained in [Chapter 1](#), a RT architecture was used to integrate a total of six power electronic equipment in the experimental platform (three grid emulators and three electronic load emulators). Their quantity obeys to the need to evaluate different applications at the same time. These emulators are suitable for the majority of test applications in the field of renewable energies, energy load, smartgrids, batteries and electric vehicles (Cinergia, 2020).

[Figure 2.4](#) shows the internal architecture of the grid emulator (GE) and the electronic load (EL) emulator. This architecture is based on a Back-to-Back power conversion topology, where, the grid side stage produces clean sinusoidal currents with a low harmonic distortion and the EUT side is configured for AC voltage source controlled by using digital controllers. Bidirectional and regenerative functions are included in the emulators by the manufacturer for saving in energy and power without impacting in the simulation procedure.

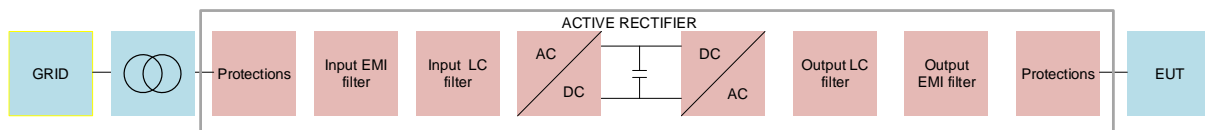


Figure 2.4: GE & EL internal power architecture (Cinergia, 2020).

#### 2.3.3.1 Grid emulators

The GEs are power electronic devices capable to emulate AC electrical grids in normal conditions (voltage, frequency, phase, and angle), disturbed conditions, harmonics (voltage dips, frequency, voltage fluctuations, flicker, etc.) and work as a power amplifier equipment (Cinergia, 2021). These devices can generate different voltages sources and grid configurations, enabling the evaluation of a wide range of scenarios.

In the experimental platform, each emulator generates a three-phase voltages signal with an independent configuration relative to the effective value, the phase angle, the fundamental frequency and the harmonic content. They are designed to generate most of the inherent disturbances of a power distribution network such as harmonic pollution, voltage fluctuations and fundamental frequency variations, following different international test standards (IEC, LRVT, Semi-F47, CBMA).

### 2.3.3.2 Electronic load emulators

The EL emulators are flexible devices crucial for testing, research and development purposes. It allows the emulation of grid-connected devices injecting or absorbing energy from the grid.

In the Bank of Energy, each emulator can simulate the behaviour of three-phase passive or active loads such as conventional loads, traditional or renewable energy sources, energy storage systems connected to the electricity distribution network, with an independent configuration relative to voltage effective value, phase angle and harmonic components of the signal generated.

### 2.3.3.3 Electrical enclosure

This enclosure has been built for the general protection of the HIL devices in the experimental platform. It was designed mainly to supply the three GE (3 x 15 kVA), the three EL (3 x 15 kVA) and the equipment rack (3 kVA), representing a total of 93 kVA of apparent power.

It is important to highlight that this installation follows the recommendations imposed by the supplier. [Figure 2.5](#) shows the protection installation scheme for the HIL devices.

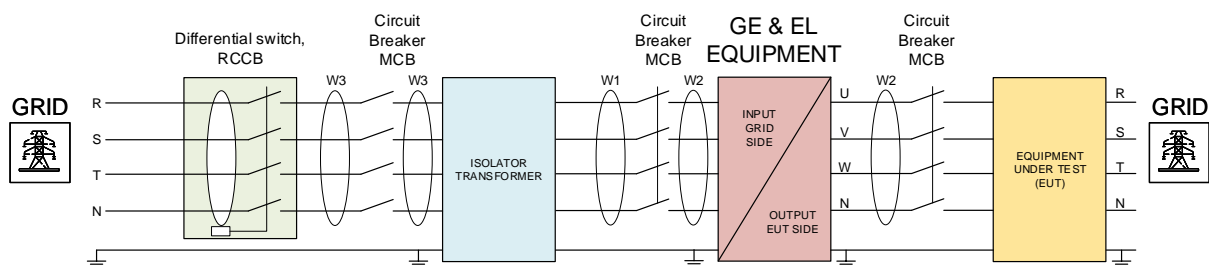


Figure 2.5: GE & EL emulator power supply protection and wiring diagram (Cinergia, 2020).

### 2.3.4 Equipment rack

The equipment rack centralizes all computational devices associated to the deployment of the experimental platform application. It also protects the equipment of harsh environment conditions enhancing the performance and longevity of critical equipment. The main characteristics of this rack are an integral ventilation, a proper sealing, a restricted accessibility and a long durability under the NEMA 12 and IP54 ratings.

[Figure 2.6](#) shows the internal equipment disposition of the rack. The technical specifications of these equipment have been selected in order to manage a large number of data in RT, ensuring a faster response of the different modules of the experimental platform. A brief description of these elements is found below.

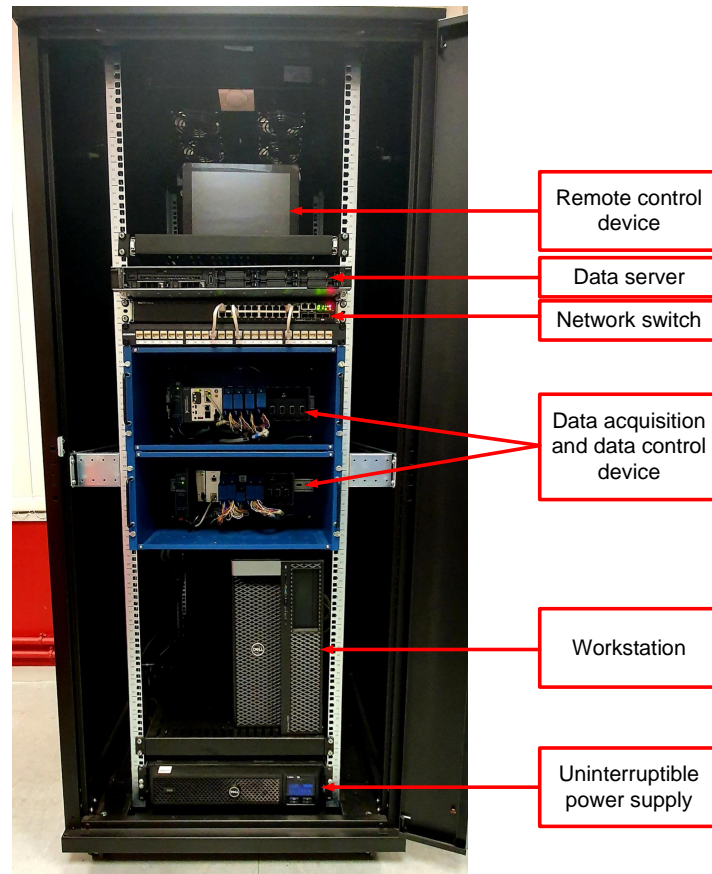


Figure 2.6: Internal arrangement of the equipment rack.

#### 2.3.4.1 Workstation

This element is the brain of the experimental platform. It stores the main application, modules and algorithms whereby the simulations are performed and interfaced with external hardware and software components.

The workstation selected is the Dell® Precision 7920. It has a central processor unit (CPU) Intel® Xeon Platinum 8168 @ 2.7-3.7 GHz Turbo, 24 physical cores and 48 logical cores (threads). It is equipped with 192 Go of memory RAM DDR4, 1 To NVMe hard drive and 2 To SATA hard drive. A double port 10 GbE network card is integrated to support an external and an internal communication network. Finally, a Nvidia® Quadro GV100 is included to optimize the machine learning algorithms. The operating system used is Windows 10®.

#### 2.3.4.2 Data acquisition and data control device

This is a unit in charge to control and manage the analog and digital signals utilized to deploy a RT simulation. Most of these signals are associated to the HIL system emulators.

The NI® cRIO-9045 is the unit chosen to deploy this task. It is based on a dual-core Intel® Atom E3930 processor @ 1.3-1.8 GHz and a field-programmable gate array (FPGA) 70T to



perform RT simulations in a deterministic manner. The NI ® 9149 RIO expansion chassis is also used to cover all signals in multiple modules.

#### 2.3.4.3 *Data server*

All data collected in the experimental platform is stored in a data server. The DELL ® PowerEdge R640 server was chosen to assure the scalability and density in the data collection. Moreover, cyber-attack protocols has been implemented to guarantee the security of the information.

It has a CPU Intel ® Xeon Silver 4208 @ 2.1 GHz, 8 physical cores and 16 logical cores (threads). It is equipped with 16 Go of memory RAM DDR4 and 480 Go SSD hard drive.

#### 2.3.4.4 *Network switch*

This device connects the experimental platform equipment by an Ethernet network. The switch DELL ® N3024 supports 48 Gigabit Ethernet ports (10 Mb/s, 100 Mb/s, 1000 Mb/s) ensuring a reliable data transmission.

#### 2.3.4.5 *Uninterruptible power supply (UPS)*

The DELL ® Smart UPS guarantees the electricity supply of the equipment rack. It has a capacity of 3 kVA enough to assure a correct functioning during 23 min in case of blackout.

#### 2.3.5 *Intelligent electronic devices*

These devices correspond to the smart meters and data concentrators installed in field. Some of them were installed in the experimental platform to evaluate its performance (1 NES ® DCN 3000 data concentrator, 2 IEC poly-phase IBox ® smart meter and 2 single-phase IBox ® smart meter).

This set of smart meters and data concentrator represent a source of data related to consumption, production and storage of electrical energy which is stored in the data server of the experimental platform. The management of these devices in site allows the development of algorithms dedicated for big data analysis and the further improvement of the communication structure and its security.

#### 2.3.6 *Remote control devices*

These units are integrated in the experimental platform to perform a remote control of certain simple simulation tasks such as simulation execution, load variation, DER production, transformers tap changer, electric vehicles (EV) insertion, among others.

Every device includes a Raspberry Pi ® 4, which integrates a Broadcom BCM2711, Quad core Cortex-A72 (ARM v8) 64-bit SoC @ 1.5 GHz. The communication is established with the workstation by Bluetooth 5.0.

### 2.3.7 Workspace

A workspace is dedicated to the experimental platform. This space assures the environmental conditions to execute simulations in high power values. For this, a cooling system has been installed to maintain the equipment in their normal temperature ratings operation. Likewise, the cooling system regulates the moisture and the temperature in the different season periods.

Figure 2.7 shows the panorama view of the workspace installation. This current distribution of the space elements allows an easy operation of the experimental platform by the user, it also respects the manufacturer recommendations to prolong the useful lifetime of equipment.

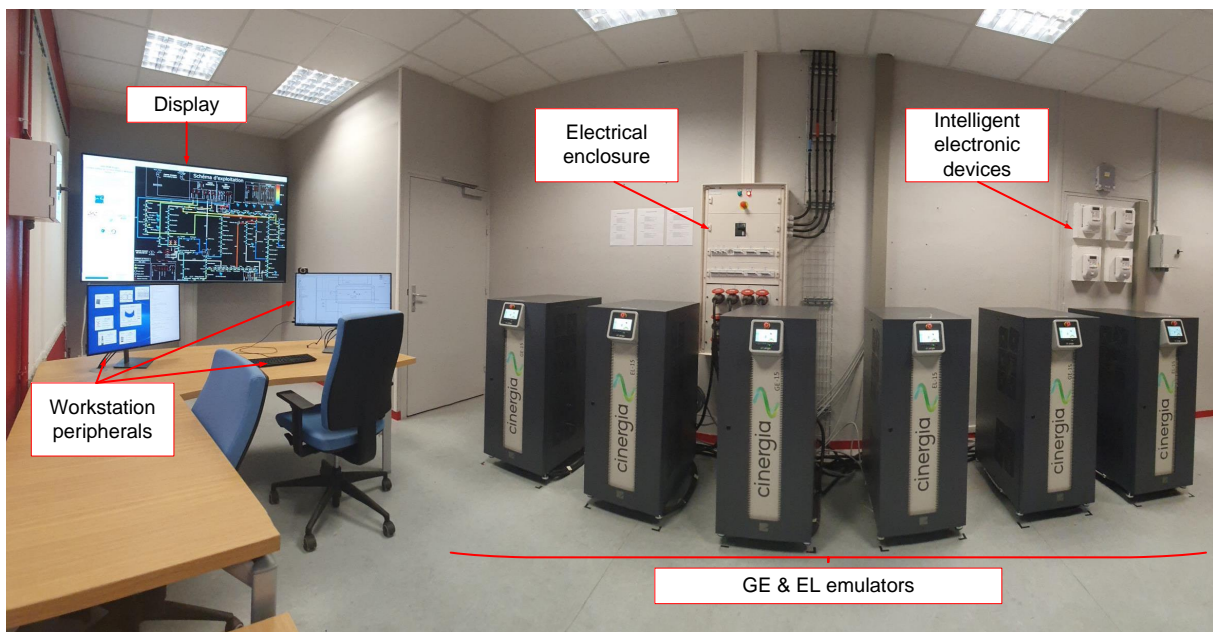


Figure 2.7: General view of the experimental platform workspace.

## 2.4 SOFTWARE ARCHITECTURE OF THE EXPERIMENTAL PLATFORM

The software structure of the experimental platform is illustrated in Figure 2.8. The type of architecture style is implemented in function to modular layers to perform efficiently all the functionalities available. This design ensures that new functionalities can be added in any layer according to its own structure.

The styles used obey certain architecture characteristics, architecture decisions, and design principles to define the suitable structure of the software developed. The architecture characteristics are based on the definition of a successful criteria in order to function the system properly. These criteria is supported in operational and structural considerations such as per-

formance, reliability, scalability, portability, upgrade-ability, security, among others. The architecture decisions has set the rules of how the styles are going to interact between them. Finally, the design principle is the guideline of the programming techniques followed in the software implementation.

The architecture styles are established in a hierarchical order to solve both the requirements and all the other architectural characteristics. A description of each style in presented below.

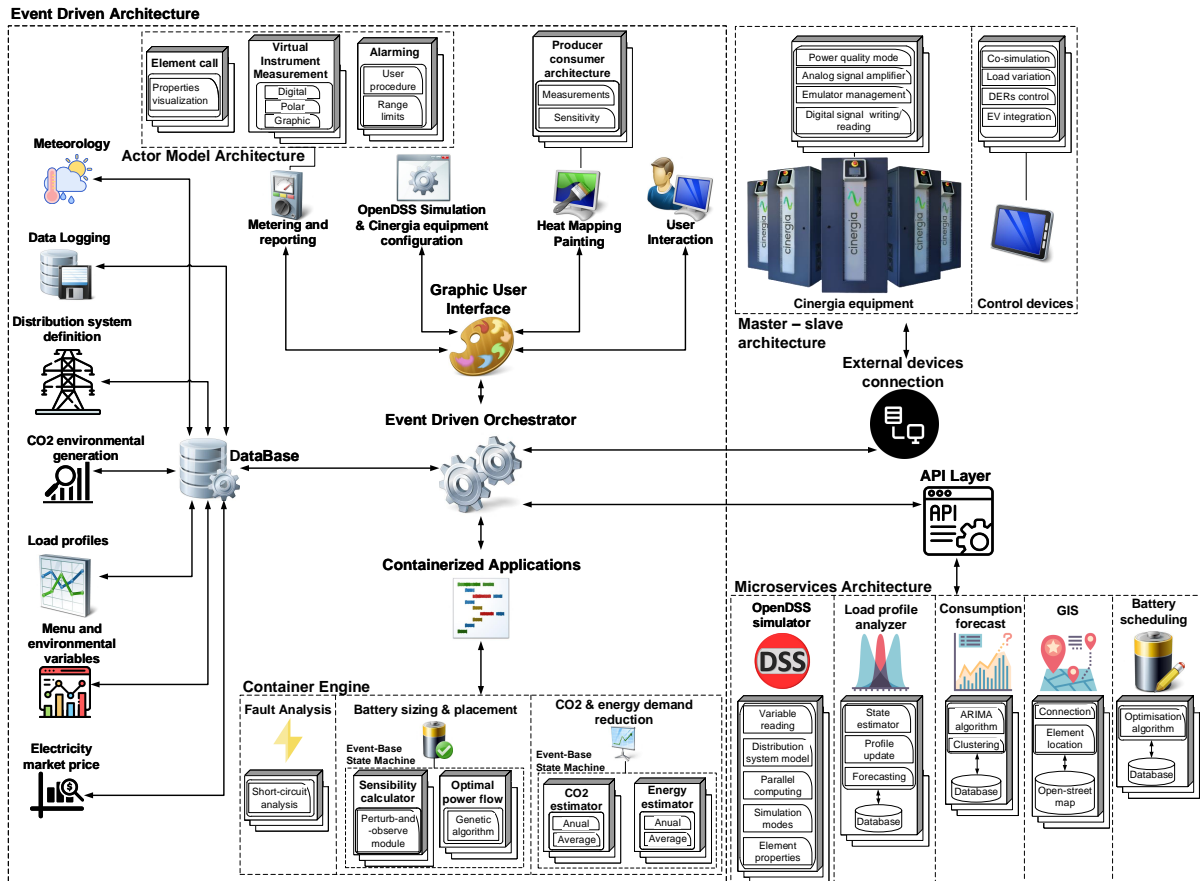


Figure 2.8: General software structure of the experimental platform.

The software architecture of the experimental platform is the most important component to the successful development of the software system. The software system is the base to accomplish the experimental platform goals.

#### 2.4.1 Event-driven architecture

This is the main architecture style of the experimental platform software. It has been chosen due to its distributed asynchronous capacity used to produce highly scalable and high-performance applications (Richards and Ford, 2020). Moreover, as a result of the nature of the experimental platform where a comprehensive interaction between the user and the platform functionalities is performed, this architecture allows to process the events in decoupled components that asynchronously receive and process events. This asynchronous communication can increase significantly the overall responsiveness of the system.

Figure 2.9 illustrates the event-driven model applied in the event-driven architecture. In this model, an event-driven orchestrator manages and controls the workflow of events started that demands the coordination of multiple event processors. The advantages of this model are related to its flexibility and the action-based levels that require a high level of responsiveness and scale in a dynamic user processing.

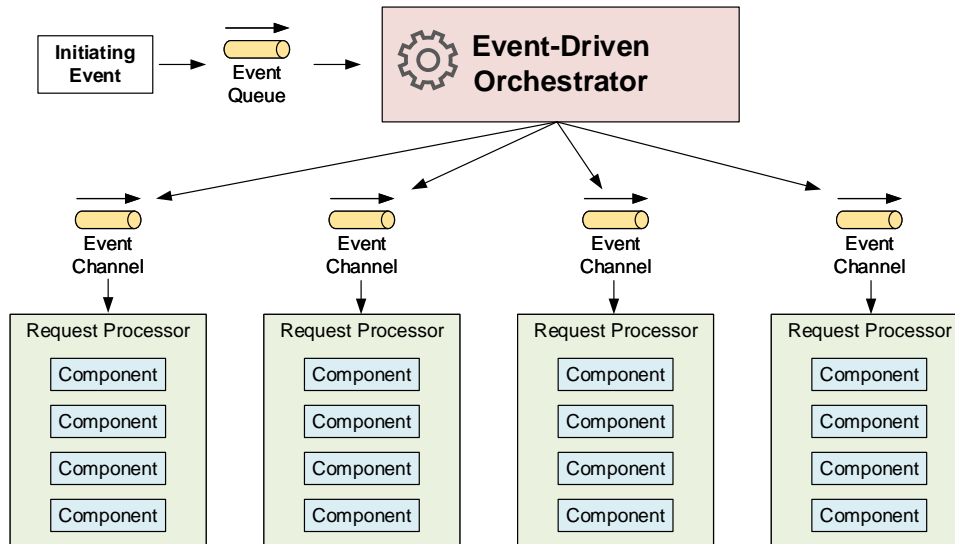


Figure 2.9: Event-driven model.

An initiating event is sent to an event queue starting the whole process. The orchestrator accepts and manages the event by sending it to a dedicated event channel (graphic user interface, containerized application, database, API layer or external device connection). The event processor listen the event channels, process the event according to the task demanded, and in some cases respond back to the orchestrator to inform that the event has been processed (mostly in simulation executions). Finally, the information is updated between the different software components.

The events are classified according to their complexity and task. Figure 2.10 shows the hierarchy between the events defined and the classification according to their execution. The orchestrator can interrogate the classification of the event, and based on that, handle the event itself or forward it to an specific software component. In this way, all events are effectively processed and delegated to the corresponding component in charge improving the efficiency of the software system. In addition, the orchestrator component has knowledge and control over the workflow.

This style is a reactive architecture that addresses both resiliency and responsiveness, it means that the system is resilient in terms of error handling without an impact on its responsiveness. It is visible in the event processing, where, the next event is immediately processed clearing the event queue handler.

#### 2.4.1.1 Graphic user interface

A graphic user interface has been designed to allow the user to supervise and interact with the different system elements which integrate the power distribution system modeled, performing

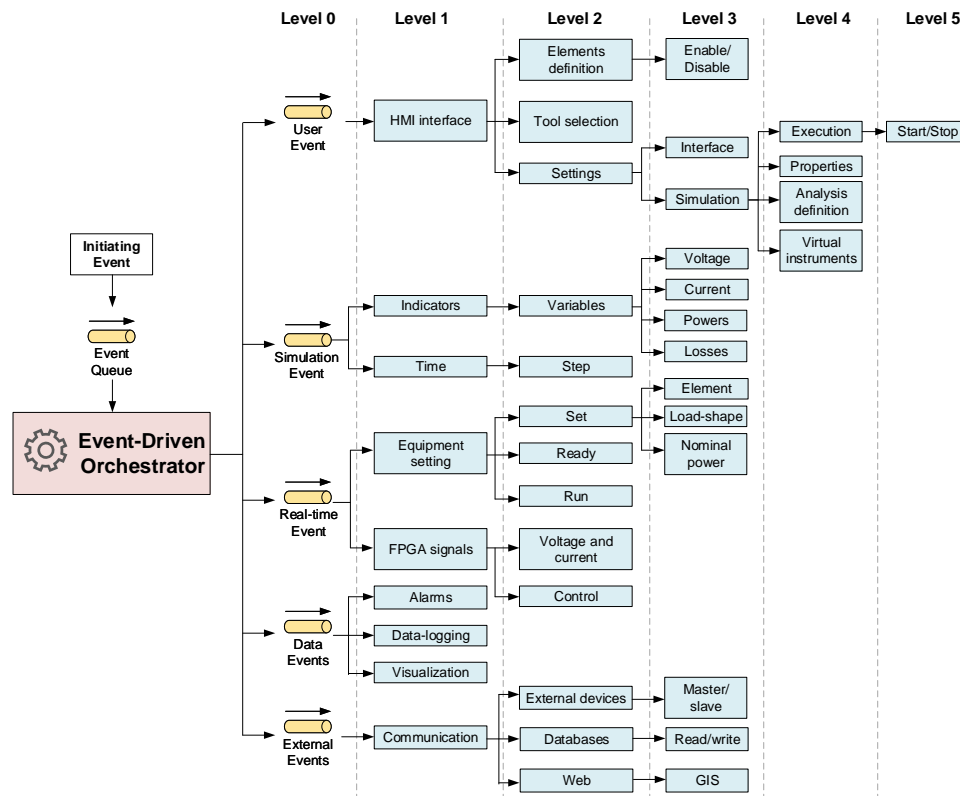


Figure 2.10: Event-driven model.

different analyses according to its physical characteristics. This kind of graphical representation provides an accurate information of all system assets and their performance. This results in a supervision and analysis interface capable to generate reports for several types of studies performed over the system network.

Figure 2.11 shows the human machine interface (HMI) developed. NI LabVIEW<sup>®</sup> has been used to develop the HMI. This interface is composed of four containers to arrange the different software functionalities. A brief description is detailed below:

1. **Tools palette:** This palette includes the software functionalities available to analyze and supervise the power distribution network.
2. **Options panel:** This panel includes the input controls, navigational components and informational components related to each functionality.
3. **Simulation step indicator:** This progress bar and date indicator help to monitor when a simulation is finished and notice the time step in a dynamic simulation (daily, weekly, yearly or duty).
4. **System panel:** This is the main container where the distribution network is modeled, whereby the user can interact and visualize the behavior of the different system elements.

## 1. Main tools palette

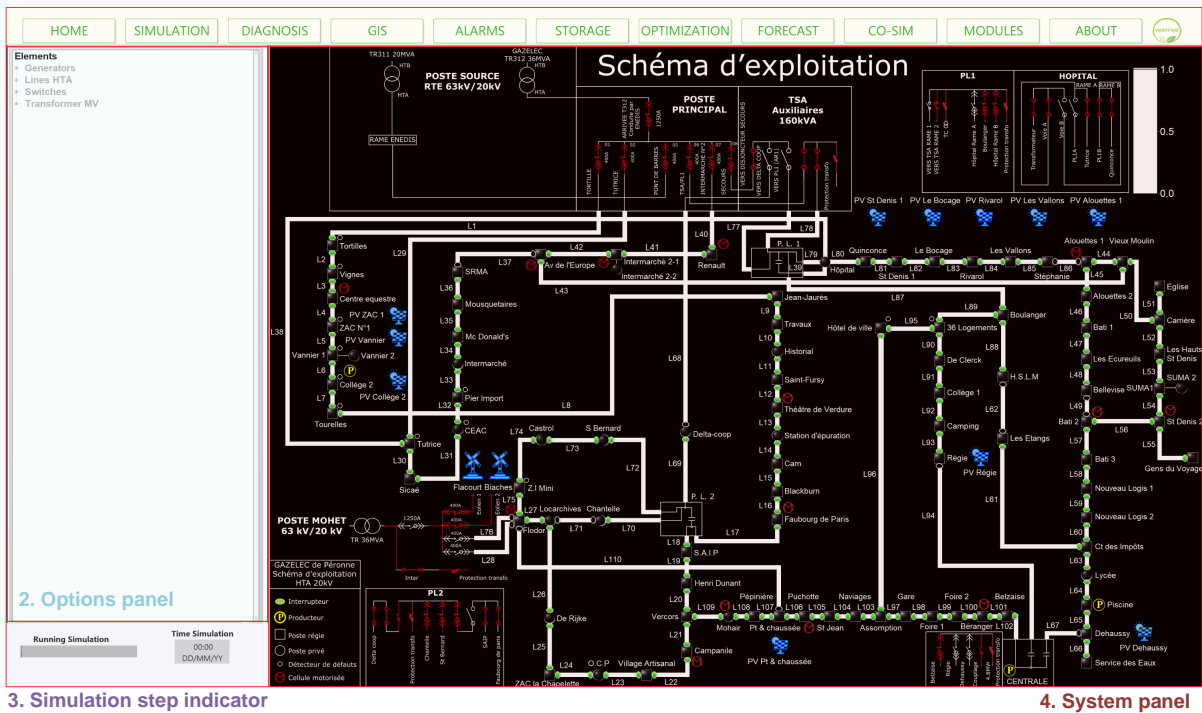


Figure 2.11: Human machine interface of the experimental platform.

2.4.1.1.1 *User interaction* The HMI has the possibility to interact with all system elements through events. This procedure allows to enable/disable the system assets and establishes a new paradigm to assess possible system re-configurations, system outages, fault isolation, etc.

Elements such as wind farms, photovoltaic panels, conventional generators, protection line switches, reclosers, storage devices are available to expand the simulation capabilities and system analysis.

2.4.1.1.2 *Metering and reporting* Different measurements can be performed in the experimental platform software (voltage, current, powers, and losses). For this task, virtual instruments pop-up windows (Figure 2.12a) were developed to display numerically or graphically these variable measurements of a specific element. The virtual instruments developed are:

- **Measurement point:** Displays a measurement graphic of a chosen element over the time after finished a dynamic simulation. The phases can be selected and the option to export the results in an Excel file is available too.
- **VI meter:** Measures numerically an element variable while the simulation is performed.
- **Polar meter:** It does the same function as a VI meter, but it is based on a polar representation (mostly used for quality power analysis and fault studies).

Furthermore, a caller pop-up window (Figure 2.12b) is available to visualize the definition and properties of the elements selected over the system distribution model. The actor-model architecture was employed to develop the pop-up management of both tools, a further explanation of this architecture is found in Chapter 4.

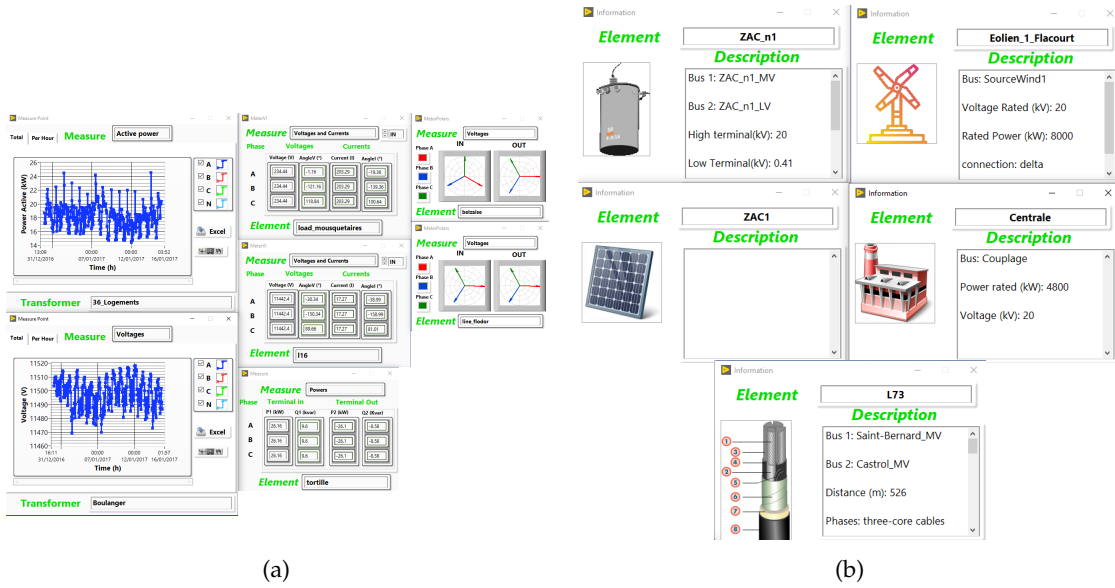


Figure 2.12: Pop-up windows: (a) Element measurement. (b) Element description.

Finally, an information panel is included to list all simulation events occurred, including the alarms and warnings generated during a simulation. An automatic data-logging file registers all the events in PDF format. This file is located in the software folder.

2.4.1.1.3 *Heat mapping* A novel graphic measurements representation is developed in the experimental platform software. This is a heat mapping representation based on a color rendering to show the results of a simulation over the lines.

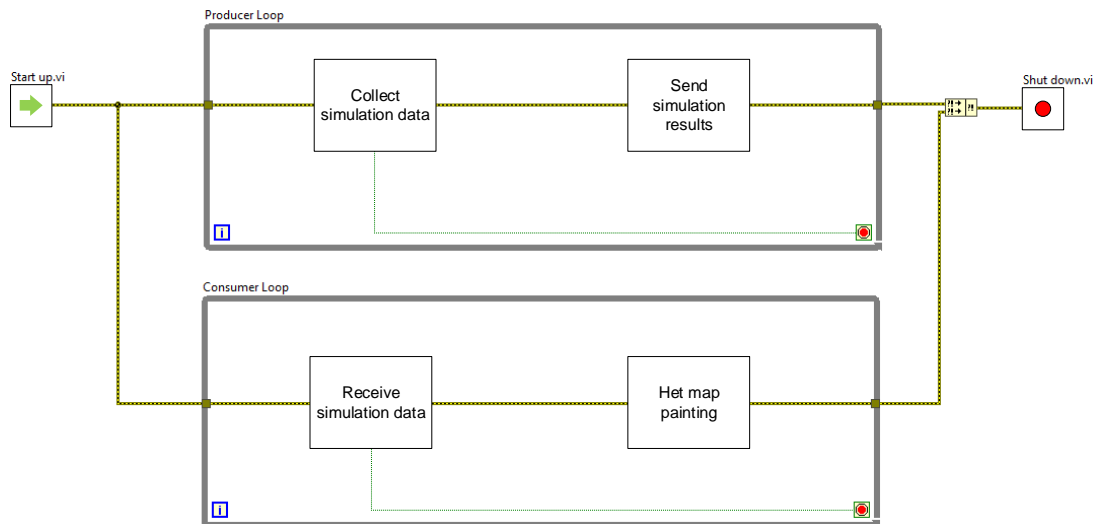


Figure 2.13: Producer/consumer architecture.

The producer/consumer architecture is used to develop the heat mapping representation. This architecture is useful to improve the data sharing across multiple loops operating at different speeds (Instruments, 2021b). Figure 2.13 shows the pattern architecture. The simulation is executed in a producer loop, then, the results are collected and sent to a consumer loop.

Finally, these results are processed and plotted using the heat mapping representation. This technique assures the refresh of the schematic in a different rate of the simulation execution.

Figure 2.14 illustrates the heat mapping representation after a static simulation execution. A heat bar is located in the upper right corner, it denotes the relationship between the color and the scoring value of the measurement. Red is a high value measurement meanwhile, blue is the opposite. The option to change the color of the heat mapping is also available.

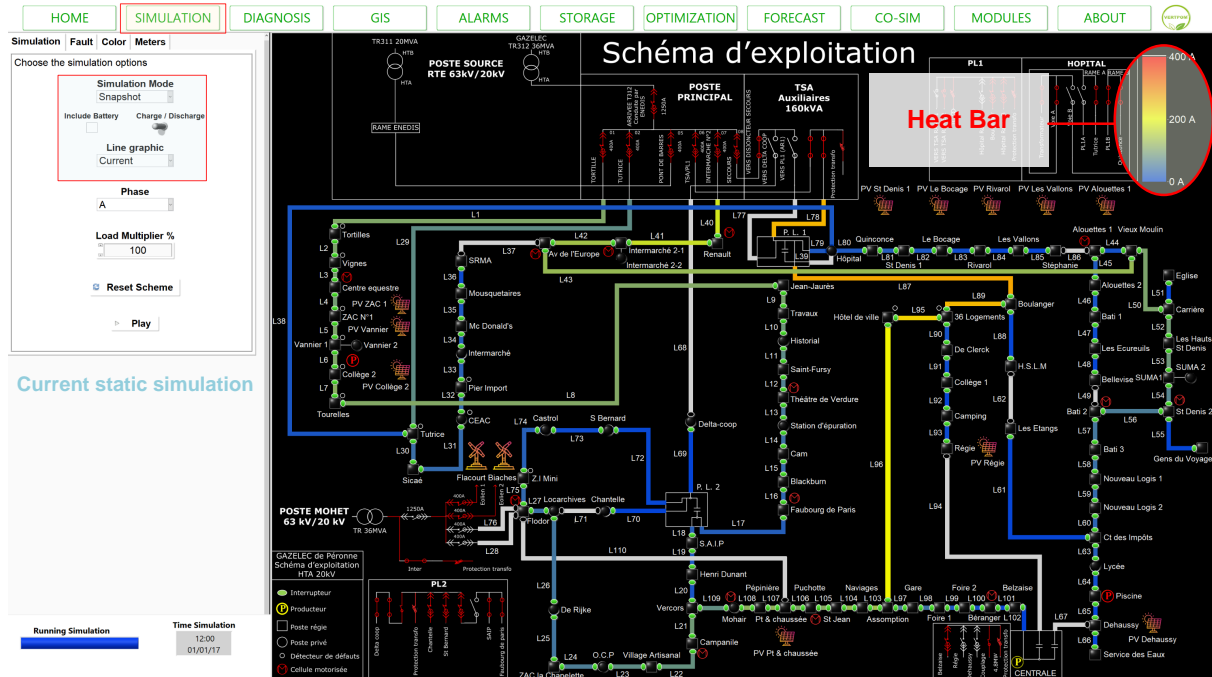


Figure 2.14: Heat mapping painting.

The relationship between the color and the type of measurement is done automatically changing the value limits and adjusting the measurement units. The heat mapping considers the phase of the line measurement selected. In a dynamic simulation, the line measurements are updated refreshing their color instantly. The possibility to change the type of measurement and phase is available too.

After an ergonomic study conducted, the results have revealed a high SO satisfaction in the use of the color mapping. The SO remarked an easy measurements interpretation and a faster decision-making response under event conditions.

**2.4.1.1.4 Simulation and equipment configuration** The user operator can manage the simulation options and emulators equipment using the software interface. In the main tools palette, a dedicated button is available for each task. A more detailed explanation in the simulation and equipment configuration is done in the following sections.

#### 2.4.1.2 Containerized applications

The containerized applications are those applications which are contained in the experimental platform software. In other words, those applications which were developed using NI Lab-



VIEW<sup>®</sup>. The applications and all their dependencies are packaged in a standard unit of the software, running quickly and reliably in the experimental platform environment.

The container engine isolates the applications to execute stand-alone studies. One example of these containers is the battery sizing and placement tool which is launched using the storage button of the tools palette. Other containerized applications are fault analysis and energy demand reduction which have been already integrated in the experimental platform. [Figure 2.15](#) reveals the containerized deployment of applications.

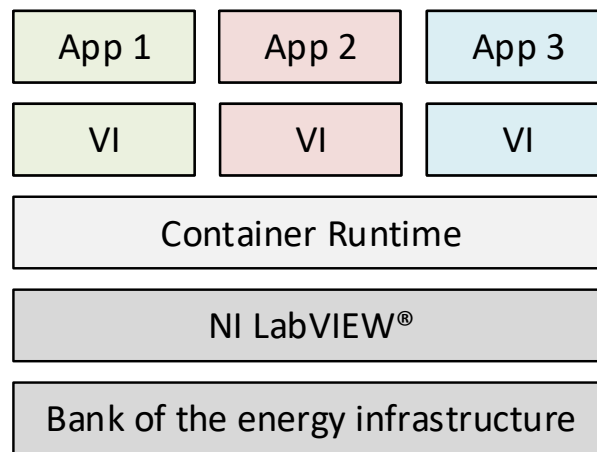


Figure 2.15: Containerized applications in the experimental platform.

This technique ensures that the application works uniformly despite differences for instance between development and staging.

#### 2.4.1.3 Database

A MySQL database is developed to store in the data server all information related to the experimental platform. This is an open source relational database which organizes the information into multiple tables relating the data type (Oracle, 2021).

A big volume of data is currently managed in the database, hence, multiple tables were built to classify the origin of the information. As a result, these tables are dedicated to store and structure the information separately such as meteorology, data logging, system modelling, CO<sub>2</sub> production, load consumption, internal software variables, electricity price, among others.

The security of the database is based on access control lists (ACLs) for all connections, queries, writing/reading operations that can be performed. Moreover, the connections between the experimental platform and other clients are SSL-encrypted.

#### 2.4.2 API layer

An application programming interface (API) is enabled in the experimental platform to interface external microservices which are not embedded in the event-driven architecture developed. Microservices allows a distributed architecture, it means that each service runs in

its own process. Figure 2.16 shows the topology of the microservices architecture. Multiple services can be run in parallel according to different client request.

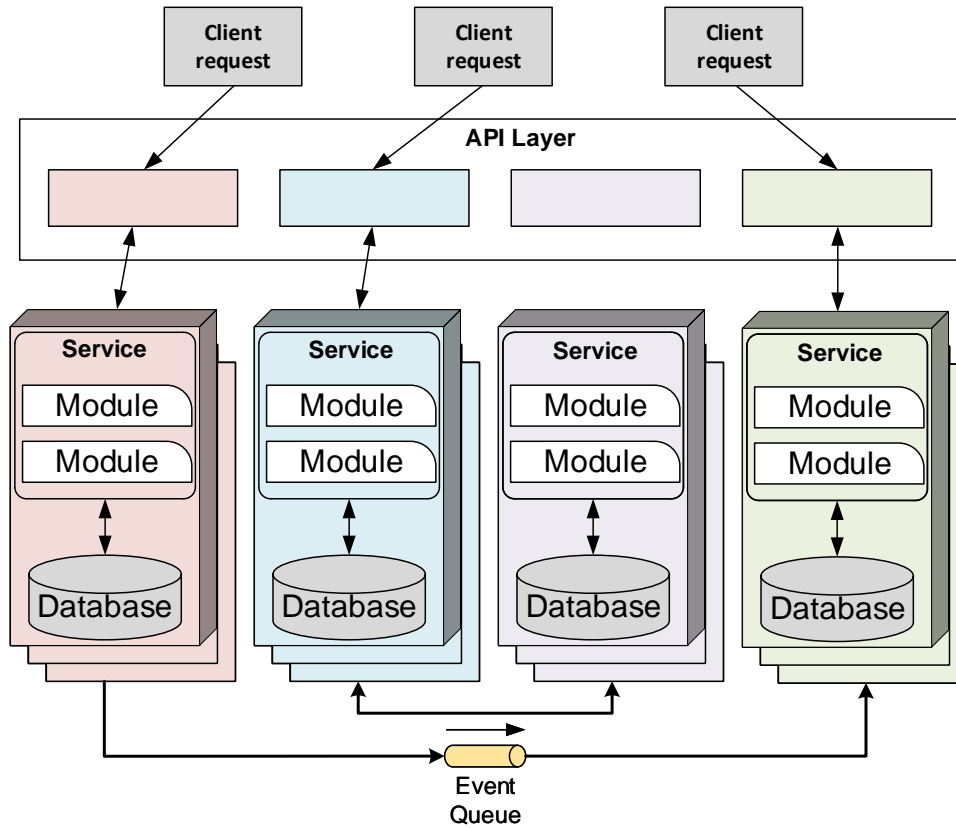


Figure 2.16: Topology of the microservices architecture.

Decoupling the services opens the possibility to execute several applications at the same time, it permits to separate each service into its own process and even execute them on different workstations (Richards and Ford, 2020). This feature improves the data analysis and simulation execution reducing the computing time to perform RT simulations in a reliable way.

Microservices represent all third-party applications, libraries or functionalities adopted in the experimental platform. The microservices integrated in the API layer are the following:

#### 2.4.2.1 *OpenDSS simulator*

The open-source distribution system simulator (OpenDSS®) is the electrical simulation software employed to support the smart grid analysis in the experimental platform. The distribution system analyzed (Appendix A) was modeled using the wide number of device models present in the simulator.

OpenDSS is developed by the electric power research institute (EPRI) (Dugan and McDermott, 2011) and it offers different simulation modes, starting from power flow simulations until quasi-static-time-series (QSTS) simulation for evaluating the behavior of power systems through time. Its capacity of performing QSTS simulations opens the possibility to analyze

distribution networks and characterize their assets by daily, yearly or another time-based simulation (Montenegro, Dugan, and Reno, 2017).

Currently, OpenDSS is evolving to a more flexible and robust simulator, exploiting the parallel processing advantages of the actual CPUs. This feature makes OpenDSS a powerful tool to be integrated in the software of the experimental platform. The interface for sending and receiving messages from OpenDSS is done by the Direct DLL API interface available for NI LabVIEW (Montenegro and Dugan, 2017).

#### 2.4.2.2 Web service applications

It is possible to integrate web services by using a client-server architecture in the experimental platform. For this purpose, a representational state transfer (REST) API is available to communicate with web services (RESTful) applications.

This communication is established using a JavaScript object notation (JSON) data object. This data object allows to send requests and receive object values from the experimental platform software to the RESTful application. Figure 2.17 shows the client-server architecture deployed to interface RESTful applications.



Figure 2.17: Client-server architecture for restful applications.

The client-server architecture has enabled a flexibility in the programming tasks of the people involved in the project, separating the client from the server. This improves the scalability in the development of the software functionalities of the experimental platform.

Applications such as load profile analyzer, energy consumption forecasting, electricity distribution network mapping (GIS) and the battery scheduling have been developed by other PhD students and research engineers belonged to the project. These functionalities are integrated in the experimental platform using the client-server architecture.

Other purposes like the connection to external databases can be done using the same model. In this way, databases for retrieving information about the load consumption, the meteorology forecasting, the energy price market and even the CO<sub>2</sub> emissions are interfaced by the client-server communication.

### 2.4.3 External devices connection

The communication with an external hardware is based on a master-slave architecture. In this architecture, the workstation functions as a *master* whereas the external devices are connected as *slaves*.

Figure 2.18 shows the communication between the workstation and the different external devices using the master-slave architecture. In both cases, the grid emulators and the remote control devices use a bidirectional communication channel to receive/send the commands to the workstation. The grid emulators process the analog and digital signals received to emulate the elements assigned, and close the loop sending the measurements obtained. On the other hand, the remote control devices can send commands to the elements defined in the workstation to change their parameters and settings, an answer from the workstation is sent to confirm these changes.

This pattern guarantees a continuous communication with the external devices that need to run simultaneously at different rates. Every task is performed separately giving a more modular approach to interact with multiple devices. This architecture also allows the deployment of a RT routine due to the control of the time management execution of every task. In NI LabVIEW, each parallel loop is treated as a separate task or thread (Instruments, 2021a). As a result, the experimental platform exploits the advantages of the parallel computing using the threads available in the workstation.

## 2.5 VALIDATION OF THE EXPERIMENTAL PLATFORM CONCEPT

For evaluating the accuracy and performance of the experimental platform, a real case and some test cases are used respectively.

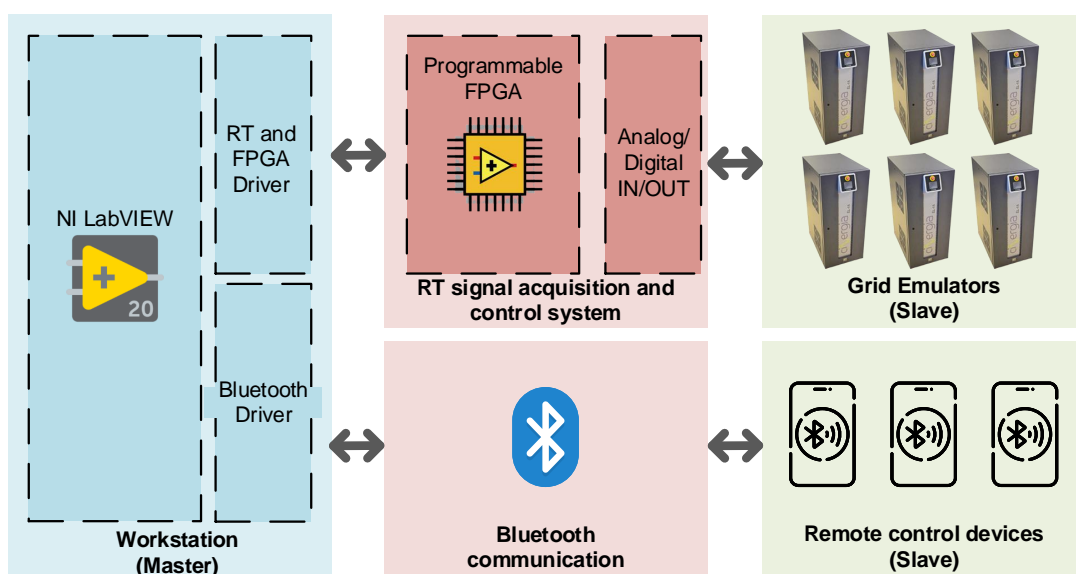


Figure 2.18: Master-slave architecture for external devices.

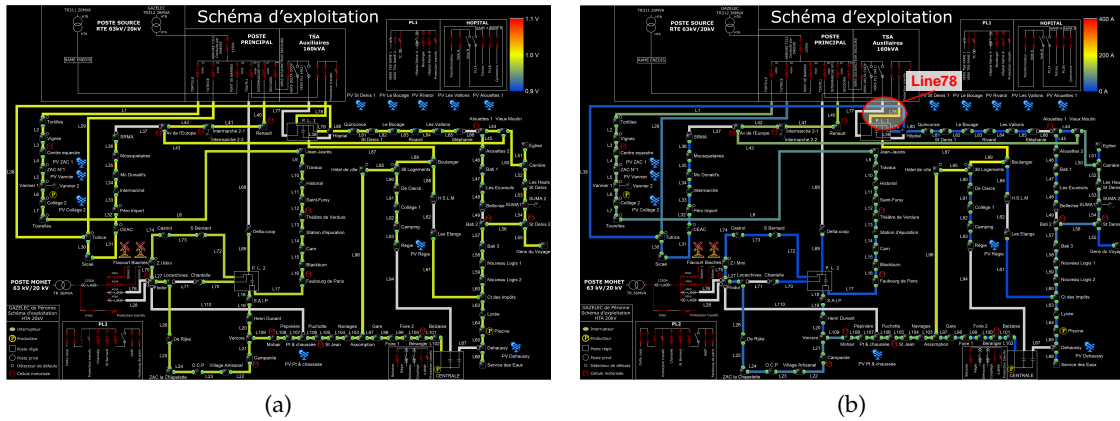


Figure 2.19: Normal state of GoP distribution system: (a) Voltage profile. (b) Current profile.

### 2.5.1 Real case: Fault study analysis

This case intends to emulate the incidents reported in a real distribution system, allowing to evaluate the accuracy of the experimental platform comparing the results obtained in the SO report. The system model and the fault analysis simulation functionalities are also tested. The short-circuits presented are emulated in the RT environment using the grid emulators to validate the phenomena. Finally, a corrective solution is proposed to avoid similar failures in the future.

#### 2.5.1.1 Case 1: Single phase short-circuit and overcurrent fault

A first real case study was conducted using the Gazelec of Peronne (GoP) system network, the fault information is retrieved from the CT-IBox meters and the technical proceedings report done by the SO.

The fault study case is about two failures detected by the SO on the same day, occurred on August 22, 2020. The normal steady-state condition for this day of GoP power distribution system is shown in Figure 2.19, the system chargeability is around 70% of its total capacity, the voltage reference is 20 kV and the average of the voltage system (2.19a) is near to 0.98 p.u.. The current (2.19b) is in a normal level, except for the the line 78, in this line the current detected is considerable and represented in a darker yellow.

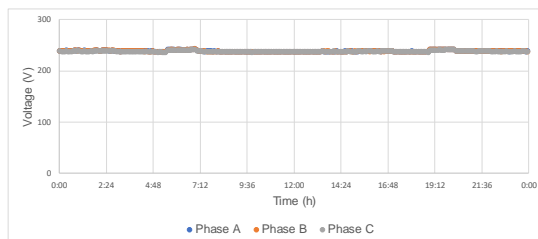
The meter data set is one-day information retrieved from 5 CT-IBox meters installed in the 400 V side of the current MV/LV transformers of the distribution system, this information reveals a fault clear procedure from the SO when a overcurrent fault is detected in one branch of the substation feeder.

Figure 2.20 and Figure 2.21 show the voltage and current measurement information retrieved from every transformer at the same period of time respectively. All phases are displayed for every measurement and the fault clearing is marked in every graphic to identify easily the event.

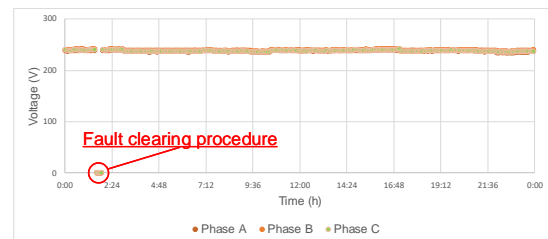
It is noticed that 4 out of 5 transformers executed the fault clearing procedure, the other one called *Alouette 1* was not affected due to its location in the opposite side of the system network. The SO reported the same short circuit, consequently, a fault clearing process was done.

The timeline of the fault incident starts at midnight with a short-circuit event detected in one of the phases of the line 78 (Figure 2.22). There is no trace in the voltage and current data sets examined, because as it is shown, the meters are installed in not affected branches. Figure 2.22a shows the simulation of a single-phase fault in the same line and phase. Figure 2.22b shows a virtual measurement instrument placed in the line 78 indicating a voltage drop in the phase affected (phase A), and an overvoltage in the other two phases; likewise, the current does not measure a big difference between the phases (Ignatova, Granjon, and Bacha, 2009).

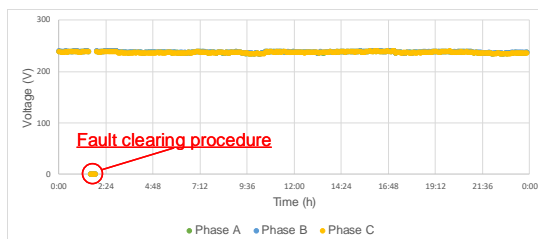
Immediately afterwards detected the fault, the line 78 is opened to clear the short-circuit, causing an unbalancing current effect in the first branch of the network (Figure 2.23a). In response the SO has closed the line 77 to activate the auxiliary services and to recover the system (Figure 2.23b). But the line 87 is now overcharged, so the SO decides to reconfigure the system: first opening the line 77 and the line 87 at the same time, unplugging one branch of the system (Figure 2.23c). Second, reconnecting this branch through the Hospital substation close connection (Figure 2.23d). And finally, opening the line 88 and 103 and closing the line 62 and 67 (Figure 2.23e).



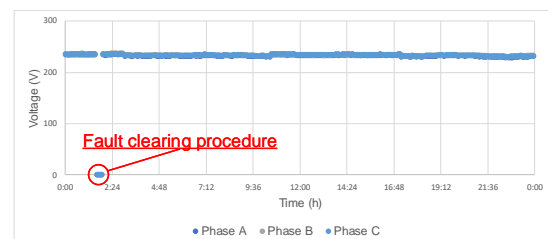
(a) Voltage profile of Alouette 1 transformer.



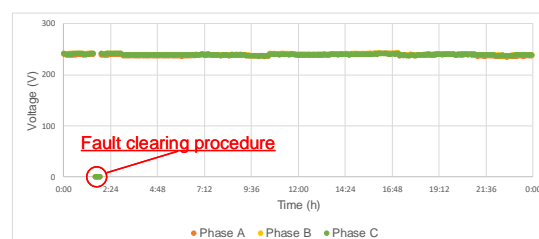
(b) Voltage profile of Cam transformer.



(c) Voltage profile of SAIP transformer.



(d) Voltage profile of Vignes transformer.



(e) Voltage profile of ZAC N°1 transformer.

Figure 2.20: One-day voltage data set from CT-IBox meters.

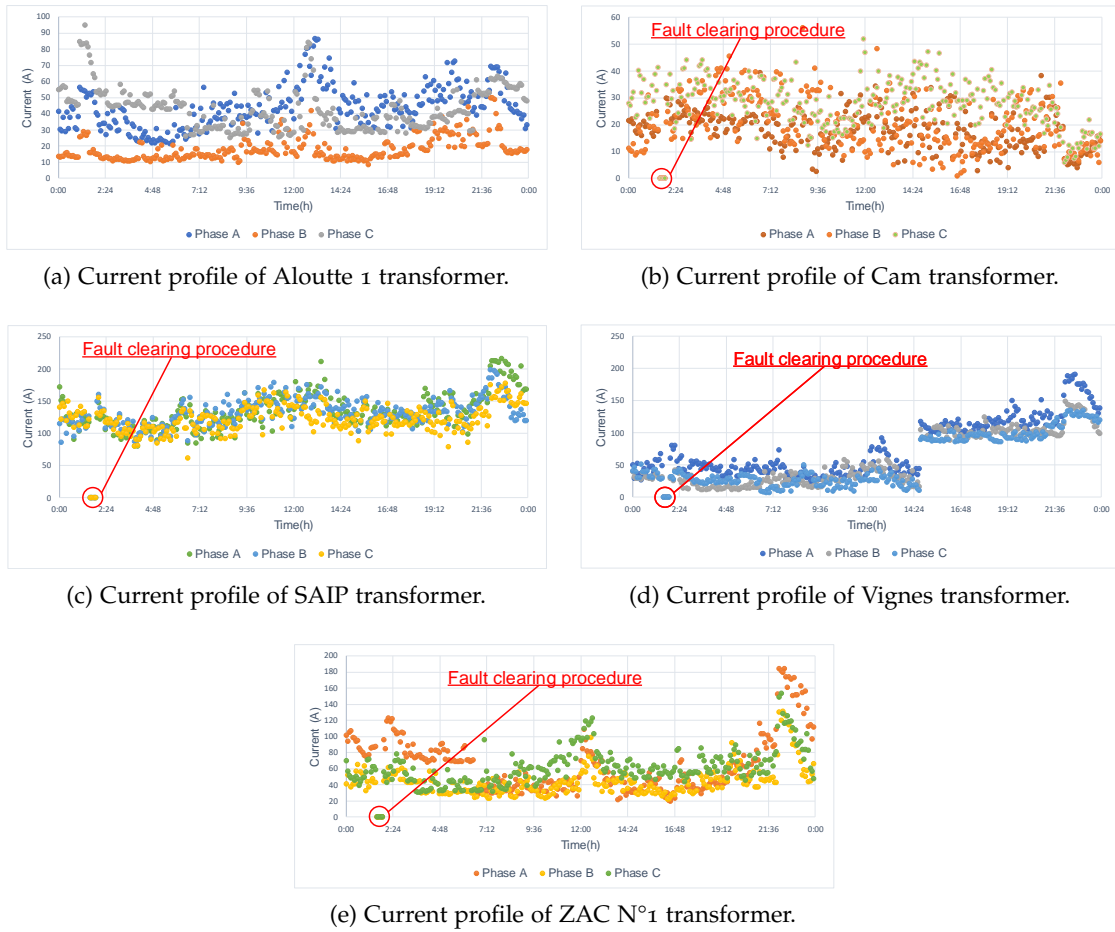


Figure 2.21: Fault clearing procedure detected by the CT-IBox meters.

At first sight the system seemed to respond well, but few hours later (01:50 am) an overcurrent is detected in the three phases of the substation protection (*Tortilles*) and, in consequence it opens the switchgear of the branch affecting at this time other substation as presented above in Figure 2.21 and Figure 2.22. Notice that those transformers where the fault is detected, they

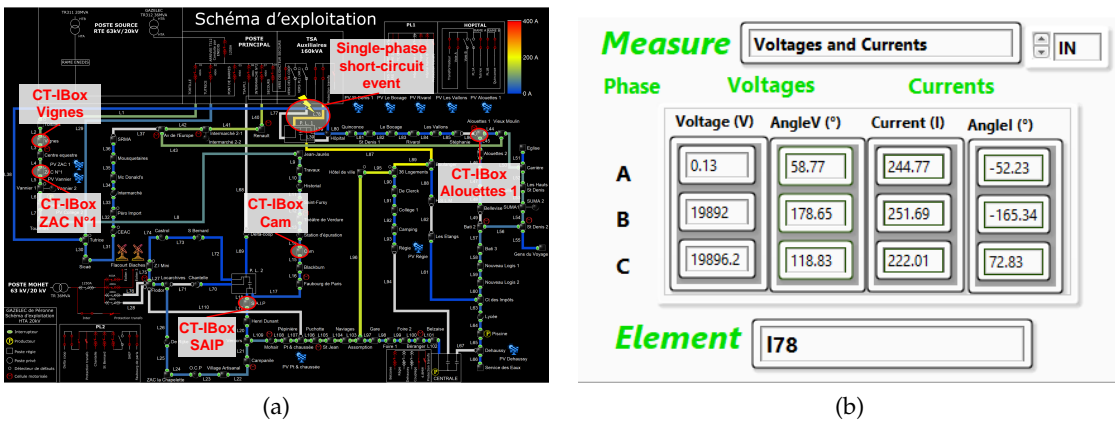


Figure 2.22: Single-phase short-circuit in the line 78: (a) Phase A current measurement in the whole system. (b) Voltage and current measurement in line 78.

are located in the same branch of the fault, contrary for the transformer *Alouette 1* which does not detect the fault and belongs to other system branch. Figure 2.24 shows the blackout at Tortille's branch after the protection is activated.

2.5.1.1.1 *Causes of faults detected* Although the two failures were detected in GoP distribution system, the cause of each fault is independent. According to the SO report, the single-

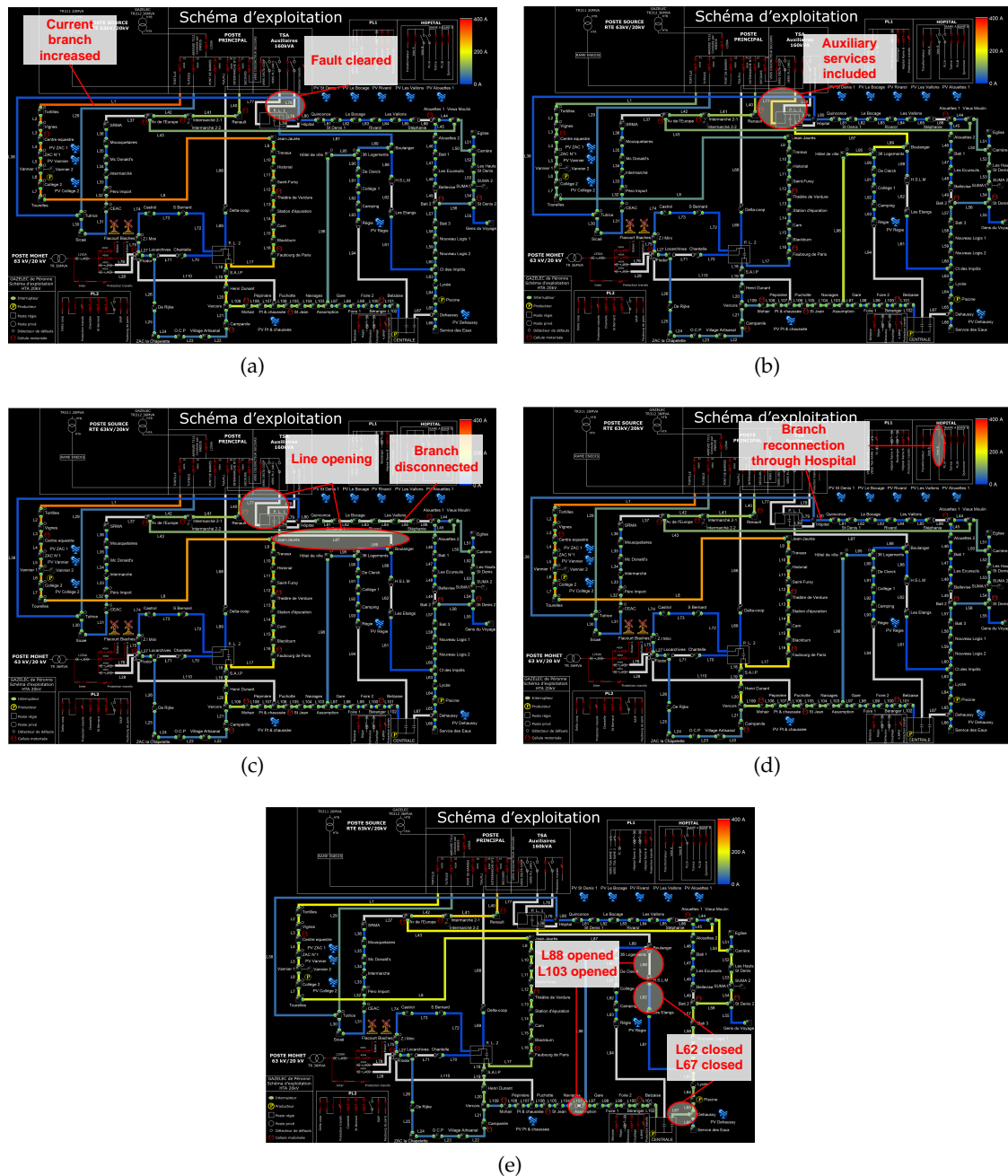


Figure 2.23: Timeline of the single-phase short-circuit case study: (a) Fault cleared. (b) Line 77 closed to recover the system. (c) First SO maneuver: Line 77 and 87 opened. (d) Second SO maneuver: Hoptal Voie B connected. (e) Third SO maneuver: Line 88 and 103 opened, line 62 and 67 closed.



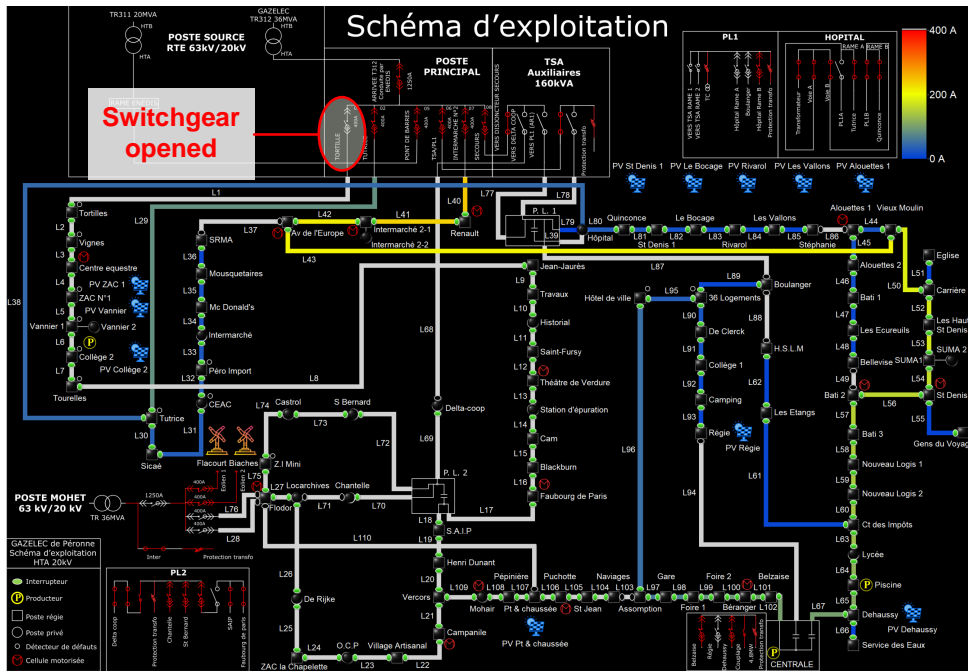
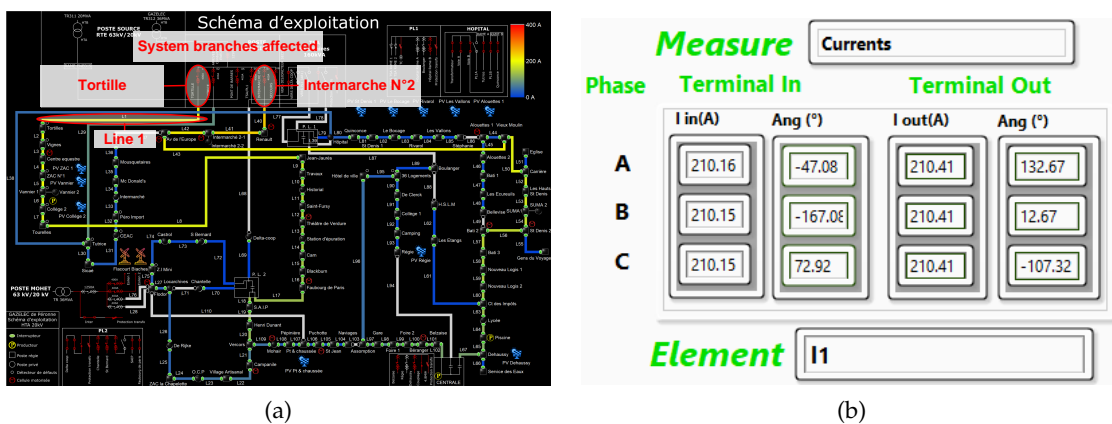


Figure 2.24: Blackout due to a three-phase short-circuit

phase short-circuit is produced by a technical malfunction of one of the phases. At the end, the correction was repairing the phase on site.

Furthermore, the presence of an overcurrent was unexpected as a consequence after the system reconfiguration procedure. But due to the analysis done in the experimental platform, it was possible to establish and clarify the nature of the fault.

Figure 2.25a reveals the last state of the system before the second fault. It is possible to realize that a high current was flowing through the branches of Tortille and Intermarche N°2. Figure 2.25b shows a virtual meter installed in the Line 1, it indicates that the current measured is slightly above 200 A. The currents are similar in magnitude but different in angle, it is due to the power delivery element used to define the lines in OpenDSS.



(a)

(b)

Figure 2.25: GoP system before the overcurrent: (a) Current increased in two branches. (b) Line 1 virtual current measurement.

Then, the equipment protection was inspected and, it was found that the set-point of this protection branch was set in 200 A. As a result, the system protection was able to detect the current peak but at the same time the recloser achieved to clear the fault. In conclusion, this fault analysis simulation allowed to determine in an efficient way the cause of the fault, in order to apply a corrective procedure of the equipment settings.

**2.5.1.1.2 Possible corrective solution** A better decision-making process could be done due to the use of the experimental platform, it is highly recommended to execute different simulations to evaluate several scenarios before to do a technical maneuver in field.

A suitable solution is based considering a better reconfiguration of the system, allowing to balance the current in the branches and improving the state of health of the system assets. Basically this reconfiguration consists in open and close some lines of the system, trying to balance the current profile. [Figure 2.26a](#) shows the final result after the reconfiguration procedure; additionally, [Figure 2.26b](#) shows the current reduction from 210 A to 158.93 A. A description of this procedure is the following:

- Open the line 109.
- And, close the lines 44, 49 and 103.

#### 2.5.1.2 Case 2: Three-phase short-circuit

A second real case study was tested in the experimental platform. For this case scenario any information could be retrieved from the smart meters and only the operator system report was available, in consequence, the simulation process is done to understand the fault phenomena.

This fault study is a three-phase short-circuit occurred in the transformer called *Gens du voyage*. [Figure 2.27a](#) shows the simulation of a three-phase fault in the same transformer. The branch which the line is located, it is affected at the same time increasing the current in all the lines

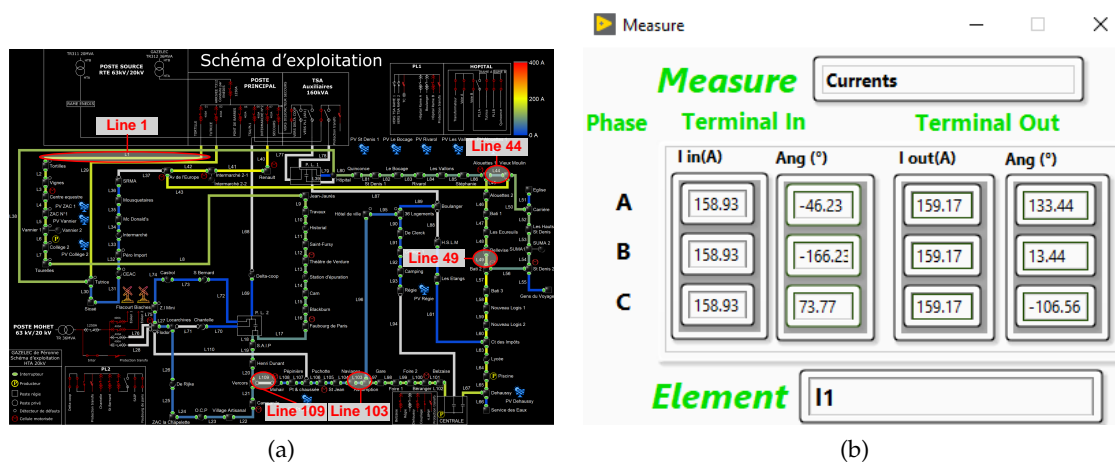


Figure 2.26: New reconfiguration suggested: (a) GoP system state after the reconfiguration. (b) Line 1 virtual current measurement.

belonged and resulting in a difficult task to find the origin of the fault. Figure 2.27b shows a virtual measurement instrument placed in the line 55 (beside the transformer) indicating a voltage drop in the medium voltage 20 kV side, likewise, an overcurrent in the three phases.

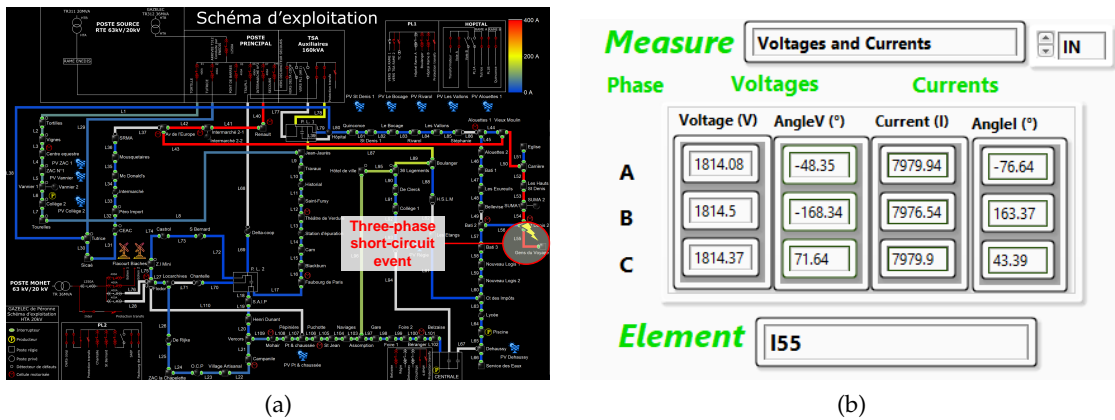


Figure 2.27: Three-phase short-circuit in the Gens du voyage transformer: (a) Phase A current measurement of the whole system. (b) Voltage and current measurement in line 55.

A major problem was that the short-circuit was not detected by the line protections, making the fault clearing process extremely difficult. But fortunately, the protection of the switchgear Interbranche N°2 was the only element to detect it, resulting in a blackout of the branch as seen in Figure 2.28a. Moreover, the recloser did not work due to the permanent presence of the fault. After several attempts by the SO, it was detected and isolated the fault origin, the system recovered its normal functioning as presented in Figure 2.28b.

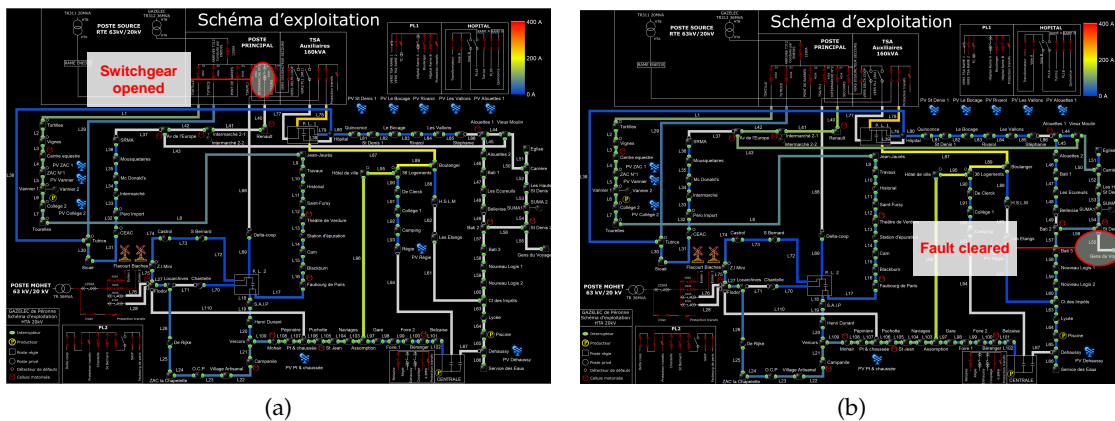


Figure 2.28: Timeline of the second fault case study: (a) Blackout in branch Interbranche N°2. (b) Fault cleared.

This case was a hard challenge to find the nature of the fault for the SO. However, the experimental platform allowed to establish a clear decision-making strategy to isolate the fault. Due to the general view of the branch affected, the SO could open the distribution network by sections until find the fault.

### 2.5.2 Test case studies

The performance and the work capacity of the experimental platform associated to the Bank of Energy is an important issue to evaluate. It allows to determine the response and the efficiency of the experimental platform before a bigger and more complex system, also, it ensures the fidelity and scalability of the HIL testing.

As a result, a series of testing scenarios were integrated in order to stress the experimental platform and evaluate their performance in the temporal parallelization process. The tables 2.1 and 2.2 summarize the characteristics of these test feeders. For a complete explanation of the test feeders, please refer to [Appendix B](#).

All test systems were modeled in the experimental platform using OpenDSS simulator. As it was explained before, NI LabVIEW is in charge to interface with OpenDSS to facilitate the supervision and integration with improved algorithms.

The use of the OpenDSS-PM (parallel machine) library for NI LabVIEW makes possible to compute the solution of each test system using a parallel environment, this allows to verify the speed calculation and the processor performance of the experimental platform.

#### 2.5.2.1 Speed test

The first test performed consists in evaluating the performance of the simulation in terms of computing time, which is measured without considering the time required for compiling the model.

The speed test has the purpose to demonstrate how long it takes to resolve a static simulation (power flow) in the workstation between 1000 iterations. [Table 2.3](#) lists the results obtained

Table 2.1: Summary of the test circuits integrated in the experimental platform (1).

Test system	Nominal voltage, kV	Radial or Meshed	Feeder type	Distribution transformer	RT series load data
IEEE 8500 Node	115, 12.47, 0.24	Radial	4-wire wye	Y	N
IEEE European LV	11, 0.416	Radial	4-wire wye	Y	Y (1 day)
EPRI Ckt5	115, 12.47, 0.48, 0.24	Radial	4-wire wye	Y	N
EPRI Ckt7	115, 12.47, 0.48, 0.24	Radial	4-wire wye	Y	N
EPRI Ckt24	230, 34.5, 13.2, 0.48, 0.24	Radial	4-wire wye	Y	N
Iowa System	69, 13.8, 0.24, 0.12	Radial	3-wire delta	Y	Y (1 year)
Gazelec of Peronne	63, 20, 0.4	Meshed	3-wire delta	Y	Y (1 year)

Table 2.2: Summary of the test circuits integrated in the experimental platform (2).

Test system	Number of nodes	Number of buses	Number of loads	Total power consumption, MW/year	Scale
IEEE 8500 Node	8531	4876	1177	11793.92	Large
IEEE European LV	2721	907	55	190.58	Low
EPRI Ckt5	3437	2998	1379	26067.91	Medium
EPRI Ckt7	2452	1255	906	28693.85	Medium
EPRI Ckt24	7522	6058	3891	120710.99	Medium
Iowa System	906	436	194	11894.56	Low
Gazelec of Peronne	561	187	450	62.96	Low

after the speed test for each test feeder. It is important to highlight that this simulation is executed just in one core of the multi-core processor. Due to the nature of the non-deterministic processor an average study was done, it means that it was executed 10 times the simulation per system and the average value is the result of time.

The results are plotted in [Figure 2.29](#) and it can be seen that there is a linear progression between the average solution time and the number of nodes of the test systems tested, except in the IEEE 8500 and the IEEE European test feeder cases for which their topology resulted in lower solution times.

These results reveal a high performance of the workstation for each model using less than 3% of the CPU utilization ([Figure 2.30](#)). The memory did not reveal a significant impact to perform the simulation of each test feeder.

Table 2.3: Speed test results using one core.

Test system	Architecture	Solution minimum time, ms	Solution maximum time, ms	Solution average time, ms
IEEE 8500 Node	Workstation	1543	1580	1556.6
IEEE European LV	Workstation	70	98	89.6
EPRI Ckt5	Workstation	1802	1843	1816.8
EPRI Ckt7	Workstation	1172	1295	1203.3
EPRI Ckt24	Workstation	5019	5309	5094.4
Iowa System	Workstation	249	275	265
Gazelec of Peronne	Workstation	131	136	134

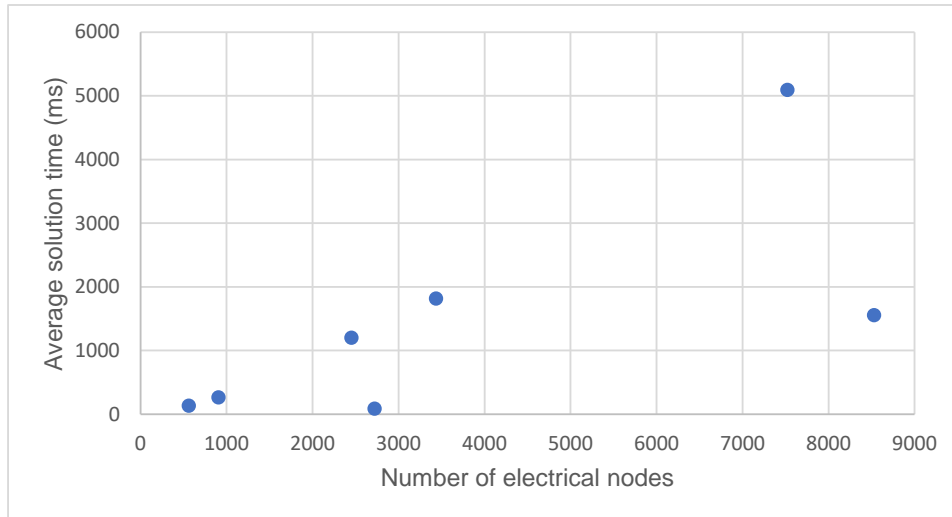


Figure 2.29: Average calculation time based on the number of electrical nodes of the simulated system.

2.5.2.2 Performance of multiple simulations concurrently using the parallel processing features

Parallel processing is very handy when performing detailed analysis that requires small simulations steps and a large number of steps. The big challenge with these simulations is that for each simulation cycle the parameters of the simulation controllers, load profiles, solar irradiance profiles, among others need to be changed. This scenario formerly required a significant

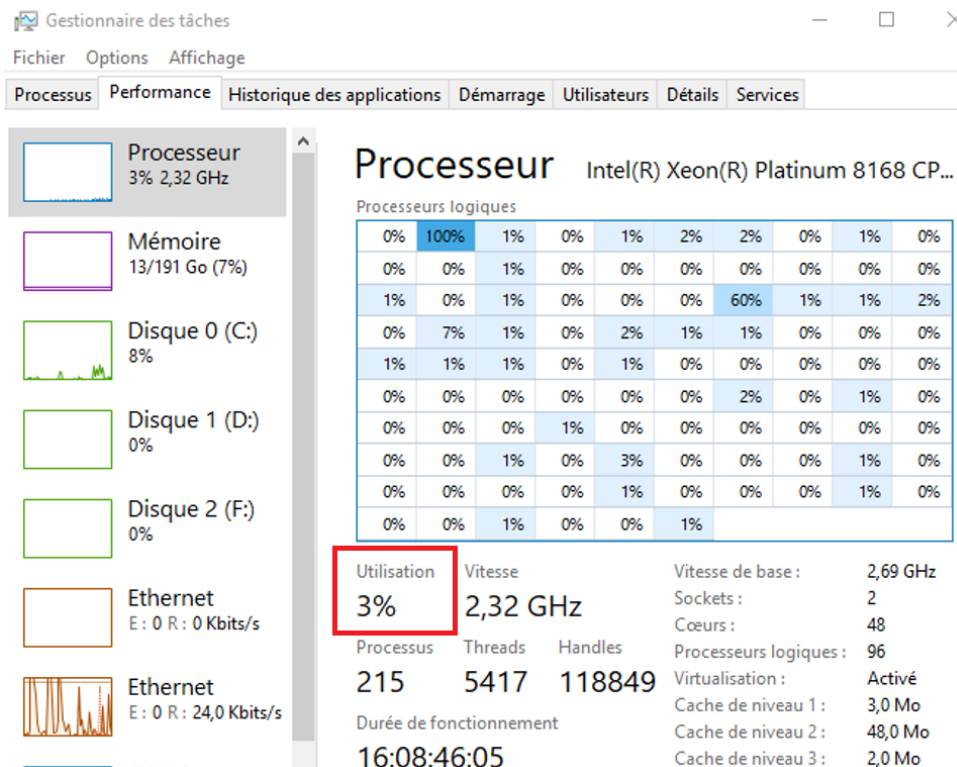


Figure 2.30: CPU utilization under speed test.

number of hours or days to be completed. Depending of the balance of the feeder test system, the system performance will be seriously affected.

By using OpenDSS-PM, it is possible to reduce this time considerably using the 32 physical and logical cores available in the workstation (one of them is left for typical CPU tasks). In this case the power flow is solved 8760 times (hours/year). This was selected to demonstrate the workstation performance in a dynamic yearly simulation.

The simulation process is divided in actors which are belonged to the number of cores disposed in the multi-core processor to execute the simulation. For this reason, it was done a simulation with just one actor equivalent to one core, and another simulation with all actors according to the core system availability.

For these cases, the simulations are performed using the co-simulation environment between NI LabVIEW and OpenDSS-PM. The overhead added by the co-simulation platform is significant compared with the performance of the OpenDSS-PM application working in stand-alone mode. To verify this, the time step of each actor is added after each simulation considering the number of actors used to solve the system.

The first test consists in performing the simulation using one actor of the system. After that, a second simulation is performed using all existing actors available in the workstation. The results of the tests are listed in [Table 2.4](#) according to each test feeder.

Table 2.4: Yearly simulation of the test feeders using single and multi-core processing.

Test system	# Cores	Simulation time per actor - 8760 h		
		Actor minimum time , ms	Actor maximum time , ms	Actor average time , ms
IEEE 8500 Node	1	53363.1	61819.6	56091.35
	31	3493.48	4873.07	3973.69
IEEE European LV	1	19815.1	21237.3	20632.8
	31	1335.52	1436	1406.18
EPRI Ckt5	1	44342.5	47706.9	46988.11
	31	10377.3	12279	11712.75
EPRI Ckt7	1	35978.9	42790.1	38881.4
	31	3407.34	4391.18	3807.92
EPRI Ckt24	1	133976	180187.4	164215.38
	31	17998.7	21837.5	19642.21
Iowa System	1	6955.95	8473.76	7582.99
	31	370.066	522.815	459.47
Gazelec of Peronne	1	6934.58	8601.5	7963.23
	31	1496.38	2123.27	1941.42

These results reveals an improved performance when the simulation is performed using parallel computing in all cases. The solution performance is evident for the more complex feeders. For instance, the Ckt24 test feeder reveals a larger solution time than the other test feeders due primarily to its complexity, however, the introduction of the parallel solver reduces significantly the computation time. On the other hand, the GoP distribution feeder does not represent a high calculation effort to the experimental platform architecture.

Figure 2.31 shows a similar progression in the results as observed in the speed test calculation. A considerable reduction in the calculation time is obtained when the parallel computing is applied. These results are valuable for dynamic simulations using short, medium and long-term basis.

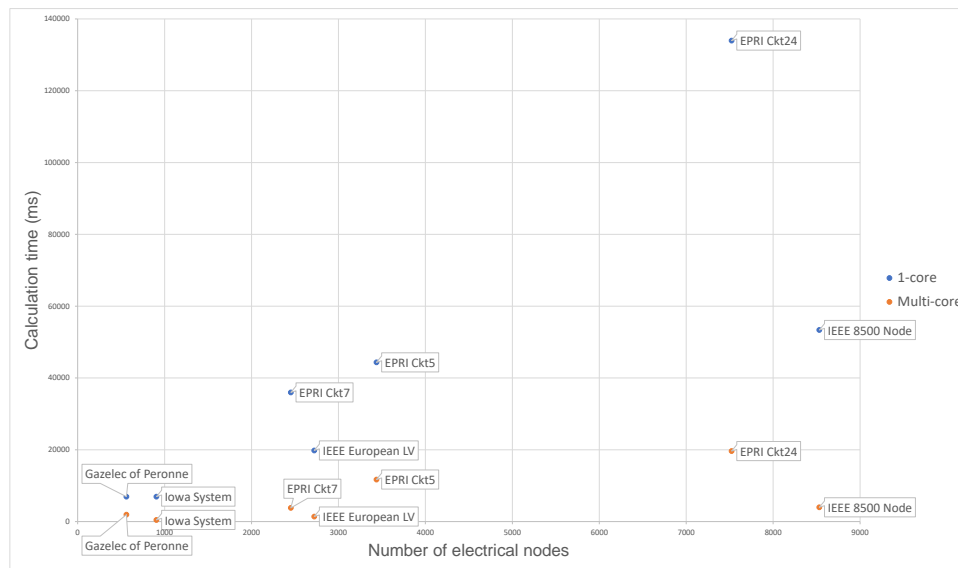


Figure 2.31: Calculation time based on the number of nodes of the simulated systems and cores of the processor.

The parallel simulation execution of the Ckt24 test feeder is shown in Figure 2.32. In this simulation, the number of actors are 31 corresponding to the number of cores available to the parallelization of the task. It is possible to notice how every task is independently parallelized in the progress bar resulting in an independent time execution by actor. The status indicates that each core is busy calculating the solution of the system.

The parallel simulation of the Ckt24 does not reveal a significant overhead in the system processors as it is shown in Figure 2.33. It is important to highlight that this test feeder is the most complex to solve.

The results presented reveal how the actors are indeed an asynchronous system. The total simulation time will be the time of the slowest actor, due to the fact that at each iteration the actors need to be synchronized to perform the extra calculations.

The use of a workstation with those specifications reveals an improved performance when is used OpenDSS in parallel mode, accelerating the simulation experience for all test feeder systems, and resulting in a reliable experimental platform for multiple applications including RT simulations.



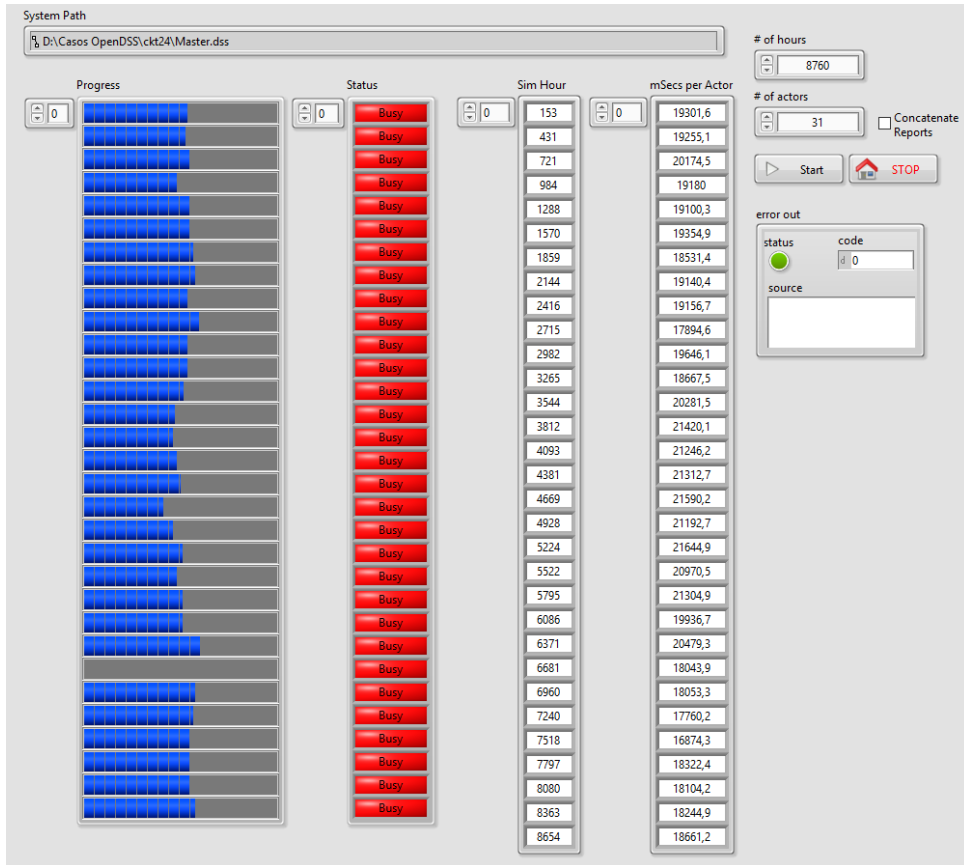


Figure 2.32: Parallel simulation execution of the Ckt24 test feeder.

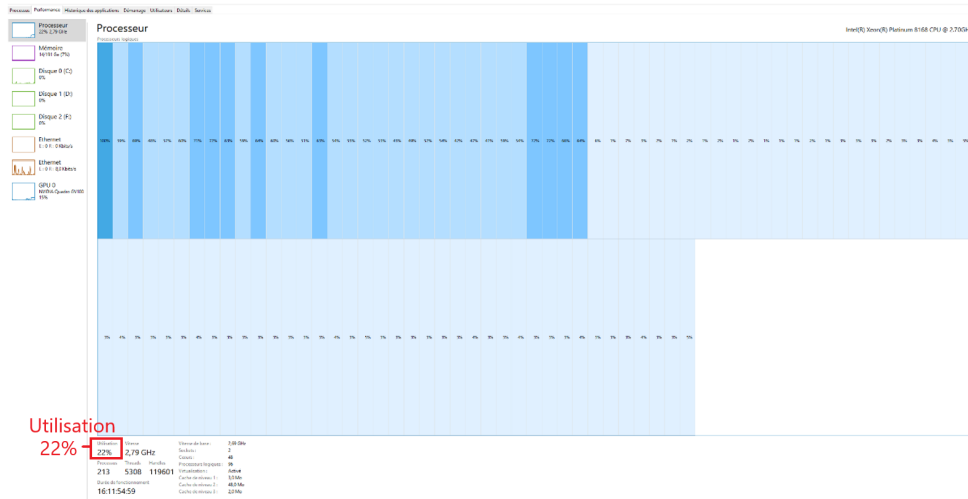


Figure 2.33: Overhead produced in the CPU during the Ckt24 test feeder execution.

2.6 ADVANTAGES OF USING THE BANK OF ENERGY

The Bank of Energy can be installed today in research centers, laboratories or smart grid distribution control centers. The use of an open-source architecture and a modular infrastructure facilitates the license agreements and installation commissioning. As a result, multiple grid

operators, researchers and students would be able to receive a beneficial utilization of the proposed approach.

The following smart grid applications existing in the experimental platform belonged to the Bank of Energy includes a starting point with some solutions that can be considered, however, there is a broad spectrum of applications that can be developed based on this concept.

### 2.6.1 *Fault analysis*

Fault incidence has an important impact in the development of the smart grid systems. The outage has been continuously monitored and investigated for a long time to anticipate the type and location of the faults. This activity is crucial to the planning and operation activities inside the smart grid evolution (Sheng, Xianzhong, and Chan, 2008).

As observed in the real case study (Section 2.5.1.1), the Bank of Energy can help to SOs to detect and understand the nature of momentary and permanent faults. Also, novel functionalities can be developed to allow to anticipate an accurate detection of a failure including power quality distortions, which will help to increase the reliability of the distribution system at a lower cost.

### 2.6.2 *System reconfiguration*

The insertion of DERs, the penetration of electric vehicles (EVs), the installation of an advanced metering infrastructure (AMI) and other technological advances promote the automation of the distribution systems. Added to these technological developments are the continuous efforts to provide a high quality service at lower rate prices to consumers and the reduction of system disruptions as possible. This results in the need of a system capable to exploit the best performance reconfiguring the electrical circuit.

Reconfiguration in distribution system plays a significant role in improving the power quality and reliability without any overcost in the current system assets (Galat and Sonawane, 2017). The typical reconfiguration objectives are destined to loss reduction, load balancing, voltage profile improvement, service restoration, among others.

The model of the distribution system and the possibility to interact with the system elements in the graphic user interface, makes the Bank of Energy an open tool to integrate reconfiguration solution methods to maximize the commonly used objectives in smart grids.

### 2.6.3 *Energy forecasting and operational planning*

The incorporation of the smart meters information and the capacity to execute dynamic simulations in the Bank of Energy, allow to develop energy forecasting and operational planning services considering the DERs installed in the system. These services could be applied as part of the French governmental plan of energy transition (ADEME, 2018a).

This suppose to reduce the energy consumption and replace the consumption of traditional energy generation by renewable energies. This could be applied as part of an advanced distribution network management system (Hayes and Prodanovic, 2016).

#### 2.6.4 *Hosting capacity*

In order to replace the traditional energy generation by renewable energies, it is necessary to consider multiple constraints at the moment to integrate the DERs. For instance when DERs penetration increases, adverse impacts may occur such as voltage variations, thermal loading of different assets, among others (Alrushoud and Lu, 2020).

Therefore, the Bank of Energy can be used to accelerate the process of DERs penetration, developing studies to evaluate the capacity penetration of renewable energy in the distribution system without affecting or updating the existing infrastructure.

#### 2.6.5 *Battery energy installation and management*

The increased installation of battery energy storage systems (BESS) in the distribution systems has to follow an economic and technical planning in order to accomplish different goals. BESS can support the distribution systems in several applications such as energy peak shaving, voltage support, distribution upgrade deferral, DER integration, among others.

In consequence, a detailed study of BESS penetration considering constraints of sizing and placement is necessary. Moreover, an effective energy management system (ESS) is required to optimize the charge/discharge process, maximizing the state of health (SOH) and the state of charge (SOC) of the BESS, and minimizing the system losses.

The experimental platform merges the necessary tools to supply this kind of studies. [Chapter 3](#) and [Chapter 4](#) explain a new methodology for placement and sizing of BESS.

#### 2.6.6 *Penetration of electric vehicles*

New challenges arise in the distribution systems with the evident penetration of electric vehicles (EVs). Environmental policies suggest a roadmap vision to achieve the widespread adoption and use of EVs by 2050, in order to provide a significant reduction in the greenhouse gas emissions and oil consumption that contributes to climate change (Kawakami, Komiyama, and Fujii, 2018). In addition, an organized strategy have to be implemented to install the necessary charge points in the distribution system to promote the use of the EVs as a real alternative to other ways of transport.

In this point, the Bank of Energy can be useful to plan and find the suitable locations to install the necessary charging infrastructure avoiding a significant impact in the energy congestion or the chargeability of the system. Likewise, a methodology to charge the EVs in a efficiently and quickly manner can be developed.

## 2.7 CHAPTER SUMMARY

This chapter has presented the hardware/software implementation of the experimental platform belonged to the Bank of Energy. This platform intends to develop a new paradigm to deploy power distribution system analysis, based on RT simulations and hardware in the loop testing.

After the execution of different test cases, it is proven that the experimental platform performance based in the architecture selected is largely enough for the RT supervision and analysis of the power distribution systems. Moreover, the scalability of the experimental platform is not unique for the GoP distribution system but for any other large-scale power system.

Multiple communication protocols and services were conducted opening a multi-functional system for power distribution analysis. Also, this architecture is protected by a cybersecurity protocol without sacrificing the quality of services.

Additional algorithms, modules or functionalities can be added to the experimental platform to increase the library of case studies for the grid modernization and, therefore, potential applications of this approach.

## Part II

# A NOVEL METHODOLOGY TO INTEGRATE BATTERY ENERGY STORAGE SYSTEMS IN POWER DISTRIBUTION NETWORKS



## BATTERY ENERGY STORAGE SYSTEM INTEGRATION IN POWER DISTRIBUTION SYSTEMS

---

### Contents

---

3.1	Introduction . . . . .	66
3.2	The power distribution system . . . . .	67
3.2.1	DERs in a power distribution system . . . . .	68
3.2.2	BESSs for an efficient power distribution system . . . . .	69
3.2.3	Impact of BESS on the power distribution system . . . . .	75
3.3	BESS testing model . . . . .	77
3.3.1	OpenDSS storage element . . . . .	78
3.3.2	Storage element operation . . . . .	79
3.3.3	Dispatch modes . . . . .	83
3.4	BESS placement and sizing background . . . . .	84
3.4.1	Optimal placement of BESSs in distribution systems . . . . .	85
3.4.2	Optimal sizing of BESSs in distribution systems . . . . .	86
3.4.3	Methodologies for placement and sizing of BESSs . . . . .	88
3.5	Chapter summary . . . . .	103

---

### 3.1 INTRODUCTION

The traditional dispatch of energy based on a one-way supply chain from production to consumption is changing, as well as the interaction between the electrical system functions (generation, transmission, distribution, and consumption), and the way to analyze it. Currently, the electrical power flow is evolving in a multi-directional distributed generation as is shown in Figure 3.1, driven by a technological development where new ways of power generation are being embedded in the distribution grids mainly.

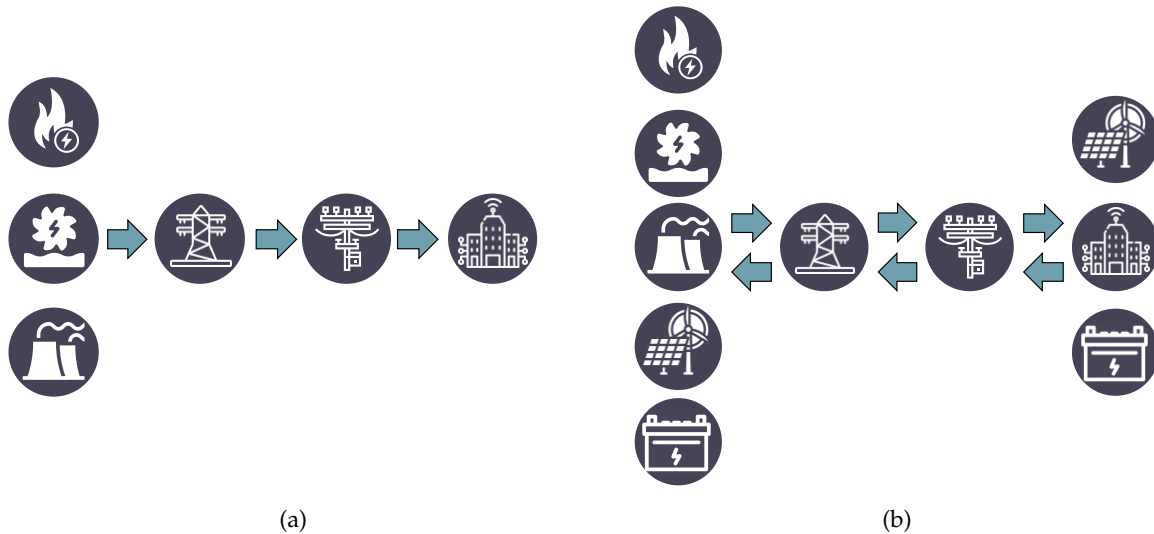


Figure 3.1: Power systems have more technologies and locations to the DERs: (a) Traditional dispatch of energy. (b) Evolving electrical power flow.

A new sets of challenges for planning and operating the power system has arisen, especially in the power distribution system where DER technologies are mostly served. However, it has been shown in several studies that the capacity of the grid to accommodate DER is highly dependent on several factors that are difficult, and so often impossible to consider entirely.

This is particularly the case with the battery energy storage systems (BESS), which are increasingly being installed around the grid, but in some cases without a clear strategy that impacts the integration of BESS concerning the electric power industry. The BESS are a determining factor into distribution economic and technical planning, so strict assessment of how to manage the growing penetration is necessary. Some recommendations are being considered at the moment to install a BESS into the electrical system (Key, 2000):

- Safe electrical integration of BESS with an appropriate response during both normal and abnormal system conditions, and with no adverse impact on local reliability or power quality.
- Minimum adverse impact by BESS on the electrical design, operation, and delivery losses of the distribution system, with no adverse impact on the system reliability, power quality, or safety; and maximum positive impact on strategic value of BESS to the distribution system operations.



- Real-time status and operating telemetry of BESS with communication and control to facilitate distribution support and an effective operating strategy.

With these challenges in mind, utilities across the world are beginning to look at new analytical methods to help assess and integrate BESS into the distribution system. The size of BESS installed in a bus depends on a wide range of factors, some of which are well known (BESS location, BESS type, feeder configuration, etc.). Similar to a load, the size, the location, the type of technology, and the energy management of connected BESS along a feeder directly impacts not only the thermal loading of assets but also the voltage profile across the feeder.

This chapter provides a description of the most common analytical methods and considering multiple criteria from the integration of BESS into the power distribution systems, taking into account mainly the aspects of placement and sizing, without taking into account the type of technology of the BESS.

### 3.2 THE POWER DISTRIBUTION SYSTEM

The power distribution grid is the side of the power grid in charge to deliver electricity to the end users. It is coupled with the transmission system through a substation. Compared with a transmission system, the distribution system is used to send relatively small amounts of electricity over relatively short distances.

In Europe, more precisely in France the distribution system operates in medium voltage (MV) and low voltage (LV) from 20 kV, and 400 V or 230 V respectively. Typical power transfer capacities range from a few tens of MW for substation transformers to as few as tens of kW for very small circuits. The total system length is around 1.3 Gm. The interface between the MV and the LV is done by using more than 700k distribution MV/LV transformers (CRE, 2018).

Distribution systems are designed to outward power flow from the substation to the end of the feeder. The power distribution system could be a radial topology nature or weakly meshed network configuration according to its architecture. Both configurations are a low voltage system with a large relation R/X ratio, and a wide range of reactance and resistance values. The constraints related to a typical distribution system could be seen in [Figure 3.2](#), where multiple phases are considered along its life-cycle.

Distribution networks could be shaped of a large number of sections and buses spread throughout the system. These sections could have unbalanced load conditions due to unbalanced three-phase loading as well as single and double phase loads in spurred lateral lines. The mutual couplings between phases are not negligible due to rarely transposed distribution lines (AlHajri and El-Hawary, 2010). All these characteristics do from the power distribution system a complex network to analyze and evolve.

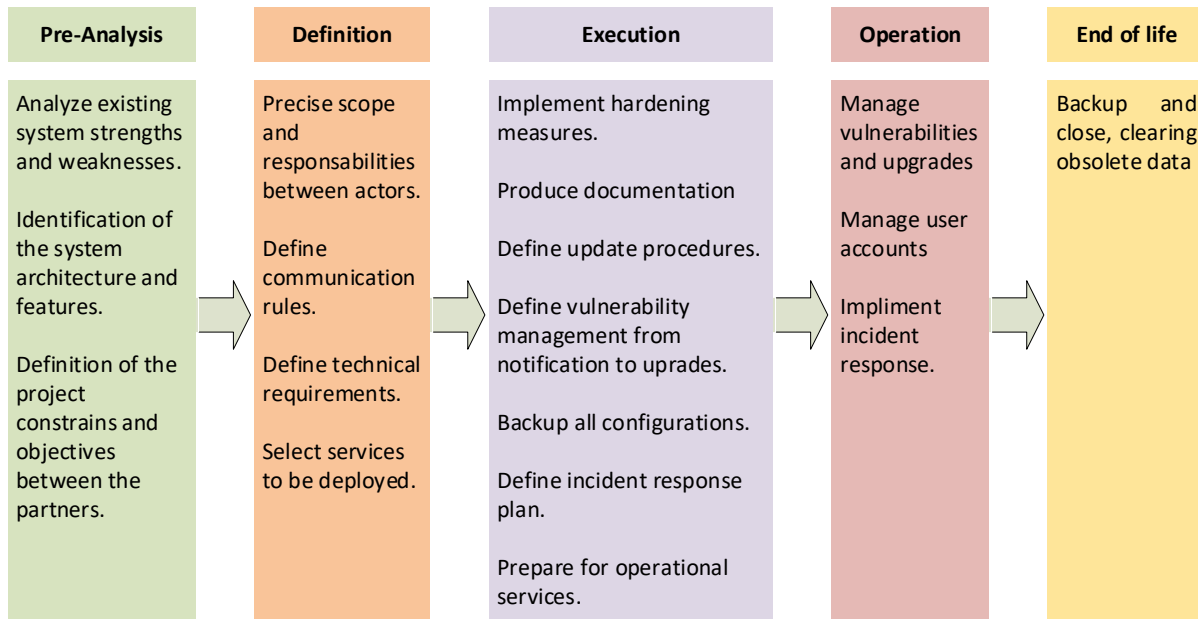


Figure 3.2: Constraints through the whole life-cycle of the distribution grid system.

### 3.2.1 DERs in a power distribution system

Due to the rapid increment in the load demand in the power distributed systems, the penetration of DERs is increasing to meet the demand efficiently, reliably and cost-effectively. Nowadays, the integration of DERs is required to improve operational efficiency and reduce network losses, being an effective means to solve the current problems. DERs allow to the grid for gaining considerable advantages respecting to provide ancillary services like improvement in the power quality, better reliability, reduction in active and reactive power system losses, enhancement in voltage profile, reduction of greenhouse emissions and an evolution towards a smart grid system.

Nevertheless, the power distribution system was not planned with DERs in mind, because of that the voltage fluctuation problem caused by reverse power flow is one of the most serious concerns in the radial distribution with high penetration of DERs (Liu et al., 2020). Adding DERs on the nodes generates a voltage and current source in a place that the system was not designed to accommodate. Figure 3.3 lists the impacts due to a high DER penetration into the system network at different penetration levels. The impacts can be classified into the following categories (Bilakanti, Lambert, and Divan, 2018):

- **Baseline Impacts:** Network issues that arise in a low penetration level of DERs, but gets worse in a higher penetration. Resolving this issues from the beginning can enable a better management increasing the penetration levels.
- **High Penetration Impacts:** Effects that become significant at a higher penetration level, impacting the distribution and transmission network mostly.
- **Feeder Configuration and Equipment Dependent Impacts:** Depends entirely on the system configuration, and the equipment setting implemented by the system operator.

Baseline Impacts	High penetration Impacts	Feeder configuration and equipment dependent impacts
Islanding	Transient and temporary overvoltages	Nuisance fuse blowing
Violations in feeder voltage profile MV/LV	Low voltage ride through	Runaway tap changer in auto-loop distribution systems
Masked Load due to DER components installed upstream	Cold load pickup	Flicker
Increased substation voltage	Low and high frequency ride through	Violation of breaker voltage rating
Relay desensitization	Reduced stability	
Reclosing out of synchronism	Ramp-rate control	
Ground fault overvoltage	Reverse power flow through substation transformer	
Ineffective automatic voltage regulation	Violation of fault current and interrupt rating of protection devices	
Pile-up of interconnection request	Violation in ampacity	
Feeder Imbalance		
Reverse power flow to adjacent circuits		
Sectionalizer Miscount		

High Severity  
 Medium Severity  
 Low Severity

Figure 3.3: Impacts of DER penetration on grid operation (Bilakanti, Lambert, and Divan, 2018).

The impacts are dependent according to the specific characteristics of the distribution network (design and equipment), the location of DER, type of DER technologies, characteristics of existing loads, time variation of loads and generation, environmental conditions, and other local factors (Rogers, 2016).

### 3.2.2 BESSs for an efficient power distribution system

Nowadays, energy efficiency is a major issue in the power systems. Due to regulatory policies and environmental concerns, it is more practical to improve the efficiency in the electrical power flow instead of increasing the generation of electricity using conventional resources (Jewell and Zhouxing Hu, 2012). Emerging technologies such as BESSs deal with several distinct issues in energy conservation and efficiency of the power distribution system.

Energy storage is based on the process of converting electrical energy from the power system into a storable form of energy to be used back when needed. This process allows to store the electricity at times of either low demand, low generation cost or from intermittent energy

sources and to be used at times of high demand, high generation cost or when no other generation means is available (Raihan, 2016). In the BESSs, the energy is stored converting it into electrochemical energy.

Although this chapter does not focus on a specific BESS technology, the distinction between BESS technologies depends directly of the application. The applications can be power applications or energy applications (Entsoe, 2018). Power applications require high power output, usually for short periods of time, whereas, energy applications uses large amount of stored energy, often for discharge durations of many minutes to hours (Eyer and Corey, 2011). Table 3.1 categorizes some energy storage applications according to its functionality into the distribution grid.

The BESS size and the charge/discharge rates consider many variables to be calculated, including the application for which BESS is used. Table 3.2 summarizes some technical requirements considering the BESS application.

Grid-BESS connected can be useful to provide multiple services, according to the application several benefits can be identified along the entire value chain of the electrical system. Figure 3.4 lists some of the BESS applications identified in the distribution system and classify them as power or energy intensive, it means that their provision requires high energy reserve or high power capability, according to the time scale of deployment indeed (Stecca et al., 2020). In this section, some of these benefits applied to the distribution system are discussed.

Table 3.1: Distribution grid-related BESS Applications (Eyer and Corey, 2010).

Category	Application
Electric supply	Energy Peak Shaving Supply Capacity
Ancillary services	Load Following Frequency Regulation Electric Supply Reserve Capacity Voltage Support
Grid system	Distribution Upgrade Deferral Substation On-site Power
End user/utility customer	Time-of-use (TOU) Energy Cost Management Demand Charge Management Electric Service Reliability Electric Service Power Quality
DER integration	Renewables Energy Time-shift Renewables Capacity Firming DER Grid Integration

Table 3.2: Technical considerations for some grid applications of battery energy storage systems (Alme-hizia et al., 2020).

Grid application	Technical consideration
Energy Arbitrage	Typical storage size: 1–500 MW Discharge duration: < 1 h Minimum cycles/year: + 250
Electric supply capacity	Typical storage size: 1–500 MW Discharge duration: 2–6 h Minimum cycles/year: 5–100
Frequency control	Typical storage size: 10–40 MW Discharge duration: 15 min to 1 h Minimum cycles/year: 250–10,000
Voltage support and regulation	Typical storage size: 1–10 Mvar Discharge duration: Not applicable Minimum cycles/year: Not applicable
Peak shaving and load levelling	Typical storage size: 1–100 MW Discharge duration: 15 min to 1 h Minimum cycles/year: Not applicable
Distribution upgrade deferral	Typical storage size: 500 kW–10 MW Discharge duration: 1–4 h Minimum cycles/year: 50–100

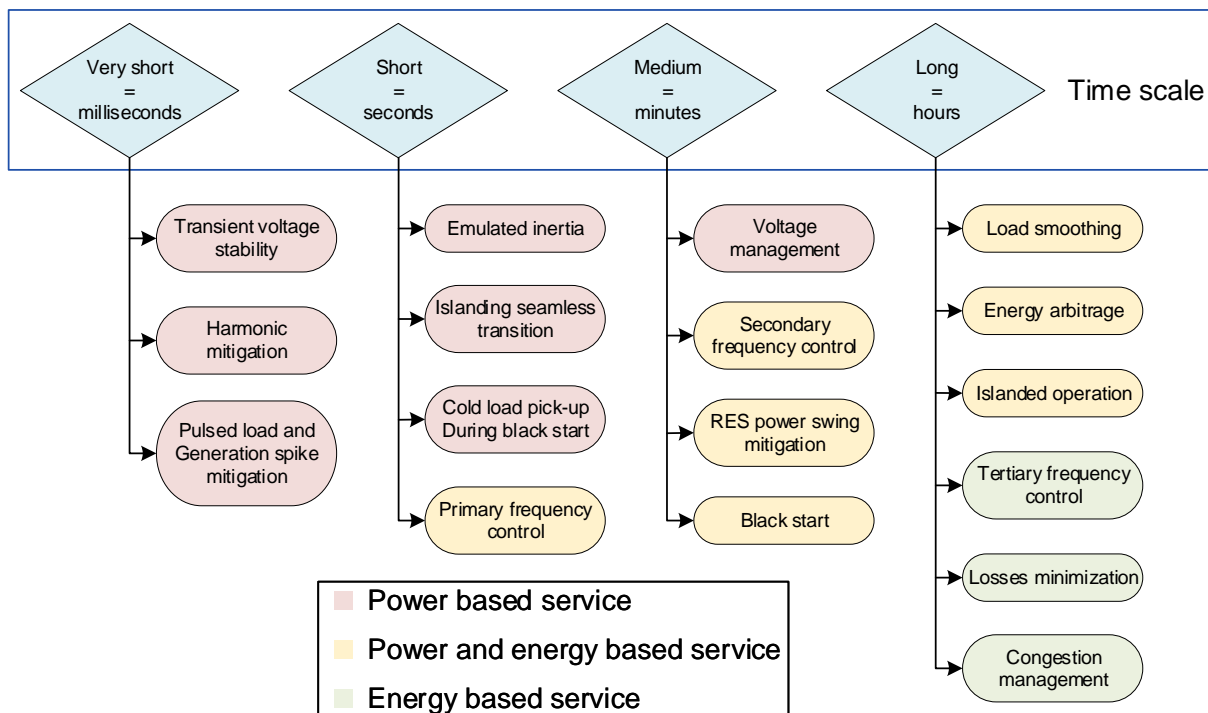


Figure 3.4: Services provided by BESS according to the time scale (Stecca et al., 2020).

3.2.2.1 Power quality

As mentioned earlier in Section 3.2.1, DERs for distributed generation specially wind and solar power, remains unsolved problems due to a high uncertainty in its energy production,

high variability related to weather conditions, and potential power over-generation injected into the feeder. The rise of these intermittent power sources has a direct incidence of power swing in the network. This can negatively affect the network due to the sudden variations in the generation.

In this context, the BESSs can be added beside the DERs and be used to buffer the short term power variation, improving the efficiency of DERs devices to deliver the energy required for the distribution grid. However, the BESS installation for this scope represents an additional cost component for a DER installation, decreasing the system revenue.

High penetration of DERs can be effectively regulated by BESSs, allowing a safe operation also during unintentional islanding. In this case, BESS is a major key to mitigate the transients due to the fault and the sudden unbalance when the system is recovered.

Some other power quality application involves using BESS to protect the consumers downstream the LV network against the electromagnetic transients occurred in short periods of time that affect the quality of power delivered to the load.

#### 3.2.2.2 *Voltage support and regulation*

In order to prevent voltage fluctuation issues in distribution systems, different voltage control regulation strategies can be performed through several devices, conventionally acting on transformers with load tap-changing mechanisms and on switched capacitors (Džafić et al., 2014). However, it is important to add some extra flexibility in managing distribution grids, and BESSs seems to have more opportunities to support the voltage management and offer an ancillary service.

The literature has demonstrated the effectiveness of the BESSs in the voltage control scheme, mostly to limit the impact on the grid's voltage because of DERs (Jamroen, Pannawan, and Sirisukprasert, 2018). The BESS is a practical solution for improving the voltage regulation and the hosting capacity of distribution grids in the near future. Most of the new voltage control strategies exploits the fast response capability of BESS to stabilize the grid operation (Zhao et al., 2019).

An effective BESS control strategy can mitigate the over-voltage and under-voltage conditions and reverse power flow caused by a voltage rise or drop problems respectively. The voltage support can be achieved by the provision of active power coming from the BESS.

The usage of BESS arrays continues to grow due to their capability in restoring system voltage and frequency following an outage, reducing the outage duration and the number of customers affected by the outage (Eguía et al., 2019). The BESSs have the capability to supply active power in order to support the voltage in post-fault scenario, this facilitates the black start procedure and allow islanding operation of the distribution feeder.

### 3.2.2.3 Frequency control

The use of DER concerns about its impact on the frequency stability of the network. A large scale DER penetration decreases the overall system inertia and reduces the frequency regulation capabilities. In order to reduce this frequency fluctuation, the BESSs has been tested as a load frequency control (LFC) solution (Amano et al., 2012).

The BESS have high energy density and fast dynamic response, suitable for high frequency and high power cycling operation. Then, the incorporation of BESS in the distribution network have significant potential to compensate the intermittent output variation of DER and hence improve frequency stability. The most prominent feature is that BESS has the ability of two-way regulation.

The LFC of the BESSs evaluates the changes in the system frequency. If the supplied active power is bigger than the load power demand, the frequency of the system increases, and the BESS is acting as a load absorbing energy from the distribution grid. In the other hand, if the supplied active power is lower than the load power demand, the BESS is discharging to the distribution grid as a power supply. The rapid response and accurate power control for the BESSs allow a quickly and a correct functioning of the frequency regulation, anticipating as well frequency deviations (Hongyan Piao et al., 2015).

### 3.2.2.4 Peak shaving and load levelling

Distribution system operators (DSO) are obligated to meet the load demands at any moment. But peak consumption only occurs a few times per day, it means that the distribution grids have to be oversized regarding to the simultaneity of peak demands.

At the same time, the growing decentralized demand of energy due to the rise of electric vehicles, residential, commercial, and industrial loads with a high peak demand in certain hours and in certain buses locations, hinder the correct decision-making of the DSOs.

Peak shaving strategy has been practiced for many years by using either diesel generators and gas turbines. However, currently is possible to be smoothed improving the flexibility and the regulation capacity of the distribution system by dispatching the BESSs. The peak shaving BESS application aims to reduce peak loads by storing energy when electricity is cheap and discharging when peak demands occurs, hence reducing the peak demand charge (Oudalov, Cherkaoui, and Beguin, 2007). It demonstrates the importance of BESS for power demand management applications

Peak shaving and load levelling by using BESS might be useful when grid development is very expensive or not possible due to a lack of space. [Figure 3.5](#) shows the peak load shaving due to the BESS discharging behaviour during a day, as well as the energy price reduction as a consequence of this utilization.

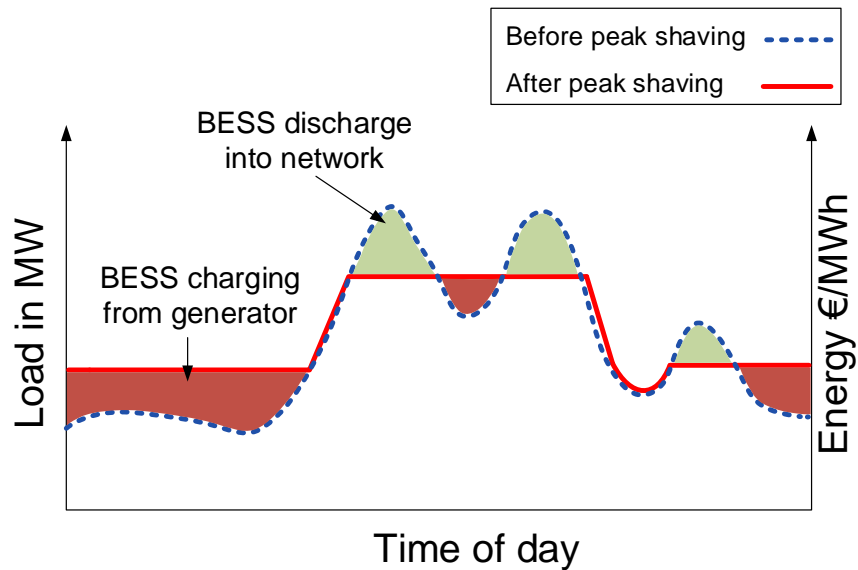


Figure 3.5: Peak load shaving using BESS.

#### 3.2.2.5 Energy arbitrage

Energy arbitrage consists of buying and selling energy in the spot energy market. The operation of BESS in energy arbitrage implies the purchase of low cost energy during cheap (off-peak) times, and furthermore have the option of selling back the excess of the energy stored in the BESSs and the DERs production during the expensive (peak-usage) times, thereby making it economical over time to provide such load shifting energy services to the market (Uddin et al., 2018).

BESSs is a promising candidate among other technologies to monetize the energy price fluctuations, due to their fast response, high efficiency, and declining investment costs (Kumtepe et al., 2020). However, the economic benefits of an arbitrage operation depends on the difference between the energy price and the marginal cost of the system operation. This marginal cost is an additional cost resulted of the charging and discharging BESS operation. Thus, their optimized operation plays a major role to increase the possible revenues (Schimpe et al., 2018).

Moreover, the authors in (Hashmi et al., 2020) use a BESS for a power factor control without any significant effect on arbitrage profit, for a range of price, and consumption. Because of the high cost of the BESS deployment, researchers have proposed using it for co-optimization additional goals along with energy arbitrage for financial feasibility.

#### 3.2.2.6 Distribution upgrade deferral

The distribution system capacity expands at a rate dictated by the population and economic factors. Utility distribution planning studies analyzes the growing demand in order to avoid exceeding violations in the rate limits of the system assets, and therefore to plan for upgrades or new installations in the distribution system. Moreover, this planning is driven by projections of the magnitude and duration of peak loads, which typically follow daily, weekly, and seasonal pattern (Zhang, Emanuel, and Orr, 2016).



According with some studies (Zhang, Emanuel, and Orr, 2016; Garcia-Garcia, Paaso, and Avendano-Mora, 2017), the high investment and deferral situations in distribution systems can be avoided by the installation of properly located BESS, as an affordable solution to meet additional peak demand, and to relieve heavily loaded lines as well as reduce the need for upgrading distribution transformers to handle the increased demand.

The distribution upgrade deferral benefits are conditioned by the cost of the BESS and the grid update, also other factors have to be considered such the rate of load increase and the additional operational costs of the BESS. Somehow the evolution of BESS technologies, assuring a less expensive devices with a longer useful life spam will allow the increase of deferral benefits in the distribution system update.

### 3.2.3 *Impact of BESS on the power distribution system*

BESSs can have a significant impact on the power flow that occur on the distribution system. In practice, achieving 100% of the support benefits mentioned before is not possible. This can vary according to different factors, mostly because the BESSs are never optimally sized, reliably dispatched, and optimally located. The impact on the power flow could be insignificant or slightly measurable, to produce significant changes in the power flow direction affecting the system behavior.

The problems are severe when the BESS power output is enough to reverse the power flow on the feeder. For instance in the radial systems configuration, the BESS capacity which can create the reverse power flow on a feeder is also more likely to affect the under frequency load shedding schemes in the substations relays. Furthermore, large low-voltage BESS installations can affect the secondary network due to the reversed power flow through the network transformers which will trip the protections, leading to an outage.

In [Figure 3.6](#), BESS can cause problems on a secondary network if the power injected is relatively large, reverse power flow through network transformers on LV networks could trip the protections, leading to an outage. Moreover, when the network protector closes back in, there is a potential for serious damage under some conditions. Under light load, a BESS may cause all of the network protectors that are feeding the load to trip, thereby creating an island. The network protector will try to close back in to the network. If this happens and the system are no longer in synchronism, the network protector can fail and cause a significant damage (Key, 2000).

But it is not enough to mitigate the reversed power flow, the BESSs can affect the utility system interaction even when the power flow of the feeder was reduced by a BESS but not reversed. It can be depicted in several problems to the coordination of the system protection devices or the voltage regulation equipment due to the change in the voltage levels at various points of the feeder. Some of the most common impacts from the integration of the BESS over the protective devices are:

- The added current due to the charging state of the BESSs may be affect the fuse-saving schemes.

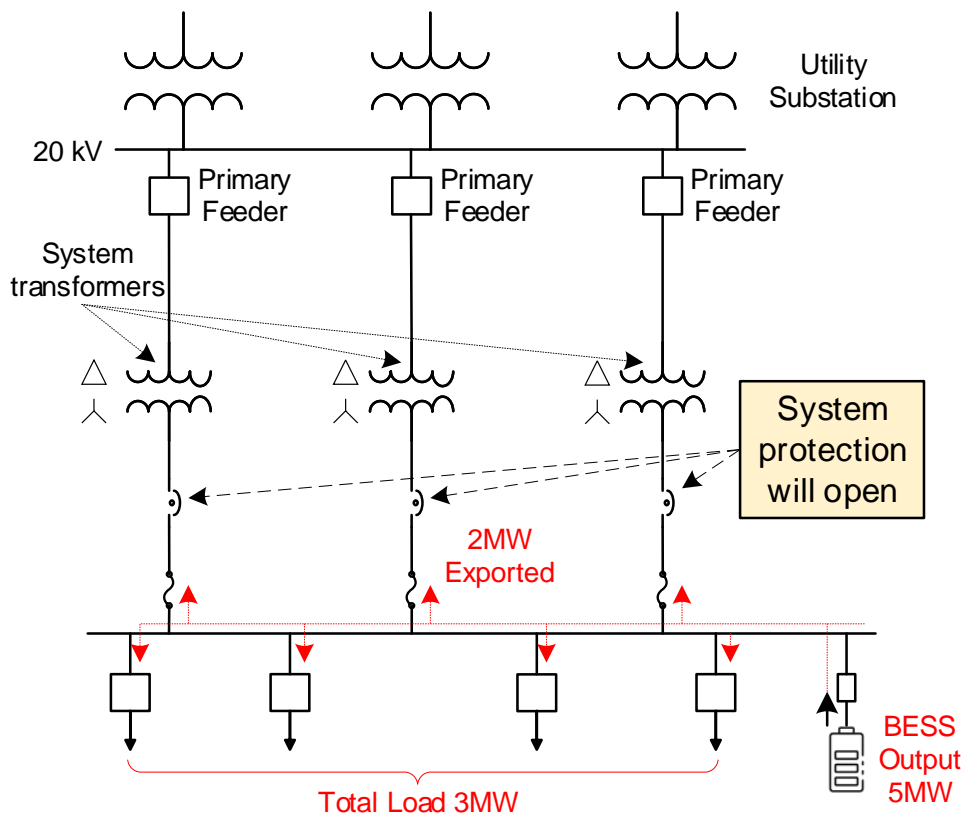


Figure 3.6: LV problems caused by a BESS installation.

- The power discharging of downstream BESSs can cause false tripping operation by upstream breakers, reclosers, sectionalizers, or fuses.
- Failure in the sectionalizers operation due to an electrical supply of a line by the BESS.
- Desensitization of breakers and reclosers due to a bad planning of the BESS operation.

Some critical voltage issues can appear at the location point of the BESS application as well, these problems can obey to the way in which the BESS is operated and controlled, and the nature of the upstream voltage-regulation equipment (Key, 2000). Two of the situations that can cause high or low voltages are:

- Low voltage due to a BESS just downstream of the line voltage regulators or the load tap changer (LTC) transformers.
- High voltage due to a BESS causing a reversed power flow.

As a result, to prevent this from happening a safe integration of BESSs, a minimum interaction between the BESSs with the existing distribution system, and a RT monitoring and control of the BESS operation are all important issues to consider.

Likewise, the interconnection of BESS installations into the distribution system requires an optimal planning of the BESS units based on different objectives. These objectives can be focused on load-management, reliability enhancement, voltage regulation, peak load-shaving, DERs power forecast, error mitigation and so on (Zhang et al., 2017). Moreover, the BESS must

meet various operating criteria related to protection, voltage control, flicker, and so on, as well as being ideally located, sized, and dispatched at the correct time.

It is worth mentioning that the purpose of this study is to develop a tool which allows to find the suitable placement and sizing of a BESS installation in a distribution system, trying to give a solution to the needs mentioned above. This tool is integrated in the experimental platform of the Bank of Energy to centralize the different studies capabilities which were explained in [Chapter 2](#). Moreover, a control operation of the charge/discharge state of the BESS is developed in parallel to this research under a macroscopic perspective of the distribution system analyzed.

### 3.2.3.1 BESS placement and sizing in MV and LV systems

Most of the applications contributions for BESS placement and sizing are related to MV distribution systems. There is still no a clear distinction between applications for MV and LV systems, considering that the formulation of a planning problem for a BESS installation in MV and LV has multiples differences.

[Table 3.3](#) summarizes the relevant differences between the LV and MV systems, these differences are important to be considered at the moment to aggregate a BESS installation.

It is noticed that the BESS installation is simpler in MV systems than LV systems, however, to achieve the best BESS performance and to maximize the overall benefits, a correct testing model is necessary.

Table 3.3: Summary of relevant differences between MV and LV systems (Mazza et al., 2019).

Characteristics	MV Grid	LV Grid	Consequences
Architecture	Weakly meshed	Radial	LV grid could not be reconfigured, so the the correct network operation has to be assured through the current assets connected to the grid.
Load	Balanced	Unbalanced	It is recommended to apply the three-phase load flow solution in the LV analysis.
Branch	$R \approx X$	$R \gg X$	There is a correlation between the voltage and the active power in the LV grid.
Load profile	Aggregate	Not aggregate	A detailed modelling of loads and DERs is necessary in the LV system, the aggregation impact is lower in the MV level.

## 3.3 BESS TESTING MODEL

Before to develop any algorithm to perform the placement and sizing of a BESS installation, it is necessary to find a suitable model of analysis in a distribution system. [Figure 3.7](#) shows a

generic architecture of a BESS testing model installed in the LV side of a distribution network. This generic BESS testing model considers the main elements to deploy a battery management system (BMS) control.

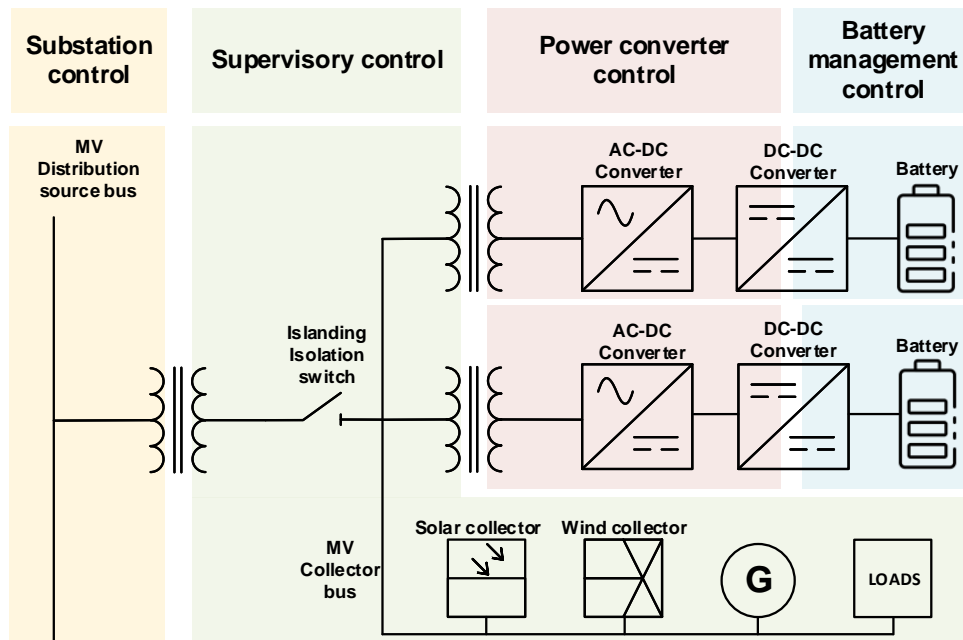


Figure 3.7: BESS generic architecture and controls (Sukumar et al., 2018).

The BESS used in the experimental platform comes from the OpenDSS simulator. This storage element is robust enough to perform any kind of storage study or BMS according to its application, and it allows to analyze the impact due to a BESS installation in the distribution grid.

This model is used to execute studies such as power flow, facilitating to compute the power flow for a selected state of the active storage element. Additionally, the strength of the model is in time-varying simulation modes, executing simulation of the system modeled in a daily, yearly or a duty cycle period of time. In a daily and a yearly simulations, the model is used to analyze the energy related issues over a period of time. While in a duty cycle simulation, the purpose is studying the effectiveness of the storage element to compensate for short-term power variations (Rocha et al., 2020).

### 3.3.1 OpenDSS storage element

The general model of the BESS element in OpenDSS is described in Figure 3.8. The storage element of OpenDSS is modelled as a constant power load during the charging state, and as a generator that can inject power into the grid during the discharging state, constrained to its nominal power rating and the energy capacity. This model is a general representation of a storage element which allows to simulate the behavior of a BESS in a distribution system. The different components identified are:

- **kWh Stored:** Represents the state of charge (SOC) of the storage element, it varies considering the state, the associated charging/discharging rates, and the element losses.

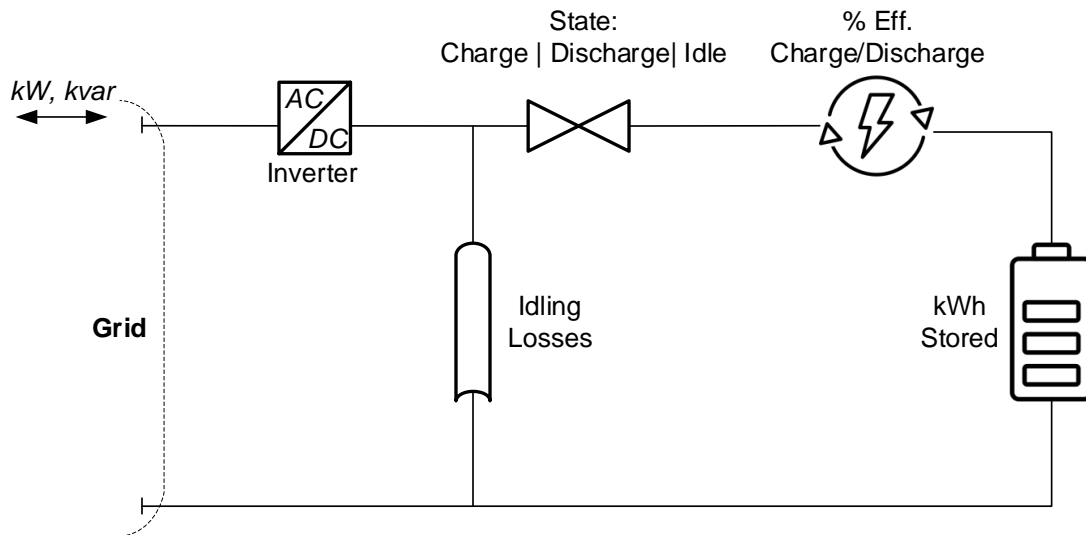


Figure 3.8: General model of the storage element in OpenDSS (Rocha et al., 2020).

- **% Efficiency Charge/Discharge:** It is related to the efficiency percentage of the charging/discharging state.
- **State:** It is the state which the storage element operates. It can be: charging, discharging and idling.
- **Inverter:** This block allows to dispatch reactive power to the system, as of modeling the inverter losses and limiting the rate of charge and discharge based on its rating.
- **Idling Losses:** It represents the storage self-depletion losses and auxiliary loads due to the inverter and the SOC block. When the storage element is discharging, the self-depletion losses and auxiliary loads are supplied by the SOC, increasing the discharging rate of the element. When the storage element is charging, it is supplied by the inverter. In the idling state, it is supplied by the grid through the inverter.

### 3.3.2 Storage element operation

The storage element operation is conditioned by the three possible states explained before (charging, discharging and idling). The calculation operation is performed within the storage element from the interface with the grid to the energy stored. Firstly, the  $kW$  and  $kvar$  are determined at the interface with the grid. All the losses are subtracted (charging/discharging losses, idling losses, inverter).

The power flow solution at an instant  $t$  is determined based on the power definition at the storage element. For time-varying simulations, OpenDSS assumes this flow is constant over the time interval until the next time instant  $t + \Delta t$ , where  $\Delta t$  is the time step selected. the nomenclature used is the following:

$P_{in}[t]$  = Power flowing into the storage at  $t$  when it is either in charging or idling states.

$P_{out}[t]$  = Power flowing out into the grid at  $t$  when it is in discharging state.

$P_{idl}$  = Constant idling losses.

$\eta_{inv}[t]$  = Inverter efficiency at  $t$ .

$\eta_{ch}$  = Charging efficiency.

$\eta_{dch}$  = Discharging efficiency.

$E[t]$  = Energy stored at  $t$ .

### 3.3.2.1 Charging state

The charging state of the storage element is constrained if the amount of energy stored  $kWh_{Stored}$  is lower than the rated storage capacity  $kWh_{Rated}$ . The power flow of the storage element during the charging state is illustrated in Figure 3.9.

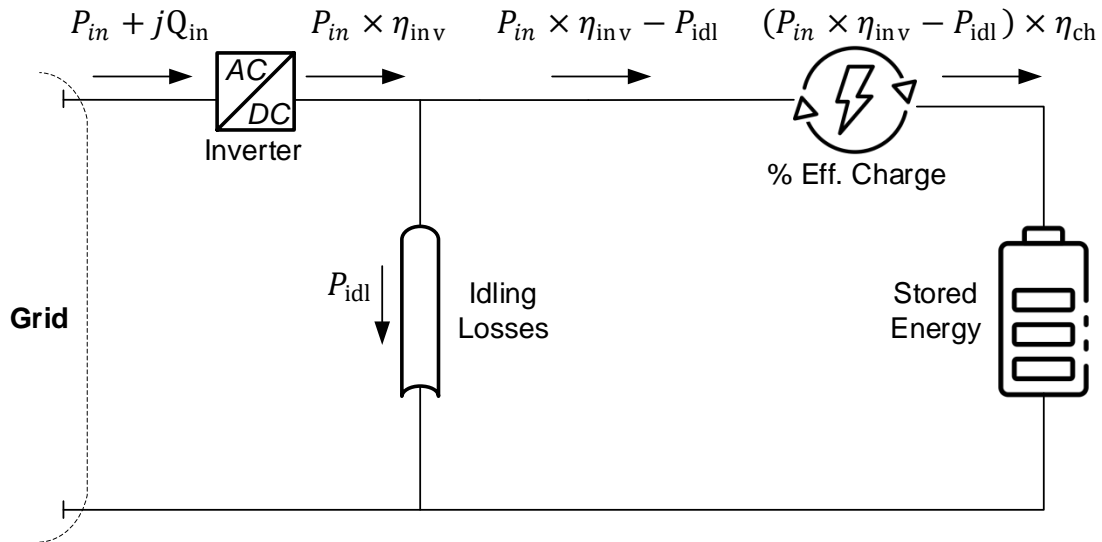


Figure 3.9: Internal power flow of the storage element during the charging state in OpenDSS (Rocha et al., 2020).

The power  $P_{in}[t]$  is calculated when the power flow is executed. After, the storage inverter losses are determined by:

$$P_{losses,inv}^{ch}[t] = P_{in}[t] \times (1 - \eta_{inv}[t]) \quad (1)$$

The power at the DC side of the storage inverter ( $P_{in}[t] \times \eta_{inv}[t]$ ), supplies the idling losses  $P_{idl}$ . The charging losses are calculated analogous to the storage inverter losses:

$$P_{losses,ch}[t] = (P_{in}[t] \times \eta_{inv}[t] - P_{idl}) \times (1 - \eta_{ch}) \quad (2)$$

Thus, the total losses are:

$$P_{\text{losses,tot}}^{\text{ch}}[t] = \text{Losses}_{\text{inv}}^{\text{ch}}[t] + P_{\text{idl}} + P_{\text{losses,ch}}[t] \quad (3)$$

And the power that effectively charges the energy stored block is determined by:

$$P_{\text{eff}}^{\text{ch}}[t] = (P_{\text{in}}[t] \times \eta_{\text{inv}}[t] - P_{\text{idl}}) \times \eta_{\text{ch}} \quad (4)$$

Equivalently:

$$P_{\text{eff}}^{\text{ch}}[t] = P_{\text{in}}[t] - P_{\text{losses,tot}}^{\text{ch}}[t] \quad (5)$$

For the time-varying simulation, the energy stored at the next simulation time step ( $t + \Delta t$ ) is given by:

$$E[t + \Delta t] = E[t] + P_{\text{eff}}^{\text{ch}}[t] \times \Delta t \quad (6)$$

### 3.3.2.2 Discharging state

The discharging state of the storage element is constrained if the amount of energy stored  $kWh_{\text{Stored}}$  is greater than the rated storage capacity to be held in reserve for normal operation ( $\% \text{Reserve} \times kWh_{\text{Rated}}$ ). The power flow of the storage element during the discharging state is illustrated in [Figure 3.10](#).

The power  $P_{\text{out}}[t]$  is calculated when the power flow is executed. After, the storage inverter losses are determined by:

$$P_{\text{losses,inv}}^{\text{dch}}[t] = P_{\text{out}}[t] \times \left( \frac{1}{\eta_{\text{inv}}[t]} - 1 \right) \quad (7)$$

The stored energy of the storage element supplies the power at the DC side of the storage inverter, taking into account the idling losses and the discharging losses. The discharging losses are given by:

$$P_{\text{losses,dch}}[t] = \left( \frac{P_{\text{out}}[t]}{\eta_{\text{inv}}[t]} + P_{\text{idl}} \right) \times \left( \frac{1}{\eta_{\text{dch}}} - 1 \right) \quad (8)$$

The total losses during the discharging state are calculated with:

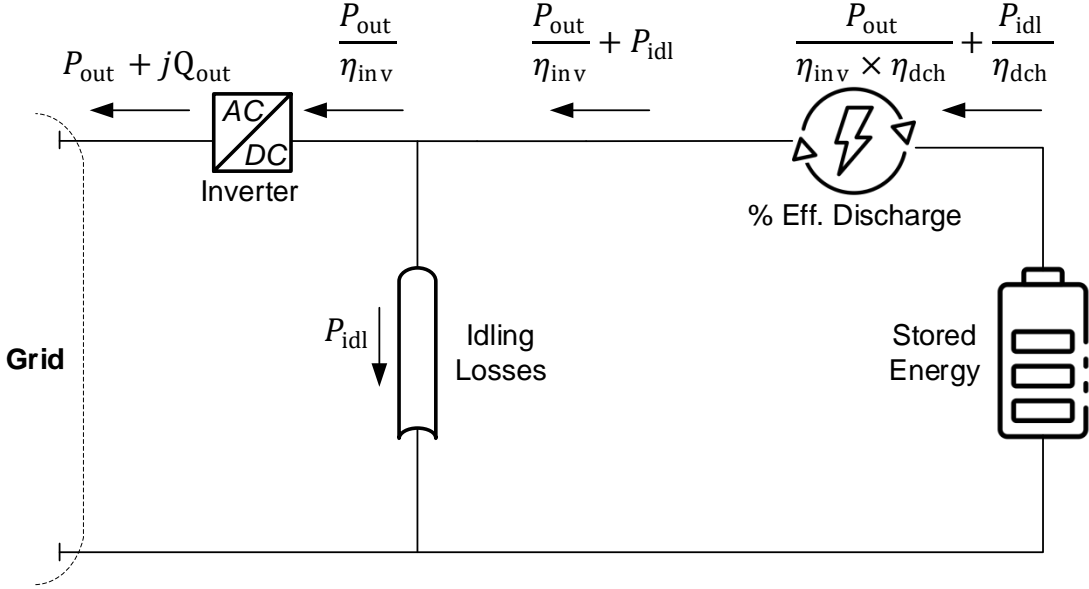


Figure 3.10: Internal power flow of the storage element during the discharging state in OpenDSS (Rocha et al., 2020).

$$P_{\text{losses,tot}}^{\text{dch}}[t] = P_{\text{losses,inv}}^{\text{dch}}[t] + P_{\text{idl}} + P_{\text{losses,dch}}[t] \quad (9)$$

And the power that effectively discharges the energy stored block is determined by:

$$P_{\text{eff}}^{\text{dch}}[t] = \frac{P_{\text{out}}[t]}{\eta_{\text{inv}}[t] \times \eta_{\text{dch}}} + \frac{P_{\text{idl}}}{\eta_{\text{dch}}} \quad (10)$$

Equivalently:

$$P_{\text{eff}}^{\text{dch}}[t] = P_{\text{out}}[t] + P_{\text{losses,tot}}^{\text{dch}}[t] \quad (11)$$

For the time-varying simulation, the energy stored at the next simulation time step ( $t + \Delta t$ ) is given by:

$$E[t + \Delta t] = E[t] - P_{\text{eff}}^{\text{dch}}[t] \times \Delta t \quad (12)$$

### 3.3.2.3 Idling state

When the storage element is in the idling state, the idling losses and the associated inverter losses are supplied by the grid, so the SOC remains unaltered as shown in Figure 3.11. The stored energy block is in standby mode waiting for a new command state.



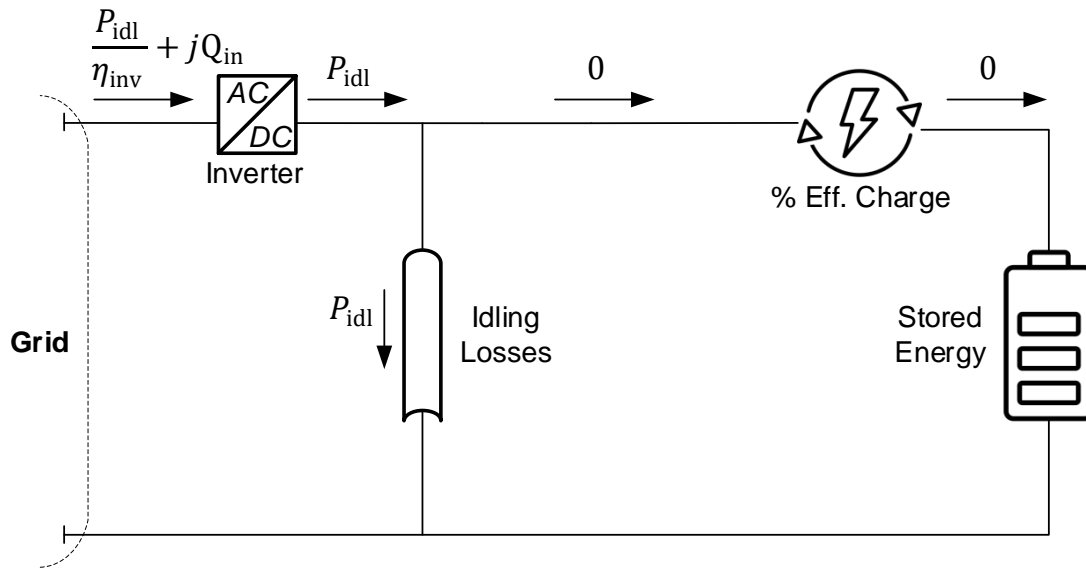


Figure 3.11: Internal power flow of the storage element during the idling state in OpenDSS (Rocha et al., 2020).

### 3.3.3 Dispatch modes

In OpenDSS, the storage element has multiple dispatch modes options mainly conceived to simulate any BESS application as seen in Section 3.2.2.

The dispatch modes can be classified into self-dispatch modes and control-dispatch mode. In a self-dispatch mode, the storage element drives its own state operation. In the other hand, the control-dispatch mode regulates the operation of the storage element by using a combination of a storage controller and the inverter control element. The dispatch modes available in OpenDSS are listed in Table 3.4.

The dispatch modes in turn are divided into active and reactive power dispatch modes. The use of these dispatch modes are normally programmed to be used separately, however, a function combination is allowed:

- Active power and reactive power dispatch driven by the follow self-dispatch mode and the volt-var function of the inverter control.
- Active power and reactive power dispatch solved between the combination of the time mode of the storage controller and the volt-var function of the inverter control.
- Active power and reactive power dispatch controlled by the storage controller using the peak shave for charging and discharging modes, and the volt-var function of the inverter controller.

The dispatch method used is the external control function to fulfill the project objectives. In this mode, the storage state and dispatch values are defined by an external algorithm which aims to find the suitable size and location of the BESS. Due to this external communication, it is necessary to use the API interface of OpenDSS to perform the simulation (Dugan, 2012).

Table 3.4: Dispatch modes of the storage element available in OpenDSS (Rocha et al., 2020).

Measure	Means	Mode/Function
Active power	Self-Dispatch	Default Follow Load level Price External control Time charge trigger
	Storage controller	Peak shave (charging) Follow Support Load shape Peak shave low (discharging) Time Schedule
Reactive power	Self-Dispatch	Constant pf Constant kvar
	Inverter control	volt-var (VV) Dynamic reactive current (DRC) VV + DRC VV + Volt-Watt (VW)

The external mode is also recommended to take more direct control over the storage operation in a BMS, using the different properties associated to the storage element.

### 3.4 BESS PLACEMENT AND SIZING BACKGROUND

Currently, most of the studies focuses on the optimization placement of DERs, but rarely involves the optimization of BESS placement and sizing specially. However, an effective management ability with DERs and economical benefits of the distribution system operation are limited without an exhaustive BESS placement and sizing evaluation (Zhong Qing et al., 2013).

According to an specific BESS application and an operational strategy, there is a need to execute a suitable procedure to determine the size and the location of a BESS, due to the fact that an adequate BESS size and location can assure to minimize the costs and losses in the system. So, it is pertinent to develop algorithms capable to analyze and conclude the optimal size and location of a BESS.

The utility distribution planners are faced with accommodating widespread the BESSs in regards of investment and grid stabilizing effect. Some of these decision tasks are listed below (Key, 2000):

- Define a distribution planning area (DPA) and model it for power flow analysis.
- Develop a load forecast for a selected planning horizon.
- Determine when planning limits on voltages and current capacities will be violated based on the load forecast.
- Identify one or more alternatives for correcting the violations.
- Determine the least cost BESS alternative over the planning horizon using approved economic evaluation methods.

Nevertheless, this strategy seems to be not enough to optimise the size and location of a BESS. Some other relevant variables are important to consider at the moment to select the appropriate conditions and features.

#### 3.4.1 *Optimal placement of BESSs in distribution systems*

BESS placement studies are of paramount importance for selecting a geographical flexibility using the BESSs. Find a suitable site is among the first steps in the process of a BESS installation. It is important that an optimal location corresponds to what services the BESS is meant to yield.

The BESSs are often installed in the distribution system in sites proximate to an existing substations or with an present interconnection to the grid. Some other installations consider the BESS placement beside to the DERs installation, in that way, improve the grid operations. In general, the optimal BESS placement implies several careful considerations such as (Hameed, Hashemi, and Træholt, 2020):

- The interest of all stakeholders involved.
- Legal regulations matters regarding to the grid connection.
- Technical criteria from manufacturers and suppliers must be fulfilled.
- the number of charge-discharge cycles of the BESS.
- Development timelines and costs are greatly considered.
- The customer benefits have to be evaluated considering the different use cases.
- Scalability, flexibility and control consideration on the BESS installation.

Based on these considerations and the application which the BESS is going to be used in mind, another issue is important to contemplate before a BESS installation. The deployment of BESS technologies on the power distribution systems can be centralized or decentralized.

#### 3.4.1.1 *Centralized BESS installation*

A centralized BESS installation provides a centralized energy storage at MV level, usually located at the distribution substation location.

The advantages of a centralized installation include an easy access to the substation and the supervisory control and data acquisition (SCADA) equipment, more simplified control schemes, economies of scale by increasing production and lowering the installation cost, and the use of the land available in the substation location (Hill et al., 2012).

Typically, the BESS centralized installation is used to reduce the demand deviation, avoiding the reverse power flow and the power factor correction (Kumar et al., 2019).

#### 3.4.1.2 *Decentralized BESS installation*

A decentralized BESS installation is preferred to introduce smaller energy storage systems distributed on the distribution feeders, networked together and remotely controlled at the substations. This installation offers the scalability, flexibility and increases end-user accessibility to storage, generating new income streams to the stakeholders while boosting storage saturation and strengthening support for the utility grid.

The operational advantages are as well numerous of distributed storage. The system reliability is enhanced since there is no single point for power conversion. Likewise, a distributed architecture uses lightweight storage blocks which allow to install ideally a storage system of any size. The common applications where decentralized BESS installations are used include annual energy loss reduction, reduction of the demand deviation, and improvement of the node voltage profile (Kumar et al., 2019).

#### 3.4.2 *Optimal sizing of BESSs in distribution systems*

Generally several small sized BESSs are installed in multiple locations to provide flexibility and redundancy according to the system application. In other cases, the system operator have opted to install a higher capacity than the required one to handle the application specifications and the battery degradation. Some others have decided to aggregate batteries to the initial BESS installation deferring the initial investment and exploiting a future cost reduction in batteries. Nevertheless, these techniques have resulted in a high investment cost, in technical challenges of BESS aggregation, or even in undersized BESS installations which do not meet the operational criteria (Jayashree and Malarvizhi, 2020).

Currently the BESSs are part of the power distribution systems, so it is necessary to determine the optimal size of BESS for a particular application. Figure 3.12 shows the possible applications which a careful BESS sizing can be determinant for a correct operation.

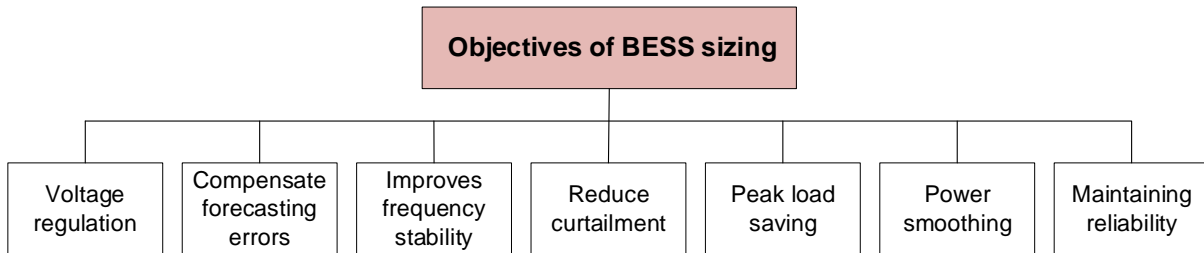


Figure 3.12: Objectives of BESS sizing.

Sizing the BESSs involves finding the optimal battery power and energy capacity with the aim of minimize the fitness function of the problem desired. It also requires to conduct a load and DERs analysis to adjust the constraints of the capacity installation. Finally, a system analysis must be deployed under critical condition to determine the effect of the BESS in the distribution system after sized.

Studies on sizing BESS can be classified in financial, technical and hybrid according to an optimization criteria (Yang et al., 2018). In this study, the voltage profile improvement and the loss minimization of the distribution system are the BESS technical applications approach considered to determine the optimal size. In Chapter 4 is presented the formulation of these optimization problems.

#### 3.4.2.1 Financial criteria

An important point considered for the size of a BESS is the financial profit as a result of its installation into the distribution system. The financial criteria allows to evaluate and compare the overall cost and benefit due to a BESS installation along the operational lifetime of the system. Another approach is related to the energy arbitrage and as seen before, the objective is to maximise the market benefit of the inclusion of a BESS.

#### 3.4.2.2 Technical criteria

Technical criteria is associated to achieve an optimization goal or to include them as a constraints in the problem formulation process. The technical criteria can be quantified in accordance to an specific value goal to evaluate if they meet or not the requirements. Then, the technical indicator measures the support of the BESS for the dynamic or steady state operation of the distribution system.

#### 3.4.2.3 Hybrid criteria

Hybrid criteria is the combination between financial and technical indicators simultaneously with regards to BESS sizing. There are to major approaches for this criteria, first, where techni-

cal criteria is used as a constraints and the financial indicator is the fitness function to optimise. The second approach is related to multi-objective optimisation of both financial and technical variables.

### 3.4.3 Methodologies for placement and sizing of BESSs

The placement and sizing of BESS can be determined by a wide variety of approaches. The major issue of determine the placement and size of BESS is that in general this problem is a complex, non-linear, non-convex and requires a high dimensional formulation. The problem is highly complex because the BESS definition uses discrete/integer variables whereas the power supply is modeled as a continuous variable which affect the quality of the optimal solution.

The formulation is indeed a mixed-integer non-linear optimization problem, it handles the combinatorial difficulty of optimizing over discrete variable sets combined with the complexity of handle with non-linear functions. Moreover, non-convex functions are an added difficulty due to the multiple local optimal in the problem (Kumar et al., 2019).

On account of this problem complexity, various types of methods with different objective functions are suggested in the literature. Figure 3.13 categorizes the methodologies in five ways (Jayashree and Malarvizhi, 2020). These methods have evolved and are still evolving, with their own strengths and weaknesses.

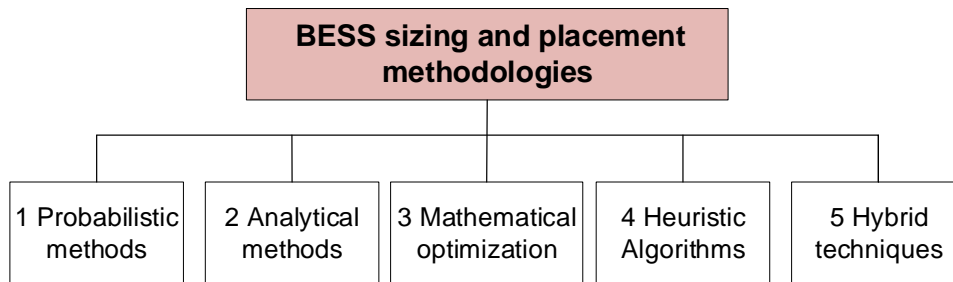


Figure 3.13: Methodologies for BESS placement & sizing (Jayashree and Malarvizhi, 2020).

Additionally, the fitness function in these methodologies can obtain a different result in the optimal BESS placement and sizing. It might be because of the network structure, renewable resources position, and the line-flow limits which can have a considerable impact in the calculation. Figure 3.14 reveals a general algorithm for the placement and sizing of BESS, which the evaluation of the fitness function will depend on the method chosen.

The following sections provide a greater detail on each of the methods listed including common misconceptions, advantages, disadvantages, and recommendations.

#### 3.4.3.1 Probabilistic methods

The probabilistic methods are used for data generation. These methods are the simplest way to determine the placement and sizing of a BESS. The basis is to use the stochastic nature of

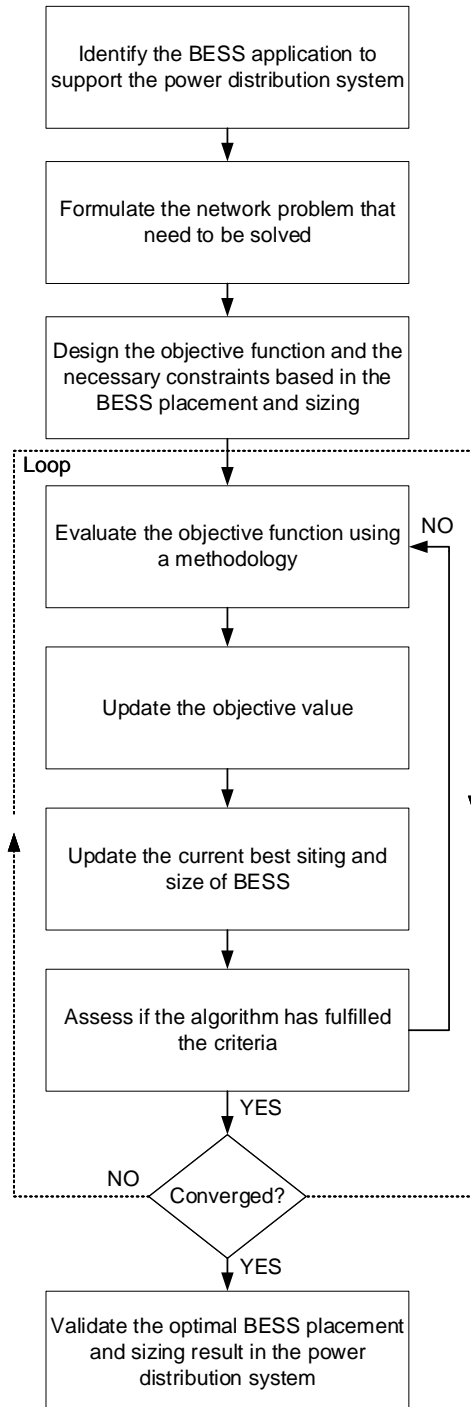


Figure 3.14: General placement and sizing algorithm (Carpinelli et al., 2013).

the active elements of the grid such as DERs and customers, to optimise the BESS siting and size. A flowchart explaining probabilistic methods is shown in [Figure 3.15](#).

The advantage of the probabilistic methods is that it could be deployed when there is limited data availability. However, a disadvantage is that the number of criteria which can be optimised in these approaches are limited, reducing its applicability for larger designs.

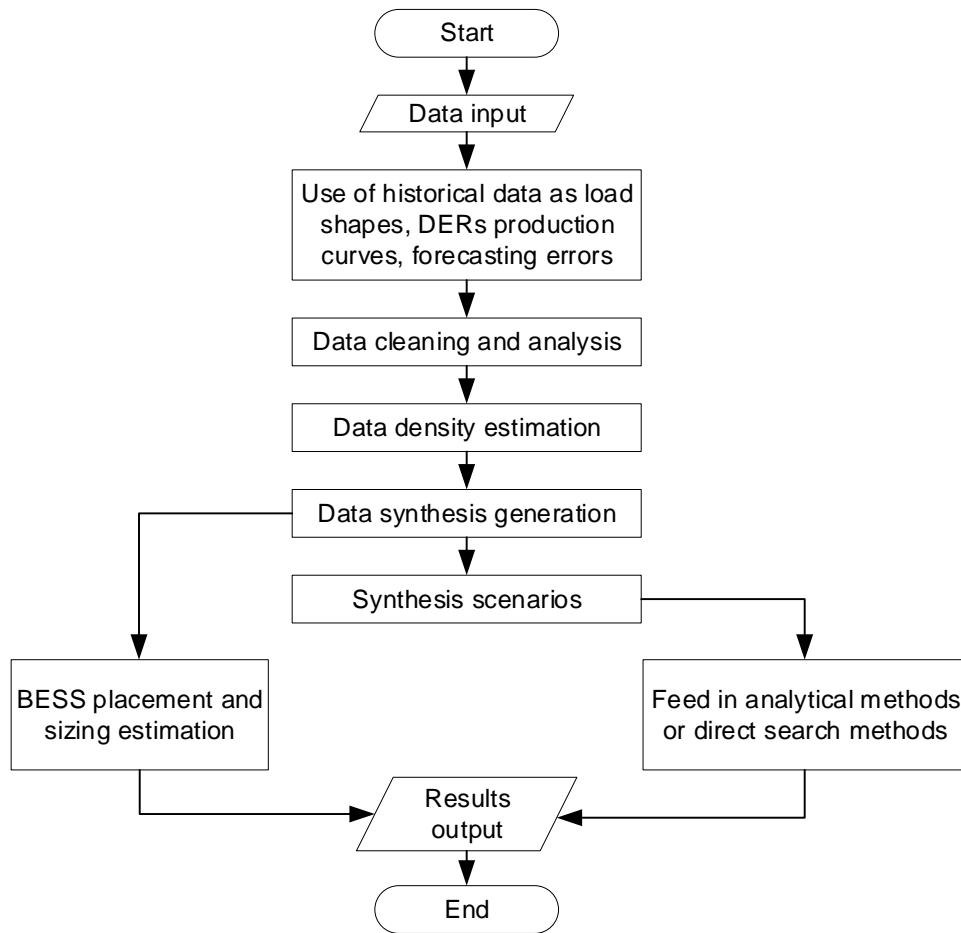


Figure 3.15: Flowchart of probabilistic methods (Yang et al., 2018).

In parallel of probabilistic methods, the stochastic optimisation methods are highly used in several studies. These methods presents some or all of the parameters of the optimization problem as random variables. Approaches as chance-constrained optimisation, robust optimisation and stochastic control strategy have been employed to determine the placement and sizing of BESS considering uncertain random variables. One of the most relevant stochastic method applied is the Monte Carlo approach (Yang et al., 2018).

*Monte Carlo approach* The Monte Carlo approach is a flexible and powerful algorithm, in which the purpose is to generate a large number of samples (scenarios) obtained by a discrete approximation of probability density function by using random variables. The Monte Carlo approach is largely used in problems that involve a huge number of degrees of freedom (Amar, 2006).

The source of the random variables depends on the nature of the problem. For instance, many random variables can be generated using Monte Carlo approach for a power system operation and planning problems, such as weather conditions, forecasting error, availability of generation production, operational BESS parameters, among others.

Moreover, this approach allows to solve the BESS placement and sizing problem when the statistical data is not enough. Monte Carlo simulations can be performed to determine the



random distribution of cost and operational benefits of installing a BESS unit. The following methodology proposed by (Ross, Abbey, and Joós, 2013), demonstrates the application of the Monte Carlo approach:

- **BESS control scheme:** First, establish how the BESS is going to be operated.
- **Perform Monte Carlo simulations:** This simulations can be performed over the time. Historical system data will allow to generate the possible scenarios to be evaluated. The power and energy rating of the BESS are chosen according to a random distribution which results in the optimisation of the fitness function over the simulation period. The optimization constraints depends on the system simulation and it will be assigned to a specific BESS placement and sizing.
- **Problem formulation:** After, formulate the cost function based on the BESS power and energy ratings. It is possible to apply linear or non-linear least squares error regression techniques. The least-squared error is useful to determine the mean cost of the probability density function of the costs for different power and energy ratings.
- **Determine the optimal BESS placement and sizing:** Finally, analyze the optimal location and size of the BESS according to the fitness function.

#### 3.4.3.2 Analytical methods

Also known as deterministic methods and one of the most important methods used for placement and sizing of BESS. The analytical methods are broadly suitable for analyzing the dynamic behavior of the system, and thus allowing to find the suitable location and size of a BESS.

The analytical methods are based on the variation of the system elements in the power system configuration to find the optimal performance criteria. In the context of BESS siting and sizing, these methods use the load profiles, the energy/demand charge rates, and the battery characteristics as an input to construct a standard programming problem, which normally implies several constraints and decision variables. In other words, the optimal BESS placement and sizing are determined through derivation and evaluation of a series of mathematical equations and algorithms.

The problem is solved by the use of optimization solvers to obtain numerical solutions. The fitness function and its related constraints are evaluated repeatedly with different set of parameters during the optimization process, then BESS siting and capacity with the best performance is chosen as the optimal solution. A flowchart explaining the analytical methods solution is seen in [Figure 3.16](#).

The analytical methods use perform repetitive calculations over a fixed interval for the relevant system element. Thus, a selection of BESS placement and sizing can be made considering the performance variation of the storage system against financial and/or technical criteria.

These methods do not use a specific mathematical programming to solve the optimization problem (Wong et al., 2019). In consequence, the advantage of these methods include an easy implementation and a faster computational resolution due to a set of simplified assumptions.

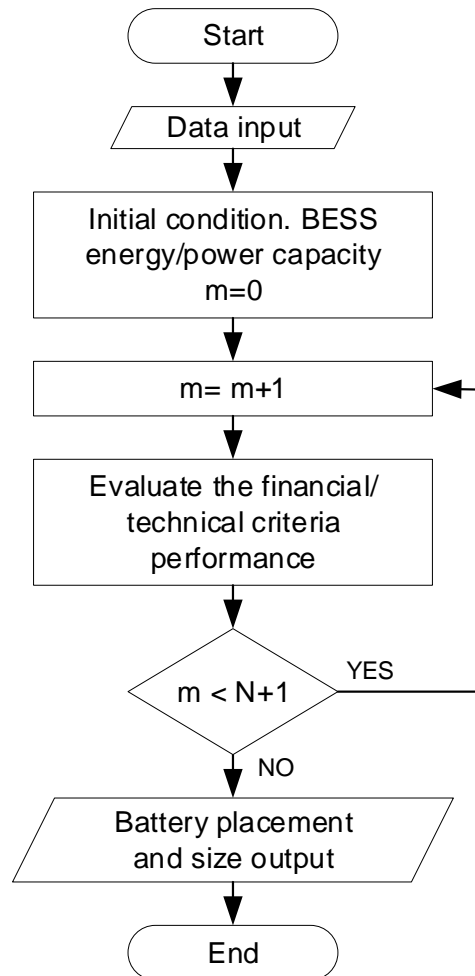


Figure 3.16: Flowchart of analytical methods (Yang et al., 2018).

However, these are not robust enough to provide the optimal global solution for complex distribution systems.

Another drawback is the need of a large number of simulations with a multiple combination of technical/financial indices. While a smaller interval solution can provide accurate results, the quantity of simulation iterations will often increase at an exponential rate. From this point of view, this becomes problematic due to a limited computational resources, and in overwhelmed cases, becoming untenable the calculation of the complete solution.

Finally, these methods are applied mostly in short problems like the BESS allocation through the derivation of the cost-benefit. For instance, in (Jayashree and Malarvizhi, 2020), the authors deploy a BESS installation to reduce the customer payment for electricity use. So, an analytical sizing method is developed to provide a comparison on how the optimal BESS size varies with the system characteristics.

### 3.4.3.3 Directed search-based methods

An efficient way to reduce the computational calculations and to reach the global solution is by the use of the direct search-based methods. There are already a vast quantity of methods oriented to solve the BESS placement and sizing problem. Hence, these methods can be divided in two different approaches: mathematical optimization methods and heuristic methods. Figure 3.17 shows the flowchart of direct search-based methods.

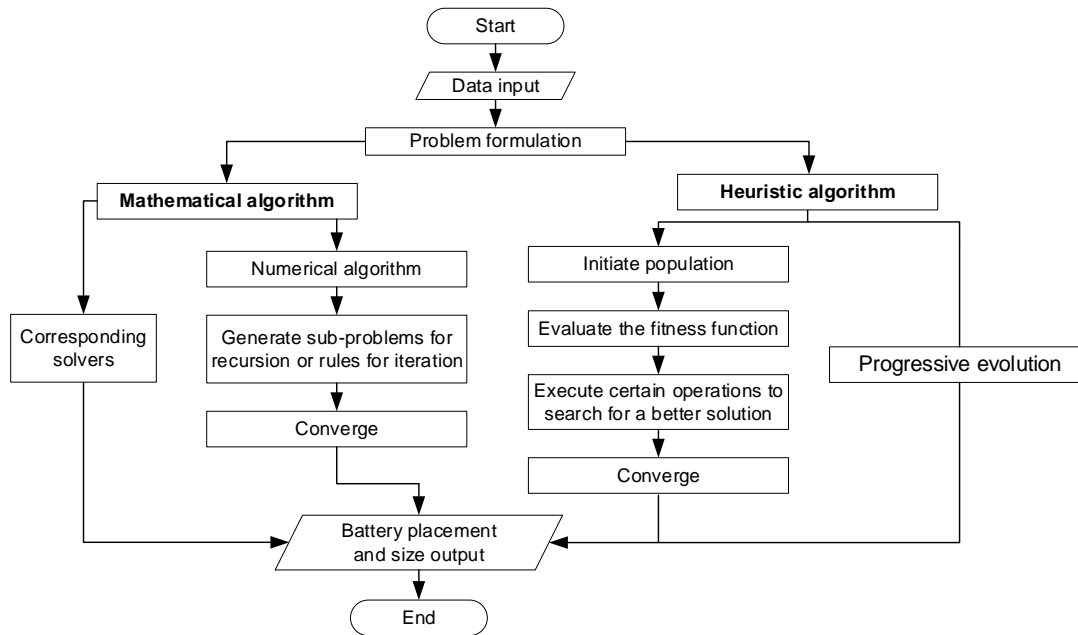


Figure 3.17: Flowchart of direct search-based methods (Yang et al., 2018).

**3.4.3.3.1 Mathematical optimisation based methods** The BESS placement and sizing problem can be expressed as linear programming, mixed-integer programming or even non-linear programming problems (Yang et al., 2018). Expressed the problem as a fitness function, the objective is to find the optimal solution by an iterative process.

It is also possible to find the best result in the BESS siting and sizing problem by implementing classic numeric methods like interior point algorithm, gradient descending algorithm, or Newton Raphson method.

The advantage of these methods is the capacity to solve complex problems with very simple operations in a very short time, reducing the computation effort and maximising the calculation power in the CPU. However, these methods cannot converge to a global solution. In consequence, this issue has allowed that heuristic methods become more popular due to its robustness to find the global solution.

**3.4.3.3.2 Heuristic methods** The heuristic method are widely used in real problems where the exact optimal solution is not mandatory and it is possible to have an approximate solution. The major advantage of heuristic methods is that they can avoid complex calculations such as

derivatives for non-linear optimisation problems, improving the CPU memory usage and the computation time required to find a solution.

Heuristic approaches offer a fast convergence, simple implementation and strong flexibility, even if they cannot often count on a robust mathematical basis to find the optimal solution (Yang et al., 2018). In some cases the heuristic methods are not enough to solve complex problems, as a result, meta-heuristic approaches were developed as a global optimization technique for solving this kind of problems (Okwu and Tartibu, 2021). Meta-heuristic methods are based on a nature-inspired behavior, capable to search a near optimal, exploiting the search space in a randomized manner.

Some of the most used heuristic and meta-heuristic algorithms implemented to solve the BESS placement and sizing problem are explained below.

*Sensitivity analysis* The sensitivity analysis is a helpful algorithm that aims to overcome the difficulty of making use of network data by projecting the complex equations that govern network voltages into a linear space. There are three ways to calculate the sensitivity coefficients (Christakou et al., 2013):

- **Circuit theory method:** This method apply the Tellegen’s theorem to find the computation of the sensitivity indexes. This method requires to build an adjoint network by using a base-case solution of a load flow, then, this can be solved to infer the desired sensitivities.
- **Newton-Raphson method:** This method allows to determine the voltage sensitivity coefficients as submatrices of the inverted Jacobian matrix, resulted of the Newton-Raphson formulation of the load flow calculation.

$$\mathbb{J} = \begin{bmatrix} \frac{\partial P}{\partial |\bar{E}|} & \frac{\partial P}{\partial \theta} \\ \frac{\partial Q}{\partial |\bar{E}|} & \frac{\partial Q}{\partial \theta} \end{bmatrix} \quad (13)$$

This is an iterative method, whereby the voltages are determined in every iteration until the changes in calculated values are smaller than a predetermined threshold (Tamp and Ciufu, 2014). The equation 14 shows the update formula for the Newton-Raphson method. The sensitivity is obtained from the inverse of the standard *Jacobian* matrix used for the calculation of the network bus voltages.

$$\begin{bmatrix} \Delta\delta_2 \\ \vdots \\ \Delta\delta_n \\ \frac{\Delta|V_2|}{|V_2|} \\ \vdots \\ \frac{\Delta|V_n|}{|V_n|} \end{bmatrix} = \mathbb{J}^{-1} \begin{bmatrix} \Delta P_2 \\ \vdots \\ \Delta P_n \\ \Delta Q_2 \\ \vdots \\ \Delta Q_n \end{bmatrix} \quad (14)$$

where  $\mathbb{J}^{-1}$  is:

$$\mathbb{J}^{-1} = \begin{bmatrix} \frac{\partial\theta}{\partial P} & \frac{\partial\theta}{\partial Q} \\ \frac{\partial|\bar{E}|}{\partial P} & \frac{\partial|\bar{E}|}{\partial Q} \end{bmatrix} \quad (15)$$

Once the load flow has converged, the *Jacobian* specifies the partial derivatives (16), in other words the sensitivities, of  $P_x$  and  $Q_x$  with respect to  $|V_Y|$  and  $\delta_Y$  as a function of current network state.

$$\mathbb{J} = \begin{bmatrix} \frac{\partial P_2}{\partial \delta_2} & \cdots & \frac{\partial P_2}{\partial \delta_n} & |V_2| \frac{\partial P_2}{\partial V_2} & \cdots & |V_n| \frac{\partial P_2}{\partial V_n} \\ \vdots & \mathbf{J}_{11} & \vdots & \vdots & \mathbf{J}_{12} & \vdots \\ \frac{\partial P_n}{\partial \delta_2} & \cdots & \frac{\partial P_n}{\partial \delta_n} & |V_2| \frac{\partial P_n}{\partial V_2} & \cdots & |V_n| \frac{\partial P_n}{\partial V_n} \\ \hline \frac{\partial Q_2}{\partial \delta_2} & \cdots & \frac{\partial Q_2}{\partial \delta_n} & |V_2| \frac{\partial Q_2}{\partial V_2} & \cdots & |V_n| \frac{\partial Q_2}{\partial V_n} \\ \vdots & \mathbf{J}_{21} & \vdots & \vdots & \mathbf{J}_{22} & \vdots \\ \frac{\partial Q_n}{\partial \delta_2} & \cdots & \frac{\partial Q_n}{\partial \delta_n} & |V_2| \frac{\partial Q_n}{\partial V_2} & \cdots & |V_n| \frac{\partial Q_n}{\partial V_n} \end{bmatrix} \quad (16)$$

A simplified expression which shows an incremental change in voltage  $Y$  as a function of active and reactive power incremental changes in all the other buses  $X$  of the network is given by 17, this equation results of combining the equations 14 and 16.

$$\Delta|V_Y| \approx \sum_X \left( \frac{\partial|V_Y|}{\partial P_X} \times \Delta P_X + \frac{\partial|V_Y|}{\partial Q_X} \times \Delta Q_X \right) \quad (17)$$

Some inconveniences are found using this methodology such as the limited access for the *Jacobian* matrix in most simulators, the computing limitation over some distribution elements, the time computing and the CPU capacity required to solve the *Jacobian* matrix, and some assumption not applicable to the distribution systems solutions.

- **Perturb-and-Observe Approach:** This methods consists of estimating the voltage and current sensitivity coefficients by a series of load flow calculations, each performed for a small nodal power injections as given in the following equations (Christakou et al., 2013):

$$\frac{\partial |\bar{E}_i|}{\partial P_l} \cong \frac{\Delta |\bar{E}_i|}{\Delta P_l} \bigg|_{\substack{\Delta P_{i,i \neq l} = 0 \\ \Delta Q_{i,i \neq l} = 0}} \quad (18)$$

$$\frac{\partial |\bar{I}_{ij}|}{\partial P_l} \cong \frac{\Delta |\bar{I}_{ij}|}{\Delta P_l} \bigg|_{\substack{\Delta P_{i,i \neq l} = 0 \\ \Delta Q_{i,i \neq l} = 0}} \quad (19)$$

$$\frac{\partial |\bar{E}_i|}{\partial Q_l} \cong \frac{\Delta |\bar{E}_i|}{\Delta Q_l} \bigg|_{\substack{\Delta P_{i,i \neq l} = 0 \\ \Delta Q_{i,i \neq l} = 0}} \quad (20)$$

$$\frac{\partial |\bar{I}_{ij}|}{\partial Q_l} \cong \frac{\Delta |\bar{I}_{ij}|}{\Delta Q_l} \bigg|_{\substack{\Delta P_{i,i \neq l} = 0 \\ \Delta Q_{i,i \neq l} = 0}} \quad (21)$$

where:

$\bar{E}_i$  = Positive sequence phase-to-ground voltage of node  $i$ .

$\bar{I}_{ij}$  = Positive sequence current flow between nodes  $i$  and  $j$  ( $i, j \in \{1 \dots K\}$ ).

$P_l$  = Active power injection at node  $l$ .

$Q_l$  = Reactive power injection at node  $l$ .

To determine the voltage sensitivity coefficients, a link between the power injections  $S_i$  and the bus voltages is necessary as shown in 22.

$$S_i = E_i \sum_{j \in \text{SUN}} \bar{Y}_{ij} \bar{E}_j, \quad i \in N. \quad (22)$$

Then, the equation 22 can be derived with respect to active and reactive power variations in correspondence to the  $N$  buses of the network to define the voltage sensitivity coefficients resulting in the following expression:

$$\frac{\partial E_i}{\partial P_l} \sum_{j \in \text{SUN}} \bar{Y}_{ij} \bar{E}_j + E_i \sum_{j \in N} \bar{Y}_{ij} \frac{\partial \bar{E}_j}{\partial P_l} = \mathbb{1}_{\{i=l\}} \quad (23)$$

$$\frac{\partial E_i}{\partial Q_l} \sum_{j \in \text{SUN}} \bar{Y}_{ij} \bar{E}_j + E_i \sum_{j \in N} \bar{Y}_{ij} \frac{\partial \bar{E}_j}{\partial Q_l} = -j \mathbb{1}_{\{i=l\}} \quad (24)$$

Where it has been taken into account that:

$$\frac{\partial S_i}{\partial P_l} = \frac{\partial \{P_i - jQ_i\}}{\partial P_l} = \mathbb{1}_{\{i=l\}} \quad (25)$$

$$\frac{\partial S_i}{\partial Q_l} = \frac{\partial \{P_i - jQ_i\}}{\partial Q_l} = -j\mathbb{1}_{\{i=l\}} \quad (26)$$

Finally, the partial derivatives of the voltage magnitude can be expressed as:

$$\frac{\partial |\bar{E}_i|}{\partial P_l} = \frac{1}{|\bar{E}_i|} \operatorname{Re} \left( \bar{E}_i \frac{\partial \bar{E}_i}{\partial P_l} \right) \quad (27)$$

A similar equation is found for derivatives with respect to reactive power injections.

A pseudo code of the perturb-and-observe network algorithm exploitation is presented in [Listing 1](#). This code is used to generate sensitivities from electrical network models from a system simulator.

Listing 1: Perturb-and-Observe algorithm for sensitivity generation

- 
- ```

1 Obtain the complex voltages for the current network state,  $v_0$ .
  For each bus  $X$  on the network:
    i) Add a generator injecting a predetermined  $\Delta P$  to the bus.
    ii) Re-run the simulation to find the new set of complex network voltages  $v_1$ .
    iii) Subtract the magnitudes and angles of  $v_0$  from  $v_1$  to obtain  $\Delta|V|$  and  $\Delta\delta$ .
6    iv) Divide  $\Delta|V|$  and  $\Delta\delta$  by  $\Delta P$  to obtain approximations for  $\partial|V|/\partial P_x$  and  $\partial\delta/\partial P_x$ 
        at each bus.
    v) Repeat for a generator injecting a predetermined  $\Delta Q$ 

```
- 

This strategy has the benefit of being loosely-coupled from the simulation approach, allowing in the side of simulation a more resilient calculation, a specific application approach, and an efficient simulation technique to be selected. In the side of experimentation and co-simulation techniques, it opens the possibility to integrate existing models constructed with existing simulators to be used.

*Genetic algorithm (GA)* This algorithm is probably the most popular evolutionary algorithm in terms of the diversity of their applications. It is an optimization algorithm that is often categorized as a global search technique, inspired from the biological evolution theory of natural selection (Okwu and Tartibu, 2021).

The GA approach aims to encode an optimization function as arrays of bits or character strings to represent it as a function called *chromosomes*. Then, some genetic operations are applied to guarantee the offspring to a next generation, and finally, a selection of the best solution (*chromosome*) of the problem concerned is evaluated.

The basic components of the GA include:

- **Fitness function used for optimization:** It is the function that has to be optimized by the solution produced by the GA.
- **The population of chromosomes or individuals:** Encodes the objectives or the optimization function.
- **Selection of chromosomes which reproduce:** This selection is based on the probability of the *chromosomes* to be used for reproduction.
- **Production of next generation of chromosomes by crossover operations:** Several strategies can be employed such as single-point crossover, uniform crossover, or multipoint crossover.

Figure 3.18 shows the crossover operation of two *parents*, which is carried out by swapping one segment of one *chromosome* (single-point crossover) with the corresponding segment on another *chromosome* at a random position.

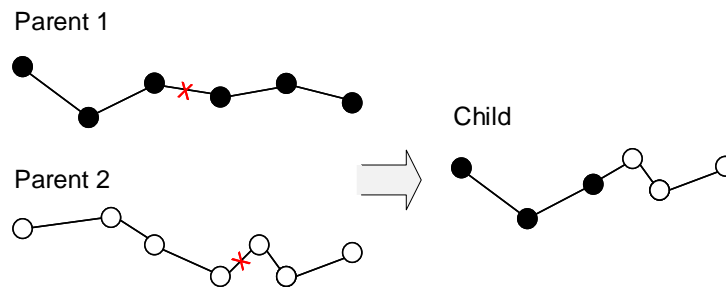


Figure 3.18: Crossover GA operator: Single-point.

- **Mutation of chromosomes in a new generation in a random manner:** Normally achieved by applying the mutation operations (Figure 3.19) in the randomly selected bits.

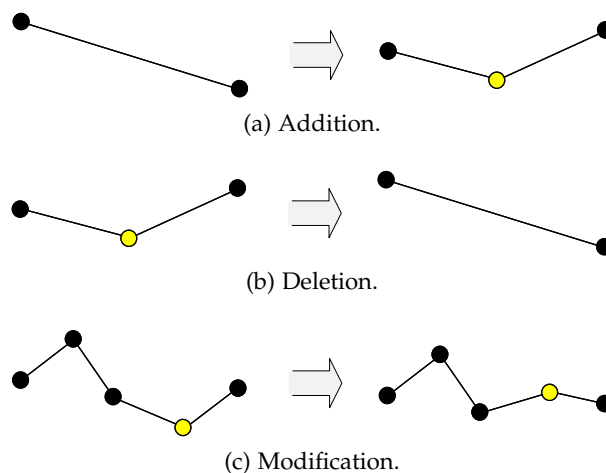


Figure 3.19: Mutation GA operators.

- **Elitism selection of the best solution:** This process is done evaluating the fitness of an *individual*. If the solution is not the best, it can be considered in a new *generation* if a certain threshold of the fitness is reached.



The elitism procedure selects the most fit individual which go through every *generation*, ensuring that the best solution is achieved more quickly.

Listing 2 shows the procedure of the GA implementation.

Listing 2: Pseudo code of GA algorithm

---

```

Objective function  $f(x)$ ,  $x = (x_1, \dots, x_n)^T$ ;
Encode the solution into chromosomes (binary strings)
3 Define fitness  $F$  (eg,  $F \propto f(x)$  for minimization/maximization)
Generate the initial population
Initial probabilities of crossover ( $p_c$ ) and mutation ( $p_m$ )
  while ( $t < \text{Max number of generations}$ )
    Generate new solution by crossover and mutation
8    if ( $p_c > \text{rand}$ ), Crossover; end if
    if ( $p_m > \text{rand}$ ), Mutate; end if
    Accept the new solution if its fitness increases
    Select the current best for the next generation (elitism)
  end while
13 Decode the results and visualization

```

---

Some advantages are remarkable from GA algorithm over traditional optimization algorithms, especially the ability of dealing with complex problems and parallelism. GA algorithms can also solve multiple types of optimization being the fitness function stationary or non-stationary (change with time), linear or nonlinear, continuous or discontinuous, or with random noise. The way how a population can explore the search space in many directions, makes the GA ideal to parallelize the algorithm for implementation (Yang, 2021).

Some disadvantages are related in the formulation and selection criteria of the algorithm parameters where any inappropriate selection can block the algorithm convergence. Otherwise, GA is highly used in modern nonlinear optimization. Also, GA can have a difficult implementation of equality and inequality constraints.

*PSO algorithm* Particle swarm optimization (PSO) algorithm is a population based optimization technique which has been widely applied to solve various optimization problems in the electric power systems (Saboori, Hemmati, and Jirdehi, 2015). The PSO nature is inspired on the swarm social behaviour such as fish and bird schooling in nature. There are three vectors associated with the PSO algorithm:

- A first vector used to know the location of particles.
- A second vector in charge to look for the best solution introduced by an individual or particle.
- A third vector which address the direction and velocity of the particles in an undisturbed manner to search the best solution.

The PSO algorithm starts with a random population matrix where each row is a particle. Every particles in the population moves toward the best solution  $g^*$  with a velocity  $v_i(t)$ . In the PSO algorithm, a particle is defined by its position and velocity. So in every iteration of

the PSO algorithm, it is determined the local and global best solutions, updating the velocity and position of the particle using the equations 28 and 29.

$$v_i(t+1) = w(t) \times v_i(t) + C_1 \times \text{rand} \times (x_{\text{best}}(t) - x_i(t)) + C_2 \times \text{rand} \times (g_{\text{best}} - x_i(t)) \quad (28)$$

$$x_i(t+1) = x_i(t) + v_i(t+1) \quad (29)$$

where:

- rand = Random value in the range of [0,1].
- w = Shows the inertial and is linearly decreased from 0.95 to 0.2.
- $x_{\text{best}}$  = Local best solution.
- $g_{\text{best}}$  = Global best solution.
- $x_i(t)$  = Population matrix in iteration  $k$ .
- $v_i(t)$  = Velocity matrix in iteration  $k$ .
- t = Number of iterations.
- $C_1, C_2$  = Acceleration constants, typically equal 2.

The velocity vector is determined by the equation 28. The initial locations of all particles should distribute relatively uniformly so that they can sample over most regions, which is specially important for multi-modal problems. The initial velocity of a particle can be taken as zero, and its position can be updated by using the equation 29. The steps to implement the PSO algorithm are summarized in the pseudo code shown in Listing 3.

Listing 3: Pseudo code of PSO algorithm

---

```

Objective function  $f(x)$ ,  $x = (x_1, \dots, x_p)^T$ ;
2 Initialize locations  $x_i$  and velocity  $v_i$  of  $n$  particles.
Find  $g^*$  from  $\min\{f(x_1), \dots, f(x_n)\}$  (at  $t=0$ )
while (criterion)
     $t = t+1$  (pseudo time or iteration counter)
    for loop over all  $n$  particles and all  $d$  dimensions
7    Generate new velocity  $v_i^{t+1}$  using equation 28
    Calculate new locations  $x_i^{t+1} = x_i^t + v_i^{t+1}$ 
    Evaluate objective functions at new locations  $x_i^{t+1}$ 
    Find the current best for each particle  $x_i^*$ 
    end for
12    Find the current global best  $g^*$ 
end while
Output the final results  $x_i^*$  and  $g^*$ 

```

---

The movement of particles is represented in Figure 3.20, where  $x_i^*$  is the current best solution for particle  $i$ , and  $g^* \approx \min\{f(x_1)\}$  for  $(i = 1, 2, \dots, n)$  is the current global best solution.

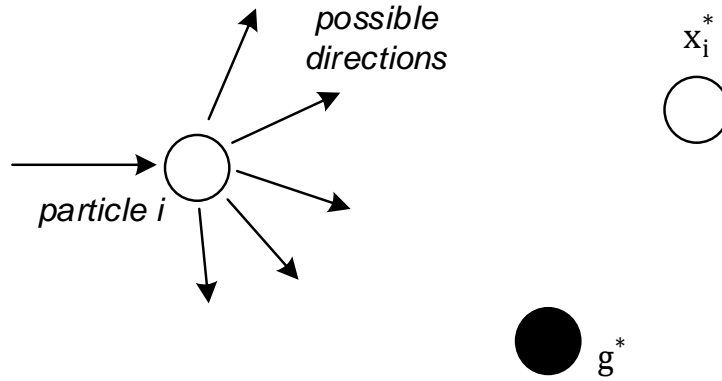


Figure 3.20: Schematic representation of the motion of a particle in PSO, moving towards the global best  $g^*$  and the current best  $x_i^*$  for each particle  $i$  (Yang, 2021).

PSO algorithm is a population-based search algorithm used to solve complex stochastic and non-linear optimization problems. The estimation of the current best particle gives a better and faster convergence towards the optimal solution. However, the fact that PSO algorithms do not record the trace of each particle, produce some limitations keeping all individuals as members of the population, and resulting in less accurate solutions compared than other techniques.

#### 3.4.3.4 Hybrid techniques

The methodologies described to solve the BESS placement and sizing problem have all advantages and disadvantages in their implementation and performance. Table 3.5 summarizes the methodologies analyzed, adding some extra information in their implementation, advantages and weaknesses.

In some cases these methodologies are not enough to deal with the BESS placement and sizing problem by themselves. Then, a way to exploit most of the benefits of these methodologies is combining them to enhance the effectiveness and efficiency of the optimization procedure, reducing significantly their weaknesses. This procedure is known as hybrid techniques, whereby it combines the robustness of each method while it searches for the global optimal with the required resolution.

The hybridisation of different methods can occur in either a decoupled or coupled way (Yang et al., 2018). A decoupled way refers that the methodologies applied are in a mutually exclusive process. In the other hand, a coupled way indicates that the methods work together simultaneously.

The comparison between these methodologies can be difficult due to their implementation in custom-fit applications. However, more advanced solution techniques are being continually developed, considering new hybrid methods to exploit the advantages for different optimization approaches.

Table 3.5: Summary of BESS sizing techniques. (Yang et al., 2018).

| Technique (Time Horizon)                                                                                                              | Implementation                                                                                                                                                                                                      | Pros                                                                                                                                                                                                      | Cons                                                                                                                                                                                                                             |
|---------------------------------------------------------------------------------------------------------------------------------------|---------------------------------------------------------------------------------------------------------------------------------------------------------------------------------------------------------------------|-----------------------------------------------------------------------------------------------------------------------------------------------------------------------------------------------------------|----------------------------------------------------------------------------------------------------------------------------------------------------------------------------------------------------------------------------------|
| Probabilistic methods (intra-hour, hourly data for long duration).                                                                    | <ul style="list-style-type: none"> <li>- Deploy several synthetic scenarios for stochastic optimization optimization such as the Monte Carlo approach.</li> </ul>                                                   | <ul style="list-style-type: none"> <li>- Overcomes the restriction of limited data availability.</li> <li>- Gives results with confidence levels.</li> </ul>                                              | <ul style="list-style-type: none"> <li>- Accuracy relies on the availability of historical data.</li> <li>- May require computational extensive resources.</li> </ul>                                                            |
| Analytical methods (Applications for optimisation horizons ranging from repeated intra-hour simulations to several years assessment). | <ul style="list-style-type: none"> <li>- Direct calculation based on intuitive criteria.</li> <li>- Repeated computation/simulation with fixed intervals.</li> <li>- Sensitivity analysis.</li> </ul>               | <ul style="list-style-type: none"> <li>- Better visualization with the change of battery siting and sizes.</li> <li>- Strong flexibility for all criteria and simulation environments.</li> </ul>         | <ul style="list-style-type: none"> <li>- Computational intensive.</li> <li>- May miss global optimum if the data resolution is not high enough.</li> </ul>                                                                       |
| Mathematical optimisation (Applications for hourly, intra-day or daily optimisation).                                                 | <ul style="list-style-type: none"> <li>- Linear, mixed-integer, quadratic programming problems.</li> <li>- Problems that can be linearized.</li> <li>- Problems that can be solved by numerical methods.</li> </ul> | <ul style="list-style-type: none"> <li>- Strong in finding the global optimum.</li> <li>- Fast convergence and good computational performances.</li> <li>- Mature in power systems.</li> </ul>            | <ul style="list-style-type: none"> <li>- Efficiency limited to linear, mixed-integer, and quadratic programming problems.</li> <li>- Convergence difficulties.</li> <li>- Explicit mathematical formulation required.</li> </ul> |
| Heuristic (Applications for hourly, intra-day or daily optimisation).                                                                 | <ul style="list-style-type: none"> <li>- Non-linear optimisation problems.</li> <li>- Apply nature-inspired algorithms such as GA, PSO, Tabu search and Bat algorithms.</li> </ul>                                  | <ul style="list-style-type: none"> <li>- Flexibility to solve all problems.</li> <li>- Avoid complex derivations.</li> <li>- Less computationally demanding.</li> <li>- Simple implementation.</li> </ul> | <ul style="list-style-type: none"> <li>- May converge to local optimum.</li> <li>- Less robustness and accuracy for linear problems.</li> </ul>                                                                                  |
| Hybrid (Applications for hourly, intra-day or daily optimisation).                                                                    | <ul style="list-style-type: none"> <li>- Decoupled methods combined sequentially.</li> <li>- Hybridisation of different methods in a coupled way.</li> </ul>                                                        | <ul style="list-style-type: none"> <li>- Combines the strengths of different methods.</li> <li>- Improves robustness and ensures global optimum found.</li> </ul>                                         | <ul style="list-style-type: none"> <li>- Likely to increase the complexity.</li> <li>- May require high computational resources than heuristic methods</li> </ul>                                                                |

### 3.5 CHAPTER SUMMARY

There is a latent necessity to integrate energy storage systems into the smart grids. It has been demonstrated that ESS can be useful to guarantee the proper operation of the network in several applications.

Currently, multiple types of ESS technologies are available. However, it is the BESS technology which has received more attention in recent years, mainly explained by the advantages offered like fast response, controllability, geographical independence, and a wide scope of applications which it can be fully utilized.

A correct sizing and placement evaluation of the BESS has resulted crucial in the integration into a smart grid. The development of algorithms for placement and sizing for BESS provides a higher efficiency and reduces the installation cost.

A review of the different algorithms used in the literature for placement and sizing problem in BESS is done. This review discovered the differences between each method and indicates the advantages and disadvantages in their implementation and efficacy.

Finally, the literature reveals a large use of the analytical and heuristic algorithms for BESS placement and sizing problem. This can happen due to the flexibility and easy implementation of both algorithms, also, the flexibility to solve all criteria of a problem. However, these methods often converge to a local optimal of the problem.



## METHODOLOGY FOR BESS PLACEMENT AND SIZING USING PARALLEL COMPUTING

---

### Contents

---

|       |                                                                                                 |     |
|-------|-------------------------------------------------------------------------------------------------|-----|
| 4.1   | Introduction . . . . .                                                                          | 106 |
| 4.2   | Diakoptics and the actor-oriented model concept . . . . .                                       | 107 |
| 4.2.1 | Diakoptics for tearing networks . . . . .                                                       | 107 |
| 4.2.2 | Actor-oriented model . . . . .                                                                  | 108 |
| 4.2.3 | Actor based diakoptics in OpenDSS . . . . .                                                     | 109 |
| 4.3   | BESS installation based on A-Diakoptics framework . . . . .                                     | 117 |
| 4.3.1 | Sensitivity analysis algorithm for BESS placement applying parallel<br>computing . . . . .      | 119 |
| 4.3.2 | BESS sizing methodology for power distribution systems applying<br>parallel computing . . . . . | 125 |
| 4.4   | Other future applications . . . . .                                                             | 145 |
| 4.5   | Chapter summary . . . . .                                                                       | 147 |

---

#### 4.1 INTRODUCTION

Most of the BESS placement and sizing simulation techniques are exceedingly slow and the necessity to model full power distribution system adds further to the complexity issues. Due to an emerging massively parallel architectures such as a general-purpose processors, an important demand is increasing to perform new methods to deploy architectural simulation algorithms. With the complexity to speed up algorithms and performance demands, multi-core platforms are becoming a popular trend in computer design. Effective utilization of these parallel computers requires development of new computational models and parallel algorithms exploiting their particular architecture and computing environments. The increased use of parallel algorithms deployed in multi-core CPUs platforms, are improving the analysis performance to manipulate large amounts of data in parallel.

Parallel programming within a multi-core architecture also can lead to improve computing performance of fast simulators and real-time hardware in the loop (RT-HIL), which can improve the performance for supporting management activities as advanced distribution automation (ADA) and the coordination of energy management systems (EMS) (Montenegro, Ramos, and Bacha, 2017).

It is very relevant for power system simulation platforms to display analysis results without any lack of time, to make meaningful predictions of design alternatives, as well as to be able to assess the performance of an equipment before it is installed into the power system. But in most of the cases power system simulators are conceived for just one core, and can not fully exploit its multi-core capability without a parallelizing restructure; being slow and with a poor scalability, which leads an unacceptable performance for a making-decision tool.

The deployment of algorithms with a fast development cycle and able to provide good trade-offs between speed and accuracy is required. The current computing architectures are composed of several cores, allowing to adopt these technologies as a target to run simulations considering parallelism, concurrency, and asynchronous events. Furthermore, a widely-availability in the service and a cost reduction, leverage the use of multiple physical processing architectures to increase the simulation rate (Raghav et al., 2015).

Extensive efforts are being made to develop the software design methods for multi-core systems, but due to the complexity to develop parallel programming, most of the programs are still being written for single processor computers. The methods for solving distribution systems are still considered to run in a single core architecture, regardless of the existence of multiple cores available for improving the simulation performance. Parallel applications have certain complexity involved, such as processor allocation and mapping, task partition, deadlock, granularity, load balancing, communication and synchronization (Fujimoto, 2007).

Recently the implementation of heterogeneous systems and the use of parallel computing has been resulted more flexible by using actor's framework. According to the literature (Montenegro, 2015), some of the most representative actor libraries and frameworks include NI LabVIEW environment; and due to the integration of A-Diakoptics in EPRI's OpenDSS (Montenegro, Dugan, and Reno, 2017), the deployment of control algorithms based on a parallel computing architecture results in a tool that is both flexible and efficient; thus, facilitating



increasingly-complex and large distribution system simulations, and allowing the test for new power technologies in realistic situations.

This scenario has motivated to develop a novel methodology for placement and sizing BESS technologies using parallel computing, to accelerate the power distribution analysis using multi-core platforms. In this novel methodology the purpose is to distribute the simulation workload over the hardware resources available, exploiting the BESS placement and sizing algorithms seen in [Chapter 3](#) to the many hardware-threads on a highly parallel CPU performance.

## 4.2 DIAKOPTICS AND THE ACTOR-ORIENTED MODEL CONCEPT

### 4.2.1 *Diakoptics for tearing networks*

Diakoptics method is an efficient method used mainly to solve electromagnetic problems of large-scale systems and complex structures. Diakoptics was firstly thought for the analysis of transmission systems to reduce the computational burden, nevertheless, because the evolution of computing hardware architecture, this method was not used anymore.

Diakoptics basically is a mathematical method for tearing networks. It is used for tearing large physical circuits into several sub-circuits to reduce the modeling complexity and accelerate the solution of the power flow problem using a computer network. Each computer will handle a separate piece of the circuit to find a total solution (Montenegro, Ramos, and Bacha, 2016).

In other words, diakoptics proposes the total separation of the areas to find partial results, which will be complemented by including the effect of the link branches separately (Jiang, Vittal, and Heydt, 2008). Some features of diakoptics method are:

- The circuit formulation is done using the  $Y_{BUS}/Z_{BUS}$  matrix.
- The implementation mode could be parallel or distributed.
- It is totally independent on other subareas information.
- The dependency on communication is critical.
- It is a method coordinated to calculate the complementary voltages.

The intention of applying diakoptics method is to consider each primitive subsystem as an independent system. This is possible by decomposing the entire system into a number of subsystems known as primitive and orthogonal networks. Primitive systems are the non-overlapping subsystems formed when separating the interconnected system; orthogonal systems are the tie lines that interconnect the primitive subsystems. The primitive subsystems do not consider the frontier effects produced by the tie lines, they are declared like if the other networks did not exist. On the contrary, the orthogonal networks include the information about the network view from the link branch.

As shown in Figure 4.1, the overall power system can be decomposed into a certain number of primitive subsystems on a geographical basis. Without loss of structural integrity, three non-overlapping subsystems  $S_1$ ,  $S_2$ , and  $S_3$  are considered to depict the main aspects of decomposition. These subsystems are connected by orthogonal networks.

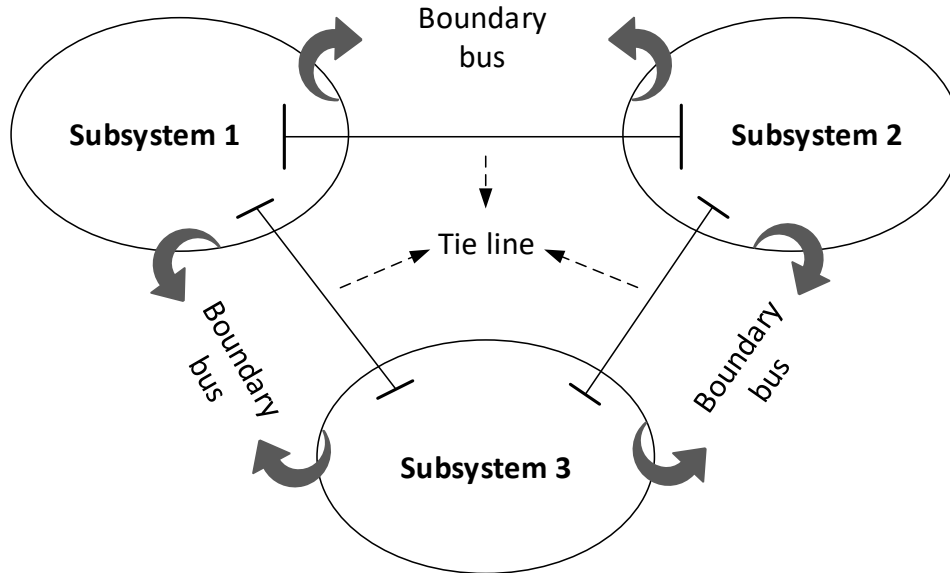


Figure 4.1: Power system decomposition in primitive subsystems.

#### 4.2.2 Actor-oriented model

The actor-oriented model is a well-known mathematical model of concurrent large scale computation, used mostly in a time-sensitive context, such as, RT simulation processes to coordinate the interaction between sub-circuits. The actor-oriented model is commonly established as a framework in different programming languages, allowing the modelling and implementation of distributed asynchronous systems.

An actor is a queue-driven state machine (QDSM) that exchanges data with other actors by using messages (Montenegro, 2015). The messages are sent by using dedicated channels, which are addressed to guarantee the high flow of data samples or dependencies between actor executions. An actor selectively retrieves messages (one at a time) from its mailbox and either creates new actors, sends messages to other actors, or invokes different kinds of task based on the pattern of the retrieved message.

Figure 4.2 illustrates the relation among actors, task and channels. The actor behavior is controlled by the internal state and the messages received. Actors run isolated helping to keep data private in a multi-tenant environment (Park et al., 2011).

For its implementation it is used the actor framework available in the NI LabVIEW environment, where actors are defined as objects within a virtual environment. As objects, they can be cloned automatically and executed independently in parallel concurrently. An application is specified using a variant of the actor-based concurrency model, where an application consists of a number of actors.

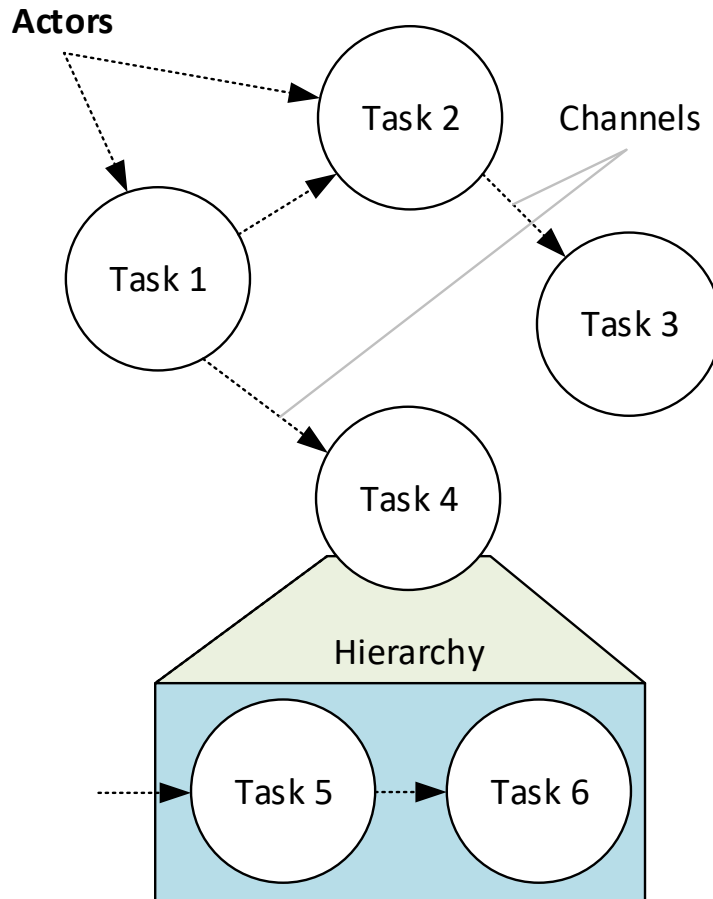


Figure 4.2: Actor-oriented specification of an application.

The advantage of the actor model for parallel computing is that the potential task parallelism of an application is explicitly specified by actors, so the parallelization of the application is nothing more than mapping the actors to the processing elements. Actors are very light weight single-threaded applications but in a multi-tenant environment they may bring down the device or drain the battery if they are not controlled (Masud, Lisper, and Ciccozzi, 2018).

#### 4.2.3 Actor based diakoptics in OpenDSS

The combination between diakoptics and the actor-oriented model is known as diakoptics based on actors (A-Diakoptics). Diakoptics suggests that many processes are happening concurrently and is then when the actor model appears for handling these processes.

The scope of A-Diakoptics is to make traditional transient stability analysis (TSA) methods suitable for multicore processing and improve the simulation performance, improving standard and real-time (RT) computing architectures (Montenegro, Ramos, and Bacha, 2017).

A-Diakoptics enhance the simulation step to achieve a faster solution in power flow problems, reducing the overall time to execute quasi-static time series (QSTS), and consequently, improving the performance to run RT simulations and the possibility to accelerate the analysis in the use of heuristic algorithms. This technique has been implemented in OpenDSS (Montene-

gro and Dugan, 2019). Figure 4.3 shows how the use of multi-core architectures allows its implementation and enables the acceleration of QSTS simulations. In OpenDSS, A-Diakoptics coordinates and uses the parallel processing to allocate and solve the distributed subsystems resulted in Diakoptics algorithm by using the actor model as a framework.

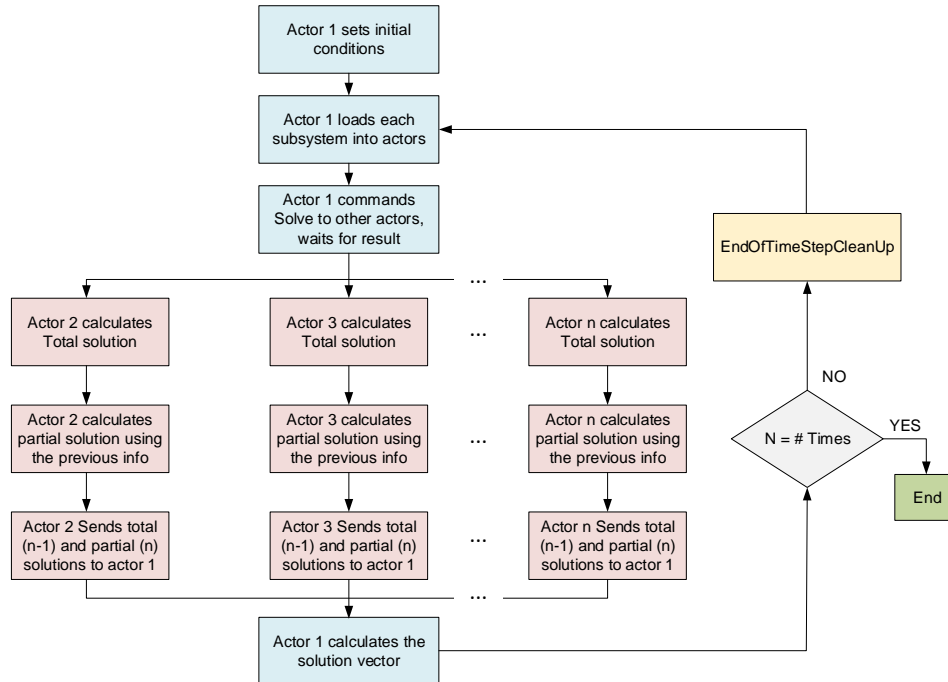


Figure 4.3: A-Diakoptics algorithm in OpenDSS (Montenegro and Dugan, 2019).

The main application of A-Diakoptics is the simulation of small-scale, medium-scale and large-scale power systems looking for improving the performance of existing simulation platforms for offline and RT-HIL. This application considers the integration of several technologies within a heterogeneous computing system for calculating the power system values, to export and import digital and analog signals (PHIL), to communicate with external controllers and monitoring devices (CHIL), guaranteeing deterministic computing times in real-time (RT).

Other applications are related to management activities called advanced distribution automation (ADA), these activities are dedicated to monitor and control distribution systems, including the different threats proposed in smart grid studies. A-Diakoptics is proposed for performing the distributed state estimation of a power distribution system.

#### 4.2.3.1 Using the OpenDSS parallel processing suite

OpenDSS has a parallel processing suite that makes from it a more modular, flexible and scalable parallel processing platform, which has the following guidelines (Dugan, Montenegro, and Ballanti, 2020):

- The parallel processing machine is interfaced independently.
- Each component of the parallel machine works independently.

- The simulation environment delivers information consistently.
- The data exchanged between the components of the parallel machine obeys the interface rules and procedures.
- The user handle of the parallel machine supports the already functioning of OpenDSS.

To create the parallel machine, OpenDSS uses the actor model. Each actor is created by OpenDSS-PM, it runs on a separate processor (if possible) using separate threads and it has its own assigned core and priority (real-time priority for the process and time critical for the thread).

The interface for sending and receiving messages from other actors is based on the Direct DLL API. With this interface is possible to create a new actor (instance), send/receive messages from these actors, and define the execution properties of the actors such as the execution core, simulation mode, and circuit to be solved, among others. Using the existing interface, it is possible to:

- Request the number of available cores and the number of physical processors available.
- Create/Destroy actors.
- Execute the simulation of each circuit concurrently and in parallel (hardware dependent).
- Assign the core where the actor will be executed.
- Modify the simulation settings for the active actor.
- Set the name of the circuit that will be simulated.

As a result, each actor can be considered as a *child* and it behaves as an independent OpenDSS solver. As can be seen in [Figure 4.4](#), the interface will work as the communication medium

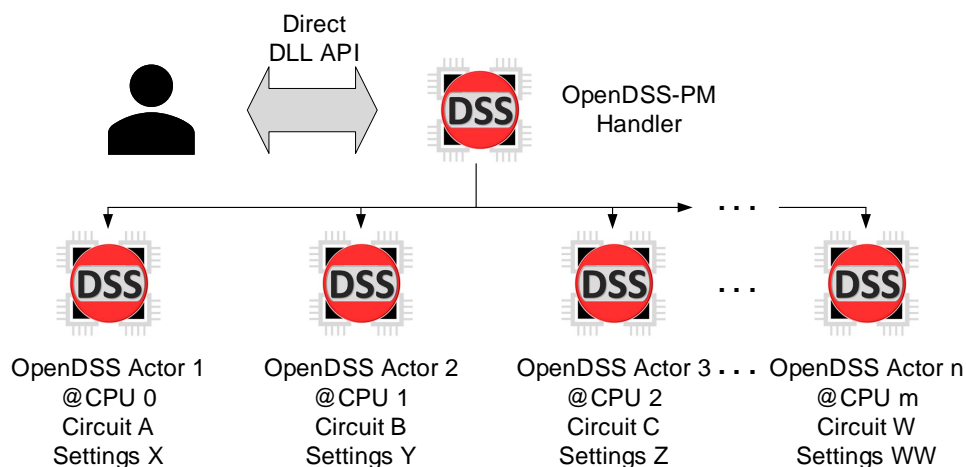


Figure 4.4: Operational architecture for A-Diakoptics algorithm in OpenDSS (Dugan, Montenegro, and Ballanti, 2020).

between the different actors on the parallel machine. This feature enables several simulation modes inspired in parallel computations such as temporal, diakoptics, among others.

These types of simulations will be driven by an external program that will handle the actors within the parallel machine, in keeping with the actor concept as a message driven state machine. To operate the parallel machine, the suggested procedure is as follows:

- The program will create a new default actor every time the start function is called in an OpenDSS-PM DLL interface when the EXE version is started. OpenDSS-PM will create *Actor 1*, designate a memory space, open an instance for KLU Solve, and define the execution thread. In return, OpenDSS-PM will return to the user an *ID* (integer) to identify the created actor.
- After the program has started the user issues the *NewActor* command to create a new actor.
- After a new actor is created, the user will designate the core in which the actor is to be executed using the *Set Core = nn* command. This command will apply to the active actor using the selected interface. *Core 0* is the default core for the initial actor created at start up, but this can be changed.
- To change the active actor, the user will issue the *Set ActiveActor = nn* command.
- After the active actor is set, the user can execute OpenDSS commands as done for the classic version using the selected interface. The commands will apply to the process executed by the active actor.
- There are two options for solving the systems with actors:
  - Solve the active actor
  - Solve all of the actors
- If the user selects to solve only the active actor while there are other actors created, the user can continue to interact with the other actors while the solving actor is working. On the other hand, if the user selects to solve all the actors, the ability to exchange information with an actor will depend on the availability of its core. If there are not enough cores to handle the request, the user program will have to wait until one of the actors finishes the solution routine.
- Each actor can be asked for data and can store its own monitor and energy meter samples locally.

To make this possible it is necessary to clone essential classes of OpenDSS. This cloning process must be done every time the user requests it. By default, there will be at least 1 actor active for performing simulations and the default core will be the first core available (*Core 0*).

The configuration of each instance (actor) can be made sequentially, however, the parallel processing of each actor circuit is done using multi-threading, defining the process and thread affinity and its priority.

#### 4.2.3.2 Parallel computing communication between NI LabVIEW® and OpenDSS

The use of the Direct DLL API of OpenDSS allows an easy integration to use OpenDSS-PM in NI LabVIEW environment (NI, 2020). Based on a design pattern of an event-base state machine architecture described in Figure 4.5, it is possible to define all possible behaviors to manage each actor in OpenDSS. For building the event-driven algorithm, it is necessary to be modeled an action-reaction functional graph based on a state machine, which will consider all possible actions that could drive the system from one state to another.

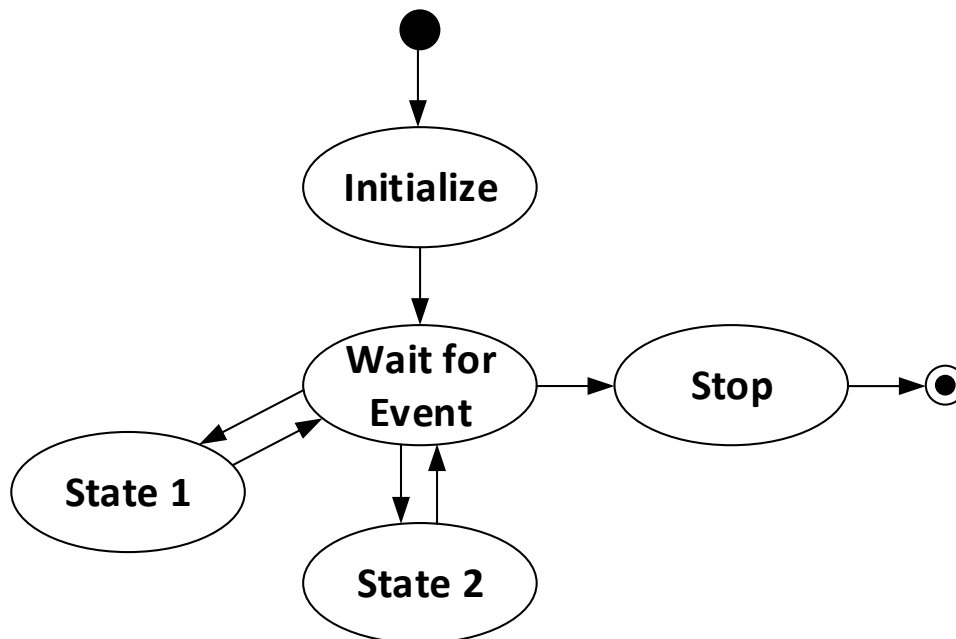


Figure 4.5: Event-base state machine design pattern.

As can be seen in Figure 4.6, the state machine can also be used to implement complex decision-making algorithms, such as heuristic algorithms, represented by state diagrams, allowing to pass from one state to another when a certain event occurs. The passing from states is unidirectional, requiring a different event-driven definition to return to the previous state. Each state in a state machine does something unique and calls other states.

The diagram description of the event-driven state machine architecture is seen in Figure 4.7, to create the event-driven state machine architecture using NI LabVIEW, it is necessary the following block diagram components:

- **While loop:** It is the container structure that permits to execute current state continuously and monitor events occurrence.
- **Shift Register:** Used to store and transit next state to current state.
- **Case structure:** Contains program code for each state.
- **Event Structure:** Contains program code for each detected event.
- **Timeout terminal:** Control when a possible timeout event executes.

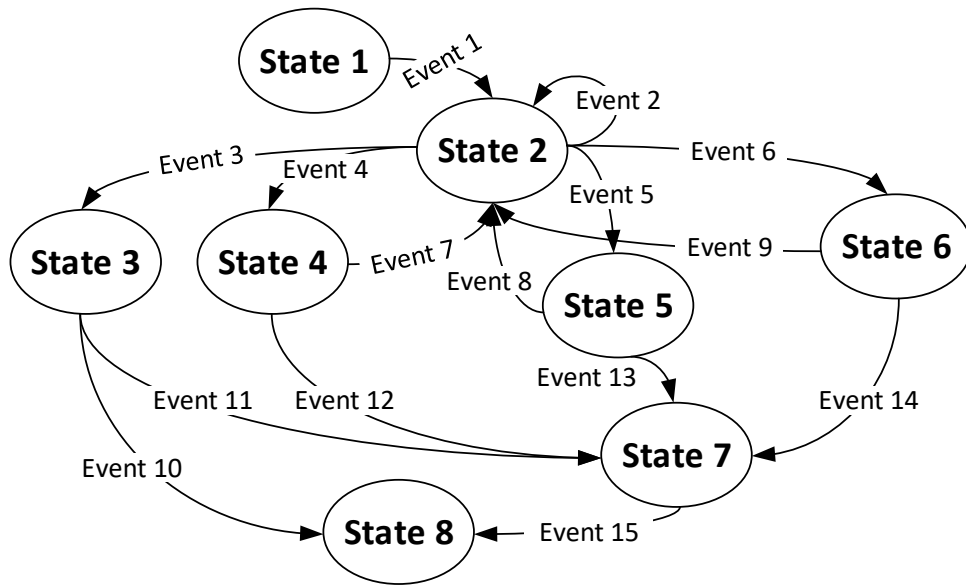


Figure 4.6: Event-Based State Machine structure.

- **State Functionality code:** Program code for each state in case structure.
- **Transition code:** Determine next state.
- **Error handler:** Used to directing errors when they occur.

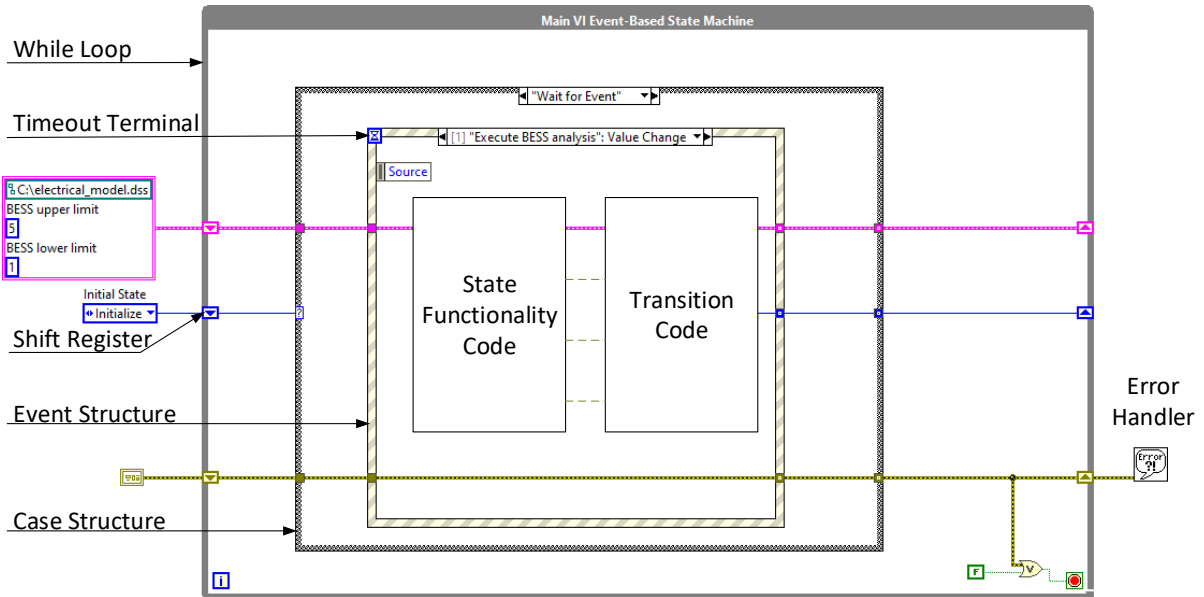


Figure 4.7: Functional Event-Based State Machine using NI LabVIEW.

After the design pattern is done, the next step is to integrate the direct DLL API library from OpenDSS for NI LabVIEW. This direct connection is a shared DLL library that implements the classes, properties and methods to control the OpenDSS interface. This connection accelerates the in-process co-simulation between OpenDSS and NI LabVIEW (Montenegro, 2017).



This library is a polymorphic virtual instrument (VI) that includes all the functionalities of OpenDSS. It was created by using the direct DLL interface, which will guarantee the best performance when including OpenDSS in any NI LabVIEW development. The OpenDSS and OpenDSS-PM libraries are open, available and can be installed in NI LabVIEW® environment (Montenegro and Dugan, 2017).

The procedure to establish a DLL connection between OpenDSS and NI LabVIEW starts initializing the parallel machine. After started the connection with OpenDSS as shown in Figure 4.8, the procedure to activates the parallel processing is done, consecutively, the scan of the system to know the number of CPU's core available is made to asses the number of parallel subsystems possible to form.

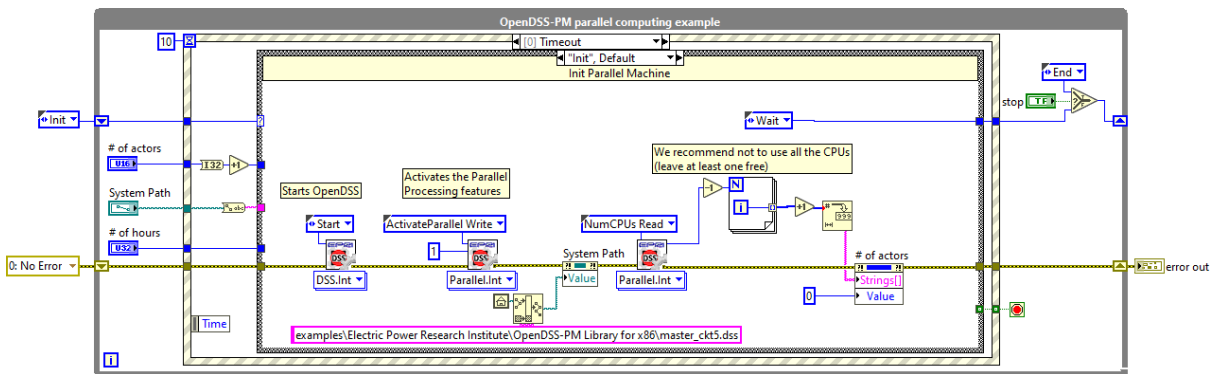


Figure 4.8: OpenDSS-PM parallel computing example. Actor's initialization.

Then, each actor is created in OpenDSS assigning the electrical system to analyze in every processor systematically, it is performed the first system solution using separate threads. Each new actor is an independent OpenDSS engine waiting for commands as shown in Figure 4.9. The circuit compiled by each actor can be the same or different. Likewise, the simulation settings can be the same or different.

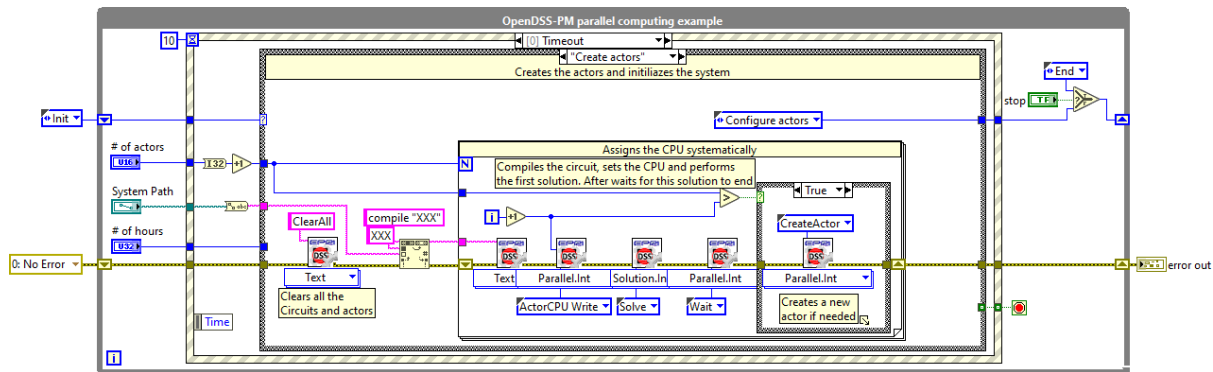


Figure 4.9: OpenDSS-PM parallel computing example. Actor's definition.

The next step is to define the execution properties of the actors such as the execution core, simulation mode, and circuit to be solved among others. Figure 4.10 shows how the features of each actor are set, a for loop iteration is defined based on the number of actors created, allowing to configure each actor considering the simulation mode and the number of iterations.

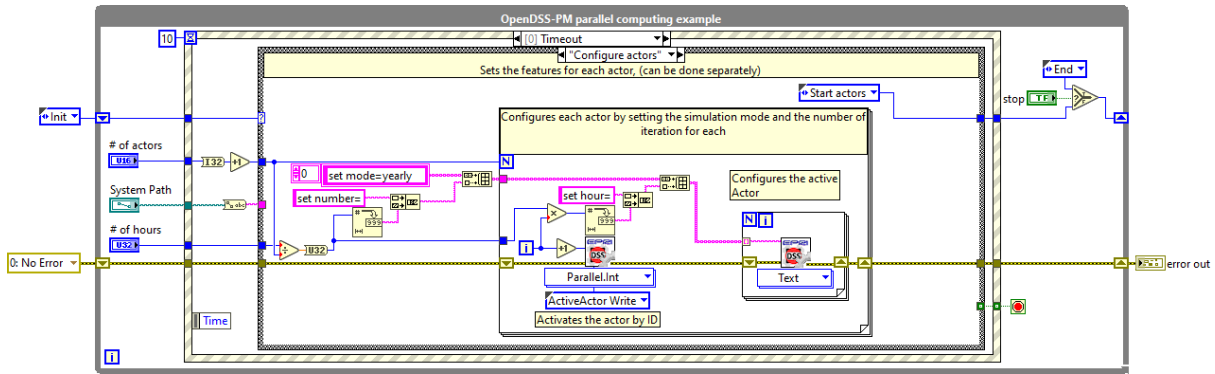


Figure 4.10: OpenDSS-PM parallel computing example. Actor’s configuration.

Configured all instances and actor’s behaviour, it is possible to start the solution for each actor. OpenDSS-PM executes a power flow iteration for each actor, processing an independent result according to the subsystem loaded in the corresponding actor. Figure 4.11 shows the actor command simulation process, this state has a high priority due to its importance to accomplish the QSTS simulation.

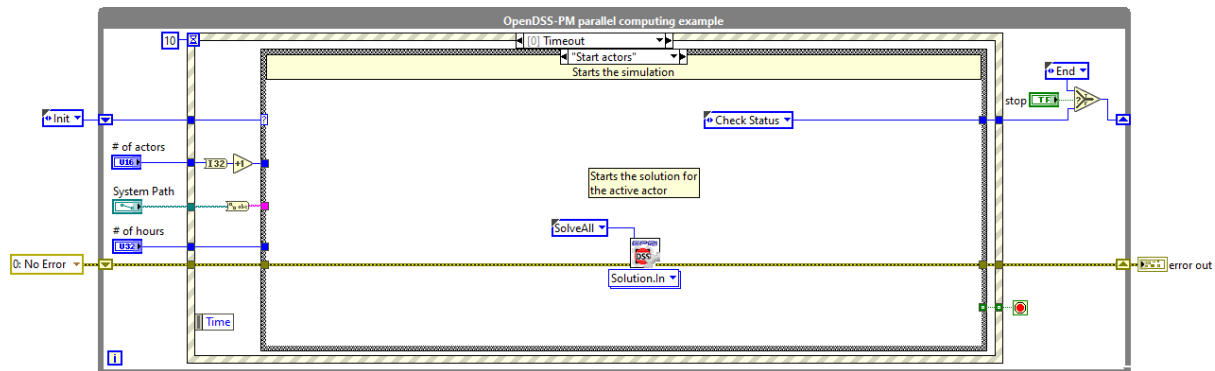


Figure 4.11: OpenDSS-PM parallel computing example. Simulation execution.

Because the occupancy of each actor is a critical task, the actor’s progress can be consulted in any moment, Figure 4.12 establishes the formulation to read the simulation step of an actor, as well as, the percentage of the total simulation progress separately.

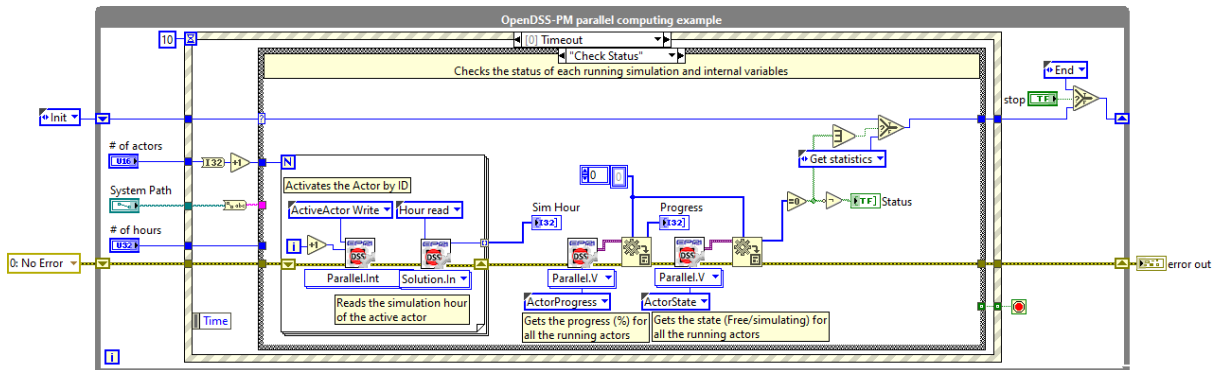


Figure 4.12: OpenDSS-PM parallel computing example. Actor’s progress status.

An interesting feature is shown in Figure 4.13, where each instance is being executed in a separate thread, all the actors can exchange information “on the fly” asynchronously. When a simulation is being performed by an actor the user can ask for a progress report and values from the simulation without interrupting the simulation process. Everything is happening at the same time, a feature that can be widely exploited in advanced applications.

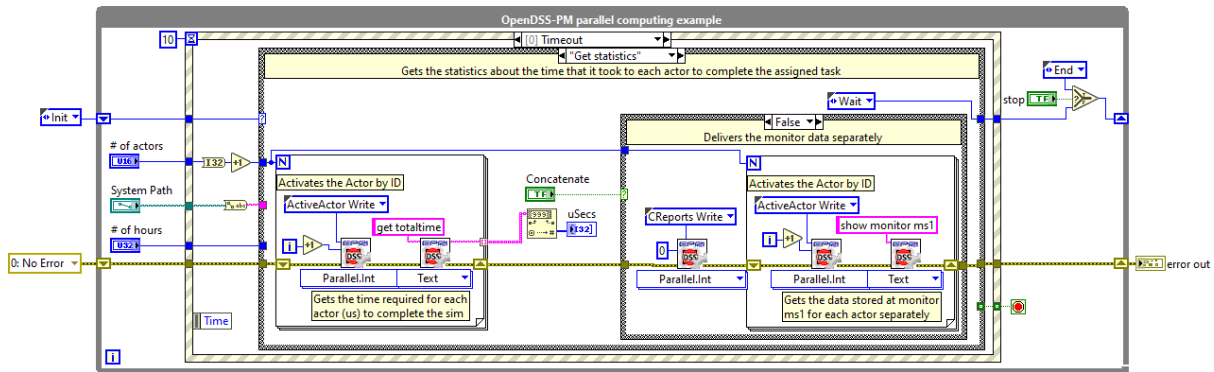


Figure 4.13: OpenDSS-PM parallel computing example. Actor's statistics.

Parallel processing is very handy when performing detailed analysis that requires small simulation steps and a large number of steps. One example is a detailed BESS placement and sizing impact studies, where many power flow simulations have to be performed using several steps. The big challenge with this kind of simulations is for each simulation cycle, the parameters of the BESS and its localization has to be recalculated. This evaluation formerly requires a significant amount of scenarios to be completed.

Depending on the type of operative system (OS), the hardware resources of the actor must be handled in a different way. For instance when it is used a personal computer, the actors computing resources will be managed by the local OS due to the non-deterministic computing environment. A multitask OS must distribute computing resources to all the software executing in the same time instant. As a result, the performance of the application could vary depending on the number of services, applications and nature of the applications running at certain moment. In case of RT applications deployed in a dedicated OS, it is possible to allocate each actor on specific cores and threads to guarantee the performance of the application.

By using OpenDSS-PM, it is possible to reduce this time considerably just using standard computers. Multiple actors can deploy simultaneously different simulations, reducing considerably the total simulation time. The literature demonstrates a better performance when performing temporal parallelization techniques, where the reduction in time is around 60% to 70% depending on the number of cores available (Montenegro and Dugan, 2017).

#### 4.3 BESS INSTALLATION BASED ON A-DIAKOPTICS FRAMEWORK

In this new methodology, BESS placement and sizing analysis is combined using an strategy of the A-Diakoptics framework of EPRI's OpenDSS<sup>®</sup>. It means that everything is treated as an actor, giving the capacity to handling placement and sizing scenarios in a parallel and concurrent way. The use of the Direct DLL API of OpenDSS, allows an easy integration of this kind of heuristic methods suitable for multi-thread processing in NI LabVIEW.

The complexity of large-scale systems and the integration of DERs technologies, boost the necessity to implement faster decision-making tools to improve the output of data under events. In response of this requirement, some of the algorithms analyzed in Chapter 3 for BESS placement and sizing are implemented in a paralleling computing strategy, which allows to create a new methodology to improve the analysis performance of the algorithm and to reduce the computing response time.

This new methodology works as a toolkit of the experimental platform belonged to the Bank of Energy concept, which simplifies the introduction of BESS in the power distribution system of Gazelec of Peronne (GoP). A flow chart of this solution is presented in Figure 4.14, where an hybrid solution of two different algorithms are used to find the suitable placement and sizing of BESS, first, a sensitivity analysis is performed to evaluate the introduction of BESS elements (placement) which supports the system without affecting or disturbing its correct operation. Knowing the most sensitive buses, a second algorithm based on a genetic algorithm (GA) approach determines the optimal output power rating (sizing) of every BESS evaluated.

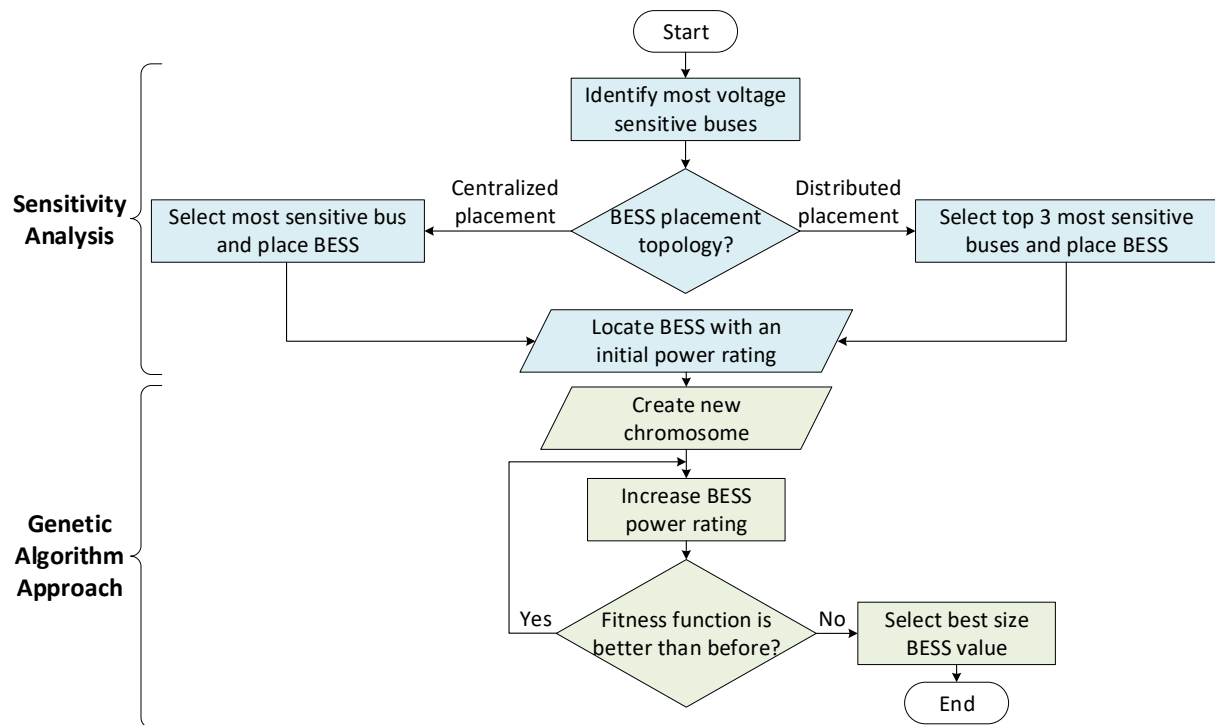


Figure 4.14: A flow chart of the novel placement and sizing BESS methodology.

This solution is programmed under a design pattern of event-based state machine to reduce the complexity of the states and to assure the use of the OpenDSS parallel processing suite. All together allows an effective use of the computational resources and electric system evaluation, to ensure a proper installation of BESS associated to the local renewable energies electricity generation towards a positive energy territory.

Based on the multi-core architecture property of the server used in Chapter 2, a parallel based computing connection between OpenDSS-PM and NI LabVIEW is assured. Figure 4.15 shows how the algorithms scenarios are introduced considering a parallel computing methodology.

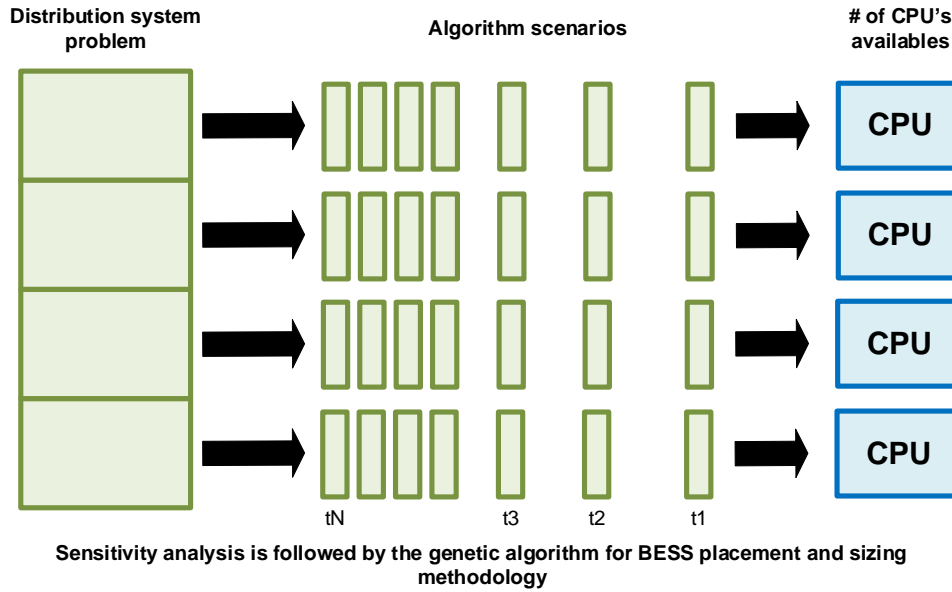


Figure 4.15: Parallel computing methodology for the integration of the sensitivity analysis and the genetic algorithm.

This methodology has resulted in a relatively low overhead to achieve better speedup, which is dependent on the size and nature of the distribution network, and its configuration. The efficiency is ensured by:

- A suitable distribution over processors of the BESS placement and sizing algorithms.
- Robust electrical system model, considering real cables and load information.
- Efficient sampling of the distribution system nodes.
- All possible event-state scenarios evaluation.

#### 4.3.1 Sensitivity analysis algorithm for BESS placement applying parallel computing

Although a number of approaches have been proposed for sensitivity analysis applied in power distribution systems, they have still some limitations related to performance and faster response for large-scale systems. The sensitivity analysis is one of the most time-consuming computational process applied to BESS placement regardless its effectiveness to determine the sensitive nodes in a power system network.

So far, a number of approaches have been proposed for speedup sensitivity analysis to BESS placement in power distribution simulation. For example, in (Christakou et al., 2013), an improved computation of sensitivity coefficients of node voltages and line currents in unbalanced radial electrical distribution networks is developed. In (Tamp and Ciufo, 2014) a software toolkit one-core based is developed to simplify the development of voltage management strategies by the application of sensitivity analysis. In (Aziz, Deeba, and Nahid-Al-Masood, 2016) is proposed a BESS system placement based on the most sensitive buses of a micro-grid to support quick voltage recovery at distributed generation terminals. In (Arif, Rabbi, and

Aziz, 2018), a sequential methodology is applied to find the suitable placement and rating of BESS in an islanded micro-grid identifying the most sensitive buses. In (Zad, Lobry, and Vallee, 2018), an improved sensitivity analysis incorporates variations of power losses in the system branches due to the nodal power changes and their eventual impacts on the node voltages.

Despite the efforts done to improve the algorithm efficiency, these global sensitivity analyses still appear to be insufficient to exploit completely the modern multi-core architectures, and thus improve the sensitivity analysis deployment. By introducing parallel computing techniques for sensitivity computation, significant speedup is deployed in the sensitivity analysis. Computation of design sensitivities is characteristically uncoupled, thus opening the option to apply parallelization.

In this section, it is proposed a novel methodology for sensitivity analysis based in a parallel distributed environment. This methodology takes a unique paradigm, which is completely different from those of sensitivity analysis methods developed so far. By combining massively parallel computation and an interactive data visualization toolkit for the experimental platform developed.

#### 4.3.1.1 Formulation of the parallel sensitivity analysis

Parallel sensitivity analysis applied for BESS placement is an opportunity to speedup the most time-consuming computational part of the traditional algorithm used over the years, which itself can be decomposed into parallel subsystem tasks. The change in voltage at a bus  $Y$  as a response to changes in  $P$  and  $Q$  at each network bus  $X$  is simplified by (Christakou et al., 2013):

$$\Delta|V_Y| \approx \sum_X \left( \frac{\partial|V_Y|}{\partial P_X} \times \Delta P_X + \frac{\partial|V_Y|}{\partial Q_X} \times \Delta Q_X \right) \quad (30)$$

This approximation of Equation 30 can be deployed splitting the problem in an actor-model architecture, where each actor will evaluate separately the response in voltage at bus  $Y$ , when a perturbation in  $P$  is done at each network bus  $X$  (for BESS placement assessing), completing the task in a reduced time. In other words, the proposed approach for this method is based on simulating the actual perturbation-state of the system in an available actor.

Because in OpenDSS everything is based on a physical model, the first task is to have the distribution system modeled with the correct physical behavior of the system elements, and a near demand of the system load. Then based on the perturb and observe algorithm for sensitivity analysis discussed in Chapter 3, a generator is defined and moved it all along the medium voltage feeders (20 kV), solving a power flow at each location. Each state demonstrates the reaction in voltage when a perturbation is done, represented in the sensitivity of the distribution system.

After all the simulations steps are finished, a post-processing of the sensitive data is done to arrange the values from the highest to the lowest sensitive bus. This list is then prepared as an input of the visualization toolkit for the experimental platform belonged to the Bank of

Energy, generating a sensitive heat map of the distribution system. This panorama allows a comprehensible understanding of the system sensibility and hence, the suitable placement of BESS. Figure 4.16 shows the flow chart of this novel methodology using a parallel computing processing.

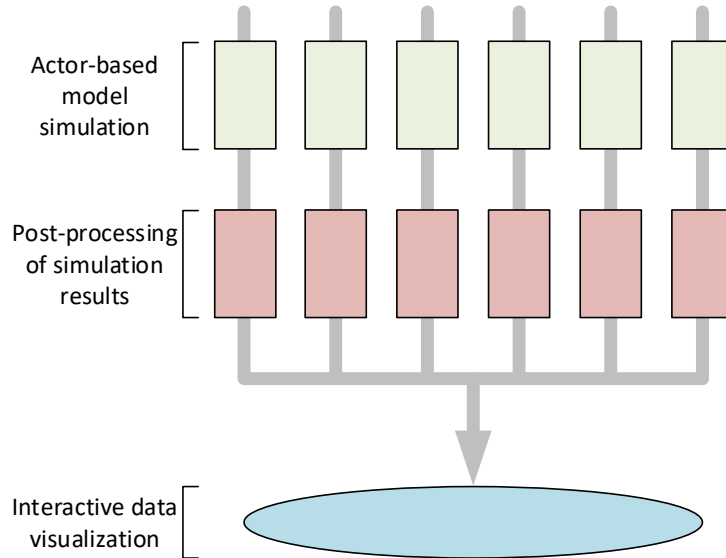


Figure 4.16: A flow chart of a novel sensitivity analysis using parallel computing.

#### 4.3.1.2 Test case study

In order to validate the developed method, it was used a simple test network topology illustrated in Figure 4.17. It is an hypothetical 230 kV transmission network, with a total loading of 570 MW and 309.86 Mvar and it was chosen because it has been already verified according to (Tamp and Ciufu, 2014).

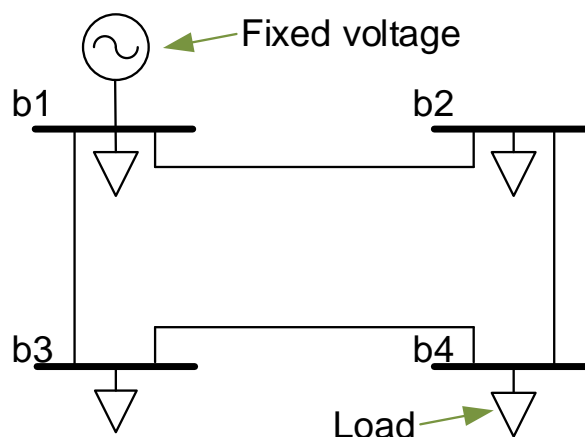


Figure 4.17: Test network topology taken from (Tamp and Ciufu, 2014).

The test network is implemented in OpenDSS, and the perturb and observe algorithm for sensibility analysis is developed using NI LabVIEW. Then, the sensitivities obtained are compared to the reference set.

4.3.1.2.1 *Sensitivity results* The sensitivity calculation results are shown in Table 4.1. The bus  $b_4$  is the most sensitive bus of the test case system. The results are compared and validated with those obtained by (Tamp and Ciufu, 2014).

Table 4.1: Sensitive results for the test case system.

| Bus name | $\delta V/\delta P$    |
|----------|------------------------|
| $b_4$    | $2.45 \times 10^{-5}$  |
| $b_2$    | $1.84 \times 10^{-5}$  |
| $b_3$    | $1.34 \times 10^{-5}$  |
| $b_1$    | $2.41 \times 10^{-10}$ |

4.3.1.2.2 *Error validation* The error statistics between the sensitivities obtained from the algorithm developed and the sensitivities given by the reference set are presented in Table 4.2. As expected, there was a negligible difference between all sensitivities obtained with the perturb and observe strategy and the reference set.

Table 4.2: Error statistics for the sensibility test case between the algorithm developed and the reference set.

| Sensitivity                          | Median error, %       | Maximum error, %      |
|--------------------------------------|-----------------------|-----------------------|
| $\frac{\partial  V }{\partial P}$    | $2 \times 10^{-3}$    | $6 \times 10^{-3}$    |
| $\frac{\partial  V }{\partial Q}$    | $6.3 \times 10^{-2}$  | $2.64 \times 10^{-1}$ |
| $\frac{\partial \delta}{\partial P}$ | $4.68 \times 10^{-7}$ | $2.05 \times 10^{-6}$ |
| $\frac{\partial \delta}{\partial Q}$ | $2.45 \times 10^{-8}$ | $1.07 \times 10^{-7}$ |

The error is purely due to a mathematical precision approximation. This error validation probes a correct operation of the algorithm developed, contributing a new toolkit for sensitivity calculation applied for any power distribution network within the Bank of Energy experimental platform frame.

As the perturb and observe algorithm performance must be tested, Table 4.3 reports the results obtained from the solution time required to deploy the algorithm between the data set and the parallel computing development considering one-core or multi-core architecture. The test consists of solving a complete sensitivity analysis of the network topology proposed, where the

Table 4.3: Solution time for selected test case.

| Speed test       | Reference set | One-core | Multi-core |
|------------------|---------------|----------|------------|
| Average time, ms | 170.4         | 147.4    | 82.6       |
| Minimum time, ms | 157           | 144      | 68         |
| Maximum time, ms | 183           | 156      | 98         |



total solution time was recorded in *ms*. These results reveal an outstanding performance when the algorithm is deployed in a multi-core architecture, reducing the solution time almost in a half of a normal solution. This characteristic provides an excellent opportunity for sensitivity calculation of large-scale distribution systems.

#### 4.3.1.3 Real test case: French distribution network

The algorithm is also tested in the real model network of GoP distribution system (for more details about the system see [Appendix A](#)). The sensitivities are calculated for the network using the perturb and observe approach explained in [Chapter 3](#). In this case as shown in [Figure 4.18](#), the *substation I* feeds the distribution system by the transformer *TR312* while all DERs are not considered for this scenario.

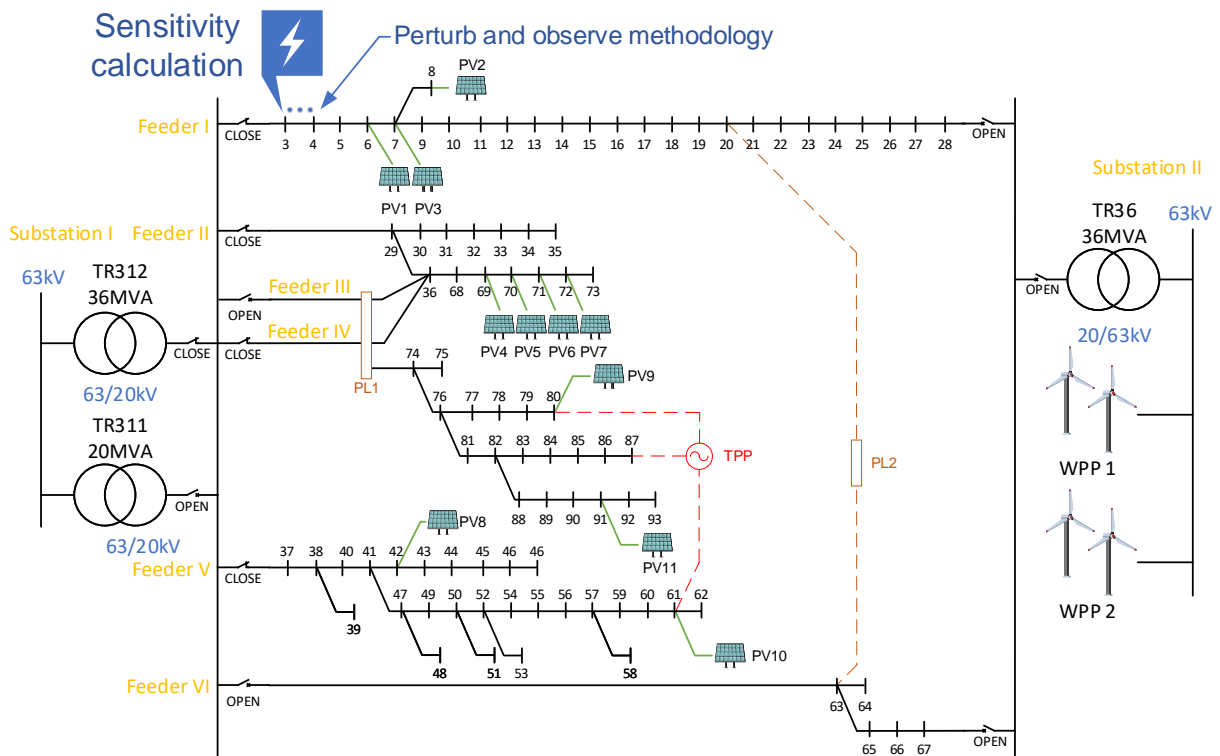


Figure 4.18: Sensitivity calculation in Gazelec distribution system

For battery placement study only  $\frac{\partial|V|}{\partial P}$  is considered, because as seen in [Chapter 3](#), BESS affects mainly the active power component in a distribution system. Hence, the  $\frac{\partial|V|}{\partial P}$  sensitivity coefficient allows to establish the suitable points to install a BESS. Each distribution node is perturbed according to the perturb-and-observe approach, this perturbation is a power generator set as a constant active power output, allowing to evaluate the impact when a perturbation is occurred in every distribution node.

**4.3.1.3.1 Sensitivity results** The sensitivity coefficients are calculated based on the sum on the MV voltage system nodes when a perturbation is done in *X* node according to [Equation 30](#).

Top 3 sensitive buses have been identified according to the voltage sensitivity indices which are given in Table 4.4. It can be seen that bus 63 is the most sensitive bus with the highest value of the voltage sensitive indices.

Table 4.4: Voltage sensitive indices of the most sensitive buses.

| Bus No. | Bus name      | $\delta V/\delta P$ |
|---------|---------------|---------------------|
| 63      | Delta-coop    | 1.01876             |
| 64      | Chantelle     | 1.01626             |
| 65      | Saint Bernard | 1.01137             |

The sensitivity calculation results are illustrated in Figure 4.19. In this way, it is possible to determine not only how sensitive is the node perturbed, but also how the others nodes of the system are affected. It is also possible to notice how the sensitivity increases when a node is farther from the feeder point.

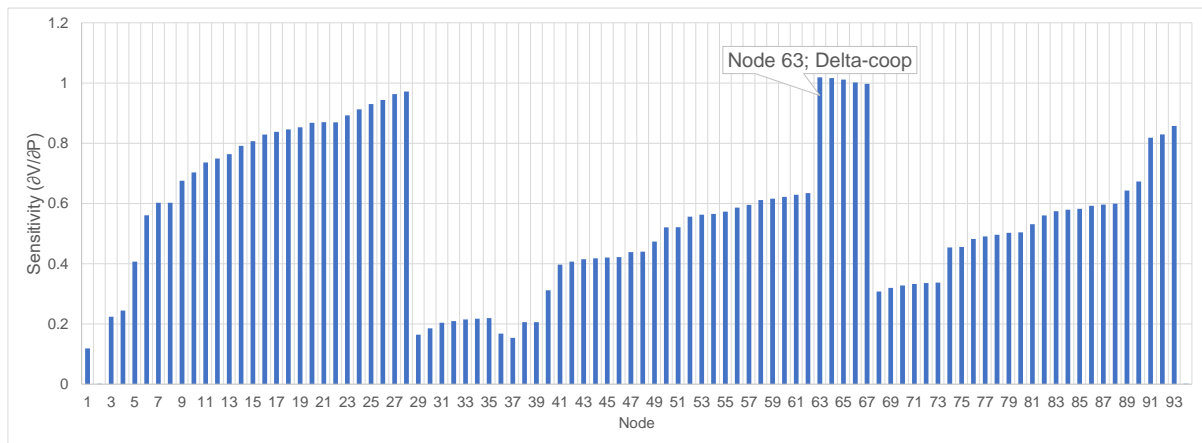


Figure 4.19: Sensitivity calculation results

**4.3.1.3.2 Interactive data visualization** To analyze massive results from different parallel simulations, it was added a visualization toolbox developed to the existing user interface of the Bank of Energy experimental platform. Basically, after all the simulations and post-processing steps are finished, the sensitivity coefficients are normalized to be represented in the user interface. Together a heat map graphic is deployed in the buses of the system, providing an comprehensible tool to analyze the sensitivity of the distribution system.

Figure 4.20 shows the sensitivity results represented in a heat map of all bus system. This visualization tool allows to identify easily the sensitive buses, as well as the sectors where the system is more sensitive. Hence, this scenario particularly shows a higher sensitivity in the buses located farther from the substation feeder. All other possible configurations and scenarios in the GoP distribution system can be evaluated.

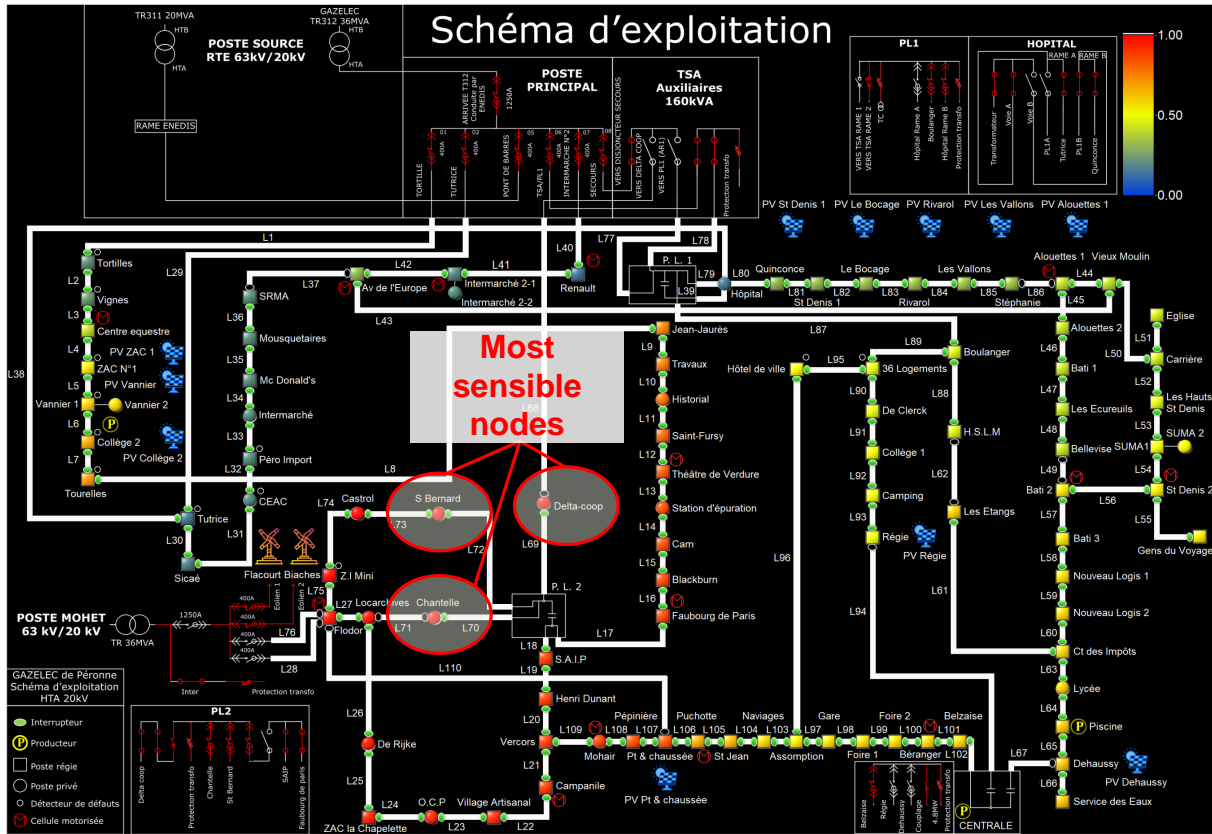


Figure 4.20: Sensitivity heat map visualization result in the Bank of Energy experimental platform marking the three most sensible buses.

#### 4.3.2 BESS sizing methodology for power distribution systems applying parallel computing

As explained in Chapter 3, different approaches are used for BESS sizing calculation. In this new methodology, the GA is chosen and implemented to cope with the complexity of the problem and compute a feasible BESS sizing value. This decision is done based on some researches that reveals the advantages of using GA over other evolutionary algorithm, demonstrating an effective function solution accuracy, reproducibility and a high speed performance (Roberge, Tarbouchi, and Labonte, 2013). Nevertheless, this methodology can be easily replaced by another algorithm.

Like the sensitive algorithm implementation, the GA is parallelized in order to achieve an improvement in the speedup and a fully exploitation of the power multi-core CPU of the experimental platform server, resulting in an effective tool capable to determine the size of the output power rating of the BESS, over a centralized or distributed installation in several nodes and under different system conditions.

##### 4.3.2.1 Parallel genetic algorithm (PGA)

The PGA is a distributed algorithm introduced in 1987 (Mühlenbein, 1996). The PGA is totally asynchronous, running especially efficient on parallel computers. Moreover, the PGA is a truly parallel algorithm which combines the hardware speed of parallel processors and the software

speed of intelligent parallel searching. It is based on multiple genetic algorithms on a parallel search by *individuals*, all of which have the same task problem description. For the PGA, the best individual of every *subpopulation* algorithm is selected, and after the best *individual* of the best *generation* is selected being the solution to a problem.

Figure 4.21 shows a general model of the PGA algorithm. In this model every *subpopulation* does not depend on each other, in consequence, it is possible to integrate them in a parallel execution, taking advantage of a multi-core CPU. Also, every *subpopulation* has a unique set of *individuals*, because they have different mutation/crossover operations. Finally, the best individual of each subpopulation will be evaluated to determine the best problem solution.

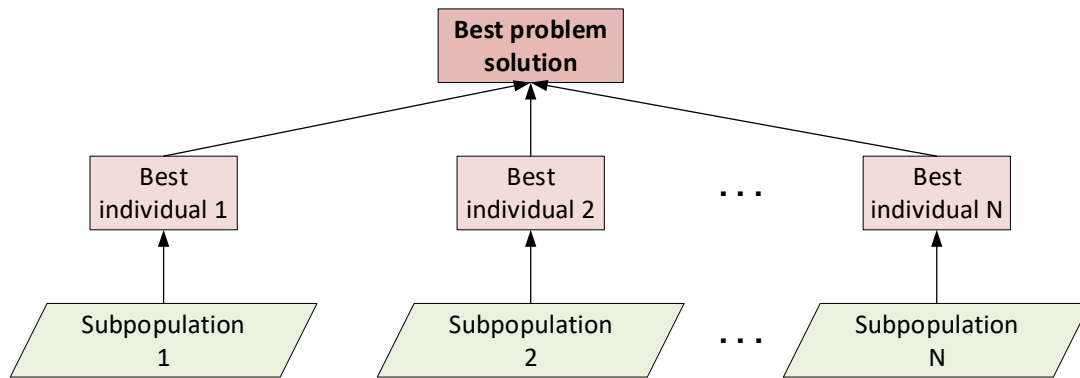


Figure 4.21: Parallel genetic algorithm.

The advantages of using PGA are the following (Umbarkar and Joshi, 2013):

- Improves the quality of the solutions
- Speedup the search strategy.
- Easy to integrate in a parallel architecture due to its asynchronism.
- Reduces the number of function evaluations.
- The algorithm uses a distributed selection schedule, it self-organizes itself.
- Explores the large populations size over the parallel platforms used for running the algorithms.
- It is able to solve multi-objective optimization problems.
- Solves the large scale, large dimensions problems with efficacy and efficiency
- High probability of achieving a global optimal solution in complex problems.
- Reduces the time to locate a solution

Now it is evident the advantages to use the PGA, however, despite the use of GA in BESS sizing problems, very little work has been done in mapping GA to an existing parallel environment. For example, in (Klansupar and Chaitusaney, 2020), evaluates the BESS size for compensating fluctuating generation of wind and solar using a single-core GA. In (Dinc and Otkur, 2020), a single-core GA based optimization study has been performed in order to find

the optimum battery size or capacity and the final drive ratio (FDR) for the given driving profiles of an electric vehicle. In (Ferreira, dos Santos, and César Rueda Medina, 2019), is proposed a sizing methodology to determine the quantity of BESS and super capacitors from a load profile to obtain maximum financial savings using a single-core GA. In (Salee and Wirasanti, 2018), is proposed the formulation of a problem that include the voltage support of BESS to the grid and the total network losses, using a single-core GA for preparing placement and sizing of BESS, as well as (Shahirinia et al., 2005), where a single-core GA approach is employed to find the optimal sizing of an hybrid power system with a battery bank.

4.3.2.1.1 *PGA classes* In Chapter 3 a review of the GA and its methodologies is done, however, the inclusion of parallel capabilities divides the GA into three general classes: master-slave, coarse-grained, and fine-grained (Nayak, Mishra, and Mohanty, 2017).

*Master-slave PGA* Master-slave PGA algorithm is the same as a simple GA but applying parallelization of the GA steps. The master executes the algorithm, controlling the slaves and distributing the tasks. The fitness function assessment is distributed among the slaves in the multi-core processors. The calculated fitness value is returned to the master to choose the best solution as shown in Figure 4.22.

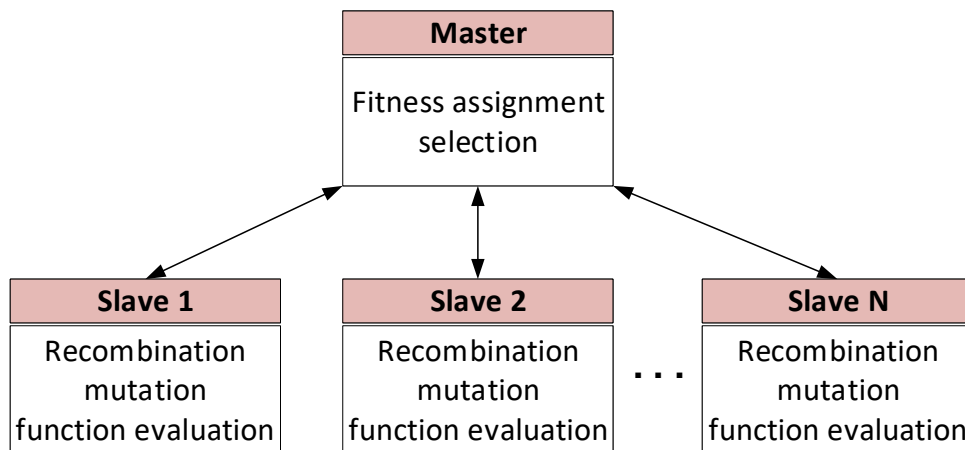


Figure 4.22: Master-Slave model (Nayak, Mishra, and Mohanty, 2017).

The slaves use the selection operation to choose the individuals that are going through crossover process as the entire population, it is known as *global parallel GA* (Johar et al., 2013).

Master-slave model has resulted in a raise of speed, scale and calculation power for GA, but some disadvantages considers the lack of performance in the synchronization between the slaves and the master.

*Coarse-grained PGA* The coarse-grained PGA divides the population into subpopulations which can be computed on separate processors. Each subpopulation is belonged to a processor and some individuals could be exchanged by migration operations. This model is know as *island model* or *distributed PGA* and the subpopulation called *deme* (Nayak, Mishra, and Mohanty, 2017).

Split the population in smaller portions is advantageous for a faster fitness calculation. But, the rapid rise of the fitness calculation stops at a lower fitness value, resulting in a low quality overall solution compared to the analysis with a single large population and a low migration rate between the individuals. The island model structure of the coarse-grained PGA is shown in Figure 4.23 demonstrating a faster solution than the master-slave model.

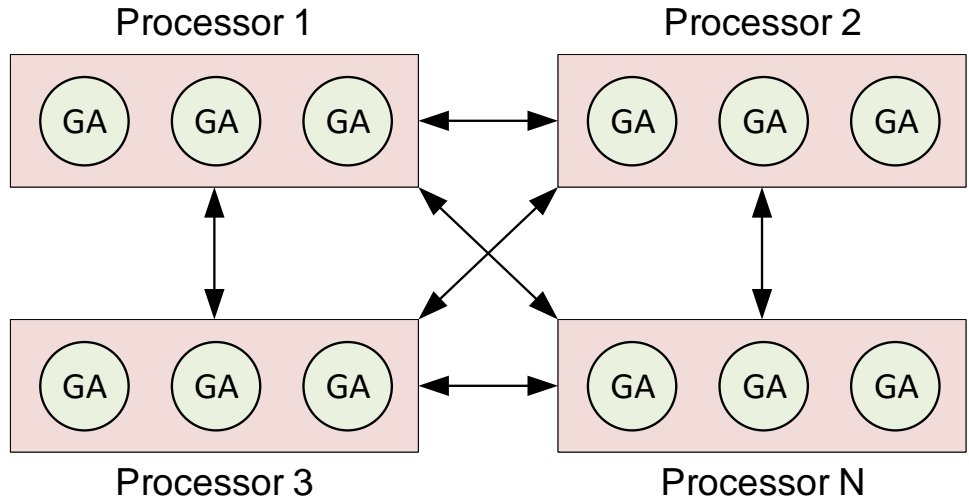


Figure 4.23: Coarse-grained parallel model (Johar et al., 2013).

*Fine-Grained PGA* As the coarse-grained PGA, the fine-grained PGA divides the population into very small subpopulations, which are maintained by different processors. It helps in maintaining better population diversity, keeping the best parallelism, therefore it improves the GA when dealing with high dimensional spaces (Johar et al., 2013). Due to its curb structure, the individuals has a direct contact with its neighbours as shown in Figure 4.24.

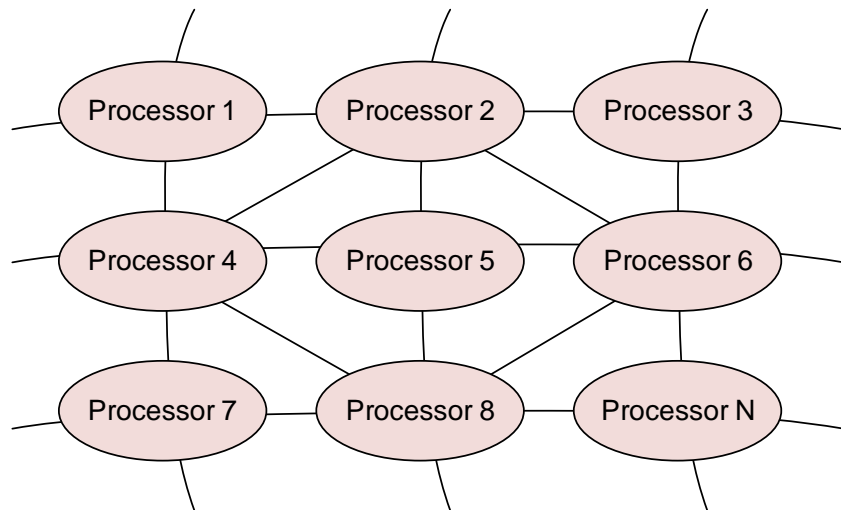


Figure 4.24: Fine-grained parallel model (Nayak, Mishra, and Mohanty, 2017).

In some cases these neighbours can be overlapping, nevertheless, the performance of this algorithm decreases when the size of the population increases. This model is suitable for massively parallel architectures, it means machines consisting of a huge number of basic processors and connected with a specific high speed topology. Most of the fine-grained PGA are used in multi-thread architectures or implemented on parallel processors, resulting in a good performance.

4.3.2.1.2 *PGA implementation* The proposed parallel evolutionary algorithm uses a master-slave GA parallelization. This decision is taken based on the results of the advantages using this model marked in the literature (Nayak, Mishra, and Mohanty, 2017; Sobuś and Woda, 2016; Johar et al., 2013; Wang, 2005). Also the easy architecture implementation, the size of the power distribution system, and the actor-oriented model used between OpenDSS and NI LabVIEW are key factors considered.

The sequence diagram of the PGA is illustrated in Figure 4.25, this model is comprised of only one population defined in the master processor. The master-slave PGA is built with one master and multiple core processors. The function of the master is allocating tasks to the

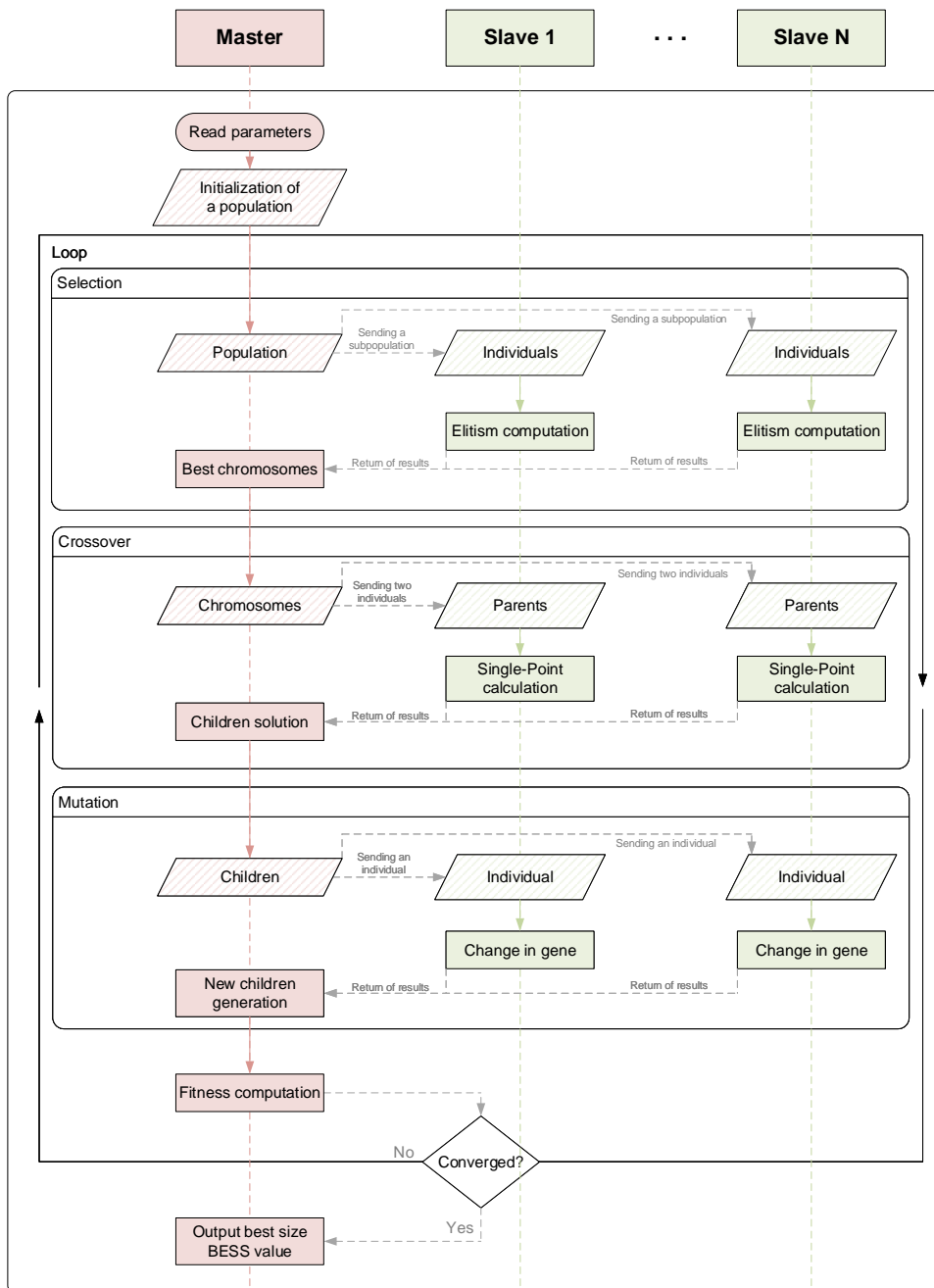


Figure 4.25: Sequence diagram of master-slave PGA.

slaves, collecting the results, and synchronizing the processes. In the other hand, the function of the slaves is to execute the genetic operations at each generation. The PGA is run in the workstation of the Bank of Energy experimental platform defined in [Chapter 2](#) to exploit its capabilities.

The PGA implementation is similar to the GA design, but it spreads the algorithm into several separate processors. The initial population is fixed in a low BESS power rating (kW) value. Subpopulations belongs to each slave processor, forming new individuals.

The first genetic operation is the elitism selection, which allows to find the best chromosome certainly with better ability and characteristics. Then, the best individual with the best fitness in this subset is chosen as the selected chromosome for crossover genetic operation. Single-point crossover is applied for two individuals called parents, so they are combined to produce other two individuals known as children. The children solutions are genetically affected by random mutations such addition, deletion, and modification of way-points. Finally, the parent generation is replaced by the children generation and the evolution cycle continues until the termination criteria has been met. The termination criteria corresponds to the maximum number of generations to be simulated or the no fulfillment of the constraints by the new generation.

In this implementation, the genetic evolution occurs synchronously maintaining a good level of collaboration between the subpopulation, and despite the lack of performance compared to other parallel implementations, this methodology has demonstrated a high quality and accuracy of the overall solution.

*Formal description of the PGA* According to (Mühlenbein, Schomisch, and Born, 1991), the PGA is a black-box solver which can be applied to the following class of problems:

$$\min \{f(x) \mid x \in X\}, \quad \text{where } X \subseteq \mathbb{R}^n, \quad f: \mathbb{R}^n \mapsto \mathbb{R}. \quad (31)$$

$$X = \{x \in \mathbb{R}^n \mid a_i \leq x_i \leq b_i, \quad i = 1, \dots, n\}, \quad \text{where } a_i \leq b_i, \quad i = 1, \dots, n. \quad (32)$$

It is possible to notice that  $f$  is not required to be differentiable, convex, continuous or unimodal. The PGA is initialized with a set (a population) of vectors (individuals). The phenotype of an individual is given by a real vector  $x$  with  $x \in X$ . The genotype of an individual is given by the bit representation  $y$  of  $x$  according to the floating point format of the workstation of the experimental platform.

A gene locus is a single bit position. The bits of the floating point representation define a chromosome. The genetic representation of an individual consists of a set of  $n$  chromosomes. In conclusion, the PGA is defined for a sizing BESS approach as:

$$\text{PGA} = (\mathbf{P}^0, \lambda, \mu, \Omega, \Gamma, \Delta) \quad (33)$$



where:

$\mathbf{P}^0$  = Initial population.

$\lambda$  = Number of subpopulations.

$\mu$  = Number of individuals of a subpopulation.

$\Omega$  = Selection operator.

$\Gamma$  = Crossing-over operator.

$\Delta$  = Mutation operator.

Each genetic operation is explained in [Chapter 3](#).

*The optimization problem* The optimization problem can be described as an optimal power flow. The goal of this optimization process is to find the optimal settings of a given power system network that optimizes the system fitness function such as total generation cost, emission of generating units, number of control actions, load shedding, system loss and bus voltage deviation, while satisfying its power equations, system security, and equipment operating limits ("[Sensitivity Calculation](#)" 2015).

Because the objective of the master problem is to find the suitable output power rating of the BESS in the GoP distribution system, two different approaches has been considered in the definition of the optimization problem according to the BESS functionalities.

*Voltage profile improvement*

$$\min VD = \sum_{i=1}^{ND} (1 - V_i)^2 \quad (34)$$

*Loss minimization*

$$\min P_L = \sum_{l=1}^{NL} P_l \quad (35)$$

where:

$VD$  = The total voltage deviation at load buses.

$V_i$  = The voltage value at load bus  $i$ .

$ND$  = The total number of load buses.

$P_L$  = The total system active power loss.

$P_l$  = The active power loss on line  $l$ .

$NL$  = The total number of lines.

[Equation 34](#) minimizes the voltage quadratic deviation at the nodes in the electrical network with regard to the desired voltage (1 p.u.), improving the voltage profile due to a BESS in-

stallation. Similarly, Equation 35 minimizes the total power losses of the distribution system when a BESS is installed, taking into account the losses of the line elements.

*Fitness function definition* From the optimization problem mentioned above, the PGA methodology is used to find the suitable power rating of the BESS. As a result, in Equation 36 the fitness value of the PGA is equal to the fitness function of the BESS application to be analyzed according to equations Equation 34 and Equation 35.

$$F_{PGA} = f(x) \quad (36)$$

*Optimization constraints*

$$x_i \leq E_{i_{max}}, \quad i \in ND \quad (37)$$

$$\sum_{i=1}^{ND} x_i = E_{max}, \quad i \in ND \quad (38)$$

$$V_{i_{min}} \leq V_i \leq V_{i_{max}}, \quad i \in ND \quad (39)$$

$$S_{L_j} \leq S_{L_{j_{max}}}, \quad j \in NL \quad (40)$$

$$P_l \leq k \cdot P_{l_{init}}, \quad l \in NL \quad (41)$$

where:

- $x_i$  = The power output rating of BESS allocated at the  $i$ -th bus.
- $E_{i_{max}}$  = The permissible power limit output rating at the  $i$ -th bus.
- $E_{max}$  = The permissible power total output rating of BESSs connected to the feeder.
- $V_{i_{max}}$  = The maximum voltage is 1.1 p.u..
- $V_{i_{min}}$  = The minimum voltage is 0.9 p.u..
- $S_{L_j}$  = The distribution line loadings.
- $S_{L_{j_{max}}}$  = The limit of distribution line loadings.
- $P_{l_{init}}$  = The initial power loss value at line  $l$ .
- $k$  = The percentage coefficient of line losses.

The subscripts *min* and *max* stand for the lower and upper bounds of a constraint respectively. The constraint 41 is applied only for the voltage profile optimization problem, avoiding to increase the line power losses in a certain  $k$  percentage after installing the BESS in the power grid.

**4.3.2.1.3 Single-core genetic algorithm** Before the PGA is implemented, a single-core GA is deployed to validate the optimization problem formulation. The flowchart of the single-core GA is shown in Figure 4.26.

The GA procedure is executed in multiple steps. First the initial system conditions are defined, choosing the number of batteries and setting their initial values and constraints. Then, the

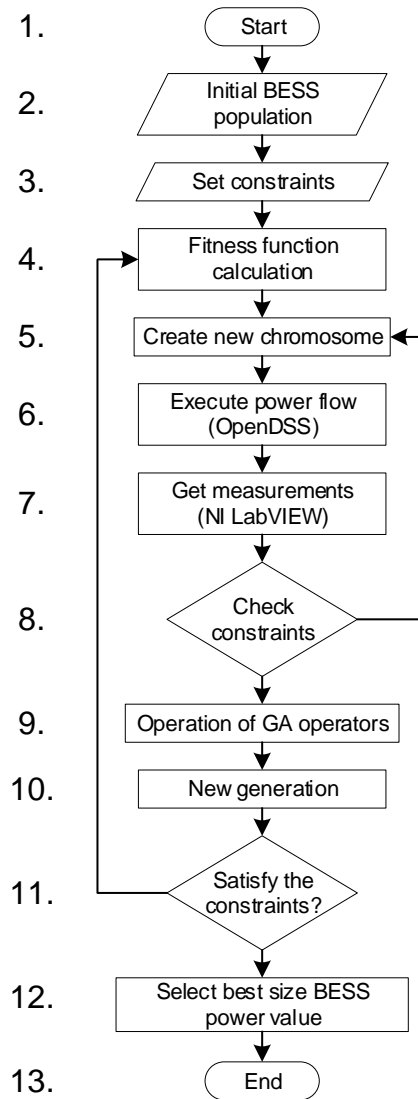


Figure 4.26: Flowchart of the single-core GA model.

fitness function is calculated for the parents generation. A new BESS chromosome is created and evaluated in the power distribution system, the co-simulation between OpenDSS and NI LabVIEW is done to review the optimization constraints.

After the constraints are validated, the GA operations are executed to determine a new generation. The algorithm is executed according to the termination criteria, finding at the end the best BESS output power rating installation for the distribution system.

#### 4.3.2.2 Test case study

The test case of [Section 4.3.1.2](#) was used to validate the optimization formulation using the single-core GA. According to the results obtained in [paragraph 4.3.1.2.1](#) from the sensitivity study, the most sensitive bus is the node  $b_4$  for this test case. Therefore, the test case system was evaluated under three conditions to validate the optimization formulation:

- The system without a BESS installation.
- The system with a BESS installation in the most sensitive bus improving the voltage profile.
- The system with a BESS installation in the most sensitive bus minimizing the system losses.

4.3.2.2.1 *Optimization results* Table 4.5 shows the results obtained after the evaluation of the three scenarios considered above. From the system without BESS, a voltage drop was encountered. A BESS is installed in the most sensitive node *b4*. The different BESS installation approaches are calculated without considering battery constraints 37 and 38, mainly to have a maximum effect in the improvement of the voltage profile and the minimization of the power losses regardless of a limit in the battery output power rating.

Table 4.5: Validation results of the optimization problem using the test case study.

|                          | Total active power, MW | Voltage range, p.u. | Total active power losses, MW | BESS output power rating, MW |
|--------------------------|------------------------|---------------------|-------------------------------|------------------------------|
| Without BESS             | 598.511                | 1-0.88              | 19.51                         | -                            |
| BESS for voltage profile | 103.257                | 1-0.929             | 10.25                         | 477                          |
| BESS for system losses   | 263.165                | 1-0.925             | 7.16                          | 314                          |

In both cases, when a BESS is installed, the voltage profile is corrected with a closed result indeed. In contrast, the active system losses are much smaller when a loss minimization approach is applied. Another effect of a BESS installation is a peak shaving in the total power consumption of the system. This test case study proves that the optimization problem can satisfy the fitness function in both approaches.

#### 4.3.2.3 *Real test case: A French distribution network*

After the optimization problem was validated, the GA is used over the French distribution network configuration shown in Section 4.3.1.3. In this case, the single-core GA and the PGA are deployed to compare the solution performance of both algorithms. Moreover, a BESS power installation is suggested according to the simulation results. For this purpose, a BESS is installed under two perspectives: centralized and decentralized localization considering the most sensitive buses found in the sensitivity analysis (see paragraph 4.3.1.3.1). The distribution system is analyzed considering the worst scenario of load chargeability (100%). Thus, the real test case system was evaluated under five case conditions:

- The system without a BESS installation.
- The system with a centralized BESS installation in the most sensitive bus improving the voltage profile.

- The system with a distributed BESS installation in the three most sensitive buses improving the voltage profile.
- The system with a centralized BESS installation in the most sensitive bus minimizing the system losses.
- The system with a distributed BESS installation in the three most sensitive buses minimizing the system losses.

Even if the sensitivity of the network nodes has been estimated for discharge only, the BESS evaluation of the size of the output power rating is done based on the charge and discharge state, assuring the compliance of the algorithm constraints for both cases of the BESS operation.

**4.3.2.3.1 Algorithm performance evaluation** As seen in [Equation 33](#), the PGA has many internal control parameters but it is not necessary to tune all these parameters for a specific function. The numerical results are obtained with a single set of parameters. This demonstrates the robustness of the search method applied.

Nevertheless, the performance evaluation of the PGA is a difficult task by itself. To do the evaluation, it is used as performance measure the average number of function evaluations to compute the optimum as well as the time needed to complete the computation. Then, these performance measurements are compared with the single-core GA to demonstrate the advantages to use this algorithm in a parallel architecture. [Table 4.6](#) shows the parameter set of each GA architecture.

Table 4.6: Architecture description of the GA tested.

|                                   | Classical GA | PGA          |
|-----------------------------------|--------------|--------------|
| # of populations                  | 1            | 1            |
| # of subpopulations ( $\lambda$ ) | 1            | 4, 8, 12, 22 |
| # of individuals ( $\mu$ )        | 50, 20       | 20           |
| Method of operation               | -            | Synchronous  |
| # of sync points                  | -            | many         |

The number of subpopulations and the number of individuals were modified to test the time needed to complete the computation and the optimum result accuracy of the algorithms respectively.

**4.3.2.3.2 Case study I: Real test case system without a BESS installation** The first analysis considers the GoP distribution system without any BESS installation. This analysis will help to compare the effects when a BESS is installed in the system. A power flow is performed and the results are shown in [Table 4.7](#).

According to the results obtained, despite this distribution system is balanced and the voltage range is inside the voltage limits, it is possible to integer a BESS to support the weak nodes

Table 4.7: Power flow results for the real test case study without a BESS.

| Total active power, MW | Voltage range, p.u. | Total active power losses, MW |
|------------------------|---------------------|-------------------------------|
| 24.99                  | 1-0.94              | 0.438                         |

and to reduce the power losses of the system. This evaluation is done under the condition of maximum load chargeability (100%), because of that the total active power is too high.

The voltage profile of the whole system is shown in Figure 4.27. The drop in the voltage level is caused mainly by the existing losses between the distance in the lines with regard to the feeder. The nodes with the lowest voltage value correspond to the furthest nodes with regard to the substation.

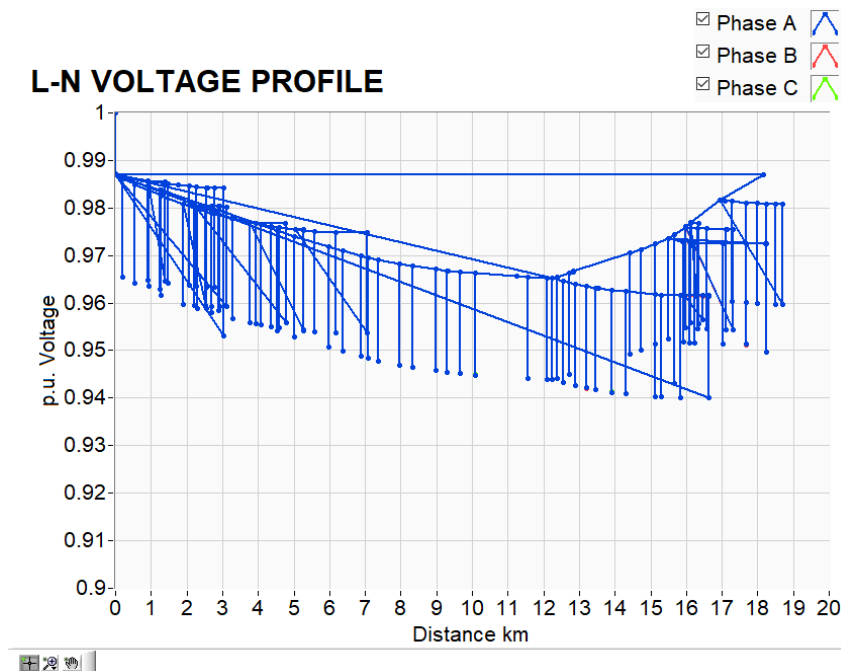


Figure 4.27: Voltage profile of GoP distribution system.

4.3.2.3.3 *Case study II: Centralized placement of BESS at the most sensitive bus for voltage profile improvement* In this case, a centralized BESS has been placed at the bus *Delta-coop* which is the most voltage sensitive bus for this system configuration according to the sensitivity results found in paragraph 4.3.1.3.1. A voltage profile improvement is the approach used in this study.

*GoP distribution system results* After deploying the PGA over the GoP distribution system, the suitable BESS installation calculated is 6.9MW. The results are presented in Table 4.8, considering the charge/discharge states of the BESS.

When the BESS is charging, the power flow analysis reveals that the system continues operating under the safe working limits. Furthermore when the BESS is discharging, the results

Table 4.8: Power flow results for a centralized BESS in the case study II.

| # BESS | Bus installation | BESS cap., MW | State     | Real distribution test system |                     |                               |
|--------|------------------|---------------|-----------|-------------------------------|---------------------|-------------------------------|
|        |                  |               |           | Total active power, MW        | Voltage range, p.u. | Total active power losses, MW |
| 1      | Delta-coop       | 6.9           | Charge    | 32.09                         | 1 - 0.9             | 1.049                         |
| 1      | Delta-coop       | 6.9           | Discharge | 17.97                         | 1 - 0.949           | 0.313                         |

show an improvement in the voltage profile of  $1 - 0.949$  p.u., the total active power consumed by the system is reduced to 17.97 MW, and the total active power losses are reduced as well to 0.313 MW. The voltage profile of the distribution system in both BESS states functioning are shown in Figure 4.28.

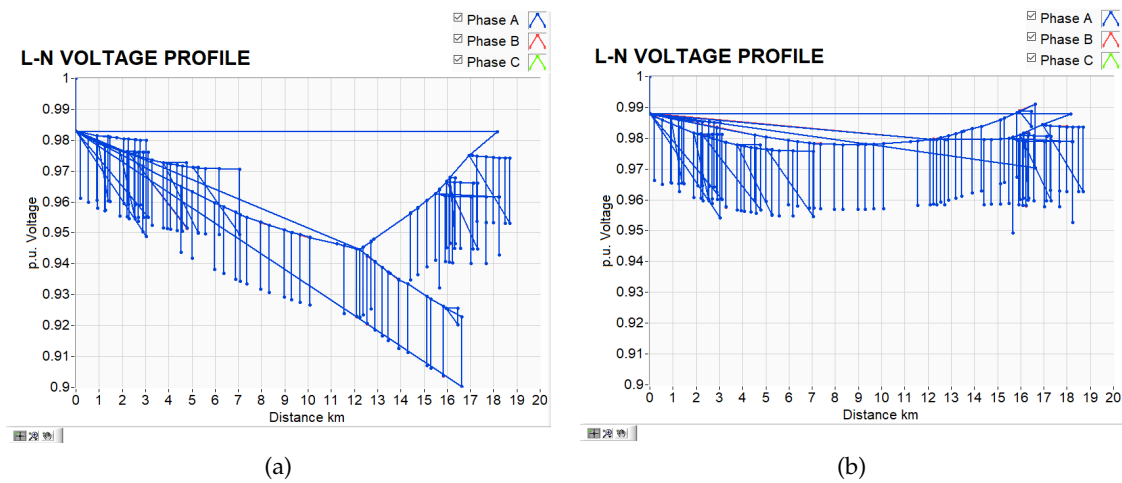


Figure 4.28: Voltage profile with a centralized BESS for voltage improvement: (a) Charging. (b) Discharging.

*GA performance* As mentioned earlier, the algorithm performance is evaluated based on the average number of function evaluations to compute the optimum and the time needed to complete the computation task. The variables modified to assess the performance are the number of subpopulations and the number of individuals. The results obtained are listed in Table 4.9. The average is based on 10 runs.

In the first two rows the results of the single-core GA are presented, proving that the variation in the number of *individuals* does not have a big impact in the accuracy of the fitness function evaluation. Meanwhile, the number of iterations is reduced significantly and consequently, the computation time is lower when the number of *individuals* is reduced indeed.

Furthermore, the PGA is tested modifying the number of subpopulations. The results demonstrate a great improvement in the reduction of the computation time, the improvement is considerable when  $\lambda = 4$ . However, the increase in the number of subpopulations, and there-

Table 4.9: GA performance in the case study II.

| Methodology    | $\lambda$ | $\mu$ | Iterations | Best       |            | Worst      |            | Average    |            |
|----------------|-----------|-------|------------|------------|------------|------------|------------|------------|------------|
|                |           |       |            | Time,<br>s | $f_{eval}$ | Time,<br>s | $f_{eval}$ | Time,<br>s | $f_{eval}$ |
| Single-core GA | 1         | 50    | 1080       | 10.98      | 1.02221    | 11.04      | 1.02221    | 11.007     | 1.02221    |
| Single-core GA | 1         | 20    | 542        | 5.53       | 1.02217    | 5.55       | 1.02217    | 5.54       | 1.02217    |
| PGA            | 4         | 20    | 241        | 2.46       | 1.02217    | 2.51       | 1.02217    | 2.48       | 1.02217    |
| PGA            | 8         | 20    | 189        | 1.96       | 1.02217    | 1.99       | 1.02217    | 1.98       | 1.02217    |
| PGA            | 12        | 20    | 182        | 1.893      | 1.02217    | 1.899      | 1.02217    | 1.896      | 1.02217    |
| PGA            | 22        | 20    | 177        | 1.853      | 1.02217    | 1.877      | 1.02217    | 1.864      | 1.02217    |

fore in the number of core-processors, does not reveal a huge difference in the improvement of the computation time when these parameters are too high.

4.3.2.3.4 *Case study III: Distributed placement of BESS at the most three sensitive buses for voltage profile improvement* In this case, a decentralized BESS has been placed at the most three sensitive buses for this system configuration. A voltage profile improvement is the approach used in this study.

*GoP distribution system results* After deploying the PGA over the GoP distribution system, the suitable BESS installations determined for each bus are: *Delta-coop* = 2.5 MW, *Chantelle* = 2.4 MW and *Saint Bernard* = 2.4 MW. The output power rating values calculated are close between every BESS balancing the voltage support in every installation node. The results are presented in [Table 4.10](#), considering the charge/discharge states of the BESSs.

Table 4.10: Power flow results for distributed BESS in the case study III.

| # BESS | Bus installation | BESS power rating, MW | State     | Real distribution test system |                     |                               |
|--------|------------------|-----------------------|-----------|-------------------------------|---------------------|-------------------------------|
|        |                  |                       |           | Total active power, MW        | Voltage range, p.u. | Total active power losses, MW |
| 3      | Delta-coop       | 2.5                   | Charge    | 32.5                          | 1 - 0.9             | 1.08                          |
|        | Chantelle        | 2.4                   |           |                               |                     |                               |
|        | Saint Bernard    | 2.4                   |           |                               |                     |                               |
| 3      | Delta-coop       | 2.5                   | Discharge | 17.55                         | 1 - 0.949           | 0.301                         |
|        | Chantelle        | 2.4                   |           |                               |                     |                               |
|        | Saint Bernard    | 2.4                   |           |                               |                     |                               |

For the BESSs charging state, the system is within the fixed constraint limits. In the other hand for the BESSs discharging state, the system presents a slight improvement with respect to a



centralized installation. Despite the voltage range in the system is almost the same compared to a centralized BESS installation (see Figure 4.29). With a decentralized BESSs installation, the total active power consumption and the total active power losses of the system are a bit lower.

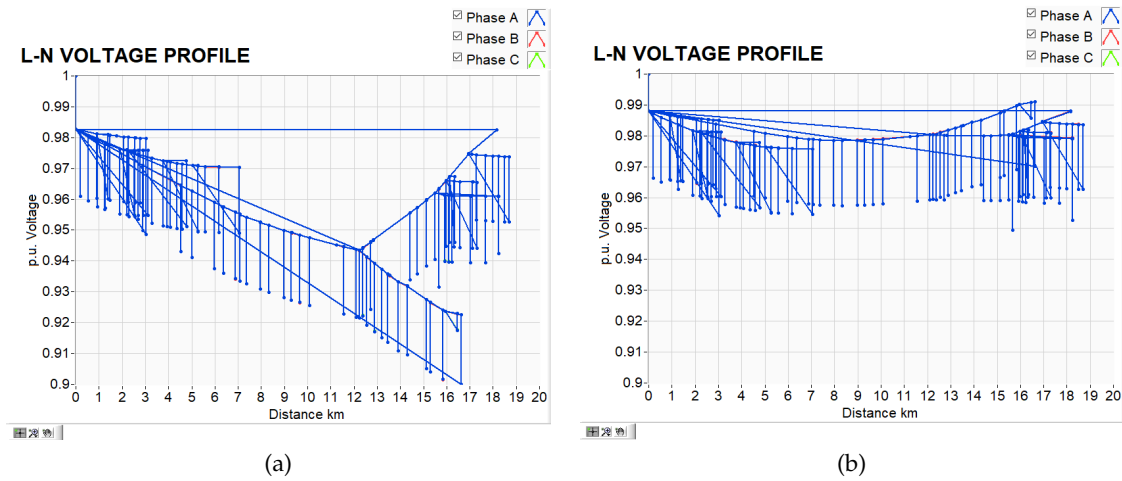


Figure 4.29: Voltage profile with decentralized BESSs for voltage improvement: (a) Charging. (b) Discharging.

*GA performance* The results obtained are listed in Table 4.11. The fitness evaluation for this scenario is a bit lower compared to a centralized installation. The computation time decreases when a PGA methodology is applied, but the results also reveal that the use of a big quantity of core-processors does not improve the performance when  $\lambda > 12$ .

Table 4.11: GA performance in the case study III.

| Methodology    | $\lambda$ | $\mu$ | Iterations | Best       |            | Worst      |            | Average    |            |
|----------------|-----------|-------|------------|------------|------------|------------|------------|------------|------------|
|                |           |       |            | Time,<br>s | $f_{eval}$ | Time,<br>s | $f_{eval}$ | Time,<br>s | $f_{eval}$ |
| Single-core GA | 1         | 50    | 1134       | 11.55      | 1.02135    | 11.61      | 1.02135    | 11.594     | 1.02135    |
| Single-core GA | 1         | 20    | 570        | 5.8        | 1.02132    | 5.83       | 1.02132    | 5.81       | 1.02132    |
| PGA            | 4         | 20    | 183        | 1.91       | 1.02132    | 1.94       | 1.02132    | 1.93       | 1.02132    |
| PGA            | 8         | 20    | 127        | 1.34       | 1.02131    | 1.36       | 1.02131    | 1.35       | 1.02131    |
| PGA            | 12        | 20    | 90         | 0.974      | 1.02133    | 0.99       | 1.02133    | 0.982      | 1.02133    |
| PGA            | 22        | 20    | 79         | 0.978      | 1.02133    | 1.032      | 1.02133    | 1.008      | 1.02133    |

4.3.2.3.5 *Case study IV: Centralized placement of BESS at the most sensitive bus for loss minimization* In this case, a centralized BESS has been placed at the bus *Delta-coop* which is the most voltage sensitive bus for this system configuration. A power loss minimization is the approach used in this study.

*GoP distribution system results* After run the PGA methodology over the GoP distribution system, the suitable BESS installation calculated is 5.6 MW. The results are presented in [Table 4.12](#), considering the charge/discharge states of the BESS installation.

Table 4.12: Power flow results for a centralized BESS in the case study IV.

| # BESS | Bus installation | BESS power rating, MW | State     | Real distribution test system |                     |                               |
|--------|------------------|-----------------------|-----------|-------------------------------|---------------------|-------------------------------|
|        |                  |                       |           | Total active power, MW        | Voltage range, p.u. | Total active power losses, MW |
| 1      | Delta-coop       | 5.6                   | Charge    | 30.8                          | 1 - 0.907           | 0.903                         |
| 1      | Delta-coop       | 5.6                   | Discharge | 19.25                         | 1 - 0.947           | 0.304                         |

Differently to the voltage improvement approach, the loss minimization algorithm has determined a lower BESS output power rating value. Moreover, the voltage range obtained is almost the same (see [Figure 4.30](#)) and the system losses are better for this approach. This could be determinant for a BESS output power rating choice considering an economical and technical perspective, because the price of a smaller BESS with an enhanced performance.

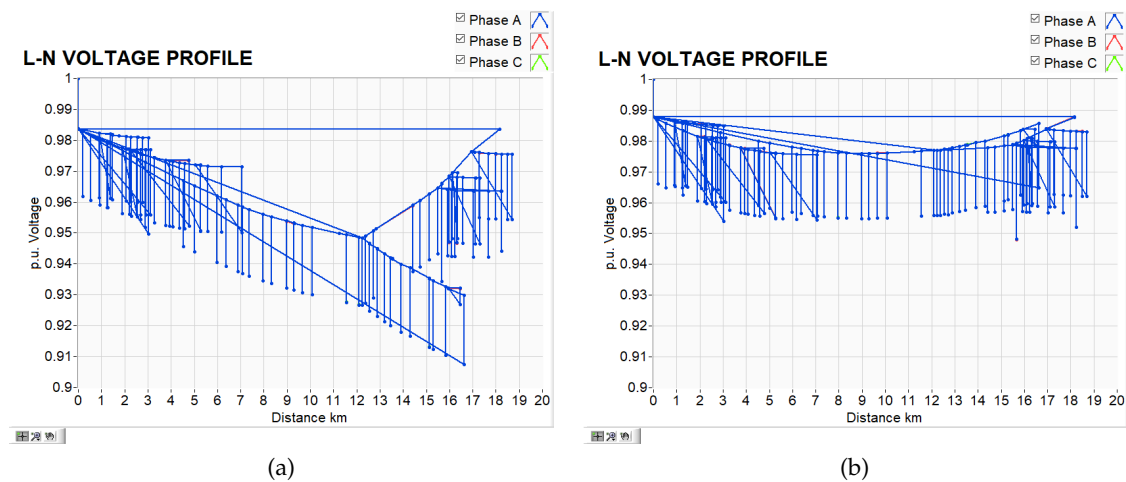


Figure 4.30: Voltage profile with a centralized BESS for loss minimization: (a) Charging. (b) Discharging.

*GA performance* The results obtained are listed in [Table 4.13](#). The fitness evaluation resulted for this scenario is different considering the loss minimization approach applied to the distribution system. The computation time of this algorithm to find a global minimum is lower than the voltage profile improvement approach, it demonstrates that the solution of the PGA is faster enough for a decision-making tool.

**4.3.2.3.6 Case study V: Distributed placement of BESS at the most three sensitive buses for loss minimization** In this case, a decentralized BESS has been placed at the most three sensitive buses for this system configuration. A power loss minimization is the approach used in this study.

Table 4.13: GA performance in the case study IV.

| Methodology    | $\lambda$ | $\mu$ | Iterations | Best      |            | Worst     |            | Average   |            |
|----------------|-----------|-------|------------|-----------|------------|-----------|------------|-----------|------------|
|                |           |       |            | Time, $s$ | $f_{eval}$ | Time, $s$ | $f_{eval}$ | Time, $s$ | $f_{eval}$ |
| Single-core GA | 1         | 50    | 450        | 4.501     | 0.311      | 4.53      | 0.311      | 4.525     | 0.311      |
| Single-core GA | 1         | 20    | 226        | 2.24      | 0.311      | 2.26      | 0.311      | 2.225     | 0.311      |
| PGA            | 4         | 20    | 100        | 0.984     | 0.311      | 1.09      | 0.311      | 1.028     | 0.311      |
| PGA            | 8         | 20    | 80         | 0.775     | 0.311      | 0.782     | 0.311      | 0.777     | 0.311      |
| PGA            | 12        | 20    | 77         | 0.759     | 0.311      | 0.775     | 0.311      | 0.765     | 0.311      |
| PGA            | 22        | 20    | 79         | 0.778     | 0.311      | 0.790     | 0.311      | 0.782     | 0.311      |

*GoP distribution system results* After deploying the PGA over the GoP distribution system, the suitable BESSs installations determined for each bus are: *Delta-coop* = 2 MW, *Chantelle* = 2 MW and *Saint Bernard* = 2 MW. The results are presented in Table 4.14, considering the charge/discharge states of the BESSs.

Table 4.14: Power flow results for distributed BESS in the case study V.

| # BESS | Bus installation | BESS power rating, MW | State     | Real distribution test system |                     |                               |
|--------|------------------|-----------------------|-----------|-------------------------------|---------------------|-------------------------------|
|        |                  |                       |           | Total active power, MW        | Voltage range, p.u. | Total active power losses, MW |
| 3      | Delta-coop       | 2                     | Charge    | 31.22                         | 1 - 0.906           | 0.93                          |
|        | Chantelle        | 2                     |           |                               |                     |                               |
|        | St Bernard       | 2                     |           |                               |                     |                               |
| 3      | Delta-coop       | 2                     | Discharge | 18.84                         | 1 - 0.948           | 0.294                         |
|        | Chantelle        | 2                     |           |                               |                     |                               |
|        | St Bernard       | 2                     |           |                               |                     |                               |

The decentralized loss minimization approach results in an affordable option, taking into account its effectiveness reducing the total power losses of the system, regulating the total power consumption and balancing the voltage profile in both BESSs states as seen in Figure 4.31.

*GA performance* The results obtained are listed in Table 4.15. This test case scenario has resulted in the lowest computing time solution of the PGA, followed by the lowest fitness function ( $f_{eval}$ ) for the loss minimization approach. The number of iterations has been reduced significantly compared to the other test case scenarios. There is a notable improvement when the PGA is implemented over a single-core GA methodology.

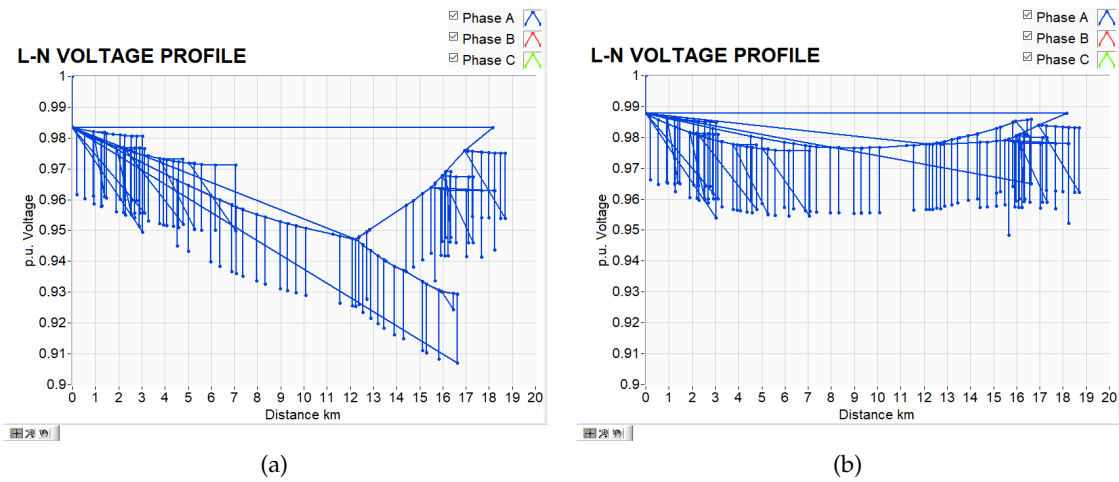


Figure 4.31: Voltage profile with decentralized BESSs for loss minimization: (a) Charging. (b) Discharging.

Table 4.15: GA performance in the case study V.

| Methodology    | $\lambda$ | $\mu$ | Iterations | Best       |            | Worst      |            | Average    |            |
|----------------|-----------|-------|------------|------------|------------|------------|------------|------------|------------|
|                |           |       |            | Time,<br>s | $f_{eval}$ | Time,<br>s | $f_{eval}$ | Time,<br>s | $f_{eval}$ |
| Single-core GA | 1         | 50    | 462        | 4.621      | 0.311      | 4.64       | 0.311      | 4.63       | 0.311      |
| Single-core GA | 1         | 20    | 234        | 2.330      | 0.301      | 2.339      | 0.301      | 2.33       | 0.301      |
| PGA            | 4         | 20    | 83         | 0.813      | 0.301      | 0.833      | 0.301      | 0.819      | 0.301      |
| PGA            | 8         | 20    | 63         | 0.596      | 0.301      | 0.653      | 0.301      | 0.628      | 0.301      |
| PGA            | 12        | 20    | 48         | 0.461      | 0.301      | 0.491      | 0.301      | 0.474      | 0.301      |
| PGA            | 22        | 20    | 49         | 0.514      | 0.301      | 0.558      | 0.301      | 0.535      | 0.301      |

4.3.2.3.7 *Results analysis* After completing the evaluation of the test case scenarios, some analysis could be done based on the algorithm methodology developed and the BESS results obtained. Moreover, a toolkit panel is presented for the experimental platform.

*PGA performance results* In order to evaluate the PGA performance capability, the speedup factor was calculated considering the algorithm performance results obtained for each test case study. The performance formula is given by Equation 42 (Harmanani, 2020).

$$S_p = T_1/T_p \quad (42)$$

where:

$S_p$  = The speedup factor.

$T_1$  = The execution time on a single processor.

$T_p$  = The execution time on a  $p$  processor system.

Despite the difficulty in the measurement of the speedup of the PGA due mainly of the probabilistic nature of the algorithm, the speedup factor demonstrates a general improvement in the use of a parallel architecture. The speedup factor results are shown in Figure 4.32.

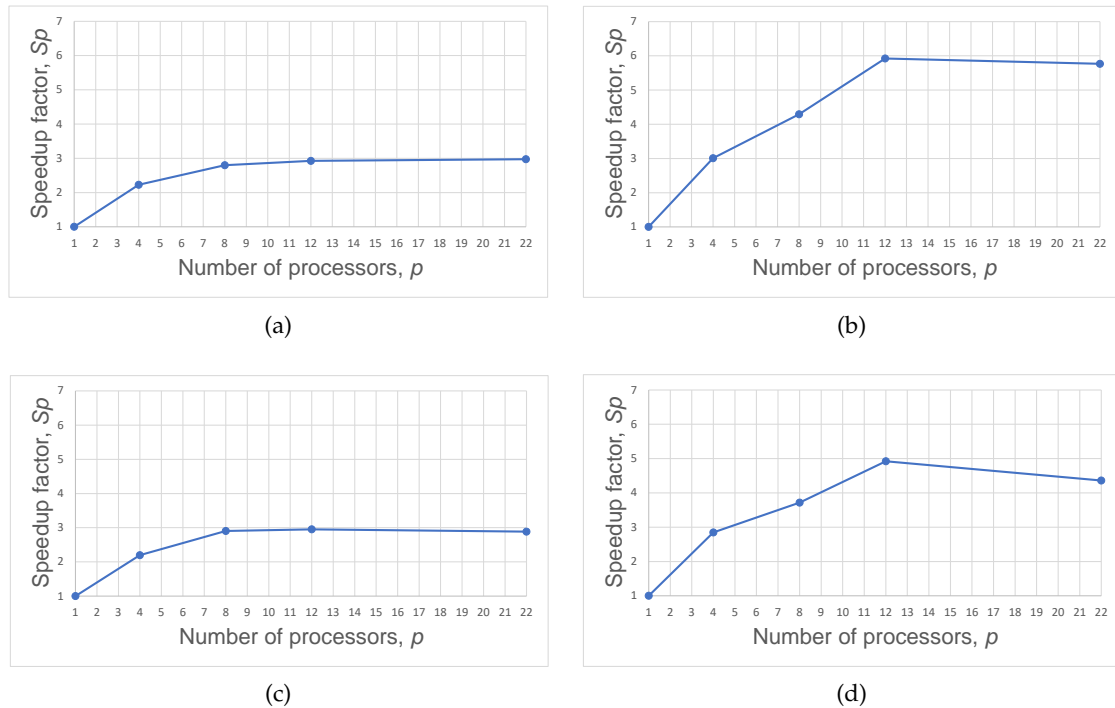


Figure 4.32: Speedup factor calculated to evaluate the PGA performance: (a) Case study II. (b) Case study III. (c) Case study IV. (d) Case study V.

In all runs the global minimum has been found to at least three digits of accuracy. The computing time needed and the number of iterations for a run was calculated between starting the computation task and arriving of the minimum function value.

According to the results obtained, the global minimum is computed faster on four processors for all test case studies. The speedup is in average 2.54 for four processors. Figure 4.32a and Figure 4.32c show the results when a centralized BESS is installed for each optimal power flow approach, it is noticed the speedup factor is not very effective for several processors; whereas Figure 4.32b and Figure 4.32d show the speedup results for a decentralized BESS installation in both approaches, revealing a largest speedup factor for almost all processors which were used. This behavior is typical for small problems, the use of more core-processors could be useful when the search space will be larger and complex.

Both optimization approaches so far have been solved efficiently by a small number of processor. However, the optimization problem seems to be small for this PGA methodology, it

could work efficiently when the distribution system results more complex and the number of parameters to be considered may increase.

*GoP distribution system results* The optimal BESS sizing results based on the different study cases using the two optimization approaches and the solution aforementioned are shown in [Table 4.16](#) and [Table 4.17](#).

Table 4.16: Optimal BESS sizing results with a charging installation.

| Case study | Optimal sizing of BESS                                              | System results when BESS is charging |                     |                               |
|------------|---------------------------------------------------------------------|--------------------------------------|---------------------|-------------------------------|
|            |                                                                     | Total active power, MW               | Voltage range, p.u. | Total active power losses, MW |
| I          | No BESS                                                             | 24.99                                | 1-0.94              | 0.438                         |
| II         | Delta-coop (6.9 MW)                                                 | 32.09                                | 1-0.9               | 1.049                         |
| III        | Delta-coop (2.5 MW)<br>Chantelle (2.4 MW)<br>Saint Bernard (2.4 MW) | 32.5                                 | 1-0.9               | 1.08                          |
| IV         | Delta-coop (5.6 MW)                                                 | 30.8                                 | 1-0.907             | 0.903                         |
| V          | Delta-coop (2 MW)<br>Chantelle (2 MW)<br>Saint Bernard (2 MW)       | 31.22                                | 1-0.906             | 0.93                          |

Table 4.17: Optimal BESS sizing results with a discharging installation.

| Case study | Optimal sizing of BESS                                              | System results when BESS is discharging |                     |                               |
|------------|---------------------------------------------------------------------|-----------------------------------------|---------------------|-------------------------------|
|            |                                                                     | Total active power, MW                  | Voltage range, p.u. | Total active power losses, MW |
| I          | No BESS                                                             | 24.99                                   | 1-0.94              | 0.438                         |
| II         | Delta-coop (6.9 MW)                                                 | 17.97                                   | 1-0.949             | 0.313                         |
| III        | Delta-coop (2.5 MW)<br>Chantelle (2.4 MW)<br>Saint Bernard (2.4 MW) | 17.55                                   | 1-0.9494            | 0.301                         |
| IV         | Delta-coop (5.6 MW)                                                 | 19.25                                   | 1-0.947             | 0.304                         |
| V          | Delta-coop (2 MW)<br>Chantelle (2 MW)<br>Saint Bernard (2 MW)       | 18.84                                   | 1-0.948             | 0.294                         |

As can be seen in [Table 4.16](#), the system measurements are within the constraint limits for all scenarios when a BESS installation is charging. In the other hand, [Table 4.17](#) shows a greatly system improvement by a BESS installation compared with non-BESS.

The loss minimization approach shows a slight improvement in the system results compared with the voltage profile improvement approach. A smaller BESS sizing is also needed with a loss minimization approach for a centralized and a decentralized BESS installation.

A decentralized BESS installation in the discharging state reveals the minimum fitness function value for both optimization approaches. In contrast, a centralized BESS installation exposes a better system performance for a charging state.

The system results shows that BESS can significantly introduce great benefits to the distribution system operation providing peak shaving, improving the voltage profile and an active power losses reduction. Moreover, the different optimal BESS test scenarios schemes with different BESS installations illustrate that the solution for optimal BESS sizing proposed can provide planners flexibility according to the system needs.

*User data visualization panel* A new toolkit panel is integrated in the software layer of the experimental platform. [Figure 4.33](#) shows the data visualization panel designed after simulated the case study II of [paragraph 4.3.2.3.3](#). This panel places a heavy emphasis on simple and analytical examination state of the distribution system, providing an infrastructure for integrate a BESS solution based upon these values.

The panel has two buttons, the first button is intended for obtain the network sensitivities, particularly, inter-bus network voltage sensitivities to changes in  $P$ . The results are published in the list box, ordered from the most sensitive bus until the less sensitive.

The user has the option to check the buses where is desirable to install a BESS system, furthermore, the user has the possibility to check as many buses as BESS installation are desired to test in a random order.

A second button is intended to execute the BESS sizing PGA, solving the optimization problem and printing the BESS output power rating result in a label layout. Two led indicators are below to each button to inform the user the completion of the algorithm execution. The total active power consumption and the total active power losses are compared in the distribution system between without/with BESS installation.

#### 4.4 OTHER FUTURE APPLICATIONS

The methodology developed has resulted in an effective solution for the BESS placement and sizing problem. Nevertheless, this problem does not require in all situations a RT solution based in a faster computation response, but, it has allowed to evaluate the robustness of the experimental platform.

In consequence, further applications can be considered to exploit the complete computational capacity of the experimental platform and the parallel efficacy of the methodology proposed which could include:

- **Placement and sizing of distributed generation:** The inclusion of DERs could be analyzed using the methodology developed. Sensitivity analysis provides a straightforward

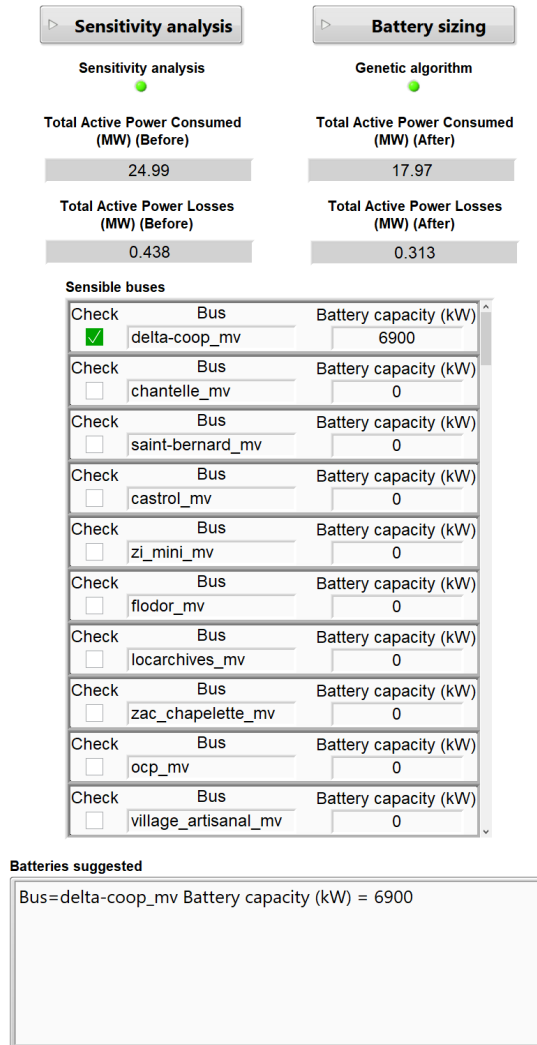


Figure 4.33: User data visualization panel of the toolkit developed.

first pass to evaluate the impact of these technologies, and to determine the suitable locations at which such technologies could provide an improved voltage support or an enhanced power consumption. The PGA technique could be used to determine the size of these technologies according to the needs.

- **Site selection for electric vehicles charging stations:** The parallel sensitivity analysis is appropriated to determine an optimal placement for the electric vehicles stations. Moreover, a PGA methodology can be useful to minimize the impact of the charging points in the distribution system.
- **Placement and control strategies of reactive power management devices:** The voltage support based on reactive power devices can be analyzed considering this novel methodology. The placement of these elements such as capacitor-banks, can be easily determined for maximum effect using the parallel sensitivity analysis technique, and control strategies can be optimized using the PGA prioritising the locations with a higher sensitivity.



- **Adjustment of local voltage controllers:** Intelligent voltage management strategies will be increasingly required as electrical networks evolve. The parallel sensitivity analysis can reinforce the speed to determine the correct adjustment of local controllers in the distribution networks. Its effective time calculation can proportionate the performance required in RT distribution system for monitoring and supervision applications.

Further, this new methodology based on parallel computing are highly extensible. The combination between the sensitivity analysis and an evolutionary algorithm lends itself to application to other.

The techniques presented become suitable for RT network control scenarios including hardware devices into the analysis. The changes in the network loading requires that the system be re-calculated periodically. As described in this chapter, the processing time could be significantly reduced using a multi-threading approach.

#### 4.5 CHAPTER SUMMARY

This chapter has presented a novel methodology for BESS placement and power sizing using parallel computing. This methodology is based on two algorithms, the parallel sensitivity analysis and the PGA to attack the complexity and produce solutions in a relatively short computation time.

Both algorithms were evaluated under a test case and a real case scenario, moreover, the PGA algorithm is assessed in two different optimization approaches. The results reveals that the use of a multi-threaded approach reduce the execution time to find an accurate answer for BESS location and output power rating.

The sensitivity analysis based on the perturb-and-observe method has resulted in an effective algorithm to find the weakness buses of the system regarding the load charging and network configuration.

PGA has demonstrated to be an effective technique to solve the optimal power flow problem, resolving the different approaches proposed with a notable convergence in an efficient computing time.

The actual fitness function considers two approaches based on the optimal power flow, the operating limits of the BESS are included as a constraints of the optimization problem. In consequence, the optimal power rating sizing formulation have to evolve to a multi-objective nonlinear integer programming problem, where it is not only considered the actual system approaches but new approaches in terms of the charge and discharge of the BESS could be added. A new schema based on the weight factors could be proposed to provide the necessary flexibility to adjust the different approaches according to the planner preferences.

An energy management system of the BESS is the next step to be integrated into the system. For this purpose, a new methodology have to be developed to determine the energy capacity of the BESS in a long-term analysis, as well as, the optimization of the number of charge/discharge cycles according to the system needs.



## GENERAL CONCLUSIONS AND PROSPECTS

---

The work reported in the present thesis covers the subject concerning the supervision, analysis and optimization of power distribution systems considering the penetration of distributed energy resources and energy storage systems. Advanced knowledge regarding condition and smart grid monitoring were required in order to allow a comprehensive understanding of the challenges that must be fulfilled for ensuring the supervision and analysis of the distribution networks. As a result, [Chapter 1](#) provides a comprehensive survey on the state of the art of the different methodologies, tools and challenges necessary to apply these concepts into distribution systems.

The experimental platform belonged to the Bank of Energy concept has been presented in [Chapter 2](#). This is a supervision platform developed in the frame of this work that aims to study and analyze different electrical phenomena in the power distribution systems, it includes the introduction of renewable energy and battery energy storage systems. The experimental platform is based in a hardware and software architecture capable to perform real-time simulations to replicate the smart grid systems with high fidelity. All together allows to supervise and evaluate the energy consumption and grid condition towards an optimized energy transition.

The experimental platform uses a well designed software architecture to guarantee a real-time supervision process. Moreover, this architecture exploits the parallel computing capacity of the equipment installed assuring the scalability in the addition of novel applications and equipment. However, the performance of the system analysis depends on the complexity of the distribution system and the number of physical cores available; so, it is expected to evaluate the experimental platform with real large-scale systems to determine its maximum efficiency.

Because the power system modeled is a real French distribution network with distributed generation composed of two wind farms and multiple photovoltaic panels installed along the grid, a study is performed to evaluate and determine the suitable integration of battery energy storage systems into the grid. For this purpose, in [Chapter 3](#) the different aspects of the integration of these elements in distribution networks is presented. It includes applications, benefits and possible impacts to consider at the moment to incorporate them in a distribution system. It has been shown that the battery storage system has the potential to strengthen and improve the electrical grid in several aspects such as frequency and voltage stability, renewable energies management, energy peak shaving, among others.

A comprehensive background is also done to know the existing methodologies to locate and size the battery energy storage systems. Most of these methodologies are applied in medium voltage distribution systems. The complexity of these methods varies depending on the approach taken, and they are continuously evolving with their own strengths and weaknesses.

New insights have been gained about which optimisation criteria prove to be the most critical for system design, and by extension the most appropriate optimisation technique for placement and sizing of a battery energy storage. In consequence, a novel methodology to locate

and size battery energy storage systems is proposed in [Chapter 4](#). This methodology is based in the diakoptics and the actor-oriented model of OpenDSS for multi-threading, which using a parallel computing approach, it can accelerate the power distribution system analysis to obtain the optimal result of the battery energy storage location and power rating.

This new methodology works as a toolkit for the experimental platform, where a technical perspective is deployed by using an hybrid technique to find the suitable battery storage integration. First, a sensitivity analysis is performed to evaluate the introduction of BESS elements in the distribution system without disturbing its correct operation. Knowing the most sensible buses, a second algorithm based in a parallel genetic algorithm approach determines the optimal size of the number of battery storage elements selected.

The results achieved have demonstrated an accuracy calculation of the system sensitivity and the size of the output power rating of the battery energy storage for both loss minimization and voltage improvement approaches. Moreover, the computing performance reveals that this method can improve the calculation process exploiting the existing computer architectures and leaving behind the classical paradigm of sequential programming. However, the use of this methodology has resulted effective in a maximum of four processors according to the speed factor calculation. It means that a maximum performance in the use of a multi-core architecture is related to the complexity of the power distribution system or the number of individuals of a subpopulation. For small-scale systems or subpopulations, it will be better to solve the system using only one processor.

This method has demonstrated to be suitable for addressing the integration of battery energy storage systems in power distribution networks. Nevertheless, future prospects are related to the addition of new variables such the charge and discharge of the battery system in the optimization problem approach, also a feasible deployment of the system integration with a real storage system, and finally, the development of new algorithms to determine the energy capacity and the number of cycles based in an energy management system strategy, the local distributed generation and the load profile consumption.

The experimental platform based in the hardware and software architecture designed opens the door to continue the R&D of new algorithms to meet the smart grid challenges. Further studies will be developed in other subjects such smart integration of electric vehicles and charging points, load demand forecast and system state estimation, artificial intelligence applied to smart grids, among others.

Likewise, the experimental platform accomplishes the objectives formulated in the VERTPOM project. This result is a first view towards to the Bank of Energy concept allowing to advance in the conception of a tool for the system operators dedicated to the analysis, supervision and monitoring of the power distribution grids.

Part III

APPENDIX AND COMPLEMENTARY MATERIAL



## POWER DISTRIBUTION SYSTEM OF GAZELEC OF PERONNE

### A.1 DISTRIBUTION SYSTEM DESCRIPTION

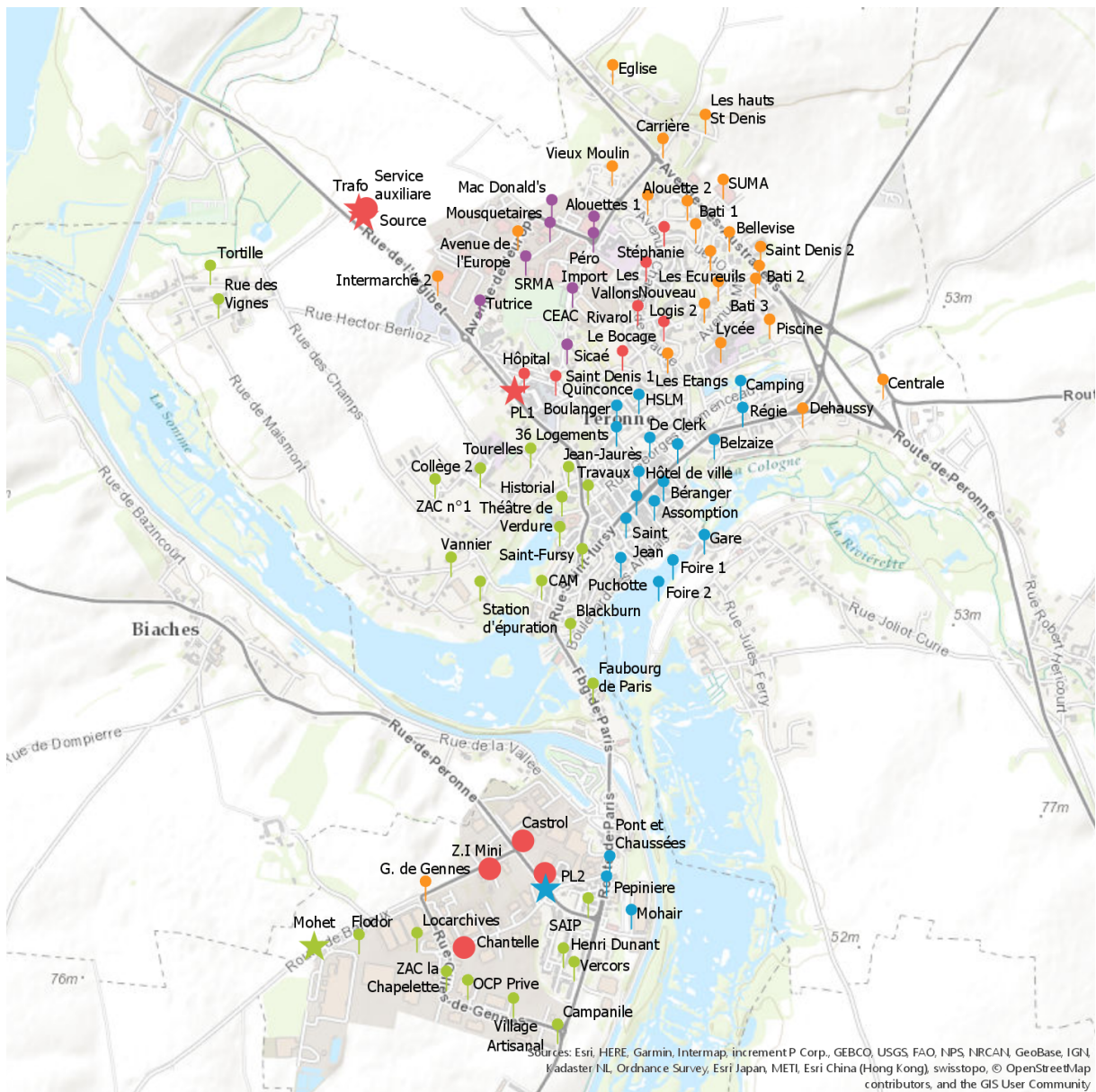


Figure A.1: Gazelec of Peronne distribution feeder map.

Gazelec of Peronne (GoP) power distribution network is a 20 kV network composed of two substations fed by RTE high voltage transmission system operator, the first substation has two 36 MVA - 63 kV/20 kV transformers ( $TR_{311}$  and  $TR_{312}$ ) and manages the conventional

power transmission energy. The second substation has one transformer ( $TR_{36}$ ) of 36 MVA - 63 kV/20 kV and controls the renewable wind energy production. Several photovoltaic panels are distributed around the city too. It also counts with one gas thermoelectric generator of 4,5 MW. Other kind of local energy production such as hydraulic, biomass or geothermal is not used.

The GoP medium-voltage (MV) network has a distance of 45,7 km of ungrounded three phase cable installation, where it connects 102 nodes, each corresponding to a MV-LV (20 kV/400 V) distribution feeder transformer. The total low-voltage (LV) distance of cable installation is calculated in 50 km, with around 4800 residential and 650 professional customers, and the different photovoltaic panels connected. [Figure A.1](#) shows the map of the city with all distribution feeders denoted by different pin colors reflecting the distribution feeders areas organized by GoP.

Considering the annual report of consumption of the city (Priour and Fau, 2015), and extrapolating the data consumption available from the year 2017 and 2019 (between 6 data concentrators installed in the secondary of some feeder transformers and almost 450 smart meters data retrieved), the total energy consumption is approximately 62,96 MWh for the year 2019. This approximation of the load profile of the city is stocked in the data server of the bank of energy and its behavior can be seen in [Figure A.2](#).

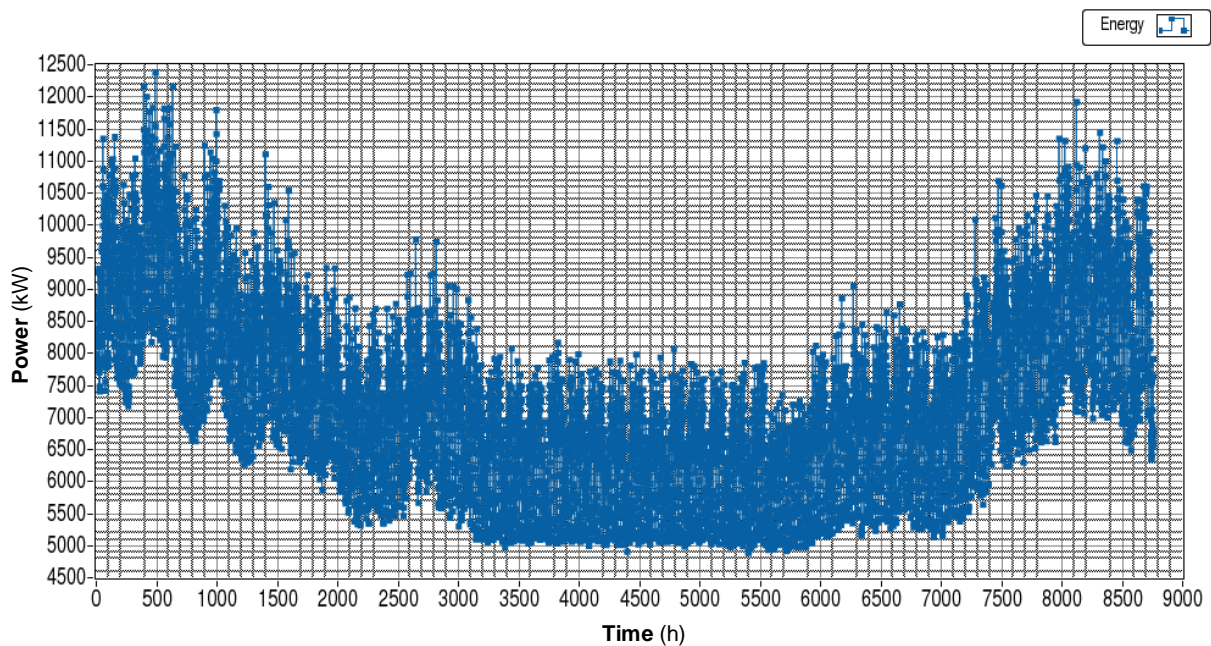


Figure A.2: Load profile curve extrapolated of the city for 2019.

## A.2 RENEWABLE ENERGY PRODUCTION

Two wind farms are located near the city as a production of renewable energy with a total generation of 37,68 MWh for the year 2017. [Figure A.3](#) and [Figure A.4](#) show the energy production extrapolated hourly for each wind farm respectively. Moreover, multiple photovoltaic panels are located around the urban area with a total power installed of 231.6 kWc for the year 2017. The energy production information is currently retrieved monthly for the wind farm in-



stallation and yearly for the photovoltaic panels installation. The reactive power production for both renewable technologies is unknown, further development considers reactive power measurement sensors in these points.

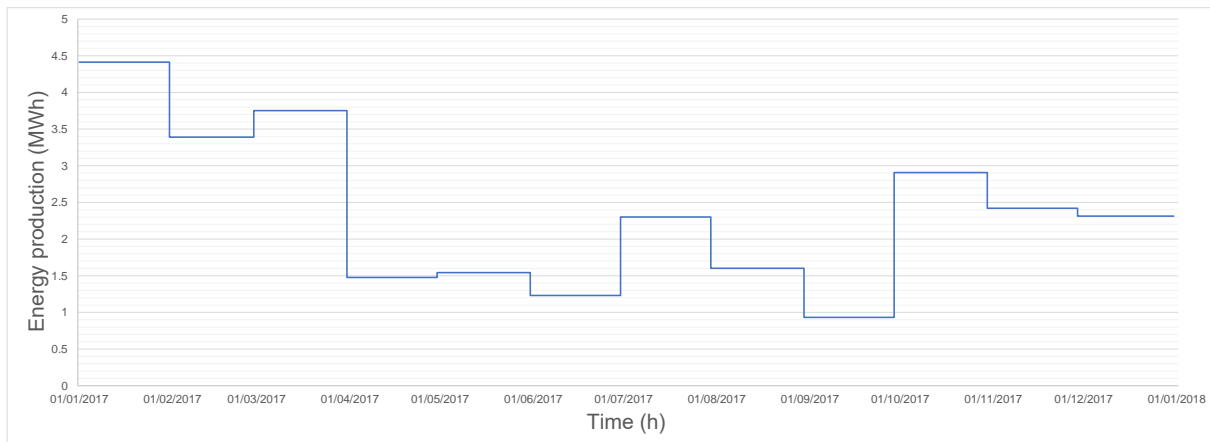


Figure A.3: Wind farm 1 power production for 2017.

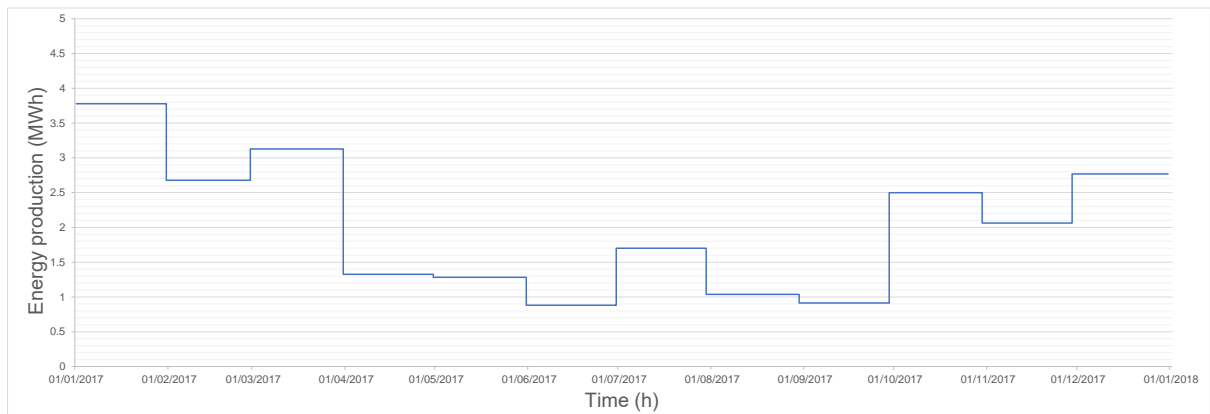


Figure A.4: Wind farm 2 power production for 2017.

Table A.1 summarizes the main features of the distribution network of the city chosen, it is important to mention that the system is in a constant evolution according to the operator proceedings.

Table A.1: Synthesis description of the distribution network of the city.

| Transmission connection | Transformers                       | Distance                        | Number of Clients        | Energy Consumption                                                                                                         |
|-------------------------|------------------------------------|---------------------------------|--------------------------|----------------------------------------------------------------------------------------------------------------------------|
| 2 substations           | 3 HV-MV 63 kV - 20 kV transformers | 45,7 km of three-phase MV cable | 4800 residential clients | 62,9 MWh of energy consumption, where 37,6 MWh comes from the wind farms and 133,9 kWh comes from the photovoltaic panels. |
|                         | 102 MV-LV 20 kV-400 V transformers | 50 km of three-phase LV cable   | 650 industrial clients   |                                                                                                                            |



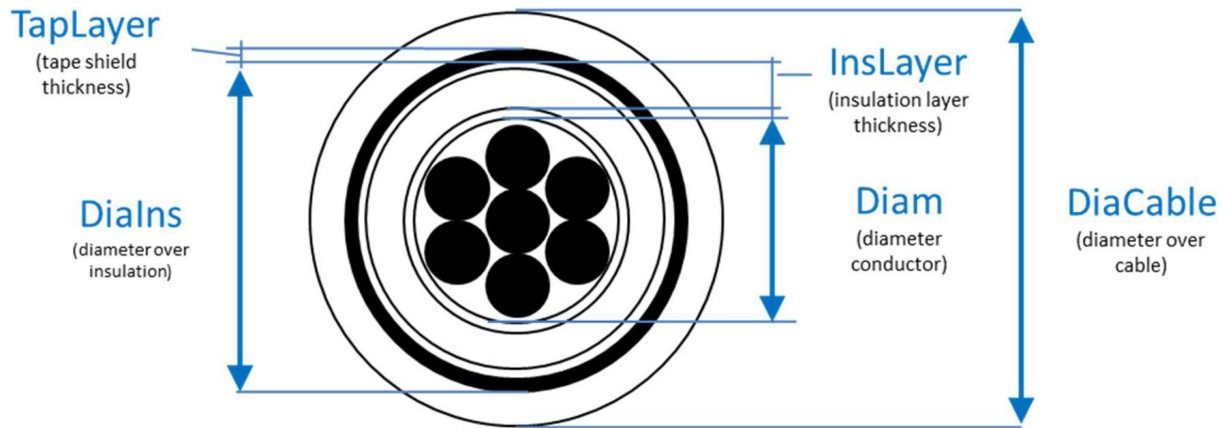


Figure A.6: Tape shielded cable geometric properties (Dugan and Ballanti, 2017).

In order to emulate a similar load consumption of the city as explained above, all customer loads were fixed as power and voltage constant. Moreover, a load profile was exploited to the transformers where is not available any information, considering a colored zone of its location

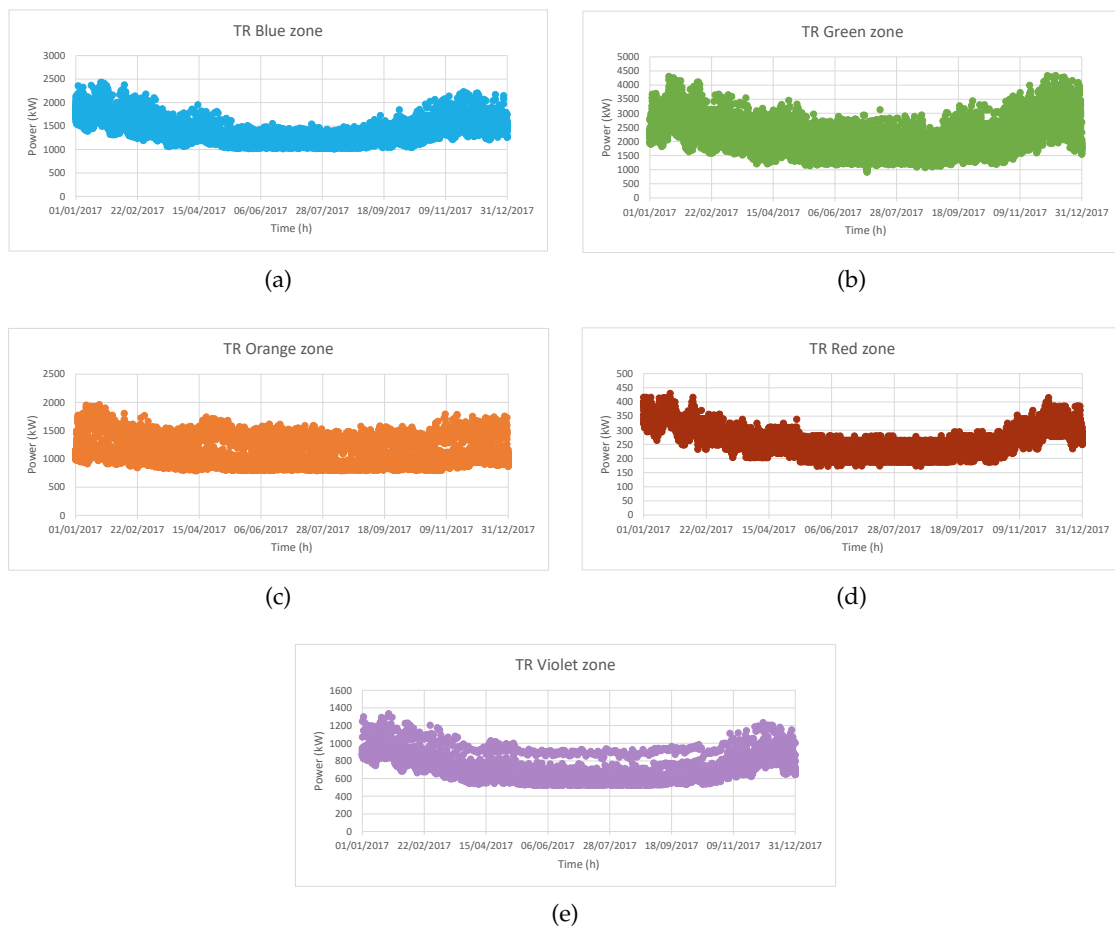


Figure A.7: Load profile extrapolation for each zone: (a) Blue zone extrapolation (15 transformers). (b) Green zone extrapolation (25 transformers). (c) Orange zone extrapolation (25 transformers). (d) Red zone extrapolation (7 transformers). (e) Violet zone extrapolation (10 transformers).

in the MV network. Figure A.7 shows the different load profiles related to the different zones of the distribution system.

Based in the French data protection and privacy law (EU, 2016; CNIL, 2018), the customer consumption information is not allowed to be treated without an explicit authorization of the client, therefore the data collected and analyzed comes from the CT-IBox<sup>®</sup> meters installed in the secondary of the MV/LV transformer.

A first data set of the load consumption is obtained from a pilot site database for the year 2017. In this case, a Thévenin load is defined for each transformer with a load profile defined. Figure A.8 shows all the load profiles where it was available a complete load consumption for the year 2017.

A second consumption load information is retrieved from the CT-Ibox meters currently installed since the year 2019, so for the load system model, an equivalent load is defined as

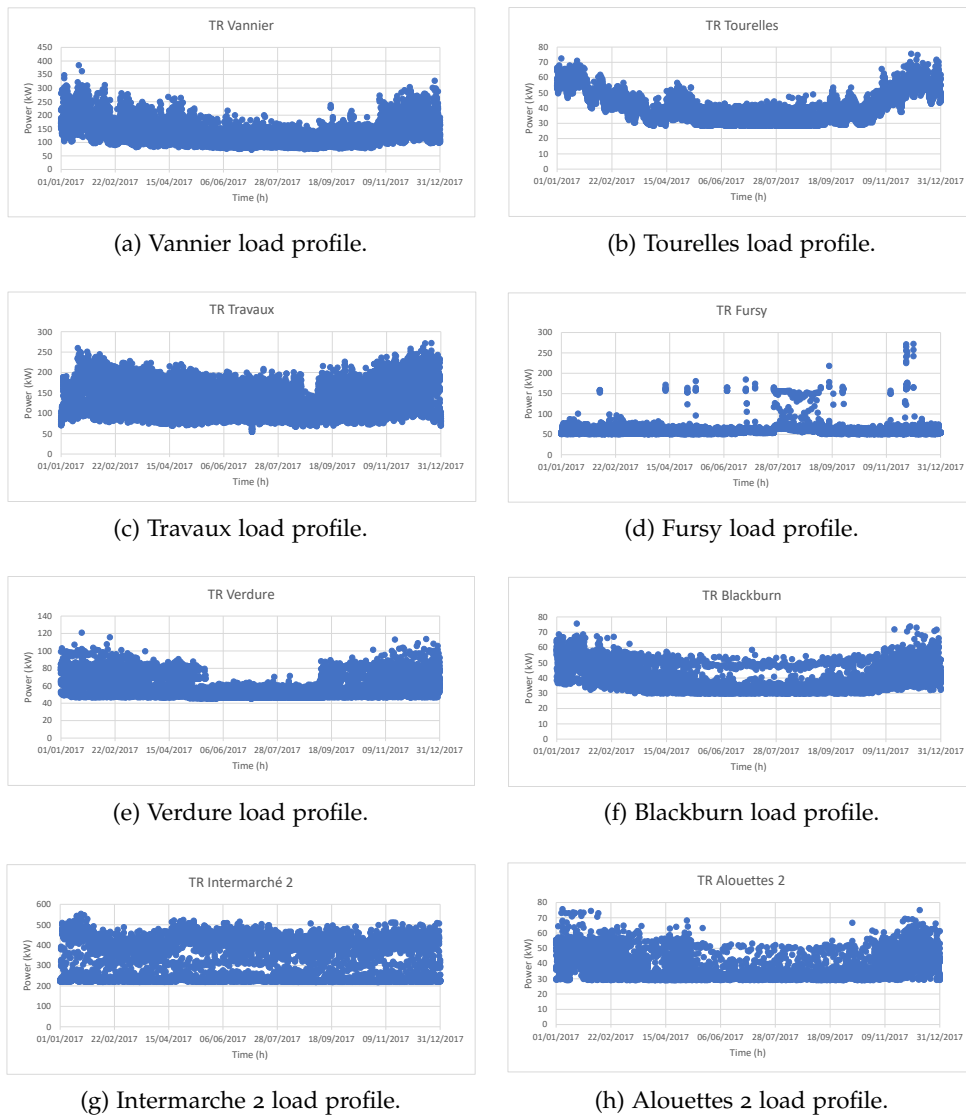
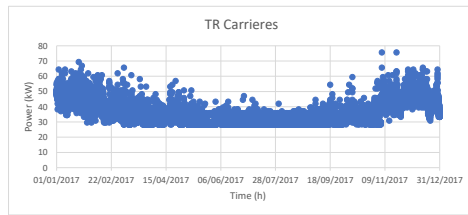
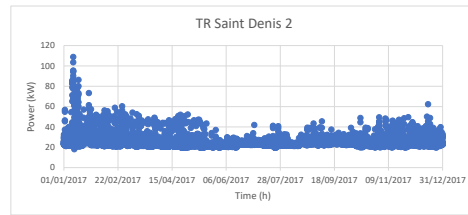


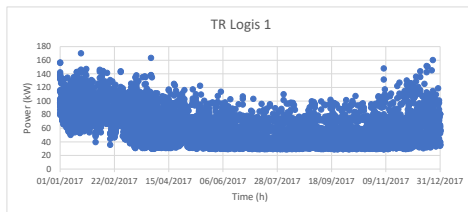
Figure A.8: Load profile consumption from transformers in the pilot site database.



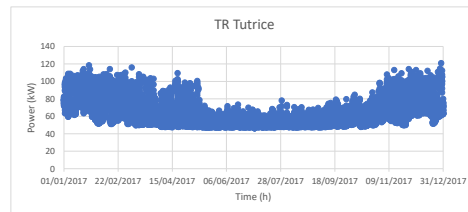
(i) Carrieres load profile.



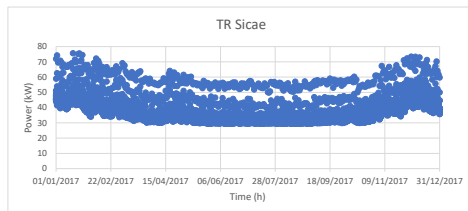
(j) Saint Denis 2 load profile.



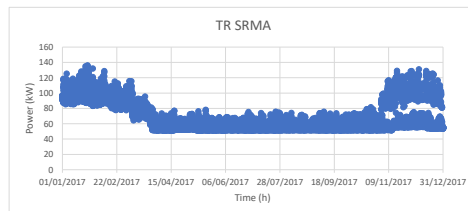
(k) Logis 1 load profile.



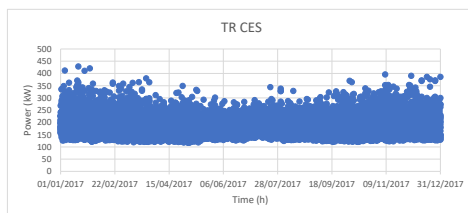
(l) Tutrice load profile.



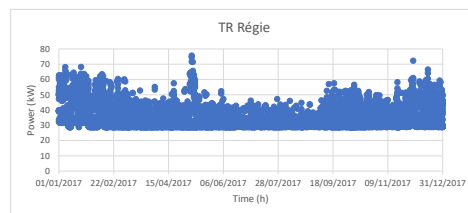
(m) Sicae load profile.



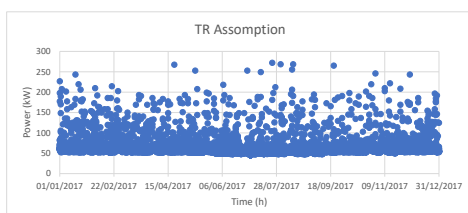
(n) SRMA load profile.



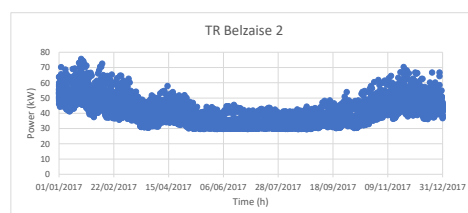
(o) CES load profile.



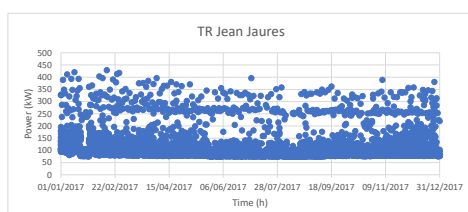
(p) Regie load profile.



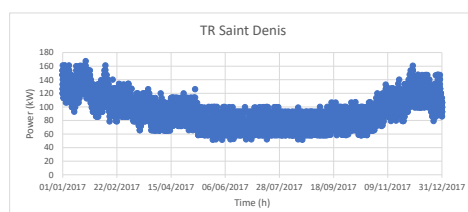
(q) Assomption load profile.



(r) Belzaise 2 load profile.



(s) Jean Jaures load profile.



(t) Saint Denis load profile.

Figure A.8: (Continued) Load profile consumption from transformers in the pilot site database.

before for each transformer with a CT-IBox meter belonged, attaching its load profile information. Figure A.9 shows the new load profiles retrieved from the CT-Ibox meters. This information allows to update the existing data consumption, refreshing the total load consumption of the system and approximating it to a real consumption behavior.

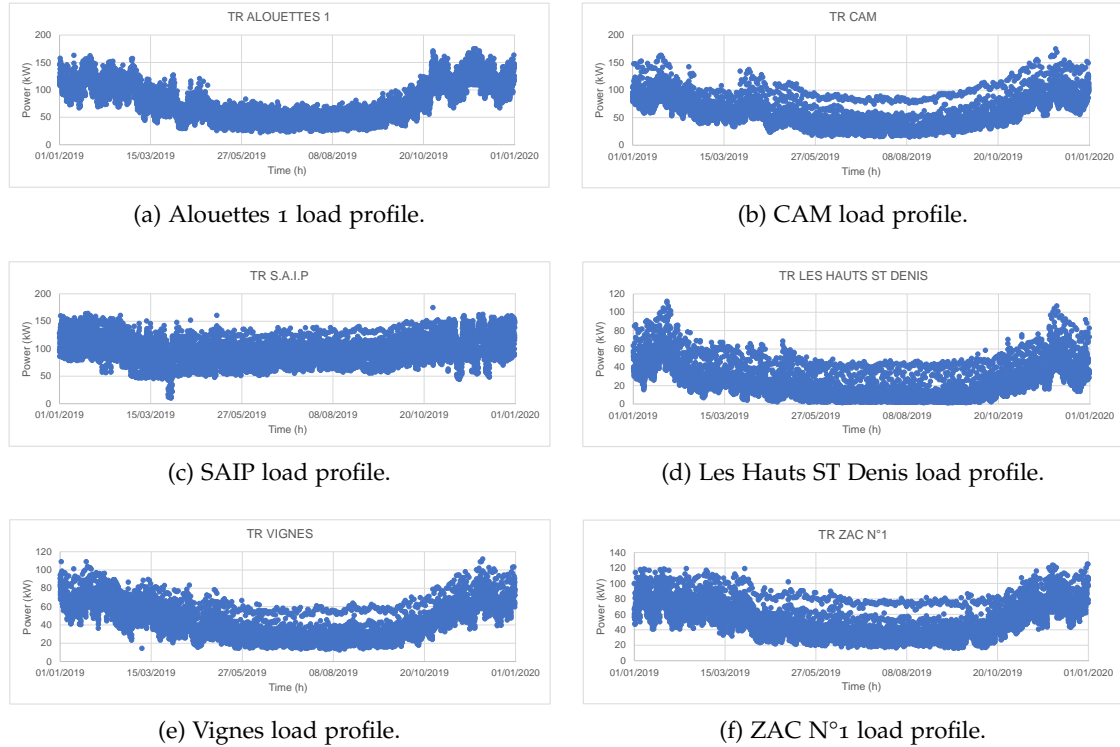


Figure A.9: Load profile for transformers with CT-Ibox installed.

#### A.4 RADIAL DISTRIBUTION DESCRIPTION

The radial diagram of the GoP distribution network test system is shown in Figure A.10. The radial structure of the system includes six typical 20 kV feeders. The nodes numbering corresponds to every transformer bus marked in the single line diagram. The load and the distributed generation resources are built based on the real information as explained before. Furthermore, the initial parameters, such as the line types, load types and renewable energy capacity are also set based on the actual data. The detailed information of the system is shown in Tables A.2 to A.7.

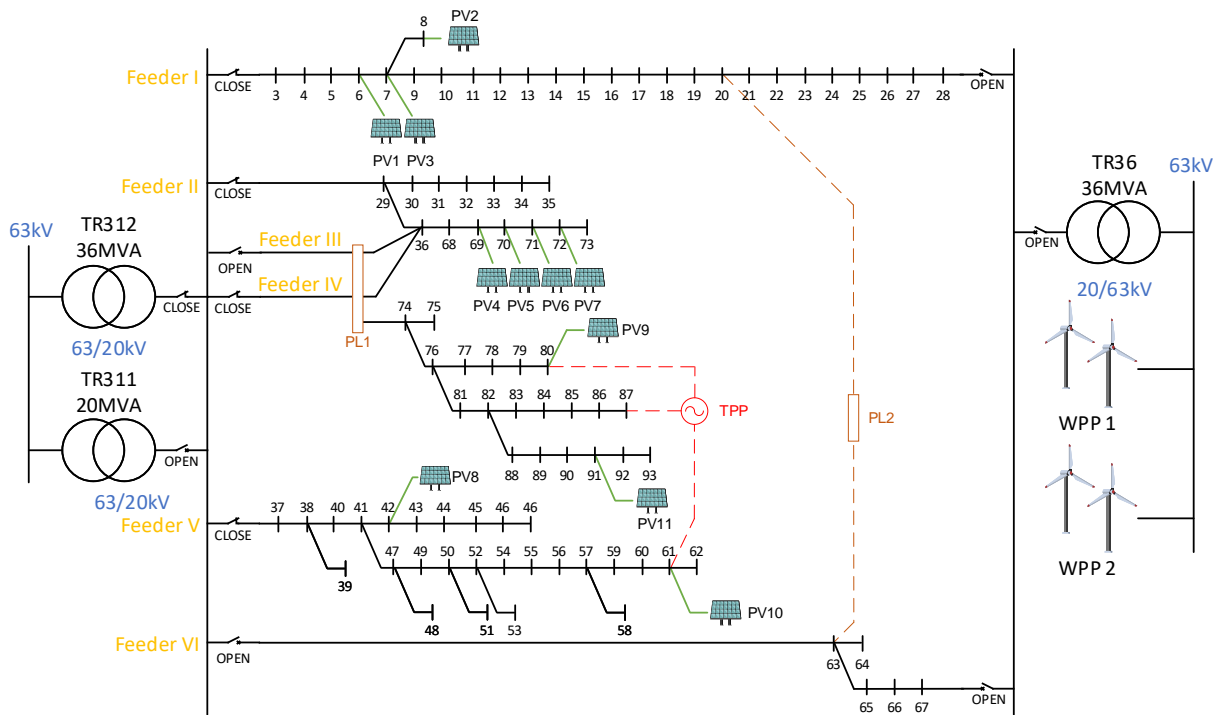


Figure A.10: Radial GoP distribution system diagram.

Table A.2: Generators.

| Generator number | Feeder  | Node       | S, kVA |
|------------------|---------|------------|--------|
| PV1              | 1       | 6          | 120    |
| PV2              | 1       | 7          | 120    |
| PV3              | 1       | 8          | 120    |
| PV4              | 2, 3, 4 | 69         | 120    |
| PV5              | 2, 3, 4 | 70         | 120    |
| PV6              | 2, 3, 4 | 71         | 120    |
| PV7              | 2, 3, 4 | 72         | 120    |
| PV8              | 5       | 42         | 120    |
| PV9              | 3, 4    | 80         | 120    |
| PV10             | 5       | 61         | 120    |
| PV11             | 3, 4    | 91         | 120    |
| WPP1             |         | 94         | 4400   |
| WPP2             |         | 94         | 3800   |
| TPP              | 3, 4, 5 | 61, 80, 87 | 4800   |

PV: Photovoltaic, WPP: Wind Power Plant, TPP: Thermal Power Plant

Table A.3: Lines characteristics.

| Name | Type   | Length,<br>km | Name | Type    | Length,<br>km | Name | Type   | Length,<br>km |
|------|--------|---------------|------|---------|---------------|------|--------|---------------|
| L1   | 150 RT | 0.945         | L38  | 150 RT  | 0.490         | L75  | 150 RT | 0.826         |
| L2   | 240 RT | 0.310         | L39  | 150 RT  | 0.040         | L76  | 240 RT | 0.431         |
| L3   | 150 RT | 1.64          | L40  | 150 RT  | 0.205         | L77  | 150 RT | 1.230         |
| L4   | 150 RT | 1.64          | L41  | 150 RT  | 0.330         | L78  | 240 RT | 1.230         |
| L5   | 150 RT | 0.466         | L42  | 150 RT  | 0.738         | L79  | 150 RT | 0.135         |
| L6   | 150 RT | 0.963         | L43  | 150 RT  | 0.618         | L80  | 150 RT | 0.192         |
| L7   | 150 RT | 0.389         | L44  | 150 RT  | 0.299         | L81  | 150 RT | 0.398         |
| L8   | 150 RT | 0.510         | L45  | 150 RT  | 0.328         | L82  | 150 RT | 0.322         |
| L9   | 150 RT | 0.213         | L46  | 150 RT  | 0.153         | L83  | 150 RT | 0.250         |
| L10  | 150 RT | 0.276         | L47  | 95 BGN7 | 0.216         | L84  | 150 RT | 0.240         |
| L11  | 150 RT | 0.585         | L48  | 95 BGN7 | 0.222         | L85  | 150 RT | 0.219         |
| L12  | 150 RT | 0.377         | L49  | 95 BGN7 | 0.349         | L86  | 150 RT | 0.190         |
| L13  | 150 RT | 0.642         | L50  | 150 RT  | 0.403         | L87  | 150 RT | 0.805         |
| L14  | 150 RT | 0.320         | L51  | 150 RT  | 0.239         | L88  | 150 RT | 0.210         |
| L15  | 150 RT | 0.353         | L52  | 150 RT  | 0.394         | L89  | 150 RT | 0.142         |
| L16  | 150 RT | 0.427         | L53  | 150 RT  | 0.569         | L90  | 150 RT | 0.330         |
| L17  | 150 RT | 1.144         | L54  | 150 RT  | 0.503         | L91  | 150 RT | 0.262         |
| L18  | 150 RT | 0.310         | L55  | 150 RT  | 0.995         | L92  | 150 RT | 0.540         |
| L19  | 150 RT | 0.545         | L56  | 95 BGN7 | 0.150         | L93  | 150 RT | 0.195         |
| L20  | 150 RT | 0.130         | L57  | 150 RT  | 0.144         | L94  | 150 RT | 0.442         |
| L21  | 150 RT | 0.332         | L58  | 150 RT  | 0.296         | L95  | 150 RT | 0.308         |
| L22  | 150 RT | 0.325         | L59  | 150 RT  | 0.217         | L96  | 150 RT | 0.186         |
| L23  | 150 RT | 0.315         | L60  | 150 RT  | 0.443         | L97  | 150 RT | 0.417         |
| L24  | 150 RT | 0.263         | L61  | 95 BGN7 | 0.230         | L98  | 150 RT | 0.192         |
| L25  | 150 RT | 0.064         | L62  | 95 BGN7 | 0.352         | L99  | 150 RT | 0.124         |
| L26  | 150 RT | 0.375         | L63  | 95 BGN7 | 0.240         | L100 | 150 RT | 0.798         |
| L27  | 240 RT | 0.382         | L64  | 95 BGN7 | 0.310         | L101 | 150 RT | 0.659         |
| L28  | 240 RT | 0.431         | L65  | 150 RT  | 0.572         | L102 | 150 RT | 0.539         |
| L29  | 150 RT | 0.902         | L66  | 150 RT  | 0.875         | L103 | 150 RT | 0.347         |
| L30  | 150 RT | 0.552         | L67  | 150 RT  | 0.090         | L104 | 150 RT | 0.412         |
| L31  | 150 RT | 0.290         | L68  | 150 RT  | 0.080         | L105 | 150 RT | 0.299         |
| L32  | 150 RT | 0.302         | L69  | 150 RT  | 0.654         | L106 | 150 RT | 1.580         |
| L33  | 150 RT | 0.215         | L70  | 150 RT  | 0.494         | L107 | 150 RT | 0.115         |
| L34  | 150 RT | 0.289         | L71  | 150 RT  | 0.240         | L108 | 150 RT | 0.338         |
| L35  | 150 RT | 0.202         | L72  | 150 RT  | 0.135         | L109 | 150 RT | 0.157         |
| L36  | 150 RT | 0.270         | L73  | 150 RT  | 0.526         | L110 | 150 RT | 0.115         |
| L37  | 150 RT | 0.347         | L74  | 150 RT  | 0.169         | -    | -      | -             |



Table A.4: Transformer characteristics.

| Node | Transformer     | S,<br>kVA | Node | Transformer      | S,<br>kVA |
|------|-----------------|-----------|------|------------------|-----------|
| 1    | TR312           | 36000     | 37   | Renault          | 400       |
| 2    | TR311           | 20000     | 38   | Intermarche 2-1  | 630       |
| 3    | Tortille        | 160       | 39   | Intermarche 2-2  | 800       |
| 4    | Vignes          | 160       | 40   | Avenue Europe    | 400       |
| 5    | Equestre        | 250       | 41   | Vieux Moulin     | 250       |
| 6    | ZAC N1          | 250       | 42   | Alouettes 1      | 250       |
| 7    | Vannier 1       | 315       | 43   | Alouettes 2      | 250       |
| 8    | Vannier 2       | 250       | 44   | Bati 1           | 400       |
| 9    | College 2       | 250       | 45   | Les Ecureuils    | 250       |
| 10   | Tourelles       | 250       | 46   | Bellevisse       | 250       |
| 11   | Jean Jaures     | 400       | 47   | Carriere         | 250       |
| 12   | Travaux         | 400       | 48   | Eglise           | 160       |
| 13   | Historial       | 630       | 49   | Hauts St Denis   | 160       |
| 14   | St Fursy        | 400       | 50   | SUMA 1           | 250       |
| 15   | Theatre Verdure | 400       | 51   | SUMA 2           | 630       |
| 16   | St Depuration   | 400       | 52   | Saint Denis 2    | 160       |
| 17   | Cam             | 250       | 53   | Gens Voyage      | 250       |
| 18   | Blackburn       | 250       | 54   | Bati 2           | 250       |
| 19   | Faubourg Paris  | 400       | 55   | Bati 3           | 400       |
| 20   | SAIP            | 250       | 56   | Nouveau Logis 1  | 250       |
| 21   | Henri Dunant    | 250       | 57   | Nouveau Logis 2  | 250       |
| 22   | Vercors         | 400       | 58   | Les Etangs       | 250       |
| 23   | Campanile       | 400       | 59   | Lycee            | 800       |
| 24   | V Artisanal     | 250       | 60   | Piscine          | 630       |
| 25   | OCP             | 630       | 61   | Dehaussy         | 400       |
| 26   | ZAC Chapelette  | 400       | 62   | Service des Eaux | 250       |
| 27   | Locarchives     | 400       | 63   | Delta-coop       | 160       |
| 28   | Flodor          | 250       | 64   | Chantelle        | 630       |
| 29   | Tutrice         | 400       | 65   | Saint Bernard    | 160       |
| 30   | Sicae           | 250       | 66   | Castrol          | 1000      |
| 31   | Pier import     | 400       | 67   | ZI Mini          | 400       |
| 32   | Intermarche     | 250       | 68   | Quinconce        | 400       |
| 33   | Mac Donalds     | 250       | 69   | ST Denis 1       | 400       |
| 34   | Mousquetaires   | 630       | 70   | Le Bocage        | 250       |
| 35   | SRMA            | 315       | 71   | Rivarol          | 250       |
| 36   | Hopital         | 1000      | 72   | Les Vallons      | 250       |

Table A.5: (Continued) Transformer characteristics.

| Node | Transformer    | S,<br>kVA | Node | Transformer       | S,<br>kVA |
|------|----------------|-----------|------|-------------------|-----------|
| 73   | Stephanie      | 250       | 84   | Foire 1           | 1250      |
| 74   | Boulangier     | 400       | 85   | Foire 2           | 400       |
| 75   | HSLM           | 250       | 86   | Beranger          | 400       |
| 76   | 36 Logements   | 250       | 87   | Belzaise          | 250       |
| 77   | De Clerk       | 250       | 88   | Naviages          | 400       |
| 78   | College 1      | 630       | 89   | Saint Jean        | 630       |
| 79   | Camping        | 250       | 90   | Puchotte          | 250       |
| 80   | Regie          | 250       | 91   | Ponts et chaussee | 400       |
| 81   | Hotel de Ville | 800       | 92   | Pepiniere         | 160       |
| 82   | Assomption     | 400       | 93   | Mohair            | 1600      |
| 83   | Gare           | 630       | 94   | TR36              | 36000     |

Table A.6: Type line properties description.

| Type    | Phases | Normal<br>Ampacity,<br>A | AC<br>Resistance,<br>$\Omega/\text{km}$ | DC<br>Resistance,<br>$\Omega/\text{km}$ | Section,<br>$\text{mm}^2$ |
|---------|--------|--------------------------|-----------------------------------------|-----------------------------------------|---------------------------|
| 95 BGN7 | 3      | 240                      | 0.247                                   | 0.193                                   | 95                        |
| 150 RT  | 3      | 307                      | 0.265                                   | 0.206                                   | 150                       |
| 240 RT  | 3      | 404                      | 0.161                                   | 0.125                                   | 240                       |

Table A.7: Type line geometric properties description.

| Type    | Diam,<br>mm | DiaIns,<br>mm | DiaCable,<br>mm | InsLayer,<br>mm | TapLayer,<br>mm |
|---------|-------------|---------------|-----------------|-----------------|-----------------|
| 95 BGN7 | 11.3        | 23.6          | 36.1            | 5.5             | 2.4             |
| 150 RT  | 14.1        | 24.1          | 30.8            | 4.5             | 2.5             |
| 240 RT  | 18.1        | 28.1          | 35.2            | 4.5             | 2.4             |

## POWER DISTRIBUTION TEST FEEDERS

---

As it is well-known, it is not possible to execute study a fully real system in the experimental platform of the Bank of Energy due to the fact that is not an easy task to have access to all data involved. Considering this reason the test feeders working group of the power systems analysis computing and economics (PSACE) committee has published several test feeders for a high development of the power distribution system (PES, 2021). The purpose of these test feeders is to provide a benchmark for mid to long term dynamic behaviors (Schneider et al., 2018).

### B.1 THE IEEE 8500 NODE TEST FEEDER

The 8500 Node Test Feeder was published in 2010 and represents an unbalanced radial system with a large number of line segments. This test feeder was specifically developed as a representation of a full-size distribution system. One-minute load shapes are integrated for time series simulations (Arritt and Dugan, 2010).

The 8500 Node Test Feeder (Figure B.1) is a 12.47 kV large radial system with 170 km of overhead lines and underground cables. The feeder has a substation load tap changers (LTC),

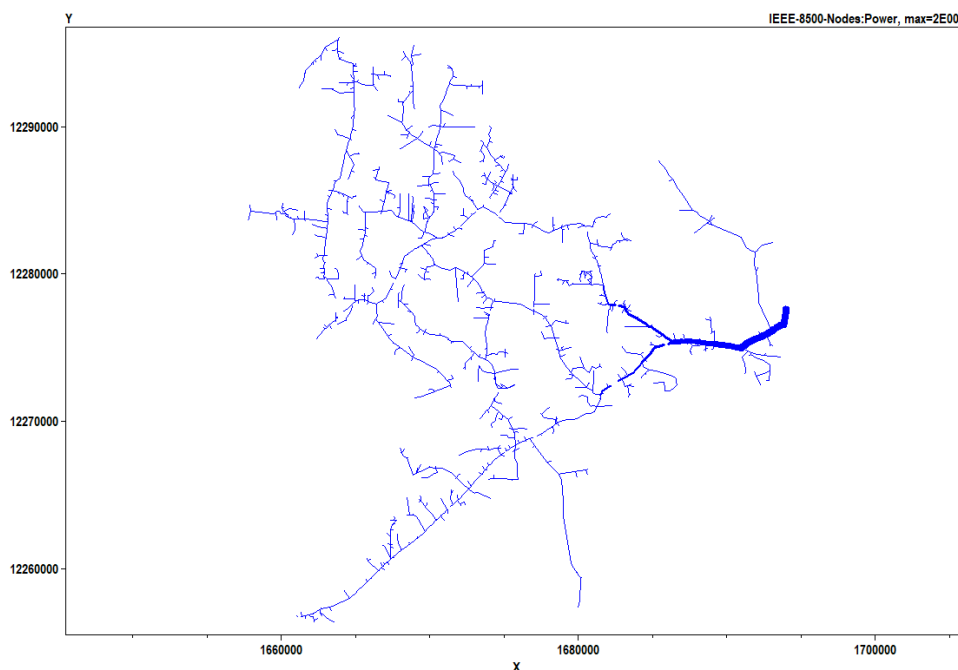


Figure B.1: One-line diagram of the 8500 node test system.

three voltage regulators, and four shunt capacitors. The end-use loads are connected to the end of radial secondary systems served by 7200/120-240 V split-phase service transformers. Figure B.2 shows the total consumption associated to this test system.

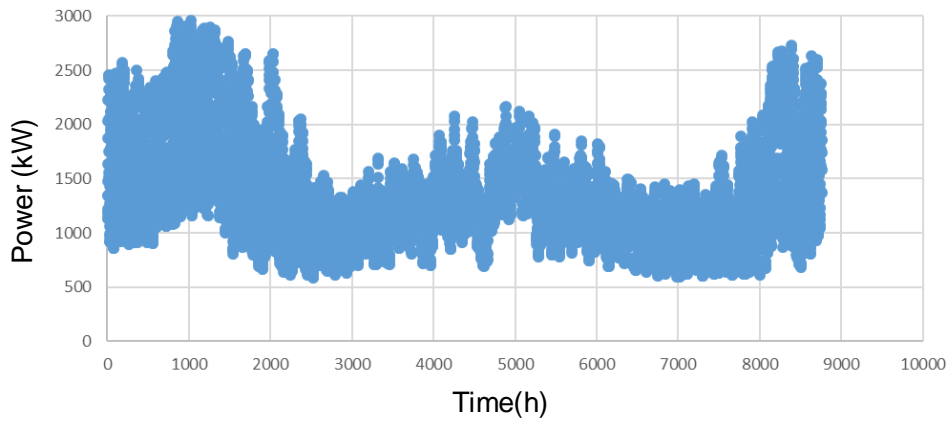


Figure B.2: Load profile curve of the 8500 node test system.

The 8500 Node Test Feeder was developed to provide a system that had a number of line segments consistent with a typical modern utility circuit model. This is a system of suitable complexity for researchers to prove the scalability of power flow, optimization, and search methods to a full-size distribution feeder.

**B.2 THE IEEE EUROPEAN TEST FEEDER**

The IEEE European Low-Voltage Test Feeder (Figure B.3) is a 400 V (nominal voltage) radial system that represents a typical feeder in Europe. The voltage at the head of the feeder is set

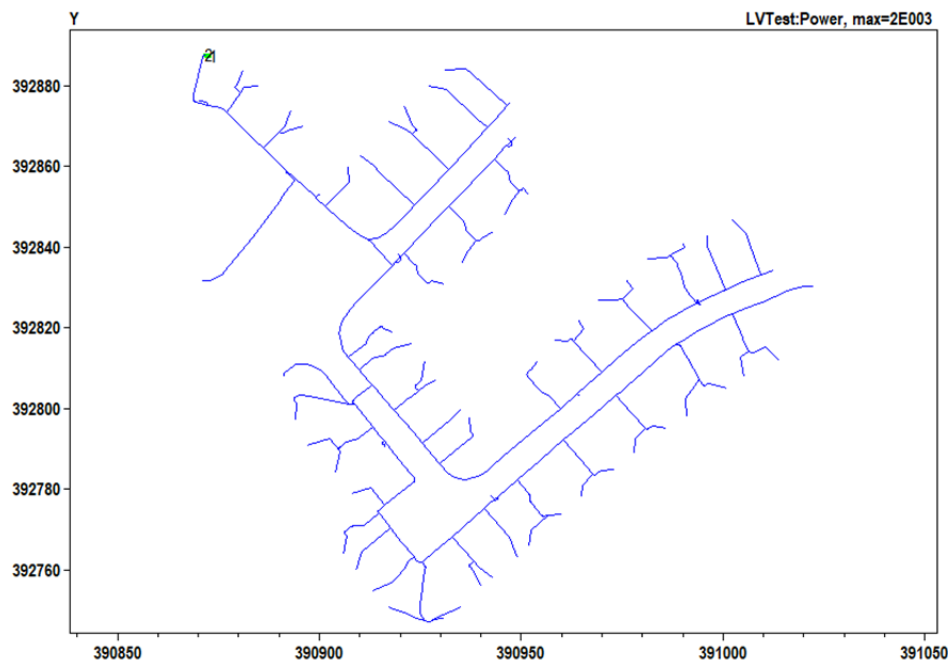


Figure B.3: One-line diagram of the IEEE European test system.

to 416 V to mimic typical operational values in Europe, the single-phase end-use loads are connected to one of the phases of the feeder. One-minute load shapes are integrated for time series simulations.

This test feeder is a radial distribution feeder with a base frequency of 50 Hz. The feeder is connected to the medium voltage (MV) system through a transformer at substation. The transformer steps the voltage down from 11 kV to 416 V. The main feeder and laterals are at the voltage level of 416 V. Time-series load shapes for the 55 loads served by the test feeder are provided with a one-minute time resolution over a one-day period (PES, 2015).

This feeder was specifically designed to address unbalanced low voltage feeders which are commonly found in Europe. The computational challenges are not significant, but the proper value of 50 Hz must be used when applying Carson's equations. Additionally, when applying the time series data for the end use loads it is necessary to run multiple power flow simulations. Because there are no state variables that are dependent on the state of the previous time-step it is possible to run these sequentially or in parallel. Figure B.4 shows the total consumption associated to this test system.

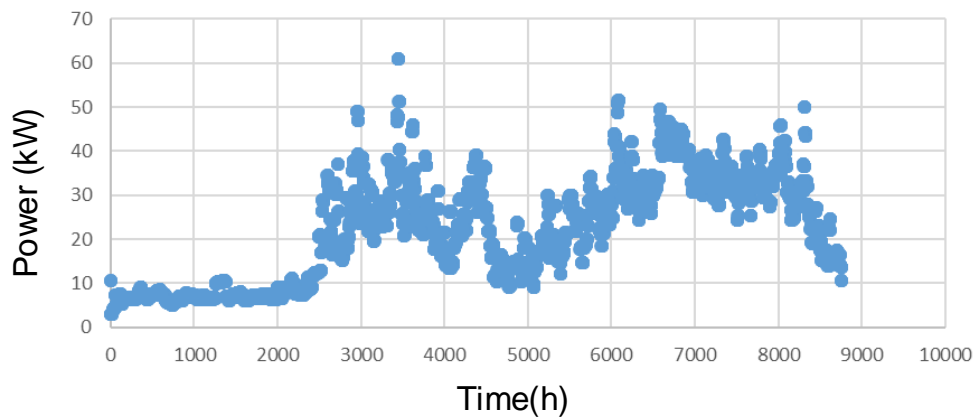


Figure B.4: Load profile curve of the IEEE European test system.

### B.3 NON- IEEE TEST CASES

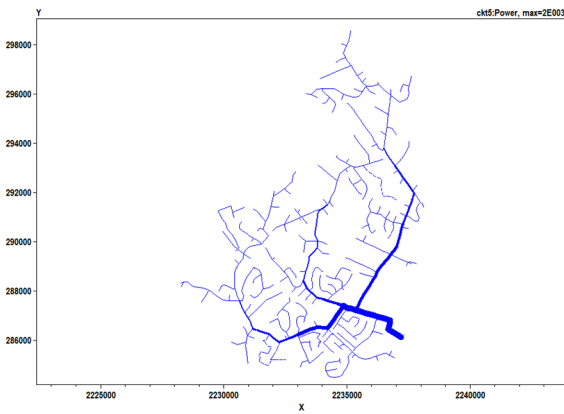
The following test cases are a working group suggestions for open-source feeder models. These models are not designed to stress the power flow solution algorithms (as the radial test feeders do), but rather as representative feeders for researchers to use in case studies.

#### B.3.1 EPRI test circuits

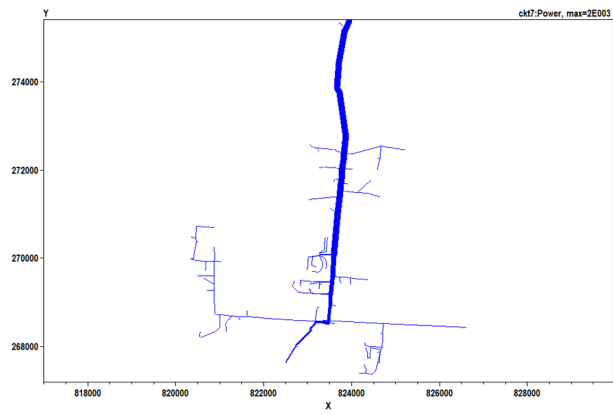
These models were designed as part of EPRI's Green Circuit project database. The models are representative of actual small, medium, and large circuits from various utilities. These models of actual electric power distribution circuits are made in OpenDSS format and they were set up to do annual simulations (PES, 2018). A summary of each, labeled Ckt5, Ckt7, and Ckt24, is given in Table B.1. The one-line diagram and load profile curve of each test feeder are presented in Figure B.5 and Figure B.6 respectively.

Table B.1: Summary of EPRI Test Circuits (Dugan, 2015).

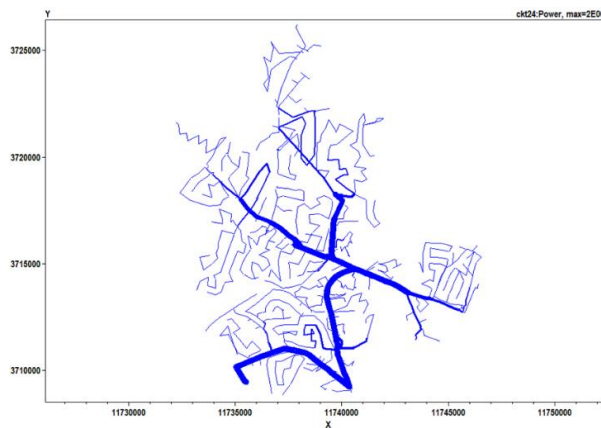
| Circuit Alias                 | CKT5  | CKT7  | CKT24 |
|-------------------------------|-------|-------|-------|
| System voltage, kV            | 12.47 | 12.5  | 34.5  |
| Number of customers           | 1379  | 5694  | 3885  |
| Service XFMR connected, kVA   | 16310 | 19320 | 69373 |
| Total feeder, kvar            | 1950  | 2400  | 3300  |
| Subtransmission voltage, kV   | 115   | 115   | 230   |
| 3-phase SCC at sub sec., MVA  | 114   | 475   | 422   |
| Primary circuit miles total   | 48    | 8     | 74    |
| Percent residential by load   | 96    | 39    | 87    |
| No. of feeders on the sub bus | 1     | 14    | 2     |



(a) EPRI Ckt5.

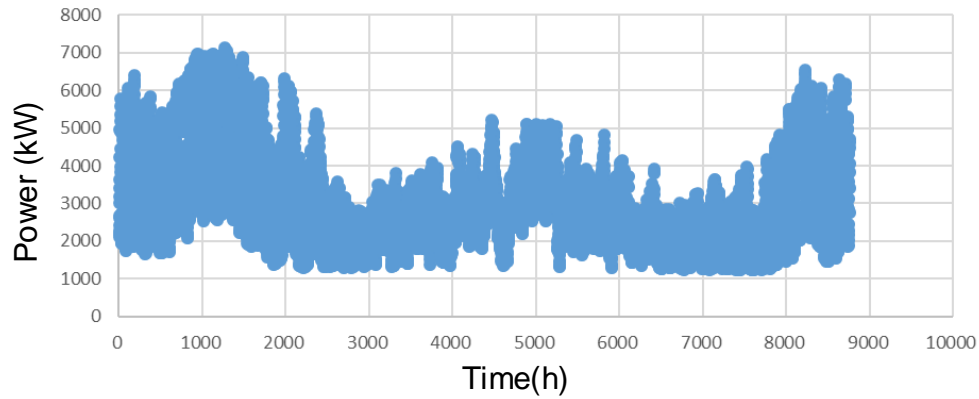


(b) EPRI Ckt7.

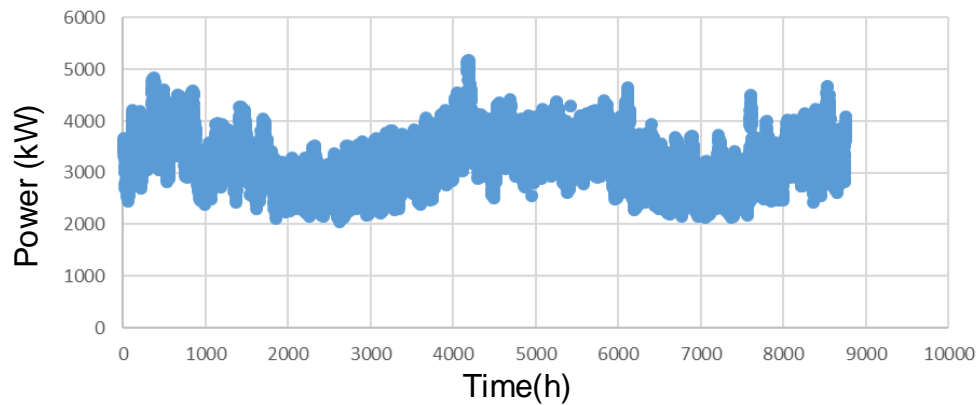


(c) EPRI Ckt24.

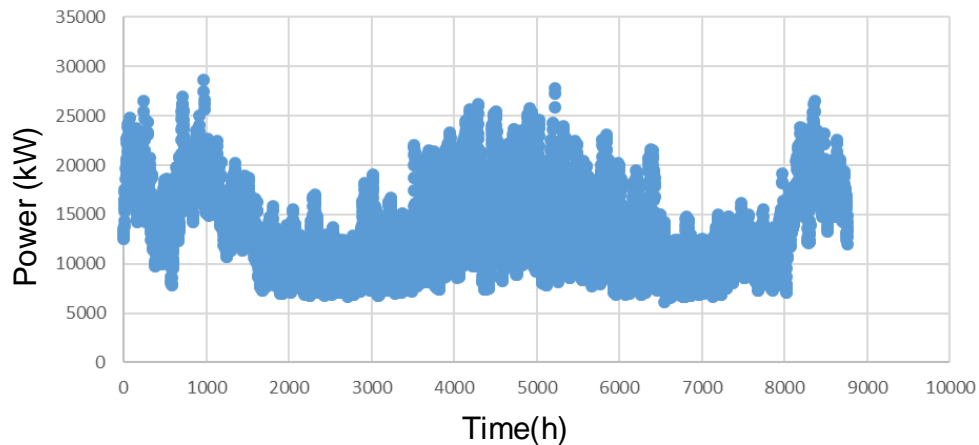
Figure B.5: One-line diagram of the EPRI test circuits.



(a) EPRI Ckt5.



(b) EPRI Ckt7.



(c) EPRI Ckt24.

Figure B.6: Load profile curve of the EPRI test circuits.

### B.3.2 Iowa distribution test systems

The Iowa Distribution test system (Figure B.7) is a radial distribution system consisting of three feeders which are supplied by a 69 kV substation. This test system is a real distribution grid located in the Midwest of the United States. The real system belongs to a municipal utility and is a fully observable network with smart meters installed at all customers. The test system has 240 primary network nodes and 23 miles of primary feeder conductor. That customers are

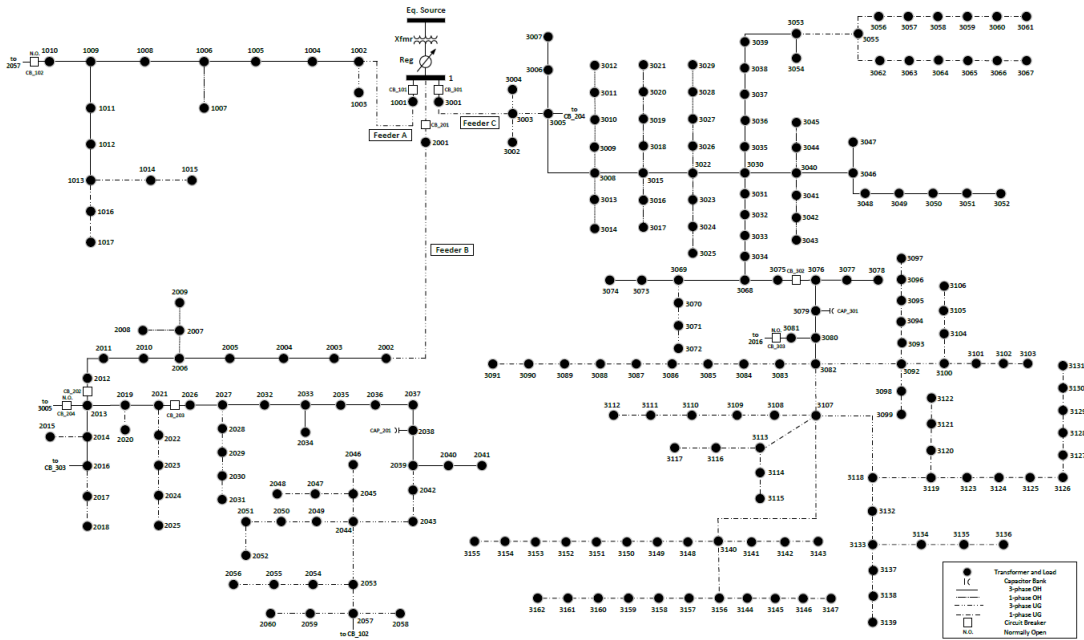
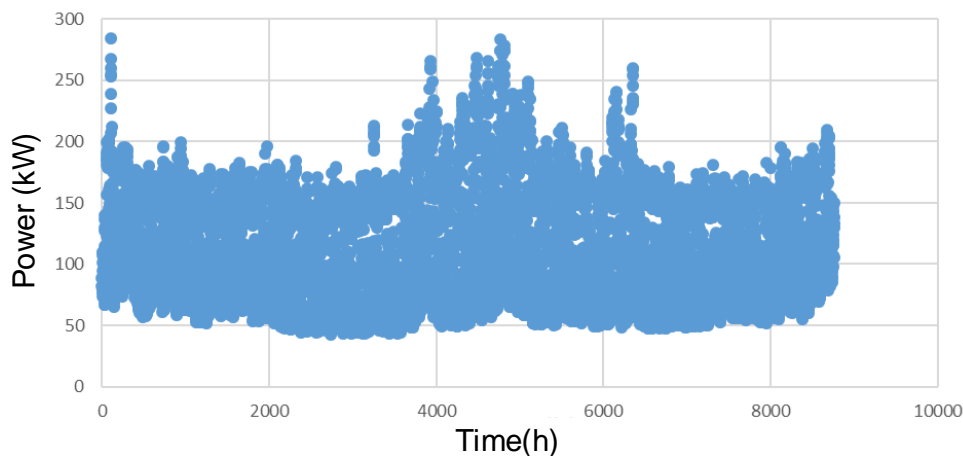


Figure B.7: One-line diagram of the Iowa State University test system (Bu et al., 2019).

connected to these primary network nodes via secondary distribution transformers (Wang, 2019).

In this test system, the time-series data of each node is directly obtained from customers of smart meters measurements. The data range is from January 2017 to December 2017. The availability of smart meter data contains hourly energy consumption (kWh) of 1120 customers. The importance of this test feeder is based on the use of real data, handling many customers compared to the distribution system of Gazelec of Peronne (Appendix A).

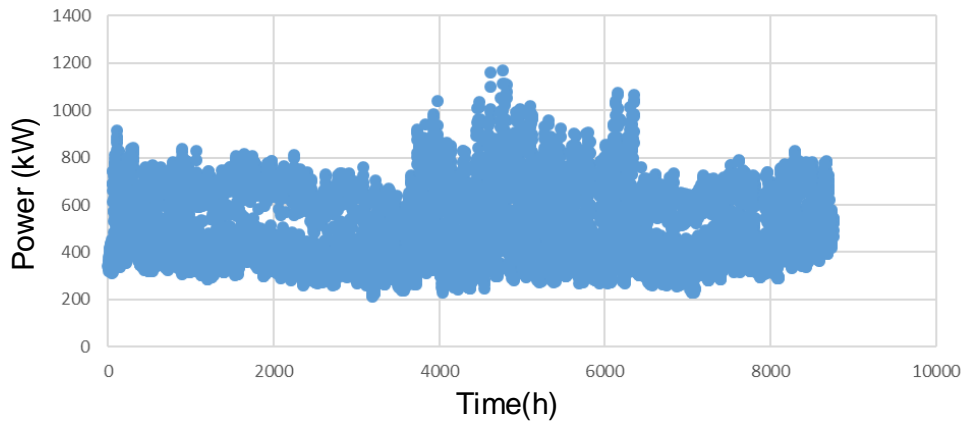
The three feeders in the test system are supplied by 69 kV/13.8 kV step-down three phase substation transformer with an on-load tap changing mechanism. The secondary distribution transformers consist of three phase transformers and single-phase transformers used for serving commercial customers at 240 V, and residential customers with nominal voltage of



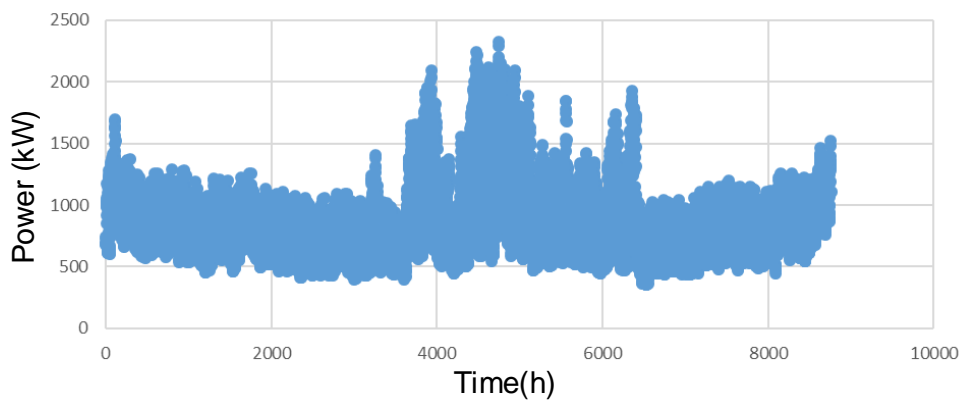
(a) Feeder A

Figure B.8: Load profile curve of the Iowa State University test system





(b) Feeder B



(c) Feeder C

Figure B.8: Load profile curve of the Iowa State University test system.

120 V/240 V respectively (Bu et al., 2019). The customers consumption are divided by three existing feeders in the system, which are illustrated in Figure B.8.

Based in the total consumption of the year 2017 (Figure B.9), this test system opens the possibility to analyze the energy demand compared to the Gazelec distribution system. Mainly, because in both systems there is a similar proportion between buses and end-users.

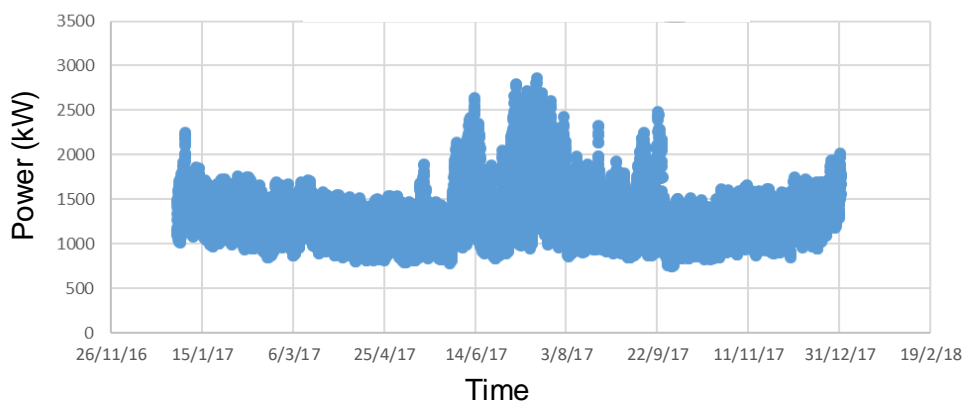


Figure B.9: Total load profile curve of the Iowa State University test system.



## BIBLIOGRAPHY

---

- ADEME (2018a). *S'engager dans la transition énergétique en France*. URL: <https://www.ademe.fr/expertises/batiment/elements-contexte/politiques-vigueur/sengager-transition-energetique-france>. (accessed: 15.03.2021).
- (2018b). *VERTPOM: Véritable éNERgie du Territoire POSitif et Modulaire*. URL: <https://www.ademe.fr/vertpom>. (accessed: 25.03.2021).
- AlHajri, M. F. and M. E. El-Hawary (2010). “Exploiting the Radial Distribution Structure in Developing a Fast and Flexible Radial Power Flow for Unbalanced Three-Phase Networks.” In: *IEEE Transactions on Power Delivery* 25.1, pp. 378–389.
- Almehizia, Abdullah A. et al. (2020). “Assessment of battery storage utilization in distribution feeders.” In: *Energy Transitions (2020) 4*, 101–112. DOI: [10.1007/s41825-020-00026-x](https://doi.org/10.1007/s41825-020-00026-x).
- Alrushoud, A. and N. Lu (2020). “Impacts of PV Capacity Allocation Methods on Distribution Planning Studies.” In: *2020 IEEE/PES Transmission and Distribution Conference and Exposition (T D)*, pp. 1–5. DOI: [10.1109/TD39804.2020.9299981](https://doi.org/10.1109/TD39804.2020.9299981).
- Amano, H. et al. (2012). “Utilization of battery energy storage system for load frequency control toward large-scale renewable energy penetration.” In: *2012 3rd IEEE PES Innovative Smart Grid Technologies Europe (ISGT Europe)*, pp. 1–7. DOI: [10.1109/ISGTEurope.2012.6465650](https://doi.org/10.1109/ISGTEurope.2012.6465650).
- Amar, J. G. (2006). “The Monte Carlo method in science and engineering.” In: *Computing in Science Engineering* 8.2, pp. 9–19. DOI: [10.1109/MCSE.2006.34](https://doi.org/10.1109/MCSE.2006.34).
- Andreev, M. et al. (2018). “Hybrid Real-Time Simulator of Large-Scale Power Systems.” In: *IEEE Transactions on Power Systems*, pp. 1–1. ISSN: 0885-8950. DOI: [10.1109/TPWRS.2018.2876668](https://doi.org/10.1109/TPWRS.2018.2876668).
- Angioni, A. et al. (2016). “Real-Time Monitoring of Distribution System Based on State Estimation.” In: *IEEE Transactions on Instrumentation and Measurement* 65.10, pp. 2234–2243. ISSN: 0018-9456. DOI: [10.1109/TIM.2016.2583239](https://doi.org/10.1109/TIM.2016.2583239).
- Anjana, S. P. and T. S. Angel (2017). “Intelligent demand side management for residential users in a smart micro-grid.” In: *2017 International Conference on Technological Advancements in Power and Energy (TAP Energy)*, pp. 1–5.
- Annaswamy, Anuradha M. and Massoud Amin (2013). “IEEE Vision for Smart Grid Controls: 2030 and Beyond.” In: *IEEE Vision for Smart Grid Controls: 2030 and Beyond*, pp. 1–168. DOI: [10.1109/IEEESTD.2013.6577608](https://doi.org/10.1109/IEEESTD.2013.6577608).
- Arif, S., A. E. Rabbi, and T. Aziz (2018). “A Battery Energy Storage Based Methodology to Accelerate Post-Fault Voltage and Frequency Recovery Process in Microgrid.” In: *2018 IEEE International WIE Conference on Electrical and Computer Engineering (WIECON-ECE)*, pp. 141–144. DOI: [10.1109/WIECON-ECE.2018.8783201](https://doi.org/10.1109/WIECON-ECE.2018.8783201).
- Arnold, G. W. (2011). “Challenges and Opportunities in Smart Grid: A Position Article.” In: *Proceedings of the IEEE* 99.6, pp. 922–927. ISSN: 0018-9219. DOI: [10.1109/JPROC.2011.2125930](https://doi.org/10.1109/JPROC.2011.2125930).
- Arritt, R. F. and R. C. Dugan (2010). “The IEEE 8500-node test feeder.” In: *IEEE PES T D 2010*, pp. 1–6. DOI: [10.1109/TDC.2010.5484381](https://doi.org/10.1109/TDC.2010.5484381).

- Arritt, R. F. and R. C. Dugan (2011). "Distribution System Analysis and the Future Smart Grid." In: *IEEE Transactions on Industry Applications* 47.6, pp. 2343–2350. ISSN: 0093-9994. DOI: [10.1109/TIA.2011.2168932](https://doi.org/10.1109/TIA.2011.2168932).
- Aziz, T., S. R. Deeba, and Nahid-Al-Masood (2016). "Investigation of post-fault voltage recovery performance with battery-based energy storage system in a microgrid." In: *2016 Australasian Universities Power Engineering Conference (AUPEC)*, pp. 1–6. DOI: [10.1109/AUPEC.2016.7749385](https://doi.org/10.1109/AUPEC.2016.7749385).
- Baki, A. K. M. (2014). "Continuous Monitoring of Smart Grid Devices Through Multi Protocol Label Switching." In: *IEEE Transactions on Smart Grid* 5.3, pp. 1210–1215. ISSN: 1949-3053. DOI: [10.1109/TSG.2014.2301723](https://doi.org/10.1109/TSG.2014.2301723).
- Bernal-Agustín, José L. et al. (2007). "Realistic electricity market simulator for energy and economic studies." In: *Electric Power Systems Research* 77.1, pp. 46–54. ISSN: 0378-7796. DOI: <https://doi.org/10.1016/j.epsr.2006.01.007>. URL: <https://www.sciencedirect.com/science/article/pii/S0378779606000228>.
- Bilakanti, N., F. Lambert, and D. Divan (2018). "Integration of Distributed Energy Resources and Microgrids - Utility Challenges." In: *2018 IEEE Electronic Power Grid (eGrid)*, pp. 1–6.
- Borlase, Stuart (2018). *Smart Grids Advanced Technologies and Solutions*. Ed. by 2. CRC Press, p. 828. ISBN: 9781498799553. DOI: [10.1201/9781351228480](https://doi.org/10.1201/9781351228480).
- Bu, F. et al. (2019). "A Time-Series Distribution Test System Based on Real Utility Data." In: *2019 North American Power Symposium (NAPS)*, pp. 1–6. DOI: [10.1109/NAPS46351.2019.8999982](https://doi.org/10.1109/NAPS46351.2019.8999982).
- Byrne, R. H. et al. (2018). "Energy Management and Optimization Methods for Grid Energy Storage Systems." In: *IEEE Access* 6, pp. 13231–13260. ISSN: 2169-3536. DOI: [10.1109/ACCESS.2017.2741578](https://doi.org/10.1109/ACCESS.2017.2741578).
- Cai, Z. et al. (2019). "A New Grouping Protocol for Smart Grids." In: *IEEE Transactions on Smart Grid* 10.1, pp. 955–966. ISSN: 1949-3053. DOI: [10.1109/TSG.2017.2756863](https://doi.org/10.1109/TSG.2017.2756863).
- Carpinelli, G. et al. (2013). "Optimal Integration of Distributed Energy Storage Devices in Smart Grids." In: *IEEE Transactions on Smart Grid* 4.2, pp. 985–995. DOI: [10.1109/TSG.2012.2231100](https://doi.org/10.1109/TSG.2012.2231100).
- Chakraborty, A. and A. Bose (2017). "Smart Grid Simulations and Their Supporting Implementation Methods." In: *Proceedings of the IEEE* 105.11, pp. 2220–2243. ISSN: 0018-9219. DOI: [10.1109/JPROC.2017.2737635](https://doi.org/10.1109/JPROC.2017.2737635).
- Chen, Y. and V. Dinavahi (2014). "Hardware Emulation Building Blocks for Real-Time Simulation of Large-Scale Power Grids." In: *IEEE Transactions on Industrial Informatics* 10.1, pp. 373–381. ISSN: 1551-3203. DOI: [10.1109/TII.2013.2243742](https://doi.org/10.1109/TII.2013.2243742).
- Chiniforoosh, S. et al. (2010). "Definitions and Applications of Dynamic Average Models for Analysis of Power Systems." In: *IEEE Transactions on Power Delivery* 25.4, pp. 2655–2669. ISSN: 0885-8977. DOI: [10.1109/TPWRD.2010.2043859](https://doi.org/10.1109/TPWRD.2010.2043859).
- Christakou, K. et al. (2013). "Efficient Computation of Sensitivity Coefficients of Node Voltages and Line Currents in Unbalanced Radial Electrical Distribution Networks." In: *IEEE Transactions on Smart Grid* 4.2, pp. 741–750. DOI: [10.1109/TSG.2012.2221751](https://doi.org/10.1109/TSG.2012.2221751).
- Cinergia (2020). *GE&EL + vAC/DC v7 ePLUS*. Tech. rep., p. 12. URL: <https://www.cinergia.coop/wp-content/uploads/2020/09/All-Terrain-v7-ePLUS-June2020.pdf>.
- (2021). *Grid Simulator (GE+)*. URL: <https://www.cinergia.coop/family/regenerative-grid-simulator/>. (accessed: 01.03.2021).
- CNIL (2018). *Le règlement général sur la protection des données - RGPD*. URL: <https://www.cnil.fr/fr/reglement-europeen-protection-donnees>. (accessed: 11.11.2020).

- CRE (2018). *Présentation des réseaux d'électricité*. URL: <https://www.cre.fr/Electricite/Recherche-d-electricite/Presentation-des-reseaux-d-electricite>. (accessed: 14.01. 2021).
- Dehalwar, Vasudev et al. (2017). "Electricity load forecasting for urban area using weather forecast information." In: *2016 IEEE International Conference on Power and Renewable Energy, ICPRE 2016*, pp. 355–359. DOI: [10.1109/ICPRE.2016.7871231](https://doi.org/10.1109/ICPRE.2016.7871231).
- Devanand, P. et al. (2020). "Advanced Distribution Management System: Improving Distribution Efficiency through an Integrated Approach." In: *IEEE Power and Energy Magazine* 18.1, pp. 55–62. ISSN: 15584216. DOI: [10.1109/MPE.2019.2945345](https://doi.org/10.1109/MPE.2019.2945345).
- Dinavahi, V., R. Iravani, and R. Bonert (2004). "Design of a real-time digital Simulator for a D-STATCOM system." In: *IEEE Transactions on Industrial Electronics* 51.5, pp. 1001–1008. ISSN: 0278-0046. DOI: [10.1109/TIE.2004.834954](https://doi.org/10.1109/TIE.2004.834954).
- Dinc, A. and M. Otkur (2020). "Optimization of Electric Vehicle Battery Size and Reduction Ratio Using Genetic Algorithm." In: *2020 11th International Conference on Mechanical and Aerospace Engineering (ICMAE)*, pp. 281–285. DOI: [10.1109/ICMAE50897.2020.9178899](https://doi.org/10.1109/ICMAE50897.2020.9178899).
- Dufour, C., V. Jalili-Marandi, and J. Bélanger (2012). "Real-Time Simulation Using Transient Stability, ElectroMagnetic Transient and FPGA-Based High-Resolution Solvers." In: *2012 SC Companion: High Performance Computing, Networking Storage and Analysis*, pp. 283–288. DOI: [10.1109/SC.Companion.2012.46](https://doi.org/10.1109/SC.Companion.2012.46).
- Dugan, R. (2012). *Storage Model Dynamics DLL (DynaDLL)*. EPRI. URL: <https://sourceforge.net/p/electricdss/code/HEAD/tree/trunk/Doc/OpenDSS\%20Storage\%20Dynamics\%20DLL.doc>.
- Dugan, R. C. and T. E. McDermott (2011). "An open source platform for collaborating on smart grid research." In: *2011 IEEE Power and Energy Society General Meeting*, pp. 1–7. DOI: [10.1109/PES.2011.6039829](https://doi.org/10.1109/PES.2011.6039829).
- Dugan, Roger (2015). *Summary of EPRI Test Circuits*. EPRI. URL: <https://sourceforge.net/p/electricdss/code/HEAD/tree/trunk/Distrib/EPRI TestCircuits/Readme.pdf>.
- Dugan, Roger and Andrea Ballanti (May 2017). *Cable Modeling in OpenDSS*. EPRI. URL: <https://sourceforge.net/p/electricdss/code/HEAD/tree/trunk/Distrib/Doc/TechNote\%20CableModelling.pdf>.
- Dugan, Roger, Davis Montenegro, and Andrea Ballanti (June 2020). *Reference Guide. The Open Distribution System Simulator (OpenDSS)*. EPRI. URL: <https://sourceforge.net/p/electricdss/code/HEAD/tree/trunk/Doc/OpenDSSManual.docx>.
- Džafić, I. et al. (2014). "A Sensitivity Approach to Model Local Voltage Controllers in Distribution Networks." In: *IEEE Transactions on Power Systems* 29.3, pp. 1419–1428. DOI: [10.1109/TPWRS.2013.2290813](https://doi.org/10.1109/TPWRS.2013.2290813).
- Eguía, P. et al. (2019). "Optimum allocation of BESS for power quality improvement. A comparative study." In: *2019 International Conference on Clean Electrical Power (ICCEP)*, pp. 450–455. DOI: [10.1109/ICCEP.2019.8890080](https://doi.org/10.1109/ICCEP.2019.8890080).
- Entsoe (2018). *Final Report*. URL: [https://www.entsoe.eu/network\\_codes/cnc/expert-groups/](https://www.entsoe.eu/network_codes/cnc/expert-groups/). (accessed: 14.04.2021).
- EU (2016). "Regulation (EU) 2016/679 of the European Parliament and of the Council." In: *Official Journal of the European Union* 59.L 119, 1–88. ISSN: 1977-0677. URL: [https://eur-lex.europa.eu/legal-content/FR/TXT/HTML/?uri=CELEX:32016R0679R\(02\)&qid=1528814703534&from=en](https://eur-lex.europa.eu/legal-content/FR/TXT/HTML/?uri=CELEX:32016R0679R(02)&qid=1528814703534&from=en).
- Eyer, J. and G. Corey (Jan. 2011). "Energy storage for the electricity grid: Benefits and market potential assessment guide." In: pp. 1–232.

- Eyer, Jim and Garth Corey (2010). *Energy Storage for the Electricity Grid: Benefits and Market Potential Assessment Guide*. Tech. rep. SANDIA. URL: <https://www.sandia.gov/ess-ssl/publications/SAND2010-0815.pdf>.
- Faruque, M. D. Omar et al. (2015). "Real-Time Simulation Technologies for Power Systems Design, Testing, and Analysis." In: *IEEE Power and Energy Technology Systems Journal* 2.2, pp. 63–73. ISSN: 2332-7707. DOI: [10.1109/JPETS.2015.2427370](https://doi.org/10.1109/JPETS.2015.2427370).
- Faruque, M. O. Omar and V. Dinavahi (2010). "Hardware-in-the-Loop Simulation of Power Electronic Systems Using Adaptive Discretization." In: *IEEE Transactions on Industrial Electronics* 57.4, pp. 1146–1158. ISSN: 0278-0046. DOI: [10.1109/TIE.2009.2036647](https://doi.org/10.1109/TIE.2009.2036647).
- Ferreira, K., W. M. dos Santos, and A. César Rueda Medina (2019). "Sizing of Supercapacitor and BESS for peak shaving applications." In: *2019 IEEE 15th Brazilian Power Electronics Conference and 5th IEEE Southern Power Electronics Conference (COBEP/SPEC)*, pp. 1–6. DOI: [10.1109/COBEP/SPEC44138.2019.9065558](https://doi.org/10.1109/COBEP/SPEC44138.2019.9065558).
- Forth, B. and T. Tobin (2002). "Right Power, Right Price [Enterprise Energy Management Systems]." In: *IEEE Computer Applications in Power* 15.2, pp. 22–27. ISSN: 0895-0156. DOI: [10.1109/67.993756](https://doi.org/10.1109/67.993756).
- Fujimoto, Richard (Dec. 2007). "Parallel and Distributed Simulation." In: *Winter Simulation Conference Proceedings*, pp. 429–464. DOI: [10.1002/9780470172445.ch12](https://doi.org/10.1002/9780470172445.ch12).
- Galat, N. S. and P. M. Sonawane (2017). "Distribution system feeder reconfiguration by robust optimization method, objectives and solution methods." In: *2017 International Conference on Intelligent Computing and Control Systems (ICICCS)*, pp. 248–251. DOI: [10.1109/ICCONS.2017.8250719](https://doi.org/10.1109/ICCONS.2017.8250719).
- Garau, Michele et al. (2018). "Co-simulation of smart distribution network fault management and reconfiguration with LTE communication." In: *Energies* 11.6. DOI: [10.3390/en11061332](https://doi.org/10.3390/en11061332).
- Garcia-Garcia, L., E. A. Paaso, and M. Avendano-Mora (2017). "Assessment of battery energy storage for distribution capacity upgrade deferral." In: *2017 IEEE Power Energy Society Innovative Smart Grid Technologies Conference (ISGT)*, pp. 1–5. DOI: [10.1109/ISGT.2017.8086030](https://doi.org/10.1109/ISGT.2017.8086030).
- Gharavi, H. and R. Ghafurian (2011). "Smart Grid: The Electric Energy System of the Future [Scanning the Issue]." In: *Proceedings of the IEEE* 99.6, pp. 917–921. ISSN: 0018-9219. DOI: [10.1109/JPROC.2011.2124210](https://doi.org/10.1109/JPROC.2011.2124210).
- Gick, B., T. Gallenkamp, and T. Wess (1996). "Introducing Digital Simulation Into An Analogue Real-time Power System Simulator." In: *Sixth International Conference on AC and DC Power Transmission*, pp. 369–374. DOI: [10.1049/cp:19960386](https://doi.org/10.1049/cp:19960386).
- Giri, J. (2015). "Proactive Management of the Future Grid." In: *IEEE Power and Energy Technology Systems Journal* 2.2, pp. 43–52. ISSN: 2332-7707. DOI: [10.1109/JPETS.2015.2408212](https://doi.org/10.1109/JPETS.2015.2408212).
- Goodman, F. and M. McGranaghan (2005). "EPRI Research Plan for Advanced Distribution Automation." In: *IEEE Power Engineering Society General Meeting, 2005*, 2620 Vol. 3-. DOI: [10.1109/PES.2005.1489389](https://doi.org/10.1109/PES.2005.1489389).
- Goswami, Kuheli, Ayandeep Ganguly, and Arindam Kumar Sil (2018). "Day ahead forecasting and peak load management using multivariate auto regression technique." In: *Proceedings of 2018 IEEE Applied Signal Processing Conference, ASPCON 2018* 1, pp. 279–282. DOI: [10.1109/ASPCON.2018.8748661](https://doi.org/10.1109/ASPCON.2018.8748661).
- Groom, S. L. (2014). "Can We Measure Our Way Out of Trouble? The Truth Behind Condition Monitoring." In: *6th IET Conference on Railway Condition Monitoring (RCM 2014)*, pp. 1–8. DOI: [10.1049/cp.2014.1007](https://doi.org/10.1049/cp.2014.1007).

- Guillaud, X. et al. (2015). "Applications of Real-Time Simulation Technologies in Power and Energy Systems." In: *IEEE Power and Energy Technology Systems Journal* 2.3, pp. 103–115. ISSN: 2332-7707. DOI: [10.1109/JPETS.2015.2445296](https://doi.org/10.1109/JPETS.2015.2445296).
- Guo, J. et al. (2015). "Design and Implementation of a Real-Time Off-Grid Operation Detection Tool from a Wide-Area Measurements Perspective." In: *IEEE Transactions on Smart Grid* 6.4, pp. 2080–2087. ISSN: 1949-3053. DOI: [10.1109/TSG.2014.2350913](https://doi.org/10.1109/TSG.2014.2350913).
- Gurralla, G. et al. (2016). "Parareal in Time for Fast Power System Dynamic Simulations." In: *IEEE Transactions on Power Systems* 31.3, pp. 1820–1830. ISSN: 0885-8950. DOI: [10.1109/TPWRS.2015.2434833](https://doi.org/10.1109/TPWRS.2015.2434833).
- Hameed, Z., S. Hashemi, and C. Træholt (2020). "Site Selection Criteria for Battery Energy Storage in Power Systems." In: *2020 IEEE Canadian Conference on Electrical and Computer Engineering (CCECE)*, pp. 1–7. DOI: [10.1109/CCECE47787.2020.9255678](https://doi.org/10.1109/CCECE47787.2020.9255678).
- Hammad, Eman, Mellitus Ezeme, and Abdallah Farraj (2019). "Implementation and development of an offline co-simulation testbed for studies of power systems cyber security and control verification." In: *International Journal of Electrical Power and Energy Systems* 104.March 2018, pp. 817–826. ISSN: 01420615. DOI: [10.1016/j.ijepes.2018.07.058](https://doi.org/10.1016/j.ijepes.2018.07.058). URL: <https://doi.org/10.1016/j.ijepes.2018.07.058>.
- Harmanani, Haidar M. (2020). *Parallel Programming for Multi- Core and Cluster Systems*. URL: <http://harmanani.github.io/classes/csc447/Notes/Lecture04.pdf>. (accessed: 18.12.2020).
- Hashmi, M. U. et al. (2020). "Arbitrage With Power Factor Correction Using Energy Storage." In: *IEEE Transactions on Power Systems* 35.4, pp. 2693–2703. DOI: [10.1109/TPWRS.2020.2969978](https://doi.org/10.1109/TPWRS.2020.2969978).
- Hayes, B. P. and M. Prodanovic (2016). "State Forecasting and Operational Planning for Distribution Network Energy Management Systems." In: *IEEE Transactions on Smart Grid* 7.2, pp. 1002–1011. DOI: [10.1109/TSG.2015.2489700](https://doi.org/10.1109/TSG.2015.2489700).
- He, M. and J. Zhang (2011). "A Dependency Graph Approach for Fault Detection and Localization Towards Secure Smart Grid." In: *IEEE Transactions on Smart Grid* 2.2, pp. 342–351. ISSN: 1949-3053. DOI: [10.1109/TSG.2011.2129544](https://doi.org/10.1109/TSG.2011.2129544).
- Hernandez, M. et al. (2017). "Visualization of Time-Sequential Simulation for Large Power Distribution Systems." In: *2017 IEEE Manchester PowerTech*, pp. 1–6. DOI: [10.1109/PTC.2017.7981076](https://doi.org/10.1109/PTC.2017.7981076).
- Hernandez, M. E. et al. (2018). "Embedded Real-Time Simulation Platform for Power Distribution Systems." In: *IEEE Access* 6, pp. 6243–6256. ISSN: 2169-3536. DOI: [10.1109/ACCESS.2017.2784318](https://doi.org/10.1109/ACCESS.2017.2784318).
- Hill, C. et al. (June 2012). "Battery Energy Storage for Enabling Integration of Distributed Solar Power Generation." In: *Smart Grid, IEEE Transactions on* 3, pp. 850–857. DOI: [10.1109/TSG.2012.2190113](https://doi.org/10.1109/TSG.2012.2190113).
- Hongyan Piao et al. (2015). "Control strategy of battery energy storage system to participate in the second frequency regulation." In: *2015 International Symposium on Smart Electric Distribution Systems and Technologies (EDST)*, pp. 53–57. DOI: [10.1109/SEDST.2015.7315182](https://doi.org/10.1109/SEDST.2015.7315182).
- Hu, X. et al. (2020). "Advanced Fault Diagnosis for Lithium-Ion Battery Systems: A Review of Fault Mechanisms, Fault Features, and Diagnosis Procedures." In: *IEEE Industrial Electronics Magazine* 14.3, pp. 65–91. DOI: [10.1109/MIE.2020.2964814](https://doi.org/10.1109/MIE.2020.2964814).
- Huang, Q. and V. Vittal (2016). "Application of Electromagnetic Transient-Transient Stability Hybrid Simulation to FIDVR Study." In: *IEEE Transactions on Power Systems* 31.4, pp. 2634–2646. ISSN: 0885-8950. DOI: [10.1109/TPWRS.2015.2479588](https://doi.org/10.1109/TPWRS.2015.2479588).

- Huang, Q. and V. Vittal (2018). "Advanced EMT and Phasor-Domain Hybrid Simulation With Simulation Mode Switching Capability for Transmission and Distribution Systems." In: *IEEE Transactions on Power Systems* 33.6, pp. 6298–6308. ISSN: 0885-8950. DOI: [10.1109/TPWRS.2018.2834561](https://doi.org/10.1109/TPWRS.2018.2834561).
- Ibarra, L. et al. (June 2017). "Overview of Real-Time Simulation as a Supporting Effort to Smart-Grid Attainment." In: *Energies* 10, no. 6, p. 817. DOI: [10.3390/en10060817](https://doi.org/10.3390/en10060817).
- Ignatova, V., P. Granjon, and S. Bacha (2009). "Space Vector Method for Voltage Dips and Swells Analysis." In: *IEEE Transactions on Power Delivery* 24.4, pp. 2054–2061. DOI: [10.1109/TPWRD.2009.2028787](https://doi.org/10.1109/TPWRD.2009.2028787).
- Ilamparithi, T., S. Abourdia, and T. Kirk (2016). "On the Use of Real-Time Simulators for the Test and Validation of Protection and Control Systems of Micro-Grids and Smart-Grids." In: *2016 Saudi Arabia Smart Grid (SASG)*, pp. 1–5. DOI: [10.1109/SASG.2016.7849658](https://doi.org/10.1109/SASG.2016.7849658).
- Ilonen, J. et al. (2005). "Diagnosis Tool for Motor Condition Monitoring." In: *IEEE Transactions on Industry Applications* 41.4, pp. 963–971. ISSN: 0093-9994. DOI: [10.1109/TIA.2005.851001](https://doi.org/10.1109/TIA.2005.851001).
- Instruments, National (2021a). *Application Design Patterns: Master/Slave*. URL: <https://knowledge.ni.com/KnowledgeArticleDetails?id=kA03q000000x1r9CAA&l=fr-FR>. (accessed: 10.03.2021).
- (2021b). *Architecture producteur/consommateur dans LabVIEW*. URL: <https://www.ni.com/fr-fr/support/documentation/supplemental/21/producer-consumer-architecture-in-labview0.html>. (accessed: 08.03.2021).
- Isaac, S. J. et al. (2011). "A survey of wireless sensor network applications from a power utility's distribution perspective." In: *IEEE Africon '11*, pp. 1–5. DOI: [10.1109/AFRCON.2011.6072184](https://doi.org/10.1109/AFRCON.2011.6072184).
- Jalili-Marandi, V. and V. Dinavahi (2009). "Instantaneous Relaxation-Based Real-Time Transient Stability Simulation." In: *IEEE Transactions on Power Systems* 24.3, pp. 1327–1336. ISSN: 0885-8950. DOI: [10.1109/TPWRS.2009.2021210](https://doi.org/10.1109/TPWRS.2009.2021210).
- Jalili-Marandi, V. et al. (2009). "Interfacing techniques for transient stability and electromagnetic transient programs IEEE task orce on Interfacing Techniques for Simulation Tools." In: *IEEE Transactions on Power Delivery* 24.4, pp. 2385–2395. ISSN: 0885-8977. DOI: [10.1109/TPWRD.2008.2002889](https://doi.org/10.1109/TPWRD.2008.2002889).
- Jamroen, C., A. Pannawan, and S. Sirisukprasert (2018). "Battery Energy Storage System Control for Voltage Regulation in Microgrid with High Penetration of PV Generation." In: *2018 53rd International Universities Power Engineering Conference (UPEC)*, pp. 1–6. DOI: [10.1109/UPEC.2018.8541888](https://doi.org/10.1109/UPEC.2018.8541888).
- Jang-Jaccard, Julian and Surya Nepal (2014). "A survey of emerging threats in cybersecurity." In: *Journal of Computer and System Sciences* 80.5. Special Issue on Dependable and Secure Computing, pp. 973–993. ISSN: 0022-0000. DOI: <https://doi.org/10.1016/j.jcss.2014.02.005>. URL: <https://www.sciencedirect.com/science/article/pii/S0022000014000178>.
- Jayashree, S. and K. Malarvizhi (2020). "Methodologies for Optimal Sizing of Battery Energy Storage in Microgrids : A Comprehensive Review." In: *2020 International Conference on Computer Communication and Informatics (ICCCI)*, pp. 1–5. DOI: [10.1109/ICCCI48352.2020.9104131](https://doi.org/10.1109/ICCCI48352.2020.9104131).
- Jeon, J. et al. (2010). "Development of Hardware In-the-Loop Simulation System for Testing Operation and Control Functions of Microgrid." In: *IEEE Transactions on Power Electronics* 25.12, pp. 2919–2929. ISSN: 0885-8993. DOI: [10.1109/TPEL.2010.2078518](https://doi.org/10.1109/TPEL.2010.2078518).
- Jewell, W. and Zhouxing Hu (2012). "The role of energy storage in transmission and distribution efficiency." In: *PES T D 2012*, pp. 1–4. DOI: [10.1109/TDC.2012.6281537](https://doi.org/10.1109/TDC.2012.6281537).



- Jiang, W., V. Vittal, and G. T. Heydt (2008). "Diakoptic State Estimation Using Phasor Measurement Units." In: *IEEE Transactions on Power Systems* 23.4, pp. 1580–1589. DOI: [10.1109/TPWRS.2008.2002285](https://doi.org/10.1109/TPWRS.2008.2002285).
- Jinming, C. et al. (2018). "Application Prospect of Edge Computing in Smart Distribution." In: *2018 China International Conference on Electricity Distribution (CICED)*, pp. 1370–1375. DOI: [10.1109/CICED.2018.8592104](https://doi.org/10.1109/CICED.2018.8592104).
- Johar, Fauzi et al. (Nov. 2013). "A review of Genetic Algorithms and Parallel Genetic Algorithms on Graphics Processing Unit (GPU)." In: pp. 264–269. DOI: [10.1109/ICCSCE.2013.6719971](https://doi.org/10.1109/ICCSCE.2013.6719971).
- Kawakami, Yasuaki, Ryoichi Komiyama, and Yasumasa Fujii (2018). "Penetration of Electric Vehicles toward 2050: Analysis Utilizing an Energy System Model Incorporating High-Temporal-Resolution Power Generation Sector." In: *IFAC-PapersOnLine* 51.28. 10th IFAC Symposium on Control of Power and Energy Systems CPES 2018, pp. 598–603. ISSN: 2405-8963. DOI: <https://doi.org/10.1016/j.ifacol.2018.11.769>. URL: <https://www.sciencedirect.com/science/article/pii/S2405896318334906>.
- Key, T. (Dec. 2000). *Engineering Guide for Integration of Distributed Generation and Storage into Power Distribution Systems*. Tech. rep. 1000419. EPRI, p. 306. URL: <https://www.epri.com/research/products/000000000001000419>.
- Khan, S. et al. (2018). "Artificial intelligence framework for smart city microgrids: State of the art, challenges, and opportunities." In: *2018 Third International Conference on Fog and Mobile Edge Computing (FMEC)*, pp. 283–288. DOI: [10.1109/TPWRS.2008.2002285](https://doi.org/10.1109/TPWRS.2008.2002285).
- Klansupar, C. and S. Chaitusaney (2020). "Optimal Sizing of Utility-scaled Battery with Consideration of Battery Installation Cost and System Power Generation Cost." In: *2020 17th International Conference on Electrical Engineering/Electronics, Computer, Telecommunications and Information Technology (ECTI-CON)*, pp. 498–501. DOI: [10.1109/ECTI-CON49241.2020.9158074](https://doi.org/10.1109/ECTI-CON49241.2020.9158074).
- Kotsampopoulos, P. et al. (2018). "A Benchmark System for Hardware-in-the-Loop Testing of Distributed Energy Resources." In: *IEEE Power and Energy Technology Systems Journal* 5.3, pp. 94–103. ISSN: 2332-7707. DOI: [10.1109/JPETS.2018.2861559](https://doi.org/10.1109/JPETS.2018.2861559).
- Kumar, Abhishek et al. (2019). "Strategic integration of battery energy storage systems with the provision of distributed ancillary services in active distribution systems." In: *Applied Energy* 253, p. 113503. ISSN: 0306-2619. DOI: <https://doi.org/10.1016/j.apenergy.2019.113503>. URL: <http://www.sciencedirect.com/science/article/pii/S0306261919311778>.
- Kumtepli, V. et al. (2020). "Energy Arbitrage Optimization With Battery Storage: 3D-MILP for Electro-Thermal Performance and Semi-Empirical Aging Models." In: *IEEE Access* 8, pp. 204325–204341. DOI: [10.1109/ACCESS.2020.3035504](https://doi.org/10.1109/ACCESS.2020.3035504).
- Lauss, Georg et al. (Sept. 2017). "Development of a Controller-Hardware-in-the-Loop (CHIL) Toolbox Applied for Pre-Certification Services for Grid-Connected PV Inverters According to the State-of-the-Art BDEW RL Guideline and FGW TR3 Standard." In: *33rd European Photovoltaic Solar Energy Conference and Exhibition*, pp. 1841–1846. DOI: [10.4229/EUPVSEC20172017-5DV.3.45](https://doi.org/10.4229/EUPVSEC20172017-5DV.3.45).
- Le-Huy, P. et al. (2006). "Real-Time Simulation of Power Electronics in Power Systems using an FPGA." In: *2006 Canadian Conference on Electrical and Computer Engineering*, pp. 873–877. DOI: [10.1109/CCECE.2006.277356](https://doi.org/10.1109/CCECE.2006.277356).
- Lin, Chih-Yuan (June 2020). *A timing approach to network-based anomaly detection for SCADA systems*. ISBN: 9789179298364. DOI: [10.3384/lic.diva-165155](https://doi.org/10.3384/lic.diva-165155).

- Liu, Jiayan et al. (Apr. 2020). "Modeling and Analysis Considering the Time Series Characteristics for Distribution Network with High Penetration of Renewable Energy." In: *IET Generation, Transmission & Distribution* 14. DOI: [10.1049/iet-gtd.2019.1874](https://doi.org/10.1049/iet-gtd.2019.1874).
- Luna, A. C. et al. (2018). "Online Energy Management Systems for Microgrids: Experimental Validation and Assessment Framework." In: *IEEE Transactions on Power Electronics* 33.3, pp. 2201–2215. ISSN: 0885-8993. DOI: [10.1109/TPEL.2017.2700083](https://doi.org/10.1109/TPEL.2017.2700083).
- Madani, V. et al. (2015). "Distribution Automation Strategies Challenges and Opportunities in a Changing Landscape." In: *IEEE Transactions on Smart Grid* 6.4, pp. 2157–2165. ISSN: 1949-3053. DOI: [10.1109/TSG.2014.2368382](https://doi.org/10.1109/TSG.2014.2368382).
- Mahseredjian, J., V. Dinavahi, and J. Martinez (2009). "Simulation Tools for Electromagnetic Transients in Power Systems: Overview and Challenges." In: *IEEE Transactions on Power Delivery* 24.3, pp. 1657–1669. ISSN: 0885-8977. DOI: [10.1109/TPWRD.2008.2008480](https://doi.org/10.1109/TPWRD.2008.2008480).
- Martinez, D., H. Henao, and G. A. Capolino (2019). "Overview of Condition Monitoring Systems for Power Distribution Grids." In: *2019 IEEE 12th International Symposium on Diagnostics for Electrical Machines, Power Electronics and Drives (SDEMPED)*, pp. 160–166. DOI: [10.1109/DEMPED.2019.8864872](https://doi.org/10.1109/DEMPED.2019.8864872).
- Masud, Abu Naser, Björn Lisper, and Federico Ciccozzi (2018). "Automatic Inference of Task Parallelism in Task-Graph-Based Actor Models." In: *IEEE Access* 6, pp. 78965–78991. DOI: [10.1109/ACCESS.2018.2885705](https://doi.org/10.1109/ACCESS.2018.2885705).
- Mazza, A. et al. (Dec. 2019). "Location and Sizing of Battery Energy Storage Units in Low Voltage Distribution Networks." In: *Energies* 13, p. 52. DOI: [10.3390/en13010052](https://doi.org/10.3390/en13010052).
- McGranaghan, M. and B. Deaver (2012). "Sensors and monitoring challenges in the smart grid." In: *2012 Future of Instrumentation International Workshop (FIIW) Proceedings*, pp. 1–4. DOI: [10.1109/FIIW.2012.6378327](https://doi.org/10.1109/FIIW.2012.6378327).
- McGranaghan, M. and F. Goodman (2005). "Technical and System Requirements for Advanced Distribution Automation." In: *CIREC 2005 - 18th International Conference and Exhibition on Electricity Distribution*, pp. 1–5. DOI: [10.1049/cp:20051374](https://doi.org/10.1049/cp:20051374).
- Moghe, R., D. Tholomier, and D. Divan (2016). "Distribution grid edge control: Field demonstrations." In: *2016 IEEE Power and Energy Society General Meeting (PESGM)*, pp. 1–5. DOI: [10.1109/PESGM.2016.7742011](https://doi.org/10.1109/PESGM.2016.7742011).
- Montaña, D. A. M. et al. (2018). "Hardware and Software Integration as a Realist SCADA Environment to Test Protective Relaying Control." In: *IEEE Transactions on Industry Applications* 54.2, pp. 1208–1217. ISSN: 0093-9994. DOI: [10.1109/TIA.2017.2780051](https://doi.org/10.1109/TIA.2017.2780051).
- Montenegro, D. and R. C. Dugan (2017). "OpenDSS and OpenDSS-PM open source libraries for NI LabVIEW." In: *2017 IEEE Workshop on Power Electronics and Power Quality Applications (PEPQA)*, pp. 1–5. DOI: [10.1109/PEPQA.2017.7981639](https://doi.org/10.1109/PEPQA.2017.7981639).
- Montenegro, D., G. A. Ramos, and S. Bacha (2016). "Multilevel A-Diakoptics for the Dynamic Power-Flow Simulation of Hybrid Power Distribution Systems." In: *IEEE Transactions on Industrial Informatics* 12.1, pp. 267–276. ISSN: 1551-3203. DOI: [10.1109/TII.2015.2506541](https://doi.org/10.1109/TII.2015.2506541).
- Montenegro, D., G. A. Ramos, and S. Bacha (2017). "A-Diakoptics for the Multicore Sequential-Time Simulation of Microgrids Within Large Distribution Systems." In: *IEEE Transactions on Smart Grid* 8.3, pp. 1211–1219. ISSN: 1949-3053. DOI: [10.1109/TSG.2015.2507980](https://doi.org/10.1109/TSG.2015.2507980).
- Montenegro, Davis (Nov. 2015). "Actor's based diakoptics for the simulation, monitoring and control of smart grids." Theses. Universidad de los Andes (Bogotá). URL: <https://tel.archives-ouvertes.fr/tel-01260398>.
- (June 2017). *Direct connection Shared Library (DLL) for OpenDSS*. EPRI. URL: [https://sourceforge.net/p/electricdss/code/HEAD/tree/trunk/Distrib/Doc/OpenDSS\\_Direct\\_DLL.pdf](https://sourceforge.net/p/electricdss/code/HEAD/tree/trunk/Distrib/Doc/OpenDSS_Direct_DLL.pdf).

- Montenegro, Davis and Roger Dugan (Feb. 2019). *Actor based Diakoptics (A-Diakoptics) suite for OpenDSS*. EPRI. URL: [https://sourceforge.net/p/electricdss/code/HEAD/tree/trunk/Version8/Distrib/Doc/A\\_Diakoptics\\_Suite.pdf](https://sourceforge.net/p/electricdss/code/HEAD/tree/trunk/Version8/Distrib/Doc/A_Diakoptics_Suite.pdf).
- Montenegro, Davis, Roger Dugan, and Matthew Reno (June 2017). "Open Source Tools for High Performance Quasi-Static-Time-Series Simulation Using Parallel Processing." In: DOI: [10.1109/PVSC.2017.8521538](https://doi.org/10.1109/PVSC.2017.8521538).
- Mtihlenbein, Heinz (1996). "Genetic Algorithms and Parallel Processing." In: *Wuhan University Journal of Natural Sciences* 1, pp. 630–639. DOI: <https://doi.org/10.1007/BF02900898>.
- Mühlenbein, H., M. Schomisch, and J. Born (1991). "The parallel genetic algorithm as function optimizer." In: vol. 17. 6, pp. 619–632. DOI: [https://doi.org/10.1016/S0167-8191\(05\)80052-3](https://doi.org/10.1016/S0167-8191(05)80052-3). URL: <https://www.sciencedirect.com/science/article/pii/S0167819105800523>.
- Nagel, I. et al. (2010). "High-speed power system stability simulation using analog computation: Systematic error analysis." In: *Proceedings of the 17th International Conference Mixed Design of Integrated Circuits and Systems - MIXDES 2010*, pp. 514–518.
- Nagel, I. et al. (2013). "High-Speed Power System Transient Stability Simulation Using Highly Dedicated Hardware." In: *IEEE Transactions on Power Systems* 28.4, pp. 4218–4227. ISSN: 0885-8950. DOI: [10.1109/TPWRS.2013.2259185](https://doi.org/10.1109/TPWRS.2013.2259185).
- Nayak, R. K., B. S. P. Mishra, and Jnyanaranjan Mohanty (2017). "An overview of GA and PGA." In: *International Journal of Computer Applications* 178.6, pp. 7–9. ISSN: 0975-8887. DOI: [10.5120/ijca2017915829](https://doi.org/10.5120/ijca2017915829). URL: <http://www.ijcaonline.org/archives/volume178/number6/28676-2017915829>.
- NI (2020). *OpenDSS Library for x86 - Electric Power Research Institute*. [Online. October 2020]. URL: <http://sine.ni.com/nips/cds/view/p/lang/fr/nid/215288>.
- Niu, Dong Xiao, Qiang Wang, and Jin Chao Li (2005). "Short term load forecasting model using support vector machine based on artificial neural network." In: *2005 International Conference on Machine Learning and Cybernetics, ICMLC 2005 August*, pp. 4260–4265. DOI: [10.1109/icmlc.2005.1527685](https://doi.org/10.1109/icmlc.2005.1527685).
- Noureen, Subrina Sultana, Nimat Shamim Vishwajit Roy, and Stephen B. Bayne (Nov. 2017). "Real-Time Digital Simulators: A Comprehensive Study on System Overview, Application, and Importance." In: *International Journal of Research and Engineering* 04 No. 11, pp. 266–277. ISSN: 2348-7860. DOI: <http://dx.doi.org/10.21276/ijre.2017.4.11.3>.
- Okwu, Modestus O. and Lagouge K. Tartibu (2021). *Metaheuristic Optimization: Nature-Inspired Algorithms Swarm and Computational Intelligence, Theory and Applications*. Ed. by 1. Vol. 927. Springer International Publishing. ISBN: 978-3-030-61111-8. DOI: [10.1007/978-3-030-61111-8\\_11-8](https://doi.org/10.1007/978-3-030-61111-8_11-8).
- Omar Faruque, M. D. et al. (2015). "Real-Time Simulation Technologies for Power Systems Design, Testing, and Analysis." In: *IEEE Power and Energy Technology Systems Journal* 2.2, pp. 63–73. DOI: [10.1109/JPETS.2015.2427370](https://doi.org/10.1109/JPETS.2015.2427370).
- Oracle (2021). *MySQL 8.0 Reference Manual*. Tech. rep. URL: <https://dev.mysql.com/doc/refman/8.0/en/introduction.html>.
- Oudalov, A., R. Cherkaoui, and A. Beguin (2007). "Sizing and Optimal Operation of Battery Energy Storage System for Peak Shaving Application." In: *2007 IEEE Lausanne Power Tech*, pp. 621–625. DOI: [10.1109/PCT.2007.4538388](https://doi.org/10.1109/PCT.2007.4538388).
- Palmintier, Bryan et al. (2015). "A Power Hardware-in-the-Loop Platform With Remote Distribution Circuit Cosimulation." In: *IEEE Transactions on Industrial Electronics* 62.4, pp. 2236–2245. DOI: [10.1109/TIE.2014.2367462](https://doi.org/10.1109/TIE.2014.2367462).

- Panwar, M. et al. (2013). "An Overview of Real-Time Hardware-In-The-Loop Capabilities in Digital Simulation for Electric Micro-grids." In: *2013 North American Power Symposium (NAPS)*, pp. 1–6. DOI: [10.1109/NAPS.2013.6666861](https://doi.org/10.1109/NAPS.2013.6666861).
- Park, Hae-woo et al. (2011). "Library Support in an Actor-Based Parallel Programming Platform." In: *IEEE Transactions on Industrial Informatics* 7.2, pp. 340–353. DOI: [10.1109/TII.2011.2123905](https://doi.org/10.1109/TII.2011.2123905).
- PES, IEEE (2015). *The IEEE European Low Voltage Test Feeder*. Tech. rep. URL: <https://site.ieee.org/pes-testfeeders/resources/>.
- (2018). *EPRI Test Circuits*. URL: <https://site.ieee.org/pes-testfeeders/resources/>. (accessed: 12.03.2021).
- (2021). *IEEE PES AMPS DSAS Test Feeder Working Group*. URL: <https://site.ieee.org/pes-testfeeders/>. (accessed: 12.03.2021).
- Phadke, A. et al. (July 2016). "Improving the performance of power system protection using wide area monitoring systems." In: *Journal of Modern Power Systems and Clean Energy* 4, 319–331. DOI: <https://doi.org/10.1007/s40565-016-0211-x>.
- Podmore, R. and M. R. Robinson (2010). "The Role of Simulators for Smart Grid Development." In: *IEEE Transactions on Smart Grid* 1.2, pp. 205–212. ISSN: 1949-3053. DOI: [10.1109/TSG.2010.2055905](https://doi.org/10.1109/TSG.2010.2055905).
- Prabakar, Kumaraguru et al. (2020). "Open-source framework for data storage and visualization of real-time experiments." In: pp. 1–6. DOI: [10.1109/kpec47870.2020.9167667](https://doi.org/10.1109/kpec47870.2020.9167667).
- Prieur, Vincent and Jean-Louis Fau (2015). *Bilan annuel 2015. ELD Régie Gazelec de Péronne*. Tech. rep. RTE. URL: <https://www.services-rte.com/fr/home.html>.
- Qi, H. et al. (2011). "A Resilient Real-Time System Design for a Secure and Reconfigurable Power Grid." In: *IEEE Transactions on Smart Grid* 2.4, pp. 770–781. ISSN: 1949-3053. DOI: [10.1109/TSG.2011.2159819](https://doi.org/10.1109/TSG.2011.2159819).
- Qiao, W. and Lu (2015). "A Survey on Wind Turbine Condition Monitoring and Fault Diagnosis—Part I: Components and Subsystems." In: *IEEE Transactions on Industrial Electronics* 62.10, pp. 6536–6545. ISSN: 0278-0046. DOI: [10.1109/TIE.2015.2422112](https://doi.org/10.1109/TIE.2015.2422112).
- Raghav, Shivani et al. (2015). "GPU Acceleration for Simulating Massively Parallel Many-Core Platforms." In: *IEEE Transactions on Parallel and Distributed Systems* 26.5, pp. 1336–1349. DOI: [10.1109/TPDS.2014.2319092](https://doi.org/10.1109/TPDS.2014.2319092).
- Raihan, M. I. A. (2016). "Impact of energy storage devices on reliability of distribution system." In: *2016 2nd International Conference on Electrical, Computer Telecommunication Engineering (ICECTE)*, pp. 1–4. DOI: [10.1109/ICECTE.2016.7879630](https://doi.org/10.1109/ICECTE.2016.7879630).
- Rehtanz, C. and X. Guillaud (2016). "Real-Time and Co-Simulations for the Development of Power System Monitoring, Control and Protection." In: *2016 Power Systems Computation Conference (PSCC)*, pp. 1–20. DOI: [10.1109/PSCC.2016.7541030](https://doi.org/10.1109/PSCC.2016.7541030).
- Ren, W. et al. (2011). "Interfacing Issues in Real-Time Digital Simulators." In: *IEEE Transactions on Power Delivery* 26.2, pp. 1221–1230. ISSN: 0885-8977. DOI: [10.1109/TPWRD.2010.2072792](https://doi.org/10.1109/TPWRD.2010.2072792).
- Richards, Mark and Neal Ford (2020). *Fundamentals of Software Architecture*. O'Reilly Media, Inc., p. 303. ISBN: 9781492043454.
- Roberge, V., M. Tarbouchi, and G. Labonte (2013). "Comparison of Parallel Genetic Algorithm and Particle Swarm Optimization for Real-Time UAV Path Planning." In: *IEEE Transactions on Industrial Informatics* 9.1, pp. 132–141. DOI: [10.1109/TII.2012.2198665](https://doi.org/10.1109/TII.2012.2198665).
- Rocha, C. et al. (May 2020). *OpenDSS storage element and storage controller Element*. EPRI. URL: <https://sourceforge.net/p/electricdss/code/HEAD/tree/trunk/Doc/OpenDSS%20STORAGE%20Element.doc>.

- Rocha-Doria, Juan S. et al. (2018). "Design and implementation of a real-time monitoring tool for power engineering education." In: *Computer Applications in Engineering Education* 26.1, pp. 37–48. ISSN: 10990542. DOI: [10.1002/cae.21859](https://doi.org/10.1002/cae.21859).
- Rogers, B. (Oct. 2016). *Time and Locational Value of DER. Methods and Applications*. Tech. rep. 3002008410. EPRI, p. 148. URL: <https://www.epri.com/research/products/3002008410>.
- Romero Aguero, J., A. Khodaei, and R. Masiello (2016). "The Utility and Grid of the Future: Challenges, Needs, and Trends." In: *IEEE Power and Energy Magazine* 14.5, pp. 29–37. ISSN: 1540-7977. DOI: [10.1109/MPE.2016.2577899](https://doi.org/10.1109/MPE.2016.2577899).
- Ross, M., C. Abbey, and G. Joós (2013). "A methodology for optimized Energy Storage sizing with stochastic resources." In: *2013 IEEE Power Energy Society General Meeting*, pp. 1–5. DOI: [10.1109/PESMG.2013.6672948](https://doi.org/10.1109/PESMG.2013.6672948).
- Saboori, Hedayat, Reza Hemmati, and Mehdi Ahmadi Jirdehi (2015). "Reliability improvement in radial electrical distribution network by optimal planning of energy storage systems." In: *Energy* 93, pp. 2299–2312. ISSN: 0360-5442. DOI: <https://doi.org/10.1016/j.energy.2015.10.125>. URL: <https://www.sciencedirect.com/science/article/pii/S0360544215015030>.
- Salee, S. and P. Wirasanti (2018). "Optimal siting and sizing of battery energy storage systems for grid-supporting in electrical distribution network." In: *2018 International ECTI Northern Section Conference on Electrical, Electronics, Computer and Telecommunications Engineering (ECTI-NCON)*, pp. 100–105. DOI: [10.1109/ECTI-NCON.2018.8378290](https://doi.org/10.1109/ECTI-NCON.2018.8378290).
- Salvadori, F. et al. (2013). "Smart Grid Infrastructure Using a Hybrid Network Architecture." In: *IEEE Transactions on Smart Grid* 4.3, pp. 1630–1639. ISSN: 1949-3053. DOI: [10.1109/TSG.2013.2265264](https://doi.org/10.1109/TSG.2013.2265264).
- Schimpe, M. et al. (2018). "Marginal Costs of Battery System Operation in Energy Arbitrage Based on Energy Losses and Cell Degradation." In: *2018 IEEE International Conference on Environment and Electrical Engineering and 2018 IEEE Industrial and Commercial Power Systems Europe (EEEIC / I CPS Europe)*, pp. 1–5. DOI: [10.1109/EEEIC.2018.8493717](https://doi.org/10.1109/EEEIC.2018.8493717).
- Schneider, K. P. et al. (2018). "Analytic Considerations and Design Basis for the IEEE Distribution Test Feeders." In: *IEEE Transactions on Power Systems* 33.3, pp. 3181–3188. DOI: [10.1109/TPWRS.2017.2760011](https://doi.org/10.1109/TPWRS.2017.2760011).
- "Sensitivity Calculation" (2015). In: *Optimization of Power System Operation*. John Wiley & Sons, Ltd. Chap. 3, pp. 51–90. ISBN: 9781118887004. DOI: <https://doi.org/10.1002/9781118887004.ch3>. eprint: <https://onlinelibrary.wiley.com/doi/pdf/10.1002/9781118887004.ch3>. URL: <https://onlinelibrary.wiley.com/doi/abs/10.1002/9781118887004.ch3>.
- Shahirinia, A. H. et al. (2005). "Optimal sizing of hybrid power system using genetic algorithm." In: *2005 International Conference on Future Power Systems*, 6 pp.–6. DOI: [10.1109/FPS.2005.204314](https://doi.org/10.1109/FPS.2005.204314).
- Sheng, S., D. Xianzhong, and W. L. Chan (2008). "Probability Distribution of Fault in Distribution System." In: *IEEE Transactions on Power Systems* 23.3, pp. 1521–1522. DOI: [10.1109/TPWRS.2008.926078](https://doi.org/10.1109/TPWRS.2008.926078).
- Shu, D. et al. (2018). "Dynamic Phasor Based Interface Model for EMT and Transient Stability Hybrid Simulations." In: *IEEE Transactions on Power Systems* 33.4, pp. 3930–3939. ISSN: 0885-8950. DOI: [10.1109/TPWRS.2017.2766269](https://doi.org/10.1109/TPWRS.2017.2766269).
- Singh, Saurabh, Shoeb Hussain, and Mohammad Abid Bazaz (2018). "Short term load forecasting using artificial neural network." In: *2017 4th International Conference on Image Information Processing, ICIIIP 2017* 2018-January, pp. 159–163. DOI: [10.1109/ICIIP.2017.8313703](https://doi.org/10.1109/ICIIP.2017.8313703).
- Sobuś, Jakub and Marek Woda (2016). "CPU Utilization Analysis of Selected Genetic Algorithms in Multi-core Systems for a Certain Class of Problems." In: *Dependability Engineer-*

- ing and Complex Systems*. Ed. by Wojciech Zamojski et al. Cham: Springer International Publishing, pp. 431–444. ISBN: 978-3-319-39639-2.
- Soliman, H., H. Wang, and F. Blaabjerg (2016). “A Review of the Condition Monitoring of Capacitors in Power Electronic Converters.” In: *IEEE Transactions on Industry Applications* 52.6, pp. 4976–4989. ISSN: 0093-9994. DOI: [10.1109/TIA.2016.2591906](https://doi.org/10.1109/TIA.2016.2591906).
- Stecca, M. et al. (2020). “A Comprehensive Review of the Integration of Battery Energy Storage Systems Into Distribution Networks.” In: *IEEE Open Journal of the Industrial Electronics Society* 1, pp. 46–65. DOI: [10.1109/OJIES.2020.2981832](https://doi.org/10.1109/OJIES.2020.2981832).
- Su, H. T. et al. (2004). “Recent Advancements in Electromagnetic and Electromechanical Hybrid Simulation.” In: *2004 International Conference on Power System Technology, 2004. Power-Con 2004*. Vol. 2, 1479–1484 Vol.2. DOI: [10.1109/ICPST.2004.1460236](https://doi.org/10.1109/ICPST.2004.1460236).
- Su, S., X. Duan, and X. Zeng (2008). “ATP-Based Automated Fault Simulation.” In: *IEEE Transactions on Power Delivery* 23.3, pp. 1687–1689. ISSN: 0885-8977. DOI: [10.1109/TPWRS.2008.923811](https://doi.org/10.1109/TPWRS.2008.923811).
- Sugumar, G. et al. (2019). “Supervisory Energy-Management Systems for Microgrids: Modeling and Formal Verification.” In: *IEEE Industrial Electronics Magazine* 13.1, pp. 26–37. ISSN: 1932-4529. DOI: [10.1109/MIE.2019.2893768](https://doi.org/10.1109/MIE.2019.2893768).
- Sukumar, S. et al. (2018). “Grey Wolf Optimizer Based Battery Energy Storage System Sizing for Economic Operation of Microgrid.” In: *2018 IEEE International Conference on Environment and Electrical Engineering and 2018 IEEE Industrial and Commercial Power Systems Europe (EEEIC / I CPS Europe)*, pp. 1–5. DOI: [10.1109/EEEIC.2018.8494501](https://doi.org/10.1109/EEEIC.2018.8494501).
- Taha, M. S., H. H. Abdeltawab, and Y. A. I. Mohamed (2018). “An Online Energy Management System for a Grid-Connected Hybrid Energy Source.” In: *IEEE Journal of Emerging and Selected Topics in Power Electronics* 6.4, pp. 2015–2030. ISSN: 2168-6777. DOI: [10.1109/JESTPE.2018.2828803](https://doi.org/10.1109/JESTPE.2018.2828803).
- Tamp, F. and P. Ciufu (2014). “A Sensitivity Analysis Toolkit for the Simplification of MV Distribution Network Voltage Management.” In: *IEEE Transactions on Smart Grid* 5.2, pp. 559–568. DOI: [10.1109/TSG.2014.2300146](https://doi.org/10.1109/TSG.2014.2300146).
- Tan, D. and D. Novosel (2017). “Energy Challenge, Power Electronics & Systems (PEAS) Technology and Grid Modernization.” In: *CPSS Transactions on Power Electronics and Applications* 2.1, pp. 3–11. ISSN: 2475-742X. DOI: [10.24295/CPSSSTPEA.2017.00002](https://doi.org/10.24295/CPSSSTPEA.2017.00002).
- Tang, Grace (2014). “Power System Fault Modeling/Simulation Protective Relay Testing and Simulation.” In: *2014 IEEE 23rd North Atlantic Test Workshop*, pp. 40–42. DOI: [10.1109/NATW.2014.16](https://doi.org/10.1109/NATW.2014.16).
- Thornton, M. et al. (2018). “Internet-of-Things Hardware-in-the-Loop Simulation Architecture for Providing Frequency Regulation With Demand Response.” In: *IEEE Transactions on Industrial Informatics* 14.11, pp. 5020–5028. ISSN: 1551-3203. DOI: [10.1109/TII.2017.2782885](https://doi.org/10.1109/TII.2017.2782885).
- Uddin, Moslem et al. (2018). “A review on peak load shaving strategies.” In: *Renewable and Sustainable Energy Reviews* 82, pp. 3323–3332. ISSN: 1364-0321. DOI: <https://doi.org/10.1016/j.rser.2017.10.056>. URL: <http://www.sciencedirect.com/science/article/pii/S1364032117314272>.
- Umbarkar, Dr. Anantkumar and M. Joshi (July 2013). “Review of parallel genetic algorithm based on computing paradigm and diversity in search space.” In: *ICTACT Journal on Soft Computing* 3, pp. 615–622. DOI: [10.21917/ijsc.2013.0089](https://doi.org/10.21917/ijsc.2013.0089).
- Valencia, F. et al. (2016). “Robust Energy Management System Based on Interval Fuzzy Models.” In: *IEEE Transactions on Control Systems Technology* 24.1, pp. 140–157. ISSN: 1063-6536. DOI: [10.1109/TCST.2015.2421334](https://doi.org/10.1109/TCST.2015.2421334).

- Vijay, A. S., S. Doolla, and M. C. Chandorkar (2017). "Real-Time Testing Approaches for Microgrids." In: *IEEE Journal of Emerging and Selected Topics in Power Electronics* 5.3, pp. 1356–1376. ISSN: 2168-6777. DOI: [10.1109/JESTPE.2017.2695486](https://doi.org/10.1109/JESTPE.2017.2695486).
- Wang, Nenzi (July 2005). "A parallel computing application of the genetic algorithm for lubrication optimization." In: *Tribology Letters* 18, pp. 105–112. DOI: [10.1007/s11249-004-1763-x](https://doi.org/10.1007/s11249-004-1763-x).
- Wang, Zhaoyu (2019). *A distribution test system with smart meter data*. Iowa State University. URL: [http://wzy.ece.iastate.edu/publication/DistributiontestsystemFinal\\_new.pdf](http://wzy.ece.iastate.edu/publication/DistributiontestsystemFinal_new.pdf).
- Westermann, D. and M. Kratz (2010). "A Real-Time Development Platform for the Next Generation of Power System Control Functions." In: *IEEE Transactions on Industrial Electronics* 57.4, pp. 1159–1166. ISSN: 0278-0046. DOI: [10.1109/TIE.2009.2038403](https://doi.org/10.1109/TIE.2009.2038403).
- Wong, Ling Ai et al. (2019). "Review on the optimal placement, sizing and control of an energy storage system in the distribution network." In: *Journal of Energy Storage* 21, pp. 489–504. ISSN: 2352-152X. DOI: <https://doi.org/10.1016/j.est.2018.12.015>. URL: <http://www.sciencedirect.com/science/article/pii/S2352152X18303803>.
- Yang, Xin-She (2021). "Chapter 6 - Genetic Algorithms." In: *Nature-Inspired Optimization Algorithms (Second Edition)*. Ed. by Xin-She Yang. Second Edition. Academic Press, pp. 91–100. ISBN: 978-0-12-821986-7. DOI: <https://doi.org/10.1016/B978-0-12-821986-7.00013-5>. URL: <https://www.sciencedirect.com/science/article/pii/B9780128219867000135>.
- Yang, Yuqing et al. (2018). "Battery energy storage system size determination in renewable energy systems: A review." In: *Renewable and Sustainable Energy Reviews* 91, pp. 109–125. ISSN: 1364-0321. DOI: <https://doi.org/10.1016/j.rser.2018.03.047>. URL: <http://www.sciencedirect.com/science/article/pii/S1364032118301436>.
- zad, Bashir bakhshideh, Jacques Lobry, and François Vallee (Aug. 2018). "A New Voltage Sensitivity Analysis Method for Medium-Voltage Distribution Systems Incorporating Power Losses Impact." In: *Electric Power Components and Systems*. DOI: [10.1080/15325008.2018.1511639](https://doi.org/10.1080/15325008.2018.1511639).
- Zambrano, C. et al. (2016). "GridTeractions: Simulation platform to interact with distribution systems." In: *2016 IEEE Power and Energy Society General Meeting (PESGM)*, pp. 1–5. DOI: [10.1109/PESGM.2016.7741563](https://doi.org/10.1109/PESGM.2016.7741563).
- Zhang, Hao-Tian and Loi-Lei Lai (2012). "Monitoring System for Smart-Grid." In: *2012 International Conference on Machine Learning and Cybernetics*. Vol. 3, pp. 1030–1037. DOI: [10.1109/ICMLC.2012.6359496](https://doi.org/10.1109/ICMLC.2012.6359496).
- Zhang, T., A. E. Emanuel, and J. A. Orr (2016). "Distribution feeder upgrade deferral through use of energy storage systems." In: *2016 IEEE Power and Energy Society General Meeting (PESGM)*, pp. 1–5. DOI: [10.1109/PESGM.2016.7968249](https://doi.org/10.1109/PESGM.2016.7968249).
- Zhang, Yongxi et al. (June 2017). "Optimal Placement of Battery Energy Storage in Distribution Networks Considering Conservation Voltage Reduction and Stochastic Load Composition." In: *IET Generation, Transmission & Distribution* 11. DOI: [10.1049/iet-gtd.2017.0508](https://doi.org/10.1049/iet-gtd.2017.0508).
- Zhao, H. et al. (2019). "Voltage and Frequency Regulation of Microgrid With Battery Energy Storage Systems." In: *IEEE Transactions on Smart Grid* 10.1, pp. 414–424. DOI: [10.1109/TSG.2017.2741668](https://doi.org/10.1109/TSG.2017.2741668).
- Zhong Qing et al. (2013). "Optimal siting sizing of battery energy storage system in active distribution network." In: *IEEE PES ISGT Europe 2013*, pp. 1–5. DOI: [10.1109/ISGTEurope.2013.6695235](https://doi.org/10.1109/ISGTEurope.2013.6695235).

Șerban, Andreea Claudia and Miltiadis D. Lytras (2020). "Artificial Intelligence for Smart Renewable Energy Sector in Europe—Smart Energy Infrastructures for Next Generation Smart Cities." In: *IEEE Access* 8, pp. 77364–77377. DOI: [10.1109/ACCESS.2020.2990123](https://doi.org/10.1109/ACCESS.2020.2990123).



## PUBLICATIONS

---

Some ideas and figures have appeared previously in the following publication:

D. Martinez, H. Henao and G. Capolino, "Overview of Condition Monitoring Systems for Power Distribution Grids," 2019 IEEE 12th International Symposium on Diagnostics for Electrical Machines, Power Electronics and Drives (SDEMPED), Toulouse, France, 2019, pp. 160-166, doi: 10.1109/DEMPED.2019.8864872.



**Abstract** This thesis presents the supervision, analysis and optimization of power distribution systems considering the penetration of distributed energy resources and energy storage systems. The power distribution system planning is becoming an increasingly issue due to the deregulation of the power industry, the environmental policy changes, the introduction of new technologies and the transformation towards a smart power distribution grid definition. In consequence, the use of modeling and numerical evaluation tools is getting more attention for the system planners and operators. This has resulted in the development of a real-time experimental platform belonged to the Bank of the Energy concept. The platform covers all aspects of the challenges of future power system requirements related to the optimization of the local energy production and consumption. A hardware/software setup with emphasis to the utilization of real-time simulation and hardware in the loop testing with some typical reference applications are described.

Additionally, it is proposed a novel methodology for battery energy storage systems (BESS) integration over a real distribution system using the parallel computing capabilities of the experimental platform. The placement of BESS is performed by a sensitivity analysis, while the output power rating sizing is deployed using a genetic algorithm. The outcomes of this methodology demonstrate the effectiveness of the proposed parallelization technique and show that voltage profile improvement and losses reduction are possible introducing the BESS into the system.

**Keywords:** Algorithm design and analysis, Battery management system, Computer interfaces, Energy storage, Genetic algorithms, Hardware-in-the-loop simulation, Power distribution networks, Power system analysis computing, Real-time systems, Renewable energy sources, Software architecture.

**Résumé** Ce travail de thèse présente la supervision, l'analyse et l'optimisation des systèmes de distribution d'électricité, considérant en particulier la pénétration des ressources distribuées d'énergie renouvelable et les moyens de stockage d'énergie. La planification de ces systèmes commence à devenir un problème croissant dû à la dérégulation dans la production d'électricité, les changements dans la politique environnementale, l'introduction des nouvelles technologies et la transformation vers la définition d'un réseau électrique intelligent. En conséquence, l'utilisation d'outils de modélisation et d'analyse pour l'évaluation de ces systèmes électriques en pleine évolution, attirent de plus en plus l'attention des planificateurs et opérateurs. Ceci a donné lieu au développement d'une plateforme expérimentale temps réel, et a permis de concrétiser le nouveau concept de gestion énergétique dans un territoire de Banque de l'Énergie, introduit dans le projet VERTPOM®. Cette plateforme couvre tous les aspects des challenges concernant les futures exigences dans un réseau électrique de distribution, relatives à l'optimisation de la gestion dans la production et la consommation locales d'énergie électrique. Une installation matérielle/logicielle avec intérêt pour l'utilisation des outils de modélisation et d'analyse temps réel, avec quelques références d'application, est décrite également.

En plus, une nouvelle méthodologie d'intégration d'un système de stockage d'énergie dans un réseau de distribution d'électricité réel est proposée, avec l'utilisation de capacités de calcul parallèle de la plateforme expérimentale. La localisation de ce système est obtenue grâce à une analyse de sensibilité, tandis que le dimensionnement en puissance est donné par le déploiement d'un algorithme génétique. Les résultats obtenus dans ces conditions démontrent l'efficacité de la technique de parallélisation proposée, qui montrent également, que l'amélioration du profil de tension et la réduction des pertes de puissance techniques, sont possibles grâce à l'intégration des moyens de stockage d'énergie dans le système électrique.

**Mots clés :** Algorithme génétique, Architecture logicielle, Conception et analyse d'algorithmes, Énergie renouvelable, Interfaces informatiques, Réseau de distribution électrique, Stockage de l'énergie, Système de contrôle des batteries d'accumulateurs, Systèmes de test hardware-in-the-loop.